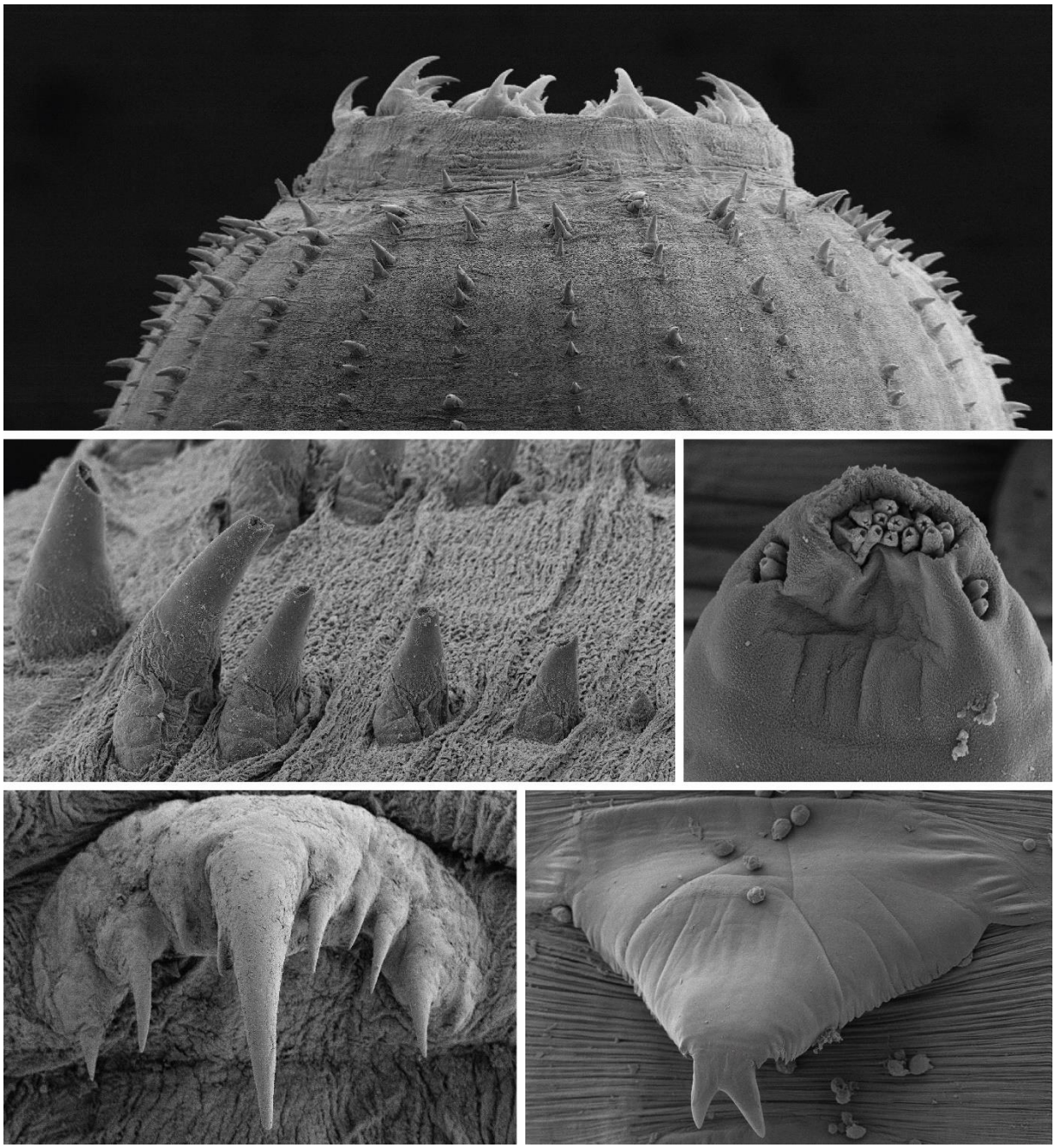

Jan Raeker

Morphology and Phylogeny of Priapulida

Dissertation

2025

Morphology and phylogeny of Priapulida

DISSERTATION

with the aim of achieving a doctoral degree (Dr. rer. nat.)
at the Faculty of Mathematics, Informatics and Natural Sciences
Department of Biology
of
University of Hamburg

submitted by
Jan Raeker

Hamburg, 2025

Examination committee:

Prof. Dr. Andreas Schmidt-Rhaesa (first supervisor and first examiner)
Prof. Dr. Katrine Worsaae (second supervisor)
Prof. Dr. Marie Herberstein (second examiner)
Prof. Dr. Jutta Schneider (head of the examination committee)
Prof. Dr. Baris Tursun (recording clerk)

Date of disputation:

23rd May 2025

List of publications

Study I:

Schmidt-Rhaesa, A., **Raeker, J.**, 2023. Morphology of larval and postlarval stages of *Priapulopsis bicaudatus* (Danielssen, 1869) (Priapulida) from the North Atlantic Ocean. *Zoologischer Anzeiger* 302, 1-16. doi: 10.1016/j.jcz.2022.11.006.

Study II:

Raeker, J., Worsaae, K., Schmidt-Rhaesa, A., 2024. New morphological structures of *Priapulus caudatus*, Lamarck 1816 (Priapulida) and analysis of homologous characters across macroscopic priapulids. *Zoologischer Anzeiger* 312, 135-152. doi: 10.1016/j.jcz.2024.08.005.

Study III:

Raeker, J., Worsaae, K., Schmidt-Rhaesa, A., 2024. David versus Goliath: an interspecific comparison between small-sized *Halicryptus spinulosus* and large-sized *Halicryptus higginsi* (Priapulida). *Zoologischer Anzeiger* 313, 1-20. doi: 10.1016/j.jcz.2024.08.003.

Study IV:

Schmidt-Rhaesa, A., **Raeker, J.**, 2024. Review of the Priapulida of New Zealand with the description of a new species. *New Zealand Journal of Zoology* (online first). doi: 10.1080/03014223.2023.2278738.

Study V:

Raeker, J., Lord, A., Herranz, M., Giribet, G., Worsaae, K., Schmidt-Rhaesa, A., 2025. The big, the small and the weird: A phylogenomic analysis of extant Priapulida. *Molecular Phylogenetics and Evolution* 204, 108297. doi: 10.1016/j.ympev.2025.108297.

Declaration of own contributions to the published manuscripts

Study I:

- Morphological investigations: LM (imaging)
- Extensive literature research for comparisons with previous studies
- Editing the drafted manuscript and figures

Study II:

- Designing the study
- Collecting *P. caudatus* in Sweden and securing live specimens of adult *P. caudatus* from Wilhelmshaven, Germany
- Morphological investigations: LM, SEM (preparation, imaging), histology (preparation, sectioning, staining, imaging)
- Extensive literature research for comparisons with published data
- Drafting the original manuscript and preparing all figures

Study III:

- Designing the study
- Morphological investigations: LM (imaging), SEM (preparation, imaging), histology (preparation, sectioning, staining, imaging)
- Molecular investigations: DNA extraction and amplification; handling and analysing sequence data (*CO1*); publishing data on NCBI GenBank
- Extensive literature research for comparisons with published data
- Drafting the original manuscript and preparing all figures

Study IV:

- Morphological investigations: LM (imaging)
- Extensive literature research for comparisons with previous studies
- Editing manuscript draft and figures

Study V:

- Collecting *T. lemburgi* in Tenerife, Canary Islands
- Morphological investigations: LM (imaging), SEM (preparation, imaging)
- Molecular investigations: cDNA synthesis and amplification; handling and analysing sequence data (transcriptomes); publishing data on NCBI Sequence Read Archive
- Coordinating the collaboration of all authors participating in this study
- Drafting the original manuscript and preparing all figures

LIB Leibniz-Institut zur Analyse des Biodiversitätswandels

Museum der Natur Hamburg - Zoologie
Martin-Luther-King-Platz 3 • 20146 Hamburg

Prof. Dr. Andreas Schmidt-Rhaesa

Leiter Sektion Wirbellose Tiere
Museum der Natur Hamburg - Zoologie
Martin-Luther-King-Platz 3
20146 Hamburg

Tel. +49 40 42838 3921
a.schmidt-rhaesa@leibniz-lib.de

12.02.2025

Statement zur Autorenbeteiligung

Herr Jan Raeker hat in seiner Dissertationsschrift die Beteiligung der Autorinnen und Autoren an den einzelnen Veröffentlichungen dargelegt. Ich bestätige hiermit, dass die genannten Werte der tatsächlichen Arbeitsteilung entsprechen.

Andreas Schmidt-Rhaesa

Table of contents

Abstract

Priapulida is a small phylum of marine worms with only 21 described species across seven genera. Although priapulidans are long-known, standardized documentations of their morphology are still lacking for many species. Some of the morphological structures are only superficially described, if at all, making comparisons among priapulidans difficult. Interestingly for Priapulida is the occurrence of two adult size classes, microscopic (<3.5 µm) and macroscopic (up to 40 cm), differing from related phyla (Kinorhyncha and Loricifera) that are exclusively of microscopic size. Due to the two size classes in Priapulida and contradicting reports of potential fossils among the three related phyla, the ancestral body size of Priapulida remains uncertain. Internal phylogenetic relationships of priapulidans have only been inferred from morphological data, as molecular data from priapulidans are scarce. Proposed phylogenies support both an ancestrally microscopic and macroscopic body size. Phylogenetic analyses based on molecular data may help to clarify the relationships in Priapulida and their ancestral body size.

In this thesis, the following macroscopic species are examined and morphological structures are described in detail using light microscopy, scanning electron microscopy and, for some species, histology: *Priapulus caudatus*, *Priapulus tuberculatospinosus*, *Priapulopsis bicaudatus*, *Priapulopsis australis*, *Halicryptus spinulosus* and *Halicryptus higginsi*. Larval and postlarval stages, as well as adult specimens were collected during multiple field trips or obtained from museum collections. Additionally, molecular data (transcriptomic and genomic) was gathered from these species and analyzed together with publicly available data. Microscopic species were not available for morphological examinations, however, few *Tubiluchus* specimens could be used for molecular analyses.

The morphological investigations conducted in this thesis describe almost all structures of these species in detail. Key findings include newly described structures on the circumoral fields of *P. caudatus* and *P. tuberculatospinosus*, as well as on the trunks of *H. spinulosus* and *H. higginsi*. Additionally, asymmetric growth of the caudal appendages and the bipartition process of first-ring teeth during postlarval development were observed in *P. bicaudatus*. The larval stages of *P. bicaudatus* were also described in greater detail compared to a previous study. While examining *P. australis* specimens, two individuals exhibit unique morphological characters, resulting in the description of a new macroscopic species, *Priapulopsis papillatus*.

Furthermore, this thesis presents the first phylogenomic analysis of Priapulida, integrating transcriptomic data from seven species across four genera (including six newly assembled transcriptomes) and conserved genomic loci from ten species across five genera. The positions of rare genera *Acanthopriapulus* and *Maccabeus*, which lack molecular data, were inferred through morphological analysis. The topology of this combined phylogenetic tree corresponds almost entirely with those of previous studies that only analyzed morphological data. Key findings include microscopic *Meiopriapulus* as sister group to all remaining priapulidans, and microscopic *Maccabeus* that exhibits morphological characters of both size classes as sister group to all macroscopic species. Ancestral state reconstructions of morphological traits on the newly conducted phylogenetic tree suggest an ancestrally small body size and an internal fertilization in extant Priapulida. These traits are consistent with their microscopic sister groups, Kinorhyncha and Loricifera.

Zusammenfassung

Priapulida ist ein kleiner Stamm mariner Würmer mit nur 21 beschriebenen Arten in sieben Gattungen. Obwohl Priapuliden schon lange bekannt sind, fehlen für viele Arten noch standardisierte Dokumentationen ihrer Morphologie. Einige morphologische Strukturen sind nur oberflächlich beschrieben oder gar nicht erfasst, was Vergleiche zwischen verschiedenen Arten erschwert. Priapuliden sind interessant, da es zwei adulte Größenklassen gibt: mikroskopisch (<3,5 µm) und makroskopisch (bis zu 40 cm). Dies unterscheidet sie von verwandten Stämmen wie Kinorhyncha und Loricifera, die ausschließlich eine mikroskopische Größe aufweisen. Aufgrund der beiden Größenklassen bei den Priapulida und widersprüchlicher Berichte über mögliche Fossilien unter den drei verwandten Stämmen bleibt die ursprüngliche Körpergröße der Priapulida ungewiss. Die inneren phylogenetischen Beziehungen der Priapuliden wurden bisher nur anhand morphologischer Daten abgeleitet, da für sie kaum molekulare Daten erhoben sind. Konstruierte Stammbäume unterstützen sowohl eine ursprünglich mikroskopische als auch eine makroskopische Körpergröße. Phylogenetische Analysen mit molekularen Daten könnten dazu beitragen, die Beziehungen innerhalb der Priapulida und daraus folgend ihre ursprüngliche Körpergröße zu klären.

In dieser Dissertation werden folgende makroskopischen Arten untersucht und ihre morphologischen Strukturen detailliert beschrieben, unter Verwendung von Lichtmikroskopie, Rasterelektronenmikroskopie und für einige Arten auch Histologie: *Priapulus caudatus*, *Priapulus tuberculatospinosus*, *Priapulopsis bicaudatus*, *Priapulopsis australis*, *Halicryptus spinulosus* und *Halicryptus higginsi*. Larvale und postlarvale Stadien sowie adulte Exemplare wurden während mehrerer Exkursionen gesammelt oder aus Museumssammlungen bezogen. Zusätzlich wurden molekulare Daten (Transkriptom- und Genomdaten) dieser Arten erhoben und zusammen mit öffentlich verfügbaren Daten analysiert. Mikroskopische Arten standen für morphologische Untersuchungen nicht zur Verfügung, jedoch konnten einige Exemplare von *Tubiluchus* für molekulare Analysen genutzt werden.

Die in dieser Dissertation durchgeführten morphologischen Untersuchungen beschreiben nahezu alle Strukturen der untersuchten Arten im Detail. Wichtige Ergebnisse umfassen neu beschriebene Strukturen an den circumoralen Regionen von *P. caudatus* und *P. tuberculatospinosus* sowie an den Rümpfen von *H. spinulosus* und *H. higginsi*. Zudem wurden ein asymmetrisches Wachstum der Schwanzanhänge, sowie eine Teilung der Zähne des ersten Zahnrings während der postlarvalen Entwicklung, bei

P. bicaudatus beobachtet. Die larvalen Stadien von *P. bicaudatus* wurden detaillierter beschrieben als in einer früheren Studie. Während der Untersuchung von *P. australis* wiesen zwei Individuen einzigartige morphologische Merkmale auf, was zur Beschreibung einer neuen makroskopischen Art führte, *Priapulopsis papillatus*.

Darüber hinaus präsentiert diese Dissertation die erste phylogenomische Analyse der Priapulida, in der Transkriptome von sieben Arten aus vier Gattungen (darunter sechs neu erstellte Transkriptome) sowie konservierte genomische Loci von zehn Arten aus fünf Gattungen integriert wurden. Die Positionen der seltenen Gattungen *Acanthopriapulus* und *Maccabeus*, für die keine molekularen Daten vorliegen, wurden durch morphologische Analysen abgeleitet. Die Topologie dieses kombinierten phylogenetischen Baums entspricht fast vollständig den Ergebnissen früherer Studien, die nur morphologische Daten analysierten. Zu den zentralen Erkenntnissen gehört, dass der mikroskopische *Meiopriapulus* als Schwestergruppe aller übrigen Priapuliden erscheint und dass der mikroskopische *Maccabeus*, der morphologische Merkmale beider Größenklassen aufweist, als Schwestergruppe aller makroskopischen Arten positioniert ist. Rekonstruktionen der ursprünglichen Merkmale auf Basis des neuen phylogenetischen Baums deuten darauf hin, dass Priapulida ursprünglich eine kleine Körpergröße und eine interne Befruchtung aufwiesen. Diese Merkmale stimmen mit ihren mikroskopischen Schwestergruppen Kinorhyncha und Loricifera überein.

1. Introduction

1.1. Marine invertebrates and the taxon Scalidophora

Marine invertebrates

Marine invertebrates are assumed to have evolved in the Neoproterozoic around 650 million years ago (e.g., Cunningham et al. 2016). Since their first appearance, this morphologically diverse group distributed throughout marine waters and they can be found in all marine environments: from intertidal to hadal ocean trenches (Jamieson 2015), and from tropical waters to cold polar oceans (Marshall et al. 2012). Marine invertebrates are experts in tolerating even extreme conditions, like anoxic hypersaline basins (e.g., Danovaro et al. 2010) or hydrothermal vents (e.g., Le Bris and Gaill 2007).

Today, more than 180,000 marine invertebrate species are described and divided into 31 phyla, among which Arthropoda (~59,600 species), Mollusca (~51,900 species) and Annelida (~14,000 species) represent the three most species-rich phyla (WoRMS Editorial Board 2024). About half of the 31 phyla exclusively inhabit marine waters (together <10,000 species). The actual number of marine invertebrates – or marine species in general – is presumed to be much higher (Appeltans et al. 2012).

Scalidophora

One group of marine invertebrates is Scalidophora Lemburg, 1995, which includes exclusively marine invertebrate animals consisting of three phyla: Priapulida Théel, 1906, Kinorhyncha Reinhard, 1881 and Loricifera Kristensen, 1983 (Lemburg 1995a; Nielsen 2012; Fig. 1A-C). This clade is part of Ecdysozoa Aguinaldo et al., 1997, a large taxon including animals that moult their three-layered cuticles during growth, like arthropods, nematodes or tardigrades (Aguinaldo et al. 1997; Schmidt-Rhaesa et al. 1998).

The most distinctive apomorphic character shared among Scalidophora is the retractable ‘introvert’ (also known as ‘proboscis’) with cuticular spine-like structures, the ‘scalids’, which give Scalidophora its name. Scalids are arranged in rings or longitudinal rows (depending on the interpretation of the arrangement) on the introvert and have a sensory function (Bang-Berthelsen et al. 2013; Neuhaus 2013; Schmidt-Rhaesa 2013; Fig. 1D-F). In Kinorhyncha and Loricifera, scalids are long and slender structures that occur in various forms (Fig. 1E, F), whereas they are mostly uniform in type and appear as conical or triangularly flattened structures in Priapulida (Fig. 1D). Other apomorphies

are a specific type of flower-shaped sensory organs (‘flosculi’; ‘sensory spots’; Fig. 1G-I) and two sets of introvert retractors (Nielsen 2012).

The adult body size differs between the three taxa. Loriciferans are the smallest among Scalidophora, as their adult body sizes are usually under 300 µm (Bang-Berthelsen et al., 2013). Depending on the species, Kinorhyncha have body sizes of up to 1000 µm (Neuhaus 2013). While Loricifera and Kinorhyncha are exclusively of microscopic size, Priapulida has microscopic (<3.5 mm) and macroscopic (up to 40 cm) adult body sizes (Schmidt-Rhaesa 2013). Detailed information on body sizes of Priapulida is shown further below.

Kinorhyncha is the most species-rich of the three phyla, with over 300 species in 31 genera (Herranz et al. 2022), and new species are regularly described (e.g., Cepeda et al. 2022; Grzelak and Sørensen 2022; Rucci et al. 2022). Loricifera, one of the most recently described animal phyla (Kristensen 1983), already includes over 40 described species in 15 genera (Neves et al. 2021), and similar to Kinorhyncha, new species are frequently described (e.g., Sørensen et al. 2022; 2023) or reported as undescribed specimens (e.g., Neves et al. 2022). Priapulida is the smallest phylum of Scalidophora with only 21 described species in seven genera (Schmidt-Rhaesa 2013; Schmidt-Rhaesa et al. 2017). Although it is the longest-known scalidophoran phylum, species have been rarely described. Species numbers only started to increase with the description of microscopic species (Van der Land 1968).

The phylogenetic relationships within Scalidophora are not distinctly solved. Interrelationships based on morphology for each possible sister-group relationship ([Priapulida + Kinorhyncha]; [Priapulida + Loricifera]; [Kinorhyncha + Loricifera]) are all supported by certain morphological characters, as summarized by Neuhaus and Higgins (2002). Similarly, the sister-group relationships of Scalidophora remain unsolved in molecular analyses (summarized by Giribet and Edgecombe 2017). Molecular studies including species of all Scalidophora taxa are scarce and mostly propose Priapulida + Kinorhyncha as sister-groups (e.g., Sørensen et al. 2008; Herranz et al. 2022; Howard et al. 2022). When only Priapulida and Kinorhyncha are included in phylogenetic analyses, they are also usually in a sister group relationship (e.g., Todaro et al. 2006; Dunn et al. 2008; Campbell et al. 2011; Borner et al. 2014). Some other studies do not support the group Scalidophora, as Loricifera (Sørensen et al. 2008) and Kinorhyncha (Hejnol et al. 2009) have been shown to have sister-group relationships with Nematomorpha. Additionally, Loricifera has been placed as the sister-group to Panarthropoda (Yamasaki

et al. 2015) or even to all ecdysozoans (Park et al. 2006). However, it has to be mentioned that molecular data for Loricifera is limited to only three genes (*18S*, *28S* and *histone H3*) and one transcriptome across three species (Laumer et al. 2015).

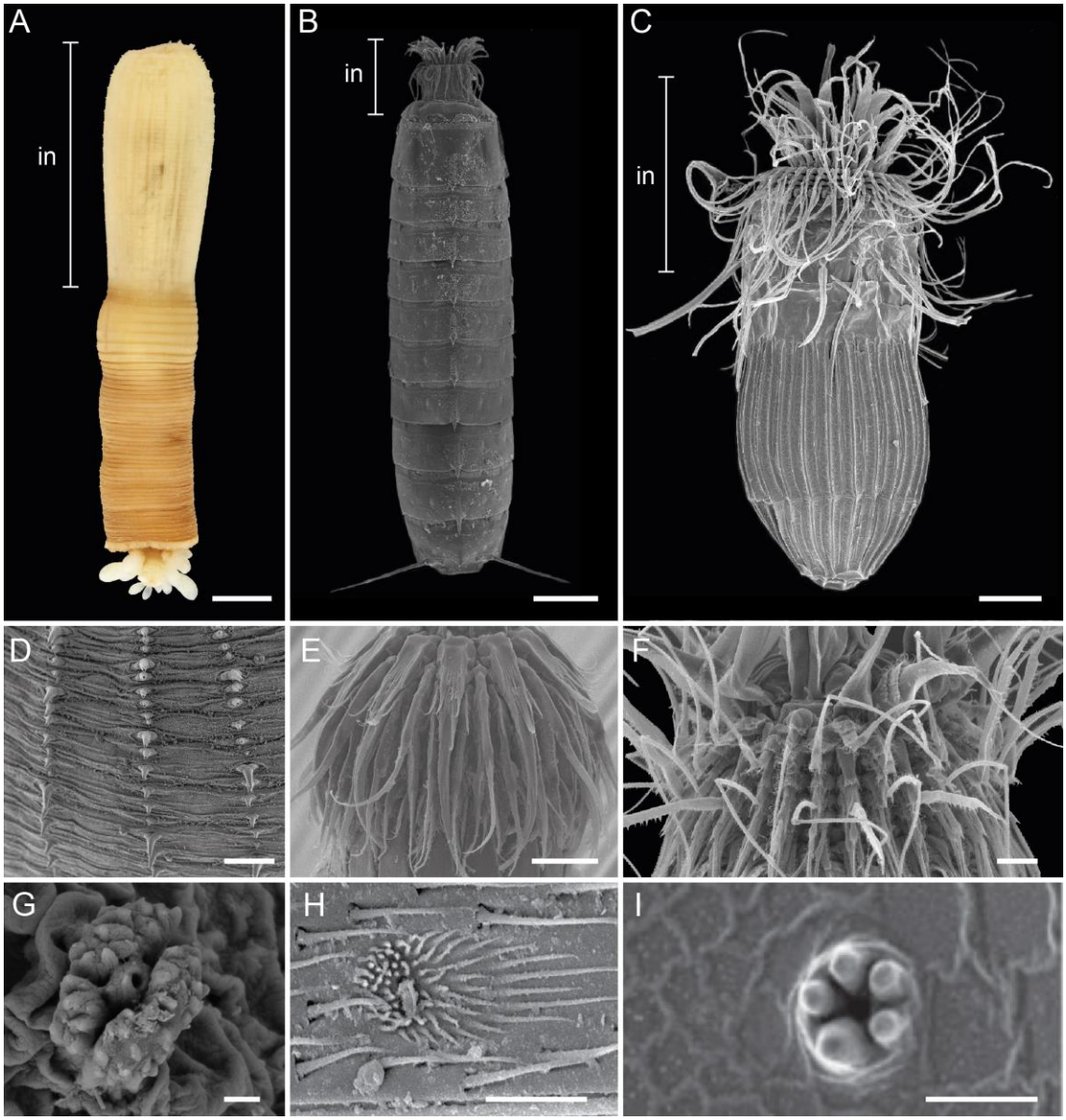

Fig. 1. Scalidophora (Priapulida [A,D], Kinorhyncha [B,E], Loricifera [C,F]), light micrograph (A) and SEM images (B-I). **A-C**. Habitus with labelled introvert (in). **A**. Small adult *Priapulus caudatus*. **B**. Adult *Cristaphyes cryopygus*. **C**. Adult *Pliciloricus leocaudatus*. **D**. Scalids of *P. caudatus*. **E**. Scalids of *Echinoderes spinifurca*. **F**. Scalids of *P. leocaudatus*. **G**. Flosculus of Priapulida. **H**. Sensory spot of Kinorhyncha. **I**. N-flosculus of Loricifera. Images B, C, and F kindly provided by Martin V. Sørensen and E by María Herranz. Image H modified from Cepeda et al. (2022) and image I modified from Bang-Berthelsen et al. (2013). Scale bars: A = 1 mm, B = 100 µm, C = 25 µm, D = 400 µm, E, F = 10 µm, G, I = 1 µm, H = 8 µm.

1.2. Priapulida

1.2.1. General information

Priapulida are benthic marine worms that develop from larval and postlarval stages to adult specimens by moulting (Van der Land 1970). The phylum derives its name from the Greek god of fertility, *Priapos*, who is often depicted with a large male genital. Therefore, priapulidans[1] are commonly referred to as 'penis worms' (see Fig. 1A). Aside from related Kinorhyncha and Loricifera, priapulidans are divided into two body size classes: macroscopic and microscopic (for details on body size see below) (Schmidt-Rhaesa 2013). The size division is only applied to the body size of adult specimens as larval stages of both size classes are exclusively of microscopic size (approximately between 80 and 1300 µm length; Lang 1939; Kirsteuer 1976; Wennberg 2009).

Classification

The 21 priapulidan species are divided into seven genera (Table 1). Eight species in four genera are of macroscopic adult size. Macroscopic genera are *Priapulus* Lamarck, 1816 (three species), *Halicryptus* Von Siebold, 1849 (two species), *Priapulopsis* Koren & Danielsen, 1875 (two species)[2] and *Acanthopriapulus* Van der Land, 1970 (one species) (Table 1). The remaining 13 species (three genera) are of microscopic adult size. Microscopic genera are *Tubiluchus* Van der Land, 1968 (ten species), *Maccabeus* Por, 1973 (two species) and *Meiopriapulus* Morse, 1981 (one species) (Table 1).

Two approaches exist for the further classification of Priapulida: the 'traditional' classification and a classification based on phylogenetic relationships. While the traditional classification tries to fill in many taxonomic ranks (e.g., family, order, class etc.) for each species, the phylogenetic classification allocates names (sometimes referred to as 'clades') to monophyla. In the traditional classification, names may be redundant, for example when a family name includes the same species as the genus (i.e., the family Tubiluchidae includes ten *Tubiluchus* species, just as the genus *Tubiluchus*). Many names introduced under traditional classificatory background turn out to name monophyla and

[1] Commonly, the vernacular term 'priapulid' is used in the literature. As this may be confusing with the vernacular term of the family Priapulidae, 'priapulidans' is used here instead. Other authors use 'Priapula' and 'priapulans', but these terms are not used here.

[2] A third species, '*Priapulopsis* (?) *cnidephorus*', was described by Salvini-Plawen (1973) on a single specimen (presumably a postlarval stage) but is widely not considered as valid and will be neglected here.

are therefore taken over in phylogenetic systematization. Named paraphyla or redundant names are not included in phylogenetic trees.

Following the traditional classification (see Table 2 for the latest traditional classification summarized by Adrianov and Malakhov, 1995), redundant names for higher hierarchical ranks exist in Priapulida for the microscopic *Tubiluchus*, *Meiopriapulus* and *Maccabeus* (*Tubiluchus*: Tubiluchidae Van der Land, 1970; *Maccabeus*: Chaetostephanidae Salvini-Plawen, 1974 and Seticoronaria Salvini-Plawen, 1974; *Meiopriapulus*: Meiopriapulidae Adrianov & Malakhov, 1995 and Meiopriapulomorpha Adrianov & Malakhov, 1995; see Table 2). The macroscopic *Halicryptus* also has redundant names (Halicryptinae Salvini-Plawen, 1974 and Halicryptomorpha Adrianov & Malakhov, 1995). However, Adrianov and Malakhov (1995) 'introduced' Halicryptidae for *Halicryptus* by misquoting Salvini-Plawen (1974), which was adopted by later authors. The remaining macroscopic genera (*Acanthopriapulus*, *Priapulus* and *Priapulopsis*) are summarized as Priapulidae Gosse, 1855. Due to morphological similarities, *Tubiluchus* and Priapulidae were summarized as Priapulimorpha Salvini-Plawen, 1974.

Table 1. Overview of valid described species of Priapulida.

No.	Species	Type locality
1	*Priapulus caudatus* Lamarck, 1816	unknown
2	*Priapulus tuberculatospinosus* Baird, 1868	Falkland Isles, Argentina
3	*Priapulus abyssorum* Menzies, 1959	South end of Mid-America-Trench
4	*Halicryptus spinulosus* Von Siebold, 1849	Beach of Stogi, Gdańsk, Poland
5	*Halicryptus higginsi* Shirley & Storch, 1999	Point Barrow, Alaska, USA
6	*Priapulopsis bicaudatus* (Danielssen, 1869)	Varangerfjord, Norway
7	*Priapulopsis australis* (de Guerne, 1886)	South Atlantic, Argentina
8	*Acanthopriapulus horridus* (Théel, 1911)	Coast of Uruguay
9	*Tubiluchus corallicola* Van der Land, 1968	Piscadera Baai, Curaçao
10	*Tubiluchus remanei* Van der Land, 1982	Near Hurghada, Red Sea, Egypt
11	*Tubiluchus australensis* Van der Land, 1985	Carter Reef, Australia
12	*Tubiluchus philippinensis* Van der Land, 1985	Sabang Island, Cebu, Philippines
13	*Tubiluchus arcticus* Adrianov, Malakhov, Tchesunov & Tzetlin, 1989	White Sea, Russia
14	*Tubiluchus vanuatensis* Adrianov & Malakhov, 1991	Efate Island, New Hebrides
15	*Tubiluchus troglodytes* Todaro & Shirley, 2003	Grotta del Ciolo, Lecce, Italy
16	*Tubiluchus lemburgi* Schmidt-Rhaesa, Rothe & Martínez, 2013	Los Cerebros, Tenerife, Canary Islands
17	*Tubiluchus soyoae* Schmidt-Rhaesa, Panpeng & Yamasaki, 2017	Suruga Bay, Honshu Island, Japan
18	*Tubiluchus pardosi* Schmidt-Rhaesa, Panpeng & Yamasaki, 2017	Tokei Beach, Kourijima Island, Japan
19	*Maccabeus tentaculatus* Por, 1973	Southeastern shores of Cyprus
20	*Maccabeus cirratus* (Malakhov, 1978)	Indian Ocean
21	*Meiopriapulus fijiensis* Morse, 1981	Korolevu Bay, Viti Levu, Fiji

Following the phylogenetic classification (see Table 3 for the latest phylogenetic classification by Lemburg, 1999), the following clades exist for Priapulida: Monocaudata Lemburg, 1999 (*Acanthopriapulus* + *Priapulus*); Megintroverta Lemburg, 1999 (Monocaudata + *Priapulopsis*); Priapulidae (Megintroverta + *Halicryptus*); Eupriapulida Lemburg, 1999 (Priapulidae + *Maccabeus*); Tubiluchidae (*Tubiluchus* + *Meiopriapulus*); Priapulida (Eupriapulida + Tubiluchidae). For further information on the phylogeny of Priapulida see Chapter 1.2.8.

Table 2. Proposed traditional classification of Priapulida after Adrianov and Malakhov (1995).

Phylum	**Order**	**Family**	**Subfamily**	**Genus**
Priapulida Théel, 1906	**Priapulimorpha** Salvini-Plawen, 1974	**Priapulidae** Gosse, 1855	**Priapulinae** Salvini-Plawen, 1974	***Acanthopriapulus*** Van der Land, 1970
				Priapulus Lamarck, 1816
				Priapulopsis Koren & Danielssen, 1875
		Tubiluchidae Van der Land, 1970		***Tubiluchus*** Van der Land, 1968
	Halicryptomorpha Adrianov & Malakhov, 1995	**(Halicryptidae)** see Adrianov and Malakhov (1995)	**Halicryptinae** Salvini-Plawen, 1974	***Halicryptus*** Von Siebold, 1849
	Seticoronaria Salvini-Plawen, 1974	**Chaetostephanidae** Salvini-Plawen, 1974		***Maccabeus*** Por, 1973
	Meiopriapulomorpha Adrianov & Malakhov, 1995	**Meiopriapulidae** Adrianov & Malakhov, 1995		***Meiopriapulus*** Morse, 1981

Table 3. Proposed phylogenetic classification after Lemburg (1999).

Priapulida Théel, 1906	**Eupriapulida** Lemburg, 1999	**Priapulidae** Gosse, 1855	**Megintroverta** Lemburg, 1999	**Monocaudata** Lemburg, 1999	***Acanthopriapulus*** Van der Land, 1970
					Priapulus Lamarck, 1816
					Priapulopsis Koren & Danielssen, 1875
					Halicryptus Von Siebold, 1849
					Maccabeus Por, 1973
	Tubiluchidae Van der Land, 1970				***Tubiluchus*** Van der Land, 1968
					Meiopriapulus Morse, 1981

The first described and most prominent priapulidan is the macroscopic *Priapulus caudatus*, which has been known since 1754 when it was described by Odhelius as '*Priapus humanus*' (Van der Land 1970). Unfortunately, the sampling localities of the investigated specimens are unknown. After some placements into different animal groups resulting in few name changes (see Van der Land 1970), Lamarck (1816) assigned the name that is now considered valid. The first microscopic priapulidan, *Tubiluchus corallicola*, was first described over two centuries after first mentioning of macroscopic species (Van der Land 1968).

The first report of larval stages of macroscopic priapulidans occurred about 150 years after the report of adults and were of *H. spinulosus* (Hammarsten 1913; 1915). The hatching larva was just recently described for *P. caudatus* (Wennberg et al. 2009) and *H. spinulosus* (Janssen et al. 2009). Through several moults, larval stages develop into adults. Between both life stages are several postlarval stages, which are morphologically very similar to adults and differ only in few aspects (Van der Land 1970). The exact number of larval stages (= number of moults) is unknown. Kirsteuer (1976) shows at least six larval stages for *Tubiluchus*, based on morphological data. The development from larval stages to the first postlarval stage takes a minimum of two years (Lang 1939).

Larval stages have been reported for the majority of priapulidans. From the macroscopic species, only the rare *A. horridus* lacks a report. Shirley and Storch (1999) mentioned the occurrence of larval stages for *H. higginsi*, but they have neither been described in detail nor imaged. For microscopic species, larval stages have been reported for half of the described species of *Tubiluchus* (Van der Land 1968; 1982; Adrianov and Malakhov 1991; Todaro and Shirley 2003; Schmidt-Rhaesa et al. 2013) and for *M. tentaculatus* (Por 1972). *Meiopriapulus fijiensis* differs from other priapulidans by having a direct development without loricate larval stages (Higgins and Storch 1991).

1.2.2. Adult body size

Size differences between adult macroscopic and microscopic priapulidans are enormous (Fig. 2). Commonly, adult specimens of *Priapulus* and *Priapulopsis* are a few centimetres long (<10 cm; Fig. 2A), but rarely large specimens of *Priapulus* (up to 20 cm) are reported (Van der Land 1970). In *Halicryptus*, *H. spinulosus* has a maximum length of about 4 cm, while its congener, *H. higginsi*, is the largest known priapulidan with reported lengths of up to 39.5 cm (Shirley and Storch 1999). For *A. horridus* only few small specimens (0.6 to 24 mm) have been recorded (see Schmidt-Rhaesa et al. 2022).

Microscopic species reach a maximum length of only a few millimetres (Fig. 2B). In *Tubiluchus*, reported trunk lengths range between 0.6 mm (*T. australensis* and *T. pardosi*; Van der Land 1985; Schmidt-Rhaesa et al. 2017) and 1.4 mm (*T. troglodytes*; Todaro and Shirley 2003). The long tail of *Tubiluchus* is usually not included in the measurements. *Maccabeus* has reported body lengths between 2 mm (*M. tentaculatus*; Por and Bromley 1974) and 3.5 mm (*M. cirratus*; Malakhov 1978). Trunk lengths of adult specimens of *Meiopriapulus fijiensis* range between 1.2 and 3.4 mm (Westheide 1990; Sørensen et al. 2012).

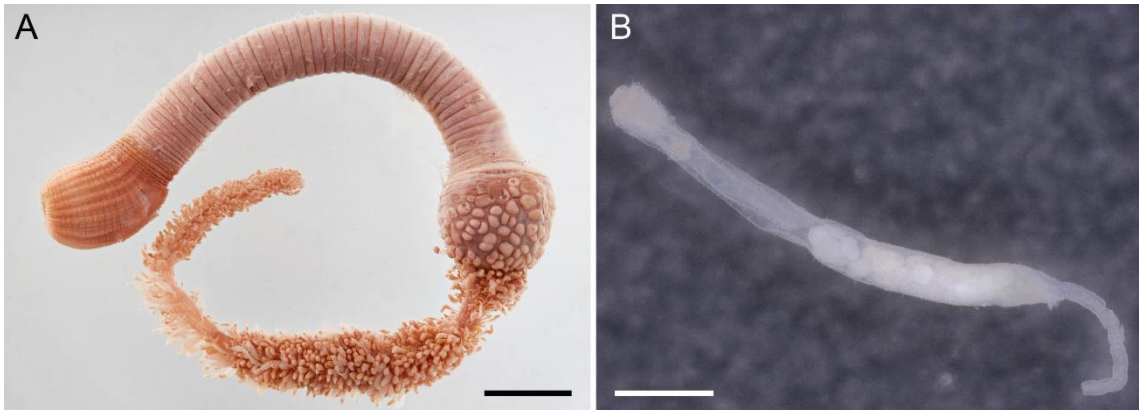

Fig. 2. Adult Priapulida, light microscopical images. **A**. Macroscopic *P. tuberculatospinosus* from Chile. **B**. Microscopic *Tubiluchus* sp. from Cuba. Scale bars: A = 5 mm, B = 500 µm.

1.2.3. Palaeontological reports

Several worm-like, fossil species from the Cambrian and one species from the Carboniferous have been brought in relation with Priapulida due to morphological similarities, like an introvert with scalid-like structures (e.g., Conway Morris 1977). Therefore, extant priapulidans are sometimes referred to as 'living fossils' (e.g., Schreiber 1996).

From the associated fossil species, the Carboniferous *Priapulites konecniorum* Schram, 1973 resembles extant Priapulida like *Priapulus* the most and is considered as extinct species within the crown group Priapulidae (see Van der Land and Nørrevang 1985). The Cambrian fossil species are considered to belong to the stem group of Priapulida or earlier lineages (Van der Land and Nørrevang 1985; Schmidt-Rhaesa 2013). Due to morphological similarities with recent Priapulida (e.g., pharyngeal teeth in pentagons; 25 rows of scalids on the introvert; annulated trunk; papillae/hooks in rings on the posterior trunk; see below for morphology of recent Priapulida), stem-group species may be *Ottoia prolifica* Walcott, 1911; *Ottoia tricuspida* Smith, Harvey &

Butterfield, 2015; *Selkirkia columbia* Conway Morris, 1977; *Xiaoheiqingella peculiaris* Huang, Vannier & Chen, 2004; *Paratubiluchus bicaudatus* Han, Shu, Zhang & Liu, 2004 (see Conway Morris 1977; Huang et al. 2004; Han et al. 2004; Smith et al. 2015). The classification of *O. prolifica* and *S. columbia* as stem-group Priapulida is further supported by findings of small carbonaceous fossils ('SCFs'), which are microscopic fossilized organic remains of organisms (see Butterfield and Harvey 2012; Smith et al. 2015; Slater et al. 2017). The identified SCFs may represent teeth, introvert structures and trunk hooks for both species and show morphological similarities with those of extant Priapulida.

A common feature for all reported priapulidan-like fossils is the macroscopic body size. *Priapulites konecniorum* has reports of 5 to 6 cm (Schram 1973), *O. prolificia* ranges between 3 and 15 cm (Conway Morris 1977), *S. columbia* has a size of about 4 cm (Conway Morris 1977) and *X. pecularis* and *Paratubiluchus bicaudatus* both have reports of just over one centimetre (Han 2004). The finding of only macroscopic priapulidan-like fossils may be due to a sampling and conservation bias (Worsaae et al. 2023). Meiofaunal fossils are found rarely, but they exist, as demonstrated by the finding of the Cambrian Loricifera *Eolorica deadwoodensis* (Harvey and Butterfield 2017) or of the Middle Cambrian *Markuelia* (Dong et al. 2004). For Kinorhyncha, potential questionable stem group fossils were described within meiofaunal size (Zhang et al. 2015; Shao et al. 2020). Although only macroscopic adult fossil species exist for Priapulida, it remains unknown whether a microscopic or macroscopic body size is ancestral in Priapulida.

1.2.4. Geographical distribution

Priapulidans have been reported from various localities across the globe (see Van der Land 1970; Adrianov and Malakhov 1996a,b; Fig. 3). Although reports of specimens represent often only punctual findings, larger distributions are estimated for some species (see distribution maps in Paulay 2024).

Macroscopic species have a polar distribution in mainly in cold marine waters of the Northern and Southern Hemisphere (Adrianov and Malakhov 1996a,b) and can be found in intertidal and subtidal regions (0 to 200 m), as well as in the deep sea (up to approximately 8000 m; see Adrianov and Malakhov 1996b). Interestingly, both genera *Priapulus* and *Priapulopsis* have each two morphologically similar species (*P. caudatus* and *P. tuberculatospinosus*; *P. bicaudatus* and *P. australis*) that are geographically separated and only occur in the Northern (*P. caudatus* and *P. bicaudatus*) or Southern

(*P. tuberculatospinosus* and *P. australis*) Hemisphere (Van der Land 1970; Adrianov and Malakhov 1996a,b). Both remaining macroscopic genera, *Acanthopriapulus* (Southern Hemisphere) and *Halicryptus* (Northern Hemisphere) only occur in their respective Hemisphere (Adrianov and Malakhov 1996a,b**).**

Microscopic species have a more restricted distribution in temperate marine waters (e.g. Caribbean Sea, Red Sea, Adriatic Sea, Andaman Sea, nearshore of Pacific islands etc.; see Fig. 3). *Tubiluchus* species have been mainly found in the intertidal or shallow subtidal (0.5 to 30 m; Van der Land 1968; 1982; 1985; Adrianov et al. 1989; Adrianov and Malakhov 1991; Schmidt-Rhaesa et al. 2017) or in marine underwater caves (Todaro and Shirley 2003; Schmidt-Rhaesa et al. 2013). One *Tubiluchus* species has been reported from the deep sea (*T. soyoae* at 260 m; Schmidt-Rhaesa et al. 2017). *Meiopriapulus fijiensis* has only few reports from the intertidal und shallow subtidal (0.5 to 35 m; Westheide 1990; Sørensen et al. 2012). *Maccabeus* has reports from the subtidal and deep sea (*M. tentaculatus*: 60 to 550 m; *M. cirratus*: 2520 m; Malakhov 1978). *Tubiluchus arcticus* is the only microscopic species from the Arctic Circle (Adrianov et al. 1989; Fig. 3), but an undescribed *Tubiluchus* species is reported from the Swedish coast in the northeastern Skagerrak (Willems et al. 2009).

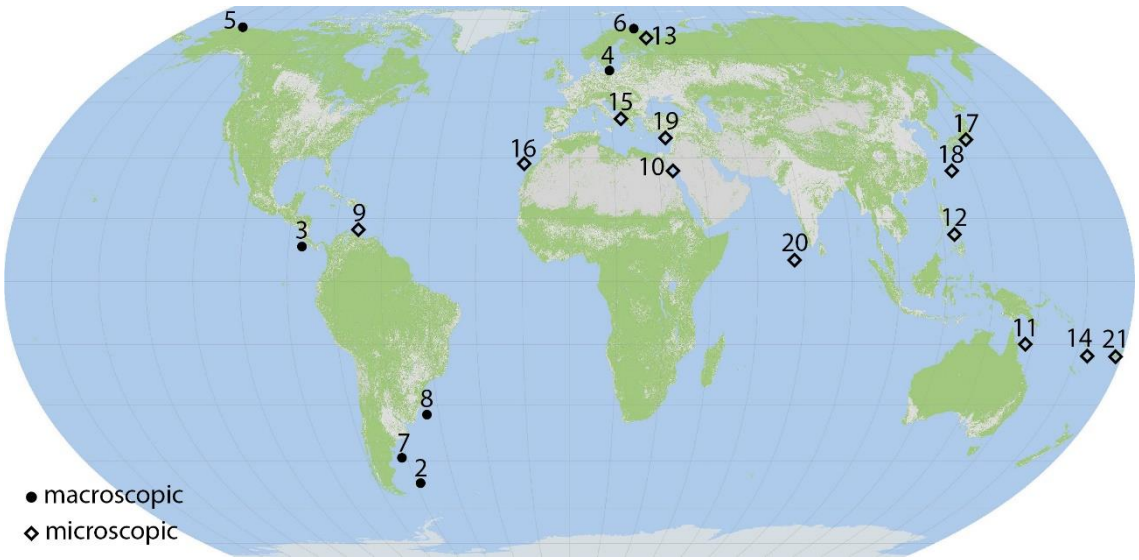

Fig. 3. Type localities of species of Priapulida. Numbers (2-21) correspond to species numbers from Table 1. Note that *P. caudatus* (1) has not been included, as the type locality is unknown. Map source: mapswire.com.

1.2.5. Morphology of adult Priapulida

The general morphology of adult priapulidans is mostly similar across the species. In this section, the morphology is shown using the example of adult *Priapulus caudatus* (see Fig. 4). Noteworthy deviations or characteristics of other species will be touched on as well. However, the microscopic *Meiopriapulus* and *Maccabeus* differ vastly in some aspects. Their major differences to the general morphology of Priapulida will be summed up at the end of this section.

Adult priapulidan bodies are divided into the movable introvert and a cylindrical trunk (Fig. 4A), forming a large body cavity that is filled with a body fluid containing numerous free cells (‘coelomocytes’; e.g., Mattisson and Fänge 1973). Some genera have additionally one (*Acanthopriapulus*, *Priapulus* and *Tubiluchus*) or two (*Priapulopsis*) caudal appendages on the posterior trunk. Terminal on the introvert is the mouth opening and almost terminal on the posterior trunk is the anus (Van der Land 1970; Schmidt-Rhaesa 2013).

The mouth opening connects to the muscular pharynx bulb. The pharynx is internally covered with numerous cuticular pharyngeal teeth (Fig. 4B). The teeth are arranged in several rings, with each of the anterior approximate seven rings composed of five teeth (Fig. 4B). The teeth of all macroscopic species and of the microscopic *Maccabeus* are of a cuspidate type, meaning the teeth have a large median cusp and some small lateral cusps on each side of the median cusp (Van der Land 1970; Fig. 4C). Contrary, the teeth of *Tubiluchus* are of a pectinate type, and they are composed of a stalk (‘manubrium’) with a comb-like structure (‘pecten’) (Van der Land 1970). The type of pharyngeal teeth is likely related to the food source, with predatory priapulidans having cuspidate teeth, and priapulidans that scratch algae from sediment for ingestion having pectinate teeth (Van der Land 1970).

A large muscular structure, the ‘polythyridium’, follows the pharynx exclusively in *Tubiluchus* and *Meiopriapulus* (e.g., Van der Land 1970; Morse 1981). The polythyridium consists of cuticular structures, the ‘valvulae’. The function of this organ remains obscure, but it is presumed to serve as a filter organ, allowing only food particles of a certain size to pass through (Van der Land 1970). Macroscopic priapulidans lack a polythyridium.

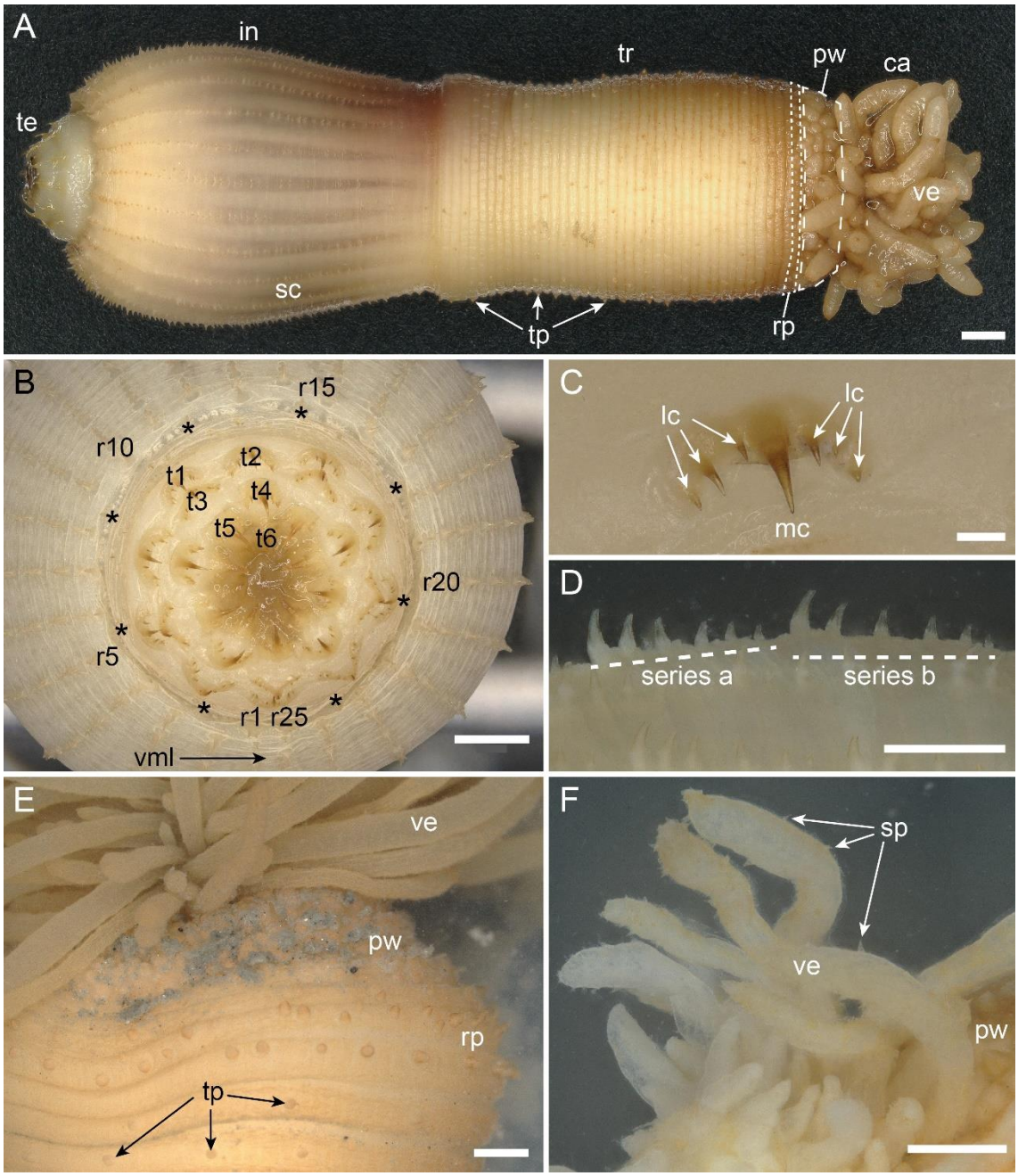

Fig. 4. General shape and morphology of adult *P. caudatus*, light microscopical images. **A**. Habitus with arrangement in introvert (in) with pharyngeal teeth (te) and scalids (sc), trunk (tr) with trunk papillae (tp), ring papillae (rp) and posterior warts (pw) and caudal appendage (ca) with vesicles (ve). **B**. Frontal view of introvert with six pentaradial rings of teeth (t1-t6) and 25 rows of scalids (r1-r25). Asterisks (*) show position of primary scalids. **C**. Higher magnification of cuspidate tooth of the first ring with median cusp (mc) and lateral cusps (lc). **D**. Lateral view of scalid series. **E**. Posterior trunk with three rings of ring papillae and posterior warts on the last annulus. **F**. Higher magnification of vesicles with spinulets (sp). Further abbreviations: vml, ventral midline. Scale bars: A, B, E = 1 mm; C = 100 µm; D, F = 500 µm. Figure modified from **Study II**.

The most distinct structures on the surface of the introvert are the scalids that are arranged in 25 longitudinal rows (Fig. 4A, B). The distance between two scalid rows is constant, except between both scalid rows next to the ventral midline, where the distance is about half of the regular distance (see Adrianov and Malakhov 2001a; Fig. 4B). Scalids typically have a conical shape (*Acanthopriapulus*, *Priapulus*, and *Priapulopsis*; Fig. 4D). In *Halicryptus* and *Tubiluchus*, the basal part of scalids are flattened, giving their scalids a triangular shape with a median cone (e.g., Calloway 1975; Storch et al. 1990). In macroscopic species (except *Halicryptus*), scalid rows consist of several scalid series that consist of up to seven scalids decreasing in size (Van der Land 1970; Fig. 4D). In *Halicryptus* and microscopic species, such scalid series are lacking.

Anterior of the scalid rows (i.e., towards the mouth opening) is a ring of specific scalids that are termed as 'primary scalids'. Sometimes they are also named as 'circumoral scalids' (Adrianov and Malakhov 1996a) or 'sensory spines' (Storch et al. 1994). There are always eight primary scalids in all species that are not aligned with the scalid rows (Schmidt-Rhaesa 2013; Fig. 4B). Primary scalids are arranged in a specific pattern: three scalid rows are between two primary scalids, while four scalid rows separate the two primary scalids adjacent to the ventral midline (Adrianov and Malakhov 2001a; Fig. 4B). Primary scalids have only been shown superficially for some species. In macroscopic species, they are similarly composed as the 'regular' scalids of the respective species (e.g., Storch et al. 1994; Lemburg 1999). In microscopic *Tubiluchus*, primary scalids are more slender than the 'regular' scalids (e.g., Todaro and Shirley 2003; Schmidt-Rhaesa et al. 2017).

All scalids have sensory functions. In macroscopic species, scalids have subapical openings with tubular receptors (Storch et al. 1990; 1994; 1995; Schmidt-Rhaesa et al. 2022). In *Tubiluchus*, tubular receptors occur apically on the scalids (e.g., Calloway 1975; Todaro and Shirley 2003; Schmidt-Rhaesa et al. 2017).

Additional structures on the circumoral field (i.e., the area between pharyngeal teeth and scalids) have been mentioned for some species. These structures are often referred to as 'buccal papillae' by several authors. They have been briefly mentioned (e.g., *T. corallicola* in Calloway 1975; *P. caudatus* and *P. tuberculatospinosus* in Storch et al. 1994; *P. bicaudatus* and *P. australis* in Storch et al. 1995), but detailed descriptions of these structures have yet to be made. Only buccal papillae of *Halicryptus* have been described in more detail (see Storch et al. 1990; Lemburg 1999).

The trunk follows the introvert. It has a circular diameter in all species. In macroscopic species, the trunk is distinctly annulated (Fig. 4A, E) and has a smooth cuticular surface. Only *Priapulopsis* has a dense covering of small, round structures on the trunk surface, the 'tumuli' (Van der Land 1970). Annuli lack in microscopic *Tubiluchus*. Instead, they have quadrangular cuticular elevations organized in rings and rows along the body, which are also called 'tumuli' (Van der Land 1968; 1970). Additionally, *Tubiluchus* has a differentiated anterior neck region on the trunk, which is defined by smaller, more densely set tumuli (Van der Land 1968; Schmidt-Rhaesa et al. 2013; 2017).

The trunk is beset with different types of sensory structures. Some structures are randomly scattered and some occur only in specific regions on the trunk, or they are organized in patterns. In *Acanthopriapulus*, *Priapulopsis* and *Priapulus*, small conical papillae, the 'trunk papillae', are randomly scattered on the trunk annuli (Fig. 4A, E). The ultrastructure of trunk papillae has been shown briefly for *P. caudatus* (Hammond 1970b) and *A. horridus* (Schmidt-Rhaesa et al. 2022), revealing apical tubular structures. *Halicryptus* has numerous spine-like structures on the trunk, giving its spiny appearance (Scharff 1885). In *Tubiluchus*, two types of randomly distributed structures appear on the trunk. The first type are tubuli, which seem to be arranged more densely on the ventral side (Schmidt-Rhaesa et al. 2017). The second type are the flower-shaped flosculi on the anterior trunk and neck (Van der Land 1970).

On the posterior trunk of macroscopic species (excluding *Halicryptus*) occur papillae that are arranged in one to five rings, the 'ring papillae' (Van der Land 1970; 1972; Fig. 4A, E). Although ring papillae are conspicuous structures, they have not yet been described in detail, but a sensory function is assumed (Van der Land 1970). Ring papillae are also described for *Halicryptus* (see Merriman 1981); however, the images of these structures are unconvincing. For *Tubiluchus*, ring papillae are not reported.

Priapulus has on the posterior trunk large, elevated, wart-like structures, known as the 'posterior warts' (Fig. 4A, E). The surface of posterior warts is beset with numerous fine tubular structures (Hammond 1970b). Internally, the warts are filled with large secretory cells (Scharff 1885; Adrianov and Malakhov 1996a), assuming a secretory function. Posterior warts were reported for *A. horridus* (Tommasi 1968), but later investigations do not confirm them (Van der Land 1970; Schmidt-Rhaesa et al. 2022). Merriman (1981) reported posterior warts for *Halicryptus*, but these structures differ from those of *Priapulus*.

Some priapulidans have a caudal appendage (also referred to as ‘tail’) connected to the posterior end of the trunk. The caudal appendage of macroscopic species is composed of a muscular stem, which appears segmented (Van der Land 1970). The stem connects directly with the body cavity and expands its lumen (Ehlers 1862). In adult specimens, the caudal appendage is covered with numerous balloon-like structures, the ‘vesicles’ (Fig. 4A, E, F). On the stem and vesicles are small pointy structures scattered, the ‘spinulets’ (Fig. 4F). In *A. horridus*, only the anterior part (i.e., near the trunk) of the stem is covered in vesicles, whereas the posterior part is densely covered with small spines (Schmidt-Rhaesa et al. 2022). The length of the caudal appendage of macroscopic species varies from small stumps (mostly in postlarval stages) to similar lengths than the remaining body (Van der Land 1970). The slender caudal appendage of *Tubiluchus* differs from those of macroscopic species, as it can reach lengths of up to 4.5 mm (Schmidt-Rhaesa 2013) and it is only covered with tumuli and scattered flosculi (Van der Land 1968; 1970). *Halicryptus* does not have a caudal appendage. Instead, it has two short, spiny structures lateral of the anus, which are referred to as ‘anal setae’ (Shirley and Storch 1999).

Priapulidans have a simple organization of internal structures. The midgut runs straight through the body cavity, connects the pharynx with the anus, and it is encircled by musculature (Storch et al. 1990). Most priapulidan species are dioecious, meaning they have either male or female gonads (Van der Land 1970). Interestingly, the fertilization mode differs between priapulidans, as macroscopic species are external fertilizers and microscopic species are internal fertilizers (Alberti and Storch 1983; Storch and Higgins 1991). The excretory organs are of a solenocytic protonephridial type (e.g., Lüling 1940; Alberti and Storch 1986). The gonads and excretory organs are combined to a paired urogenital system that opens with two urogenital pores lateral of the anus (Van der Land 1970; Schmidt-Rhaesa 2013).

Priapulidans are highly muscular animals. The body wall musculature consists of two continuous layers, the outer circular and inner longitudinal musculature (e.g., Candia Carnevali and Ferraguti 1979; Rothe et al. 2006). In the introvert occur additional 25 longitudinal muscle strands that correlate with the longitudinal scalid rows (Lemburg 1999; Rothe et al. 2006). The pharynx bulb consists of a complex network of longitudinal and circular muscles with additional outer pharynx protractors and circular sphincter muscles (Adrianov and Malakhov 1996a). Two sets of introvert retractor muscles (short and long retractors) encircle the pharynx bulb. The number of both retractors is

ambiguous, as studies report different numbers (8 to 9 long retractors; 8 to 25 short retractors; see Schmidt-Rhaesa 2013). The introvert can be completely retracted into the trunk and can be everted again by pushing body fluid into the introvert by contracting the trunk musculature (Hammond 1970a). These retraction and eversion movements help the priapulidans to burrow through sediment or move on its surface (Hammond 1970a; 1980; Elder and Hunter 1980).

The central nervous system of Priapulida consists of a ring nerve, which surrounds the anterior pharynx, and represents the brain (e.g., Scharff 1885; Rothe et al. 2010). On the ventral side, an unpaired ventral nerve cord connects to the brain, and runs longitudinally in the epidermis from the introvert to the caudal ganglion, which is located in the posterior trunk (Scharff 1885; Rothe et al. 2010). In macroscopic genera, the ventral nerve cord is distinctly visible as a ventral midline on the external trunk. In microscopic genera, a ventral midline is not externally visible on the trunk (Por and Bromley 1974; Morse 1981). The peripheral nervous systems consists of longitudinal and circular bundles of neurites (Rothe et al. 2010).

Morphology of *Maccabeus* and *Meiopriapulus*

As mentioned above, adults of both microscopic genera *Maccabeus* and *Meiopriapulus* differ in certain aspects vastly from the general morphology of priapulidans.

Differing from other priapulidans, *Maccabeus* has a distinct tentacle crown around the mouth opening (Por and Bromley 1974). This tentacle crown is composed of eight ‘trigger spines’ and 25 elongate ‘double tentacles’. Following the tentacle crown occur three types of sensory structures: one ring of 16 ‘sensory spines’, two rings of 25 ‘trifid spines’ and three to four rings of 25 ‘glandular spines’ (Por and Bromley 1974; Malakhov 1978). From these introvert structures, the glandular spines are assumed to be homologous with the scalids of other priapulidans (Por and Bromley 1974). The trunk of *Maccabeus* is composed of circular rows of soft, cuticular ‘tubercles’ (Por and Bromley 1974). On the posterior trunk, one ring of anterior facing ‘anal hooks’ separates the trunk from a rounded anal cone (Por and Bromley 1974; Salvini-Plawen 1974). *Maccabeus* has no caudal appendage, but two terminal structures, similar to *Halicryptus*, occur lateral of the anus (Salvini-Plawen 1974). *Maccabeus* lacks a polythyridium, but ‘gastric spines’ are present in approximately the same position, which are thought to be homologous structures to the polythyridium (Por and Bromley 1974). Differing from other

priapulidans, *Maccabeus* lives in an agglutinated tube made of plant debris (Por and Bromley 1974). As only female specimens of *Maccabeus* are documented, a parthenogenetic reproduction is assumed (Por and Bromley 1974; Salvini-Plawen 1974).

Meiopriapulus fijiensis is reported to have three rings of sensory scalids with (8+9+8) scalids (Sørensen et al. 2012), followed by up to 150 longitudinal rows of 'locomotory scalids' (Morse 1981). The locomotory scalids vary vastly from the appearance of scalids from other priapulidans, as they look more similar to pectinate teeth of *Tubiluchus* (see Morse 1981; Storch et al. 1989; Sørensen et al. 2012). Another type of scalids ('trunk scalids') occurs on the anterior trunk (Morse 1981). Small, spherical structures ('tubercles') cover the cuticle of the trunk, like the trunk structures of *Maccabeus*, but they differ in appearance (Morse 1981). Similar to *Maccabeus*, one ring of recurved 'preanal hooks' is present on the posterior tapering trunk (Morse 1981; Sørensen et al. 2012). The preanal hooks have two apical hooks with a tubular structure between the hooks (Sørensen et al. 2012). *Meiopriapulus* is reported to have pectinate teeth (Morse 1981), but their shape differs from teeth of *Tubiluchus*, as they do not have a manubrium, but rather a triangularly (anterior pharynx) or rectangular (posterior pharynx) shape (Sørensen et al. 2012).

1.2.6. Morphology of larval stages

Characteristic for larval stages of priapulidans is the thick cuticular armature, the 'lorica' (Van der Land 1970; Fig. 5A, B). However, the lorica still lacks in the hatching larva and develops only after the first moult (Wennberg et al. 2009; Janssen et al. 2009). The introvert and neck region of the larvae can be withdrawn into the lorica.

The shape of the lorica differs between larval stages of both body size classes. Macroscopic priapulidans and microscopic *Maccabeus* have dorsoventrally flattened larval stages whose loricae consist of two large dorsoventral cuticular plates and six slender lateral plates (two lateral and four sublateral plates) (Schmidt-Rhaesa 2013; Fig. 5A, C). The lateral plates are connected in a 'zig-zag' pattern, creating three inner foldings and two distinct outer ridges (Higgins et al. 1993; Lemburg 1999; Schmidt-Rhaesa 2013; Fig. 5C). Microscopic *Tubiluchus* on the other hand has roundish shaped larval stages with their lorica consisting of 20 equally sized plates, separated by alternating each ten primary and secondary cuticular ridges (e.g., Kirsteuer 1976; Adrianov and Malakhov 1991; Todaro and Shirley 2003; Fig. 5B).

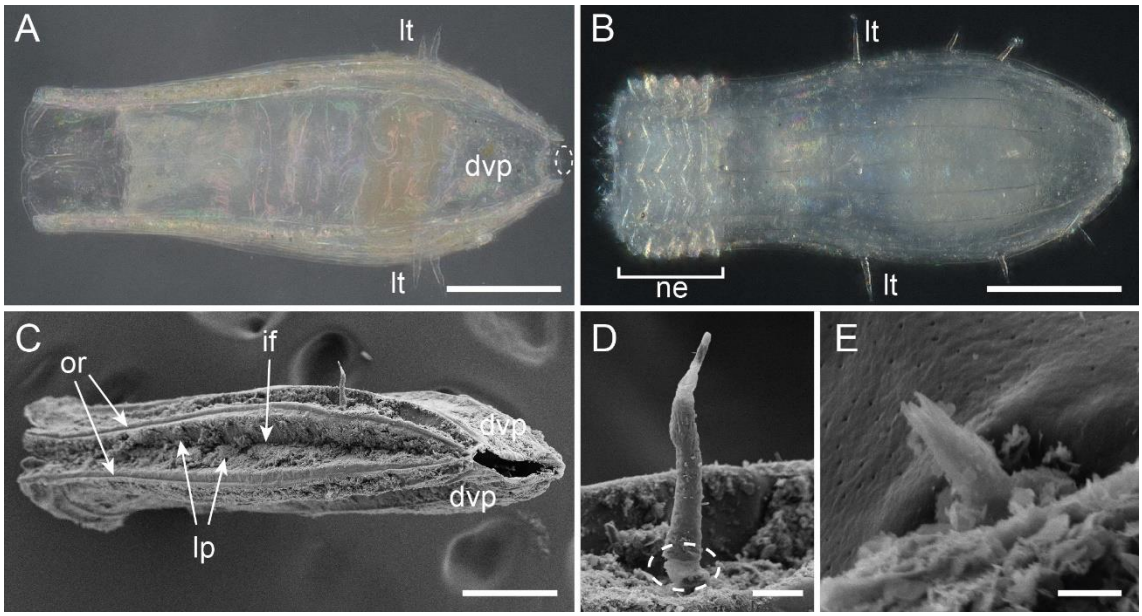

Fig. 5. Lorica larvae of *P. caudatus* (A, C-E) and *T. lemburgi* (B), light microscopical (A, B) and SEM (C-E) images. **A**. View on dorsoventral plate (dvp) from larva of *P. caudatus* with four lorica tubuli (lt). Dotted circle shows caudal gland tubulus. Note the slightly visible sculpturing on the dorso-ventral plate. **B**. Larva of *T. lemburgi* with protruded neck (ne). **C**. Lateral view of larva of *P. caudatus*. Note both outer ridged (or) and the inner fold (if) between two lateral plates (lp). Sublateral plates are not distinctly visible here. **D**. Magnification of lorica tubulus of *P. caudatus*. Dotted circle shows joint-like structure. **E**. Magnification of marginal tubulus of *P. caudatus*. Note the pores on the surface of the lorica. Scale bars: A-C = 100 µm, D = 10 µm, E = 1 µm.

On the anterior part of the lorica are further, smaller cuticular plates located that function as closing apparatus. These have been only reported for dorsoventrally flattened larvae (e.g., Lang 1948; Sanders and Hessler 1962; Lemburg 1999). Such small plates are not present in larval stages of *Tubiluchus*. Instead, the folds of the neck region (see below) function as closing apparatus, when the introvert is withdrawn into the lorica (Van der Land 1968).

The lorica only has few structures on the surface. Most prominent are the ‘lorica tubuli’ (Fig. 5A-D). Dorsoventrally flattened larvae of macroscopic priapulidans have four lorica tubuli, one pair on each lateral side approximately on the posterior third of the lorica length (Van der Land 1970; Fig. 5A, C). Lorica tubuli have a conical shape and near the base is a ball joint-like structure (Lemburg 1999; Fig. 5D). In larval stages of microscopic *M. tentaculatus*, additional four lorica tubuli appear on the anterior third of the lorica (Por and Bromley 1974; Salvini-Plawen 1974). In round-shaped larval stages of *Tubiluchus*, the lorica tubuli are arranged in circlets (Fig. 5B). In addition, the number of circlets (two to five circlets) and the number of lorica tubuli (two to five tubuli) per circlet increases with growth (= moult) of the larva (Kirsteuer 1976). Lorica tubuli of

Tubiluchus are conical shaped, but a ball joint-like structure is absent (e.g., Van der Land 1968; Kirsteuer 1976; Adrianov and Malakhov 1991).

There are few further lorica structures, which have been only shown for few species. One of these are the 'marginal tubuli' (Fig. 5E), which occur on the outer ridges of the dorsal and ventral plate of the lorica of macroscopic species as small (~2 µm) tubular cones (see Adrianov and Malakhov 1996a; Lemburg 1999). Another structure is the 'caudal gland tubulus' (Fig. 5A), which is found on the perianal field, dorsal of the anus in macroscopic species (see Hammarsten 1915; Adrianov and Malakhov 1996a; Lemburg 1999). For *Tubiluchus*, flosculi are reported on the lorica (e.g., Van der Land 1982; Todaro and Shirley 2003).

The surface of the dorsoventral plates of macroscopic species has distinct cuticular folds, which are sometimes termed as 'sculpture'. The sculpturing has been reported scarcely, but it seems to differ between species and the larval stage of a species (Higgins et al. 1993; Schmidt-Rhaesa and Freese 2019). In *H. spinulosus*, the sculpturing seems to consist of regular depressions differentiated by distinct cuticular ridges (e.g., Hammarsten 1915; Fig. 13.4F in Adrianov and Malakhov 1996a). In *P. caudatus* and *P. tuberculatospinosus*, a distinct median ridge on the anterior lorica is visible (Hammond 1970b; Adrianov and Malakhov 1996a; Schmidt-Rhaesa and Freese 2019), but older larval stages can have a median ridge along the whole lorica (Higgins et al. 1993). On the posterior lorica are horizontal ridges, forming rectangular cuticular sculptures (e.g., Hammond 1970b; Adrianov and Malakhov 1996a). In *Priapulopsis australis*, the sculpturing appears to form median 'zig-zag' patterns, created by the cuticular folds (e.g., Fig. 13.14C in Adrianov and Malakhov 1996a; Schmidt-Rhaesa and Freese 2019).

The introvert and neck have been both examined for few macroscopic (see Hammarsten 1915; Lang 1948; Lemburg 1995b; 1999; Adrianov and Malakhov 1996a; 2001b) and microscopic species (see Salvini-Plawen 1973; Kirsteuer 1976; Todaro and Shirley 2003). The most prominent structures on the introvert of larvae are the scalids. Like in adults, the first ring consists of eight slender primary scalids in both size classes (e.g., Adrianov and Malakhov 2001b). There are 25 longitudinal rows of scalids on the introvert, which do not occur in series but rather stand as individual scalids. The scalid rows of young larval stages have less scalids than those of later stages (Adrianov and Malakhov 1996a; 2001b). The scalids of larvae appear long, slender and often with cuticular hairs, similar to those of adult *Tubiluchus* (e.g., Lemburg 1995b; Adrianov and Malakhov 1996a; 2001b). Following the introvert is the distinct neck region. When the

introvert is not fully everted (or withdrawn), the neck is visible due to several distinct folds (Fig. 5B). Flosculi are reported from the neck of larvae (e.g., Adrianov and Malakhov 1996a; Todaro and Shirley 2003).

Larvae have pharyngeal teeth that, similarly to their adults, are organized in pentaradial rings. The type of the teeth (cuspidate or pectinate) is not easy to determine, as reports differ between species, their corresponding larval stage and the number of tooth ring (see Lemburg 1999). Sometimes, larval teeth resemble more cuspidate teeth (e.g., Todaro and Shirley 2003). However, Adrianov and Malakhov (1996a) show for a *P. australis* larva both types and the shape of the teeth changes between each tooth ring.

The larval anatomy has been described for a few species (e.g., Hammarsten 1915; Lang 1948; Van der Land 1968; Adrianov and Malakhov 1996a; Lemburg, 1999). The musculature and nervous system resemble those of adults (e.g., Lang 1948; Van der Land 1968; Adrianov and Malakhov 1996a; Martín-Durán et al. 2016). However, the number of long and short introvert retractors, as well as pharynx retractors and protractors, differs slightly between reports (e.g., Lang 1948; Lemburg 1999). Protonephridia are developed in larvae, while gonads are lacking (Lang 1948).

1.2.7. Diagnostic characters

Genera of the same size class can be clearly distinguished in adult specimens. In macroscopic genera, *Acanthopriapulus* has a unique caudal appendage (Théel 1911; Van der Land 1970), while *Priapulopsis* can be distinguished from *Priapulus* by having a paired caudal appendage and the first ring of teeth consists of five bipartite teeth (i.e., ten tooth structures) (Van der Land 1970). However, postlarval stages of *Priapulus* and *Priapulopsis* are morphologically similar, complicating their correct identification (see Van der Land 1970). *Halicryptus* lacks a caudal appendage and has a spiny appearance (Von Siebold 1849; Shirley and Storch 1999). In microscopic species, *Tubiluchus* has a long tail (e.g., Van der Land 1968), *Maccabeus* has a unique tentacle crown (Por and Bromley 1974; Malakhov 1978), and *Meiopriapulus* has a distinct arrangement of primary scalids and locomotory scalids (Morse 1981).

Within a genus, distinguishing species can be complicated, especially when the sampling locality of specimens is unknown. In *Priapulus* and *Priapulopsis*, the geographically separated species (*P. caudatus* and *P. tuberculatospinosus*; *P. bicaudatus* and *P. australis*) are mainly ‘identified’ by their sampling locality. However, there are few specific diagnostic characters, like smaller or bipartite teeth of the first ring of the

respective species in the Southern Hemisphere (Van der Land 1970; Storch et al. 1994). *Halicryptus spinulosus* differs from *H. higginsi* by having a unique type of scalids ('dentoscalids') in the posterior part of scalid rows and by having a much smaller adult body size (Shirley and Storch 1999). *Tubiluchus* species are all morphologically similar. Particularly, female specimens do not differ between species (Van der Land 1985). Male specimens have a distinct genital area on their posterior trunk, which differs between species (e.g., Schmidt-Rhaesa et al. 2013). Both *Maccabeus* species are reported to differ in their scalid morphology (Malakhov 1978), but as *M. cirratus* was only described on a single specimen, this report seems vague.

Species identification on larval material is difficult, as there are only two types of larval stages and not all larval stages of every species is examined in detail. In dorsoventrally flattened larval stages, the position of the lorica tubuli is potentially a diagnostic character, as it differs between *Priapulus* and *Priapulopsis* species (Lang 1951; Van der Land 1970; Schmidt-Rhaesa and Freese 2019). Larvae of different *Tubiluchus* species are reported to differ in their shape of teeth (e.g., Todaro and Shirley 2003).

1.2.8. Phylogeny and availability of molecular data

Although the phylum Priapulida contains only a few described species, it still lacks phylogenetic analyses based on molecular data. Priapulidans have been included in a few large molecular phylogenetic analyses that did not specifically focus on Priapulida, but they were represented by only a few species (e.g., Giribet et al. 2000; Sørensen et al. 2008; Laumer et al. 2015; 2019). Laakkonen et al. (2019) and Kolbasova et al. (2023) analyzed single genes from *P. caudatus* specimens from different localities across the Arctic Ocean.

Phylogenetic relationships based on morphological data

So far, only attempts based on morphological data have been made to resolve the phylogenetic relationships in Priapulida. The approaches of Salvini-Plawen (1974) and Adrianov and Malakhov (1995) both proposed the microscopic *Maccabeus* as the sister group to the remaining Priapulida. The position of *Tubiluchus* differs between both analyses: it is either the sister group to a clade of all macroscopic priapulidans (Salvini-Plawen 1974; Fig. 6A) or the sister group to Priapulidae (*Acanthopriapulus*, *Priapulus*, *Priapulopsis*) (Adrianov and Malakhov 1995; Fig. 6B). However, Salvini-Plawen's

(1974) approach excludes *Meiopriapulus*, as it had not been described at the time, and includes some obsolete morphological characters. Other studies including fossil species (e.g. Wills 1998; Lemburg 1999; Dong et al. 2004; 2005; 2010; Harvey et al. 2010; Wills et al. 2012) proposed microscopic genera *Tubiluchus* and *Meiopriapulus* as monophyletic group that constitutes the sister group to the remaining priapulidans, from which *Maccabeus* is the sister group to the macroscopic species (Fig. 6C). These inconsistent positions of some groups support the demand of phylogenetic analyses of Priapulida using molecular data.

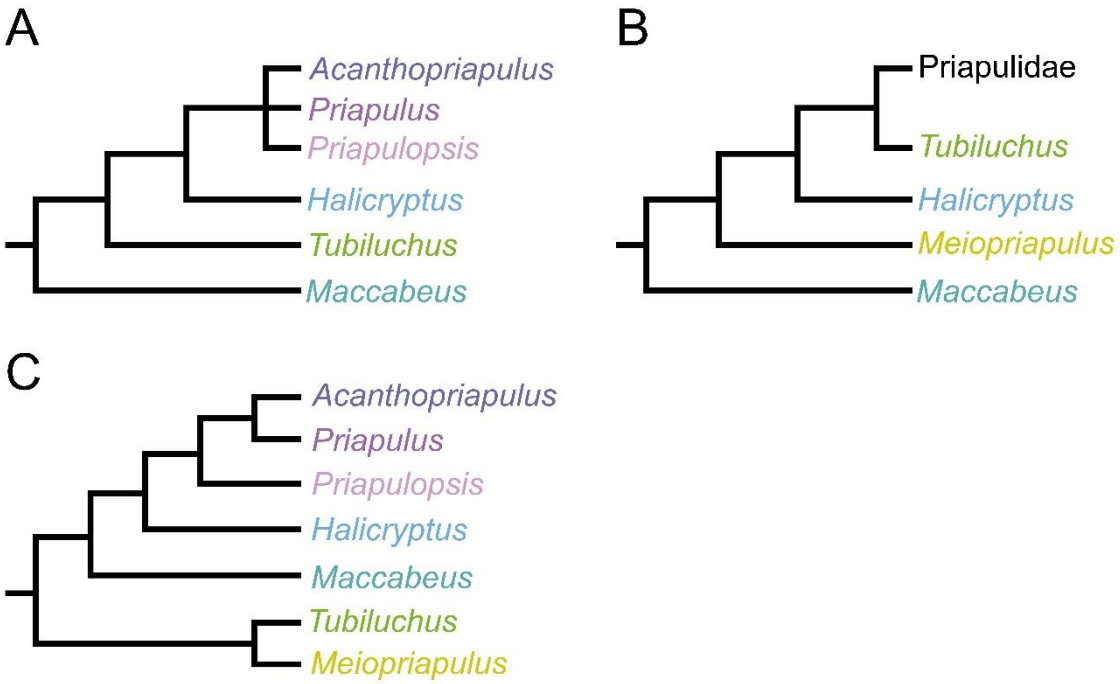

Fig. 6. Proposed phylogenetic relationships of Priapulida based on morphological data. **A**. Relationships after Salvini-Plawen (1974). **B**. Relationships after Adrianov and Malakhov (1995). Note that Priapulidae consists here of *Priapulus* + *Priapulopsis* + *Acanthopriapulus*. **C**. Relationships after Lemburg (1999). This topology corresponds to modified phylogenies (= excluding fossil species) proposed by Wills (1998), Dong et al. (2004), (2005), (2010), Harvey et al., (2010) and Wills et al. (2012).

Availability of molecular data

Publicly available molecular data of priapulidans on NCBI GenBank is present for only seven species from five genera, but they differ in their data type (single genes, transcriptomes, genomes). The majority of available molecular data represents single gene sequences (genes: *CO1*, *18S*, *28S*, *histone H3*; e.g., Giribet 2000; Mallat and Winchell 2002; Sørensen et al. 2008; 2012; Schmidt-Rhaesa et al. 2017; Kolbasova et al.

2023). Additional transcriptomes of *P. caudatus*, *H. spinulosus*, *T. corallicola* and *M. fijiensis* exist (e.g., Martín-Durán et al. 2012; Borner et al. 2014; Cannon et al. 2016), as well as genomes of *P. caudatus* (unpublished) and *T. corallicola* (Lord et al. 2023). Two genera, *Acanthopriapulus* and *Maccabeus*, and 12 species from the remaining genera entirely lack molecular data. Comparable molecular data is needed to achieve a robust phylogeny of Priapulida.

Most of the available molecular data belong to 'easily' accessible or abundant species, like *P. caudatus* or *H. spinulosus*. Other species, like *P. tuberculatospinosus*, *P. australis*, *P. bicaudatus* or *T. corallicola*, originate from more remote places, but have been stored in larger quantities in museum collections (e.g., National Institute of Water and Atmospheric Research [NIWA] Invertebrate Collection [NIC], Zoological Museum Hamburg [ZMH] and Museum of Comparative Zoology Harvard). Many other species were described based on only a few specimens from remote localities (e.g., Van der Land 1970; 1982; 1985; Malakhov 1978; Adrianov et al. 1989; Adrianov and Malakhov 1991; Shirley and Storch 1999; see Fig. 3), making access to these species difficult. In addition to limited accessibility, museum-stored specimens are often old and preserved in formalin, which leads to DNA degradation and cross-linking of DNA with proteins, resulting in short sequence fragments (Campos and Gilbert 2012). Methods to generate genomic data from museum-stored or poorly preserved priapulidan specimens could help expand the availability of molecular data for more species.

In the shallow short-read sequencing method 'genome skimming', fragmented DNA sequences are aligned to a reference genome, allowing the usage for phylogenomic analyses (Straub et al. 2012; Dodsworth 2015). Genome skimming has been successfully used on fresh and museum-stored samples of vertebrates (e.g., Literman et al. 2023), invertebrates (e.g., Taite et al. 2023) and plants (e.g., Fu et al. 2022) to obtain whole mitochondrial genomes or nuclear DNA loci. This method may help to recover usable molecular data from priapulidans of museum collections for reconstructing molecular-based phylogenies.

1.3. Aims of the thesis

Although some priapulidan species have been morphologically investigated quite well (mainly *P. caudatus*, *H. spinulosus*, *T. corallicola*), there is still a demand to investigate the whole development (hatching larva, larval and postlarval stages, young and older adults) of priapulidans. Consequently, this thesis aims to examine morphological structures of a priapulidan species during its development from larval stages, postlarval stages and adult specimens (**Study I**). The examinations have been conducted on the macroscopic *Priapulopsis bicaudatus*.

In addition, this thesis aims to reinvestigate the morphology from adult specimens of macroscopic genera (*Halicryptus*, *Priapulus*, and *Priapulopsis*) in detail by using light microscopy, scanning electron microscopy and histology (**Study I** to **IV**). With a standardized description of similar morphological structures, it will be possible to compare them across macroscopic genera and draw conclusions from potential homologous structures (**Study II**). Furthermore, the terminology of some morphological structures in *Halicryptus* is clarified, as some structures have been referred to by different names in previous studies (**Study III**).

Lastly, this thesis aims to resolve the phylogenetic relationships of extant Priapulida by combining molecular and morphological data (**Study V**). A phylogeny based on molecular data lacks for Priapulida and it is aimed to construct the first molecular phylogenetic tree of this phylum. For this, new transcriptomes are generated and analyzed alongside publicly available transcriptomes to construct a robust phylogenetic framework. This framework is further complemented by conserved genomic loci identified through the genome skimming method to incorporate additional species. Morphological data will be analyzed to infer the positions of the missing taxa that are unavailable for molecular sequencing within the reconstructed molecular phylogenetic tree.

1.4. Origin of examined specimens

The specimens examined in the studies of this thesis were obtained in different ways. While some specimens originated from museum collections, some were collected during organized sampling trips in this thesis, or they were obtained from other researchers. The following briefly outlines how specimens of each examined species were gathered.

Priapulus caudatus

Specimens of *P. caudatus* were collected during three sampling trips and additional live specimens were allocated from another work group.

The first sampling trip to the White Sea Biological Station in Russia took place from 17. to 18. September 2021 and were conducted by Andreas Schmidt-Rhaesa (Leibniz-Institute for the Analysis of Biodiversity Change) and Glafira Kolbasova (White Sea Biological Station, Lomonosov Moscow State University). A total of 44 adult *P. caudatus* specimens were obtained by searching the mud by hand. Specimens were partially used in **Study II** and **V**.

The second and third sampling trip took place to the Kristineberg Center for Marine Research and Innovation at the Gullmarsfjord in Sweden. The first sampling was conducted on 05. April 2022 by Jan Raeker, Katrine Worsaae (Marine Biological Section, University of Copenhagen, Denmark), Mará Herranz (Department of Biology and Geology, Rey Juan Carlos University, Spain) and Ekin Tilic (Senckenberg Natural History Museum Frankfurt, Germany). A total of 88 *P. caudatus* specimens (1 small postlarva, 87 larvae) were collected. The second sampling trip was conducted on 19. May 2023 by Jan Raeker and Andreas Schmidt-Rhaesa, and yielded 3 adult specimens and 11 larval stages of *P. caudatus*. On both trips, the specimens were obtained by Agassiz trawl and an Ockelmann sledge (Ockelmann 1964). Adult specimens were examined in **Study II**. The larval *P. caudatus* were not studied in detail in this thesis and are stored in the Schmidt-Rhaesa collection.

Additional ten adult live specimens were obtained on 25. August 2022 from Katherine A. Turk (Smithsonian National Museum of Natural History, USA). These specimens were originally sampled on 22. June 2022 by Van Veen grab in the North Sea and were part of the study in Turk et al. (2024). These specimens were examined in **Study II**.

Priapulus tuberculatospinosus

Five adult *P. tuberculatospinosus* specimens originated from the NIWA collection (Auckland, New Zealand) which was made available from Michelle Kelly and Sadie Mills (National Institute of Water and Atmospheric Research, New Zealand). These specimens were investigated in **Study IV**.

One additional adult specimen from New Zealand (Zoological Museum Hamburg) was morphologically investigated (**Study IV**), and three adult specimens from Chile of the Schmidt-Rhaesa collection were used for DNA extraction (**Study V**), however, without success.

Priapulopsis bicaudatus

A total of 163 *P. bicaudatus* specimens (99 larvae; 63 postlarvae; 1 adult) were made available by Saskia Brix (German Centre for Marine Biodiversity Research [DZMB], Germany) investigated in **Study I**. The specimens were collected during the IceAGE (27. August to 28. September 2011; Brix et al. 2012) and IceAGE2 (20. July to 04. August 2013; Brix 2013) expeditions in the North Atlantic by using different methods (Agassiz trawl, box corer, epibenthic sledge, Shipek grab and Van Veen grab).

Priapulopsis australis

A total of 20 *P. australis* specimens were made available for **Study IV**, from which 18 specimens originated from the NIWA collection (Auckland, New Zealand) and two specimens from the Zoological Museum Hamburg. Specimens from the NIWA collection were collected with different methods between 1982 and 2020, while both specimens from the Zoological Museum Hamburg were collected on 24. November 2020 near Cape Rodney, New Zealand. Body parts from the latter two specimens were used for DNA extraction in **Study V**.

Priapulopsis papillatus **nov. spec.**

Two *Priapulopsis* specimens of the NIWA collection distinctly differed from those of *P. australis*. Upon further examination, these specimens were described as a new species, *Priapulopsis papillatus* nov. spec. (**Study IV**). For more details and diagnosis characters see Chapter 2.2.9. and **Study IV**. Both specimens were obtained in the Hikurangi Margin by beam trawl at about 750 m (March 2004) and 950 m (April 2010) depth.

Halicryptus spinulosus

Specimens of *H. spinulosus* were obtained from two sources. Eight adult specimens originated from the White Sea, Russia (see above) and were collected in the mud by hand. Another five small adult specimens from the Beaufort Sea, Alaska were collected on 01. August 2021 and were made available by Katrin Iken (College of Fisheries and Ocean Sciences, University of Alaska Fairbanks, USA). Specimens from both localities were examined in **Study III**, whereas specimens from the White Sea were additionally used in **Study V**.

Further sampling trips to the Bay of Kiel, Baltic Sea, were conducted with the assistance of Frank Melzner (GEOMAR Helmholtz Centre for Ocean Research Kiel, Germany), but yielded no specimens.

Halicryptus higginsi

Originally, a sampling trip to Utqiagvik (former Barrow) on the north coast of Alaska, USA for obtaining *H. higginsi* specimens was planned in this thesis. However, due to the travel restrictions during the Covid-19 pandemic, this trip had to be cancelled. As alternative, one paratype specimen of *H. higginsi* (USNM No. 186062; Shirley and Storch 1999) was loaned from the Smithsonian Institution, National Museum of Natural History, USA. This specimen was examined in **Study III**, and DNA extractions were conducted for **Study III** and **V**.

Tubiluchus specimens

Specimens of two described (*T. lemburgi* and *T. corallicola*) and two undescribed *Tubiluchus* species were used in molecular analyses of **Study V**.

Tubiluchus lemburgi was obtained during a sampling trip to Tenerife, Spain on 02. September 2021. Sediment samples were received by scuba diving with the help of Alejandro Martínez García (Water Research Institute, National Research Council, Verbania, Italy). A total of seven *T. lemburgi* specimens (one adult, six larvae) were sampled.

One *Tubiluchus corallicola* specimen from Curaçao was made available by María Herranz, while the two undescribed *Tubiluchus* specimens originated from Cuba (collected by Katrine Woraaae) and Kas, Turkey (collected by Ekin Tilic).

2. Discussion

The contributions of this thesis to the research of Priapulida are divided into two parts: morphological and phylogenetic contributions. The morphological contributions (Chapter 2.2.) recaps the results of **Study I** to **IV**, in which species of macroscopic genera were reinvestigated in detail. The phylogenetic contributions (Chapter 2.3.) present the first phylogenetic analysis of extant Priapulida that combines molecular and morphological data (**Study V**), along with an additional analysis of the *CO1* gene of *H. spinulosus* specimens from various localities in the Northern Hemisphere and from the largest known priapulidan, *H. higginsi* (**Study III**).

2.1. Availability of specimens

The majority of sampling trips during this thesis did not yield a high number of specimens of the respective targeted species. For example, two sampling trips to the Gullmarsfjord, Sweden, yielded combined only three adult specimens of *P. caudatus*, although this locality had been a reliable source for this species for a long time (e.g., Hammond 1970a; Huang et al. 2004; Wennberg et al. 2009).

Another example is *H. spinulosus*, which had always been abundant in the Bay of Kiel in the Baltic Sea, presumably due to its high tolerance to low oxygen concentration and high hydrogen sulfide content present in this area of the Baltic Sea (e.g., Oeschger 1990; Oeschger and Janssen 1991). Attempts during this thesis to sample *H. spinulosus* in localities of the Bay of Kiel, where it had been regularly sampled before (Frank Melzner [GEOMAR, Kiel], pers. communication) resulted in no specimens.

Originally, it was also planned to reinvestigate the morphology of the microscopic *Tubiluchus lemburgi* within this thesis. The type locality and other cave systems on the coast of Tenerife, where specimens have previously been found, were sampled (see Schmidt-Rhaesa et al. 2013), but only a total of seven specimens (one adult and six larvae) were found.

Explanations for the small amount of newly sampled specimens are ambiguous. Usually, priapulidans are collected by searching mud or coarse sand samples. Sediment samples are mainly collected by using various tools, like Agassiz trawl, epibenthos sledges or box corer from a research vessel. While adult macroscopic specimens can be collected by hand from the mud, smaller (post-)larval stages have to be extracted from the sediment. For this, the sediment samples are often kept with some sea water over night to let the meiofauna reach the upper sediment layers, which are then carefully sieved with

a 100 or 63 µm mesh. Finally, these extracted samples are searched under a stereomicroscope. These methods have been used during this project, but they did not yield a high number of specimens.

Studies with remarks on the distribution and density of priapulidans in the sediment are scarce. For *P. caudatus*, about 58,000 larvae and 85 adults per m² were reported (Shirley 1990). For the microscopic *T. troglodytes*, between 37,000 (June) and 84,000 (November) specimens per m² were reported (Todaro and Shirley 2003). For *M. fijiensis*, however, a patchy distribution was reported, with densities between 0 and 150 specimens per liter of sand collected from a 1 m² area, and that they may live gregariously (Paulay and Holthius 1994). Assuming all priapulidans have a patchy distribution, there may be the possibility that the sampling methods used during the conducted sampling trips by mischance missed the inhabited patches. Further ecological studies on the distribution of priapulidans may help to facilitate the collection of specimens.

2.2. Morphological contributions

The morphology of Priapulida has been studied thoroughly in the past. First detailed morphological investigations (light microscopy and histology) have been done on adult *P. caudatus* and *H. spinulosus* by Ehlers (1862), Scharff (1885) and Apel (1885). Detailed SEM studies contributed new information on macroscopic species of *Halicryptus* (Merriman 1981; Storch et al 1990; Shirley and Storch 1999), *Priapulus* (Storch et al. 1994; Adrianov and Malakhov, 1996a) and *Priapulopsis* (Storch et al 1995; Adrianov and Malakhov, 1996a). From the microscopic priapulidans, *T. corallicola* (Kirsteuer and Van der Land 1970; 1976; Kirsteuer and Rützler 1973; Calloway 1975; Adrianov and Malakhov 1996a) and *M. tentaculatus* (Por and Bromley 1974; Salvini-Plawen 1974) represent the most detailed examined ones. Therefore, for some species (e.g., *P. caudatus*, *H. spinulosus*, *T. corallicola*), more information exists than for other, more uncommon and rare species or genera (e.g., *A. horridus*, *H. higginsi*, *Priapulopsis*, *Maccabeus*). Recent reinvestigations of species (*M. fijiensis* by Sørensen et al. 2012; *A. horridus* by Schmidt-Rhaesa et al. 2022) contributed new morphological insights of these long-known species.

Within this thesis, morphological reinvestigations have yielded new data on the following macroscopic species: *Priapulopsis bicaudatus* (**Study I**), *Priapulopsis australis* (**Study IV**), *Priapulus caudatus* (**Study II**), *Priapulus tuberculatospinosus*

(**Study IV**), *Halicryptus spinulosus* and *Halicryptus higginsi* (both **Study III**). Additionally, a new macroscopic species, *Priapulopsis papillatus*, has been described in **Study IV** (see Chapter 2.2.9.).

In the following paragraphs, the newly gathered morphological information of postlarval and adult specimens will be presented and discussed within the respective structure, and compared across mainly the macroscopic priapulidan species. As larval stages have only been examined in detail in **Study I**, new findings will be presented in Chapter 2.2.7.

2.2.1. Pharyngeal teeth

Pharyngeal teeth of all macroscopic priapulidan species are of the cuspidate type (Van der Land 1970; Schmidt-Rhaesa 2013; Fig. 4C). They consist of a large median cusp and a variable number of small lateral cusps on each side of the median cusp (see below). The teeth are arranged in pentagons (e.g., five teeth per ring) in the first approximately seven anterior rings of the pharynx (Van der Land 1970; **Study I-IV**). The following teeth in the middle part of the pharynx are smaller and they are not distinctly arranged in pentagons (Van der Land 1970; **Study II-IV**). Their appearance differs slightly from the anterior teeth, as they appear narrower and the median cusp decreases in size (Storch et al. 1995; **Study II-IV**). Van der Land (1970) stated in *Priapulopsis* a toothless gap between the anterior pentagons and teeth of the middle pharynx, which was not observed in **Study I** and **IV**. In the far posterior pharynx, the teeth have a papilliform shape with minute small cusps (**Study II** and **IV**).

The most prominent structure of the anterior teeth is the large median cusp. The median cusp grows from a small size in young postlarval stages to its distinct size in late postlarval stages and adults (**Study I**). Lateral on the tooth on each side of the median cusp is a variable number of small cusps. Usually, the number of lateral cusps on each side ranges between 3 and 10 cusps throughout the species (e.g., Van der Land 1970; **Study I-IV**). Specimens of the genus *Halicryptus* seem to have fewer lateral cusps than other macroscopic species. Especially large *H. spinulosus* specimens and *H. higginsi* often show only one lateral cusp starting from the second ring of teeth, or they are completely absent, leaving only the large median cusp (Van der Land 1970; Shirley and Storch 1999; **Study III**). Van der Land (1970) already reported a higher number of lateral cusps in young specimens and also assumed a geographical variation, which has not yet

been proven. **Studies I** to **IV** could not further investigate the number of lateral cusps as potential age indicator for macroscopic priapulidans due to limited specimen availability.

Teeth of the first pentagon

Teeth of the first pentagon are often used as diagnostic character to distinguish similar looking genera or species. In *Priapulus*, the morphologically similar species can be distinguished by comparing the size of the teeth of the first pentagon. They are of similar size or slightly smaller than the second pentagon teeth in *P. caudatus* (**Study II**), while in *P. tuberculatospinosus* the first ring teeth are distinctly smaller (Van der Land 1970; **Study IV**). In adult *Priapulopsis* specimens, the teeth of the first ring are bipartite. **Study I** shows for *Priapulopsis bicaudatus* that the bipartition is a process during postlarval development. In loricate larval stages and young postlarval stages, the bipartition has not yet taken place. The bipartition starts with a small furrow on the 'internal' side of the first ring teeth, which becomes larger during later postlarval stages until both parts are fully separated (**Study I**). In *Priapulopsis australis*, the bipartite tooth parts are distinctly smaller than in its congener (**Study IV**). *Halicryptus spinulosus* and *H. higginsi* are not reported to be distinguishable by the first tooth pentagon (Shirley and Storch 1999; **Study III**).

Tooth receptors

In some species, pharyngeal teeth hold tooth receptors on the surface. The tooth receptors consist of a short apical tube (~1 µm) and a round base, and they are set into small grooves in the cuticle of teeth (**Study I** and **IV**). These structures were first reported by Storch et al. (1994) on the first ring teeth of *P. tuberculatospinosus* (as 'cuticular tubules') and shortly after by Storch et al. (1995) for *P. australis*. **Study IV** shows for both species additional tooth receptors on teeth of subsequent pentagons for the first time. Tooth receptors have not been found on teeth of adult *P. caudatus* (**Study II**), although they seem to be present in loricate larval stages (see Lemburg 1999). Similarly, *Halicryptus spinulosus* lacks tooth receptors (**Study III**), and no evidence for the presence of tooth receptors is found in *H. higginsi* (Shirley and Storch 1999; **Study III**). For *P. bicaudatus*, tooth receptors have been shown for postlarval stages and adults on all examined teeth (**Study IV**). The function of tooth receptors remains obscure.

2.2.2. Cuticular structures on the circumoral field

The circumoral field describes the area between the first tooth pentagon and the primary scalids (Adrianov and Malakhov 2001a; **Study II** and **III**). On the circumoral field occur cuticular structures, which have been either overlooked or summarized as 'buccal papillae' in previous studies (e.g., Van der Land 1970; Merriman 1981; Storch et al. 1990; 1994; 1995). However, the types of the cuticular structures on the circumoral field differ between genera. **Studies I** to **IV** were able to examine the structures on the circumoral field in detail for species of *Priapulus*, *Priapulopsis* and *Halicryptus* for the first time.

Circumoral field of *Priapulus*

For *Priapulus*, three types of cuticular structures are reported: 'ring 0 scalids', 'hemispherical papillae' and 'circular folds' (**Study II** and **IV**). Ring 0 scalids look identical to scalids in scalid rows (i.e., conical shape with subapical openings and receptor tubuli). They are organized in a ring approximately in the middle of the circumoral field and occur either as individual structure or as pairs. Hemispherical papillae are laterally flattened with a distinct ridge on which receptor tubuli are located. The hemispherical papillae may have been shown before, as Hammond (1970b) described 'disc-like flattened papillae' in the same area for *P. caudatus*, but showed no images. Circular folds appear as flat, receptor-less foldings on the cuticle and are located approximately on the same level as primary scalids. These folds have been visible in images of previous studies (e.g., Fig. 2C in Hammond 1970b; Fig. 16 in Storch et al. 1994), but they were not described. While all three types are reported for *P. caudatus* (**Study II**), only hemispherical papillae have been found in *P. tuberculatospinosus* (**Study IV**).

Circumoral field of *Priapulopsis*

In *Priapulopsis*, only one structure type, the ring 0 scalids (**Study I**), has been described on the circumoral field of *P. bicaudatus*. Similar to the ones of *P. caudatus*, they have the same appearance as scalids and are organized in a ring, but in *P. bicaudatus* ring 0 scalids stand more closely together. Sometimes, there are individual scalid-like structures anterior of the ring of ring 0 scalids, which may represent the pairs that have been reported for *P. caudatus*. Storch et al. (1995) reported 'peribuccal papillae' for *P. bicaudatus* (cf. their Fig. 11), which may be these individual scalids, but they are not shown in detail. Similar papillae are reported for *P. australis* without showing images

(Storch et al. 1995), but they have not been confirmed in **Study IV**. *Priapulopsis papillatus* is also lacking structures on the circumoral field (**Study IV**).

Circumoral field of *Halicryptus*

Halicryptus differs from both previous genera, as their circumoral field has a high number of buccal papillae (e.g., Merriman 1981; Storch et al. 1990; Shirley and Storch 1999; **Study III**). The buccal papillae appear also similar to the scalids in scalid rows, but they have numerous tiny cuticular protrusions on the surface, giving them a spiny appearance (Storch et al. 1990; **Study III**). Shirley and Storch (1999) and Lemburg (1999) implied different sizes for buccal papillae of *Halicryptus*, which have been shown in detail in **Study III**. All three sizes have the same composition with a broad, triangularly flattened base and an apical cone with small tubular structures on its tip. There are eight large buccal papillae located directly anterior of each primary scalid (Lemburg 1999; **Study III**). Approximately 16 medium-sized buccal papillae occur in a loose ring slightly anterior of the large buccal papillae. The small buccal papillae are randomly scattered between the medium-sized papillae. Another structure type on the circumoral field is represented by the 'mouth papillae', which occur directly posterior of the second pentagon of teeth, approximately on the same level as the first pentagon of teeth (**Study III**). Mouth papillae appear as small conical structures with few apical tubular receptors (**Study III**). These structures have been briefly reported before as rudimentary structures by Adrianov and Malakhov (1996a) and Lemburg (1999). As there is no indication that these are rudimentary structures, **Study III** suggested to change their terminology to 'mouth papillae'.

2.2.3. Scalids

Further posterior of the structures of the circumoral field on the introvert are the scalids. In most species there are two types of scalids: eight primary scalids and the 'regular' scalids that form the conspicuous 25 scalid rows (Van der Land 1970; Adrianov and Malakhov 1996a; Schmidt-Rhaesa 2013). *Halicryptus spinulosus* has a third scalid type reported, the dentoscalids (see below) (Van der Land 1970; Storch et al. 1990). The scalids are one of the most distinct structures of Priapulida and are well-described for most species.

Primary scalids

The eight primary scalids have been shown before for adult specimens of *P. tuberculatospinosus* (Storch et al. 1994), *P. caudatus*, *P. australis* (both in Adrianov and Malakhov 1996a) and *H. spinulosus* (Lemburg 1999). All studies showed that primary scalids resemble the scalids in scalid rows of the respective species, which was confirmed here for *P. caudatus* (**Study II**) and *H. spinulosus* (**Study III**). The tip of primary scalids is either similar to those of 'regular' scalids by having a subapical depression (**Study II**), or the depression is extruded (Adrianov and Malakhov 1996a; Lemburg 1999; **Study II** and **III**). When the subapical depression is present, it is directed towards the posterior part of the priapulidan, contrary to the ones of 'regular' scalids, which are directed towards the anterior part (cf. Fig. 5D in **Study II**). Whether the orientation of the subapical depression is related to the function of scalids is unknown. On the tip of primary scalids are numerous tubular receptors, which occur in two different types (smooth or dented margin), similar to those of the scalids in scalid rows (see below) (Adrianov and Malakhov 1996a; Lemburg 1999; **Study II** and **III**). In this thesis the primary scalids of *Priapulopsis* species could not be further investigated in detail because of dirt coverings or not fully everted introverts of specimens.

Scalids composing the scalid rows

The 'regular' scalids composing the 25 scalid rows are well-investigated throughout the macroscopic priapulidans (e.g., Hammond 1970b; Storch et al. 1990; Storch et al. 1994; 1995; Schmidt-Rhaesa et al. 2022). **Studies I** to **IV** mainly confirmed previous reports and showed them in more detail. Nevertheless, reinvestigations of scalids recovered a few new findings, as follows.

Scalids of *Priapulopsis*

For *Priapulopsis* it is reported that some scalids of a series are basally fused together (e.g., Van der Land 1970; Storch et al. 1995), which could not be confirmed in **Study I** and **IV**. Interestingly though, in light micrographs of *P. australis* specimens it appears that scalids of a series are basally fused (cf. Fig. 4A in **Study IV**), but this was not visible in SEM images (cf. Fig. 4B-D in **Study IV**). Additionally, the scalids of *Priapulopsis* are assumed to have a telescopic function, meaning the apical cone can be withdrawn into the basal part (Van der Land 1970). This assumption may be due to a differentiation of the apical smooth-surfaced cone and the wrinkled base by a distinct

cuticular fold (**Study I and IV**). Such distinct cuticular fold is also present in *A. horridus* (Schmidt-Rhaesa et al. 2022), but not in *Priapulus* species (**Study II** and **IV**). However, a telescopic function was not examined.

Scalids of *Priapulus*

New observations in *Priapulus* were only made for the scalids of *P. caudatus* (**Study II**). As mentioned above, the subapical depressions of scalids are oriented towards the anterior part (e.g., towards the mouth opening) of the specimen, contrary to the ones of primary scalids (**Study II**). Whether the orientation of subapical depressions of different types of scalids has a functional reason remains open. It is assumed, that primary scalids and 'regular' scalids have the same sensory function due to the same two types of tubular receptors (**Study II**). The second new observation lays within the distribution of the tubular receptors on the scalids. Previous studies examining scalids of *P. caudatus* reported the tubular receptors to be only in the subapical depressions (e.g., Storch et al. 1994; Lemburg 1999). **Study II** shows the irregular occurrence of individual tubular receptors outside the subapical depression on the surface of the scalids for the first time. This examination was only made on specimens from the White Sea, which may represent a specific character for specimens from this location, but more material is needed for verify this assumption.

Scalids of *Halicryptus*

In *Halicryptus*, both described species hold different kinds of scalids or structures in a scalid row. *Halicryptus spinulosus* has the 'regular' scalids, dentoscalids and a small structure at the end of a row called 'flosculus-tubulus-complex' (Lemburg 1999; **Study III**). *Halicryptus higginsi* lacks the dentoscalids and no flosculus-tubulus-complex at the end of a scalid row has been reported (Merriman 1981; Shirley and Storch 1999; **Study III**). There are additional circular structures reported directly posterior of a scalid row on the border between introvert and trunk for *H. higginsi*, which are assumed to be rudimentary scalids (see Fig. 3 in Shirley and Storch 1999). **Study III** did not confirm this circular structure due to a slightly inverted introvert of the examined specimen. However, this structure may represent neither rudimentary structures nor scalids, as there is no indication of being rudimentary, and scalid rows may not extend this far (**Study III**). Detailed investigations of these structures are needed for clarification. Additionally,

Study III was able to increase the maximum number of scalids in a row of *H. spinulosus* to 13 scalids from previous ten (Van der Land 1970).

2.2.4. Trunk and trunk structures

The trunk follows directly posterior of the introvert. It is distinctly annulated in postlarval stages and adults, and it holds several types of sensory structures on the surface, from which some are specific to certain genera. However, the surface above the ventral midline remains free of sensory structures. Some sensory structures are randomly distributed across the whole trunk, whereas others are distinctly organized on the posterior trunk. Many of these structures were previously not described in detail, if at all. **Studies I** to **IV** show all cuticular structures on the trunk of the respective examined species in detail (see below). Only for *H. higginsi*, the structures on the posterior trunk could not be examined in detail.

While the cuticle of *Acanthopriapulus*, *Priapulus* and *Halicryptus* is smooth (besides the presence of sensory structures), small roundish protrusions of the cuticle, the 'tumuli', occur in *Priapulopsis*, serving as diagnostic character of this genus (Van der Land 1970; **Study I** and **IV**).

Annuli

The annuli correspond with the circular musculature of the body wall (Van der Land 1970; **own observations**). The number of annuli differs between genera and sometimes between species within a genus (**Study I-IV**). Interestingly, *P. caudatus* specimens of different sizes had between 38 and 42 annuli, suggesting a fixed number of annuli within this range for this species (**Study II**). For *Halicryptus spinulosus*, a maximum of 100 annuli was reported by Van der Land (1970), which was confirmed in **Study III**, where small (~5 mm) and medium-sized (~10 mm) specimens had between 77 and 84 annuli. In contrast, a 20 cm long *H. higginsi* specimen had 145 annuli (**Study III**) and the largest known specimen (38.5 cm) had about 180 annuli (Shirley and Storch 1999). This observation is interesting, as the number of annuli is roughly the double amount, while the body length increases drastically. Whether and how the number of annuli correlates with body size remains unclear.

Trunk papillae

Trunk papillae are randomly distributed cuticular structures on the trunk surface of *Priapulopsis* (Storch et al. 1995; **Study I** and **IV**), *Priapulus* (Adrianov and Malakhov 1996a; Lemburg 1999; **Study II** and **IV**) and *Acanthopriapulus* (Schmidt-Rhaesa et al. 2022). They are hemispherical to slightly conical structures with apical numerous tubular receptors, indicating a sensory function. The tubular receptors differ slightly from those on other morphological structures (i.e., scalids), as the apical tubulus is connected to a prolonged basal part, which again compose 'receptor units' consisting of a small number of tubular receptors (**Study II**). **Study I** and **IV** show the trunk papillae of *Priapulopsis bicaudatus, P. australis* and *Priapulus tuberculatospinosus* for the first time in detail. Trunk papillae of the newly described *Priapulopsis papillatus* differ from those of other species by composing distinct ring patterns on each annulus, and by having flosculi as additional sensory structures on their tip (**Study IV**).

Halicryptus also has small trunk papillae, but they differ in shape and composition from those of the other macroscopic genera (**Study III**). They are more conically shaped and have numerous small cuticular protrusions on the tip of the cone. A variable number of flosculi and sometimes additional small papillae encircle the cone. The small trunk papillae occur on the whole trunk, but are more accumulated on the posterior trunk.

Trunk tubuli

Trunk tubuli are unique morphological structures of *Halicryptus* that are randomly distributed in a high number on the trunk. In previous studies, trunk tubuli were assumed to be setae or spines, due to their distinct shape with a broad basal part and a tapering tip (e.g., Ehlers 1862; Van der Land 1970). Later, these structures were proposed to represent tubuli, due to a reported apical opening (Storch et al. 1999), which was shown for the first time in **Study III**. Trunk tubuli may be secretory organs, as large glandular cells are connected to the tubuli (Scharff 1885; Moritz 1972; **own unpublished histological examinations**). However, the function of the secretion is unknown.

Ring papillae

Ring papillae are organized in distinct rings on the posterior trunk of Priapulinae. The number of rings differs between one and five (Van der Land 1970; **Study I**, **II** and **IV**), but up to seven rings of ring papillae have been reported (Van der Land 1972). Although they are conspicuous structures, only Adrianov and Malakhov (1996a) showed

images of ring papillae of *P. australis*, but not in great detail. **Study I**, **II** and **IV** showed ring papillae for *P. bicaudatus*, *P. australis*, *P. papillatus* and *P. caudatus* for the first time in detail. Only for *P. tuberculatospinosus*, they could not be examined in SEM, due to dirt coverings. However, they are assumed to appear similar to those of its congener, as ring papillae are almost identical between *Priapulopsis* species.

Ring papillae differ slightly between *P. caudatus* and *Priapulopsis* species in shape. While *P. caudatus* has more hemispherical ring papillae (sometimes slightly elongated in large specimens) (**Study II**), they are elongated cones in *Priapulopsis* (**Study I** and **IV**). *Priapulopsis bicaudatus* and *P. papillatus* have an additional flat extension of the cuticle of the cone, which is directed towards the anterior of the specimen (**Study I** and **IV**).

Ring papillae are sensory structures, as they hold apically some tubular receptors (**Study I**, **II** and **IV**), confirming Van der Land's (1970) assumption that ring papillae have a sensory function. The receptors are located in an area, which is directed towards the anterior of the specimen (**Study I** and **II**). The function of ring papillae remains obscure.

Halicryptus spinulosus lacks ring papillae (**Study III**), whereas *H. higginsi* seems to have conical structures organized in a ring-like formation on the posterior trunk (Merriman 1981; **Study III**). However, images are unclear and need more material for validation.

Flosculus-tubulus-complexes

Unique to *Halicryptus spinulosus* is the presence of a loosely organized ring of flosculus-tubulus-complexes on the last annulus of the posterior trunk. These structures are, as their name suggests, composed of a conical tubulus with apical finger-like protrusions, which holds one or two accessory flosculi at the approximately half of the tubulus (**Study III**). Similarly shaped structures are present on the last annulus of *H. higginsi*, slightly posterior of the conical structures assumed to be ring papillae (see above), but these could not be examined in detail (**Study III**). Whether flosculus-tubulus-complexes of *Halicryptus* are homologous to ring papillae of other macroscopic species is uncertain, as their position on the trunk matches, but different types of sensory structures occur (**Study II**).

Posterior warts

Posterior warts are conspicuous structures on the posterior trunk of *P. caudatus* and *P. tuberculatospinosus*, following directly after the ring papillae (Van der Land 1970). In *Priapulopsis*, posterior warts are absent (Wesenberg-Lund 1930; **Study I** and **IV**). While in older specimens, the posterior warts are distinctly visible, young *P. caudatus* specimens only show small warts (Adrianov and Malakhov 1996a). Posterior warts are large cushion-like structures that encircle the stem of the caudal appendage almost completely, omitting the trunk surface near the ventral midline (cf. Figs. 4 to 6 in Théel 1911; Hammond 1970b; **own observations**). The posterior warts have been shown before briefly by Hammond (1970b), Adrianov and Malakhov (1996a) and Lemburg (1999). Each wart is distinctly elevated from the trunk surface and holds numerous tubes with apical openings. **Study II** was able to give new insights into the composition of posterior warts. Each wart consists of several wart units, which again consist of approximately three to seven wart subunits. Each subunit holds apically about one to five tubes. The tubes seem to be fragile, as they either have a distinct opening, or the tube is collapsed (as seen in Fig. 3.35D in Adrianov and Malakhov 1996a and Fig. 3C in Lemburg 1999; **Study II**).

Scharff (1885) reported large secretory cells beneath the warts and a covering of the warts with mucous material, assuming a secretory function. **Study II** confirms both observations. However, the function and composition of the secretory remains obscure. As the warts are close to the caudal appendage, the mucous excretion could function as protective or lubricate layer of the vesicles, as the caudal appendage is often covered with a mixture of mucus and dirt (Hammond 1970a; **own observations**). A second possible function could be the lining of the burrows in the mud with a mucous layer to keep them from collapsing as they remain in the mud (see supplementary videos of Turk et al. 2024), although reports of immediately collapsing burrows exist (Hammond 1970b).

The presence of posterior warts on *A. horridus* is ambiguous, as reports for their presence (Théel 1911; Tommasi 1968) and absence (Van der Land 1970; Schmidt-Rhaesa et al. 2022) exist. However, Schmidt-Rhaesa et al. (2022) reported ‘groups of small ring papillae’ (cf. their Figs. 6D and E), which resemble posterior warts of *Priapulus*. These structures are similar to the wart units and subunits of posterior warts with apically collapsed tubes (cf. Figs. 8D and E in **Study II**). As to date only small *A. horridus* specimens are known (under 25 mm; see Schmidt-Rhaesa et al. 2022), posterior warts may be inconspicuous, similar to those of young *P. caudatus* specimens. To fully confirm

the presence of posterior warts on *A. horridus*, more specimens of this rare species are needed.

Anal tubuli

Unique to *Halicryptus*, the trunk terminates on the posterior end with two distinct anal tubuli lateral of the anus (Van der Land 1970; Shirley and Storch 1999). Anal tubuli are apically tapering cones (Adrianov and Malakhov 1996a; **Study III**). Previous studies termed these structures as setae or spines, but due to apical tubular openings, they represent tubuli (**Study III**). The basal part of each anal tubulus is surrounded by small papillae (Adrianov and Malakhov 1996a; Lemburg 1999). These papillae presumably represent types of flosculus-tubulus-complexes (see above), as they occur in different compositions of smaller accessory papillae and flosculi (**Study III**).

2.2.5. Caudal appendage

Postlarval stages and adults of Priapulinae have caudal appendage(s) terminally on the posterior trunk. Species of *Priapulopsis* are unique by having a paired appendage (Van der Land 1970). **Study I** shows for *P. bicaudatus* that the caudal appendages grow asymmetrically during postlarval development, meaning one appendage grows first before the second one starts to grow. In adult *Priapulopsis*, both appendages have the same length. The length of the caudal appendage can differ drastically (short buds to as long as the introvert and trunk together), even in similarly sized specimens (Van der Land 1970; **Study II**). As the caudal appendage is contractile, it may be affected (= shortened) during the fixation process of specimens (**Study IV**).

The function of the caudal appendage is still ambiguous. The appendages of *Priapulus* and *Priapulopsis* were linked to function as respiratory organ (e.g., Fänge and Mattisson 1961), but there is also evidence against this (Nyholm and Bornö 1969). For *A. horridus*, the appendage may have an anchor function due to its composition (see below) (Van der Land 1970). Similarly, in *Tubiluchus* it may also function as anchor, as the slender appendage is contractile (Van der Land 1970).

The stem of the appendage

The stem of the caudal appendage is a slender extension of the trunk. It is directly connected with the body cavity of the trunk, expanding the body cavity (Apel 1885; Van der Land 1970; **Study II**). Sometimes, the caudal appendage is described to be segmented

(e.g., Théel 1911; Adrianov and Malakhov 1996a; **Study I** and **II**). This segmented appearance may be due to the ring musculature of the stem (**Study II**) that may contract and form distinct thickenings during the fixation of specimens.

Vesicles

During postlarval development, the balloon-like vesicles start to grow on the stem of the appendage (**Study I**). In *Priapulopsis*, the vesicles grow in distinct circles on the stem (Van der Land 1970; **Study I**), while in *Priapulus* they seem to grow randomly on the stem, but indications of a growth in circles is visible on small specimens with a long appendage (cf. Fig. 12H in **Study II**).

Vesicles are thin-walled with an external cuticle and underneath a one-layered epidermis (**Study II**). An additional muscular layer was mentioned by Ehlers (1862), but such layer was not confirmed in **Study II**. Vesicles further expand the body cavity of the specimen, as they are open at their connection with the stem (Ehlers 1862; **Study II**). The surface of the vesicles may differ between *Priapulus* and *Priapulopsis*, as it is either smooth or circularly wrinkled in *Priapulus* (**Study II** and **IV**), or have a distinct net-like wrinkles in *Priapulopsis* (Adrianov and Malakhov 1996a; **Study I** and **IV**). However, these observations may be coincidental artifacts occurring during the drying process of SEM preparation.

On the surface of vesicles, as well as on the stem of the appendage, occur randomly distributed, small spinulets (Van der Land 1970). Spinulets are conical structures with apically one to five tubular receptors (Adrianov and Malakhov 1996a; **Study I**, **II**, and **IV**). The tips of vesicles often have an accumulation of several spinulets, composing together a spinulet crown (**Study I** and **II**). The spinulet crown often has a slightly larger central spinulet (**Study I** and **II**).

Differing from other Priapulinae, *A. horridus* only has vesicles on the anterior stem (e.g., near the posterior trunk; see Théel 1911; Schmidt-Rhaesa et al. 2022). The surface of the vesicles resembles the one of *P. caudatus* (Schmidt-Rhaesa et al. 2022). Interestingly, a small number of spinulets is reported only on the apical part of the vesicle (Van der Land 1970). On the posterior vesicle-free stem of the appendage are numerous, slightly posteriorly curved hooks (Théel 1911; Van der Land 1970). These hooks are blunt-tipped and have an apical single opening (Schmidt-Rhaesa et al. 2022).

2.2.6. Musculature

During this thesis, only the musculature linked to the introvert, more precisely the long and short introvert retractors, were examined (**Study II** and **III**). As only one of each species (*P. caudatus*, *H. spinulosus* and *H. higginsi*) were histologically examined, the following results may be vague. The number of long introvert retractors is always eight (e.g., Candia Carnevali and Ferraguti 1979; Lemburg 1999) and **Study III** was able to validate this number for *H. higginsi*, which was previously reported to have nine long introvert retractors (Shirley and Storch 1999). The number of short introvert retractors is more ambiguous, as numbers differ between 8 and 25 (summarized by Mattisson et al. 1974; Storch et al. 1994; Lemburg 1999), probably due to divisions of muscle strands (Schmidt-Rhaesa 2013). **Study II** and **III** report nine short introvert retractors for *P. caudatus* and *H. spinulosus*, whereas *H. higginsi* has eight. As results differ, detailed studies on the composition of the introvert musculature are needed, potentially using µCT, as this method has shown feasible results for Priapulida (Schmidt-Rhaesa et al. 2022; Fig. 1C in Wernström et al. 2023).

2.2.7. Larval stages of *Priapulopsis bicaudatus*

Larval stages of presumably *P. bicaudatus* have only been shown before by Sanders and Hessler (1962), as they were found together with postlarval stages in the North Atlantic. As only nine larvae were reported, little is known about their morphology. Reports are limited to the number of lorica plates that hold numerous fine spines and few introvert structures (Sanders and Hessler 1962). **Study I** gives new information for medium- to large-sized larval stages of *P. bicaudatus*. The hatching larva and early larval stages (<400 µm lorica length) were not found.

Sanders and Hessler (1962) described a total of 22 lorica plates for the loricate larva of *P. bicaudatus*: two large dorsoventral plates, three lateral plates on each lorica site and 14 anterior plates (two frontal, two laterofrontal and three plates anterior of the lateral plates on each side). **Study I** shows, that both dorsoventral plates are connected by three pairs (two sublateral pairs and one midlateral pair) of lateral pairs, summing up to 14 lorica plates. Additionally, the frontal and latero-frontal plates are confirmed as previously described, but the three small lorica plates anterior of the lateral plates are absent (Fig. 7). Therefore, **Study I** confirms the number of lorica plates (22) for *P. bicaudatus*, but the arrangement is different as proposed by Sanders and Hessler (1962).

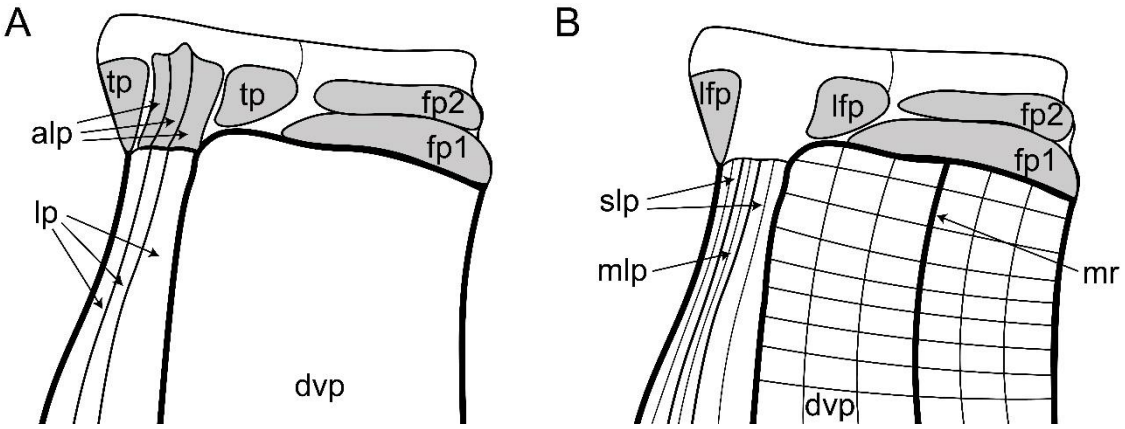

Fig. 7. Anterior lorica of larval *P. bicaudatus*. **A**. Lorica plates described by Sanders and Hessler (1962). **B**. Lorica plates described in **Study I**. Note that the sub- (slp) and midlateral plates (mlp) depict pairs. Abbreviations: alp, anterior lateral plate; dvp, dorsoventral plate; fp1/2, frontal plate 1/2; lfp, laterofrontal plate; lp, lateral plate; mr, median ridge; tp, triangular plate.

Additionally, the sculpturing of the dorsoventral lorica plates of *P. bicaudatus* was described in **Study I** for the first time. The dorsoventral plates have a distinct longitudinal median ridge with two less distinct longitudinal ridges on each side of the median ridge (Fig. 7). The median ridge reaches from the anterior to posterior end of the lorica, whereas the lateral ridges become less distinct on the posterior lorica. Together with perpendicular ridges, the lorica shows a pattern of rectangular compartments (Fig. 7). These rectangular patterns are consistent throughout larval development of *P. bicaudatus*. The lorica sculpturing differs distinctly from its congener *P. australis* (see below), *Priapulus caudatus* (Hammond 1970b; Higgins et al. 1993; Lemburg 1999) and *Halicryptus spinulosus* (Hammarsten 1915; Adrianov and Malakhov 1996a).

The relation of the position of the lorica tubuli to the lorica length of dorsoventrally flattened larvae represents a diagnostic character. The lorica tubuli of *Priapulus tuberculatospinosus* are positioned at about 62 to 67% of the lorica length (Lang 1951; Schmidt-Rhaesa and Freese 2019), while in *P. caudatus* they are positioned further posterior at approximately three-quarters of the lorica length (see Lang 1951; Van der Land 1970; **72 to 83% in own unpublished observations**). For *P. australis*, the lorica tubuli are reported to be positioned between approximately 72 and 77% (Adrianov and Malakhov 1996a) and 78 to 80% (Schmidt-Rhaesa and Freese 2019). However, the data of Adrianov and Malakhov (1996a) may be inaccurate, as their relations were measured from drawings. **Study I** raised the first data for the position of lorica tubuli in relation to the lorica length for *P. bicaudatus*. Their lorica tubuli are positioned between 71 and 77% of the lorica length, falling into the same range as its congener. As both

species have similar relations of the position of lorica tubuli, new data with a high sample size of *P. australis* is needed to clarify this. **Study IV** investigated a few dorsoventrally flattened larval stages from localities around New Zealand, but they could not be distinctly identified to species level.

The introvert of larval stages of *P. bicaudatus* has been only briefly investigated by Sanders and Hessler (1962) before. They reported only numerical data for scalids: eight large scalids (primary scalids) in a circle around the mouth opening and 25 longitudinal rows of scalids. These numbers are validated in **Study I**. Additionally, **Study I** shows the primary scalids and 'regular' scalids in detail for the first time. Primary scalids of larval stages of *P. bicaudatus* are distinct in appearance, as they are long, slender structures. The regular scalids have a leaf-like, triangular shape. The only exception is the eight regular scalids in the first ring posterior to the primary scalids, which are slightly longer than the following regular scalids. Larval stages of *P. caudatus* show similar scalid appearances (Higgins et al. 1993; Adrianov and Malakhov 1996a; Lemburg 1999), whereas all scalids are quite long and slender in larval stages of *H. spinulosus* (Storch and Higgins 1991; Lemburg 1995; Adrianov and Malakhov 1996a).

Study I shows the pharyngeal teeth of the first pentaradial ring of teeth from larval *P. bicaudatus* for the first time. The following rings were not visible. The visible teeth have all a distinct median groove on the 'outer' surface, dividing one tooth into two symmetric parts. Yet, both parts are still connected, as can be seen due to the smooth 'inner' surface without groove. Apical on the teeth are numerous short spine-like structures. Nested between these spines are two tubular receptors. A similar appearance of the teeth of the first ring was reported for older *P. caudatus* larvae by Higgins et al. (1993). However, pharyngeal teeth of larval stages are difficult to compare between species or even within a species. Often, the appearance of teeth changes between larval stages of different ages (e.g., Higgins et al. 1993; Adrianov and Malakhov 1996a). Another problem is the state of eversion of the introvert of the fixed larvae, as teeth are usually only visible when the introvert is fully everted. Further investigations of larval teeth from *P. bicaudatus* and *Priapulus* species, but also other macroscopic species, are needed for gathering data that are more comparable.

2.2.8. Are morphological characters affected by body size?

As there are two body size classes in Priapulida, this raises the question of whether the body size has an effect on the size or the number of morphological structures. The

genus *Halicryptus* is well-suited for examining this question, as it includes two species with vastly different adult body sizes: *H. spinulosus* (up to 4 cm) and the much larger *H. higginsi* (up to 40 cm), which are otherwise morphologically very similar (see Merriman 1981; Shirley and Storch 1999; **Study III**),

Study III shows that a larger body size influences some randomly distributed structures in *Halicryptus*, such as an increased number of small buccal papillae and trunk tubuli during development. In *H. spinulosus*, trunk and anal tubuli grow in size during development but do not consistently scale with body size. Contrary, in large *H. higginsi*, these structures have a much lower proportional size relative to body length than in large *H. spinulosus*. Additionally, the body wall thickness in *H. spinulosus* increases with growth, eventually resembling the proportions of large *H. higginsi*.

On the other hand, **Study III** shows that the numbers of primary scalids, scalid rows, and certain buccal papillae, remain constant regardless of body size in *H. spinulosus*. This mirrors observations in insect sensory organs, where some correlate in size with the body size while others do not (see Makarova et al. 2022). A recent geometric morphometric study of pharyngeal teeth in Priapulida shows that both *Halicryptus* species occupy a similar morphospace, suggesting potential allometric growth of their teeth (Wernström et al. 2023). Further studies on homologous sensory organs across Priapulida could clarify patterns of allometric growth in this group.

2.2.9. A new macroscopic species

New macroscopic priapulidan species are rarely described. The last described macroscopic species was *H. higginsi* (Shirley and Storch 1999), and before that *P. abyssorum* (Menzies 1959). While examining priapulidans from the NIWA collection (**Study IV**), two macroscopic specimens that were formerly determined as *Priapulopsis australis* differed in certain morphological aspects from other *P. australis* specimens. As both specimens had bipartite teeth in the first ring of teeth and a paired caudal appendage, they are classified under the genus *Priapulopsis*. However, one main difference to other *Priapulopsis* species is that trunk papillae are organized in a distinct ring on each annulus of the trunk. Due to this distinct diagnostic character, both specimens are newly described as *Priapulopsis papillatus*. Other morphological differences are: trunk cuticle without tumuli, but with radiating ridges; scalids on introvert without series; bipartite teeth of the first ring of teeth with blunt cusps; tooth receptors only present on teeth of the first ring (**Study IV**).

Unfortunately, only two specimens are documented as for now. *Priapulopsis papillatus* thus aligns with species descriptions from *A. horridus*, *M. cirratus*, *P. abyssorum*, *T. remanei* and six further *Tubiluchus* species, which all had less than 10 specimens for describing the species.

2.3. Phylogenetic contributions

Molecular phylogenetic analyses focusing on Priapulida have not been previously conducted, and molecular studies that include only a few priapulidan species are scarce (e.g. Giribet et al. 2000; Sørensen et al. 2008; Laumer et al. 2015; 2019). **Study V** presents the first molecular phylogenomic analysis based on molecular (transcriptomic and genomic) data from species representing five out of seven priapulidan genera (Fig. 8A).

2.3.1. Phylogenetic relationships of extant Priapulida

The topology of the newly proposed relationships of Priapulida corresponds almost entirely with those of the previous analyses based fully on morphological data (**Study V**; Fig. 8B). The only difference occurs in the position of microscopic *M. fijiensis*, as it forms a clade together with *Tubiluchus* in previous studies (see Fig. 6C), while molecular analyses propose *M. fijiensis* as sister group to all remaining priapulidans (**Study V**; Fig. 8). The inferred positions of *Acanthopriapulus* and *Maccabeus* based on morphological data on the tree also correspond with the majority of previous studies (**Study V**; Fig. 8B). However, further molecular analyses including fresh material of both missing genera are needed to confirm these proposed relationships within Priapulida.

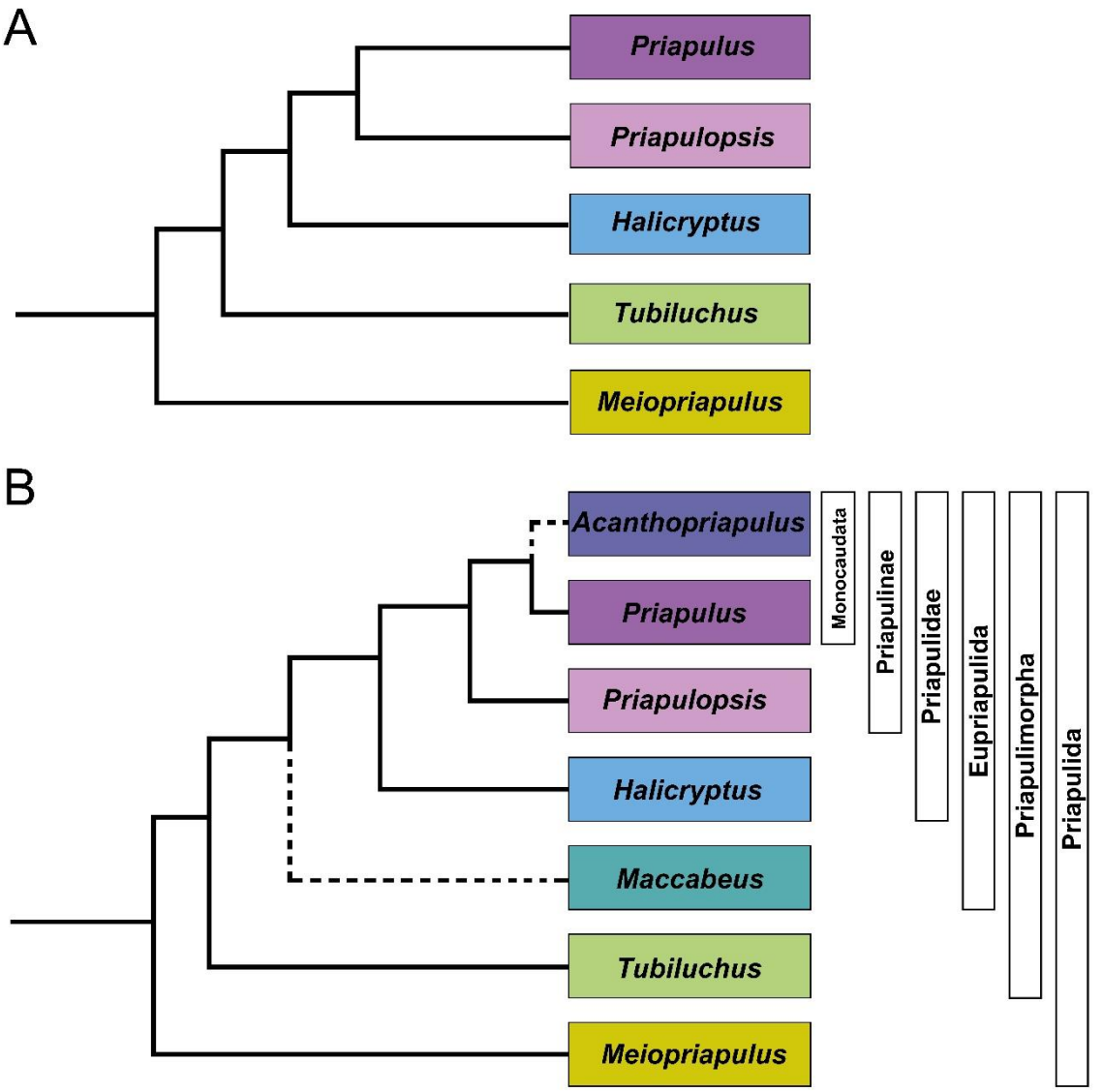

Fig. 8. Phylogenetic relationships of extant Priapulida. **A**. Relationships based on transcriptomic data. **B**. Relationships based on combined molecular and morphological data. Dotted branches show taxa added to the tree by analysing morphological data. Names on the right side show the newly proposed classification of Priapulida. Figure modified from **Study V**.

2.3.2. Classification of Priapulida

Based on the phylogenetic relationships inferred in **Study V**, the phylogenetic classification of Priapulida, as proposed by Lemburg (1999) (see Table 3), has been slightly changed. The monophylum Megintroverta (Monocaudata + *Priapulopsis*), proposed by Lemburg (1999), is renamed to Priapulinae, as this name was already introduced by Salvini-Plawen (1974) for this clade. Additionally, the monophylum Tubiluchidae (*Tubiluchus* + *Meiopriapulus*) proposed by Lemburg (1999) is not supported in the newly inferred phylogenetic relationships, as *Meiopriapulus* represents the sister group to the remaining priapulidans (**Study V**; Fig. 8). Instead, a 'new'

monophyletic group is proposed: Priapulimorpha (Eupriapulida + *Tubiluchus*) (**Study V**; Fig. 8B), named after Salvini-Plawen's (1974) proposed clade, which included *Tubiluchus* and the macroscopic priapulidans (see Table 2). However, as *Maccabeus* is inferred to be the sister group to the macroscopic species, it is now proposed for inclusion in Priapulimorpha (**Study V**; Fig. 8B), contrary to Salvini-Plawen's proposal.

Regarding the traditional classification, minor changes are suggested here. The falsely cited family 'Halicryptidae' by Adrianov and Malakhov (1995) is refused here, although it is often used in other studies (e.g., Wills et al. 2012; Schmidt-Rhaesa 2013; Giribet and Edgecombe 2020; Wernström et al. 2023). Instead, *Halicryptus* should be included in Priapulidae, as formerly proposed by Van der Land (1970) and Salvini-Plawen (1974). Due to morphological differences of *Halicryptus* to the remaining macroscopic species, it is suggested to re-establish the subfamilies Halicryptinae and Priapulinae (*Acanthopriapulus* + *Priapulus* + *Priapulopsis*), as formerly proposed by Salvini-Plawen (1974) (**Study V**).

2.3.3. Are Priapulida ancestrally small?

The ancestral body size of Priapulida, micro- or macroscopic, is ambiguous. Studies on morphological data proposing both ancestral body sizes exist. Lemburg (1999) proposes a small ancestral body size due to the most parsimonious evolution when related microscopic outgroups (Kinorhyncha, Loricifera, Gastrotricha and Nematoda) are included in analyses. Other studies including priapulidan-like fossils in their analyses tend towards a macroscopic ancestral body size (e.g., Adrianov and Malakhov 1996a).

Study V suggests that extant Priapulida ancestrally had a small body size and consequently an internal fertilization, based on phylogenomic relationships and ancestral state reconstructions. However, these reconstructions did not incorporate data from priapulidan-like fossils.

Fossil approach

From all priapulidan-like fossils, *Priapulites konecniorum* from the Carboniferous resembles recent Priapulinae the most (see Schram 1973) and is therefore classified within this group (see Van der Land and Nørrevang 1985). Other fossil species show certain morphological similarities, like teeth in pentagons, 25 scalid rows on the introvert, annulated trunk or papillae/hooks in rings on the posterior trunk (see Huang et al. 2004; Han et al. 2004). However, it remains controversial, whether these fossil species belong

within Priapulida, or whether they represent stem lineages of Priapulida, Scalidophora or other related taxa (Huang et al. 2004; Han et al. 2004; Schmidt-Rhaesa 2013).

Assuming all priapulidan-like fossils indeed represent priapulidans, they all fall within the macroscopic size range (~1.2 to 15 cm). Extinct microscopic priapulidans may have existed, but associated fossils may not have been found due to sampling and conservation bias (Worsaae et al. 2023). One potential larval priapulidan-like fossil, *Inuitiphlaskus kouchinskyi*, exists, which resembles the hatching larva of *P. caudatus* and *H. spinulosus* but it is eight times larger (~1250 µm) than extant hatching larvae (Peel 2022). Even though this fossil represents a microscopic fossil, the potential adult stage may have exceeded the microscopic body size if *I. kouchinskyi* is representing a hatching larva. For the related Loricifera, well preserved microscopic fossil specimens of *Eolorica deadwoodensis* with total lengths of 180 to 300 µm exist (Harvey and Butterfield 2017). For Kinorhyncha, two questionable microscopic fossils (both about 1100 µm) of potential stem group kinorhynch species, *Eokinorhynchus rarus* (Zhang et al. 2015) and *Zhongpingscolex qinensis* (Shao et al. 2020) exist. As potential small fossils of other Scalidophora taxa exist, microscopic fossils representing adult priapulidans may emerge.

The frequently found SCFs resemble extant priapulidan teeth or scalids (see Butterfield and Harvey 2012; Smith et al. 2015; Slater et al. 2017). Some of the teeth-like SCFs resemble the pectinate teeth of microscopic *Tubiluchus* (**Study V**). Both have a basal crescent-like shape with an anterior, spine-holding part (e.g., prong holding denticles in fossils; manubrium holding pecten in *Tubiluchus*) and a posterior part bending towards the anterior (e.g., spur in fossils; posterior part of the manubrium in *Tubiluchus*). While similarities in the composition of both exist, the teeth-like SCFs are larger (~50 µm width) than teeth of extant microscopic species (~5 to 15 µm width) (**Study V**). Comparably, the base of teeth of extant macroscopic species ranges between approximately 100 and 600 µm (see **Study I** to **III**). Therefore, the species belonging to those teeth-like SCFs may be larger than extant microscopic species, but further analyses of the phylogenetic relationships of priapulidans including extinct species are needed to support these observations.

Fertilization mode

The fertilization mode differs between both size classes of Priapulida. Macroscopic species are external fertilizers and have round-headed spermatozoa with a cilium (Van der Land 1970; Afzelius and Ferraguti 1978; Schmidt-Rhaesa 2013). In contrast, microscopic species are assumed to have internal fertilization due to sexual

dimorphism (*Tubiluchus*), modified spermatozoa (*Tubiluchus*; Alberti and Storch 1983; Ferraguti and Garbelli 2006), internal embryo brooding (*Meiopriapulus*; Storch et al. 1991), and low oocyte numbers (*Tubiluchus, Meiopriapulus, Maccabeus;* Storch et al. 1991).

Although *M. fijiensis* likely has internal fertilization, it has round-headed spermatozoa similar to macroscopic species (Storch et al. 1989). In contrast, *Tubiluchus* has elongated, corkscrewed spermatozoa (Alberti and Storch 1983; Ferraguti and Garbelli 2006). Typically, external fertilizers have round-headed sperm, while internal fertilizers have modified sperm, and body size correlates with fertilization mode (Franzén 1977; Jarvis and Marshall 2023). However, *M. fijiensis* differs from this pattern by combining round-headed sperm with internal fertilization.

Study V suggests internal fertilization as ancestral for Priapulida, contradicting the common assumption that external fertilization and round-headed sperm were ancestral. *Meiopriapulus* retaining this spermatozoa type suggests that external fertilization may have re-evolved in Eupriapulida, with modified spermatozoa occurring only in *Tubiluchus*. Related scalidophoran taxa (*Kinorhyncha, Loricifera*) are assumed to have exclusively internal fertilization (see Bang-Berthelsen et al. 2013; Neuhaus 2013), supporting the hypothesis that internal fertilization is the ancestral reproductive mode in Priapulida.

2.3.4. Wide geographical distribution of single species

Priapulus and *Priapulopsis* include morphologically similar species that are geographically separated. While *Priapulus caudatus* and *Priapulopsis bicaudatus* are found in the Northern Hemisphere, their congener *Priapulus tuberculatospinosus* and *Priapulopsis australis* occur in the Southern Hemisphere (Van der Land 1970; Schmidt-Rhaesa 2013). Usually, when a specimen of one of these genera is found, it is assigned to the respective species of the Hemisphere. This results in wide geographical distributions for these species (Van der Land 1970; Adrianov and Malakhov 1996b). This raises the question, whether specimens from such far apart localities represent the same species (e.g., Baltic Sea, White Sea, Cobscook Bay [East coast of Maine, USA] and Gulf of Alaska for *P. caudatus*; see Adrianov and Malakhov 1996b).

Two recent studies show a variable genetic population structure of *P. caudatus* from different localities, which are interpreted differently. Laakkonen et al. (2021) specify different *Priapulus* species across localities, whereas Kolbasova et al. (2023)

argue for an incomplete speciation of *P. caudatus*. Morphological examinations of *P. caudatus* specimens from different localities did not find significant differences, tending towards the same species (**Study II**).

A similar wide northern distribution is assumed for *H. spinulosus* on the basis of morphology (see Adrianov and Malakhov 1996b). **Study III** analyzed *CO1* sequences of *H. spinulosus* specimens from different localities (Baltic Sea, White Sea, East Siberian Sea, Beaufort Sea and Hudson Bay) and confirmed the belonging to the same species. A potential incomplete speciation of *H. spinulosus* was not tested.

For the species of the Southern Hemisphere with a wide distribution (*P. tuberculatospinosus* and *P. australis*), similar molecular analyses of specimens from different localities have yet to be made.

2.3.5. Generating molecular data for Priapulida

During this thesis, several attempts to generate molecular data for priapulidans have been made. While the protocols for gaining molecular data of a large scale (transcriptomes and genomic conserved loci) positively worked (see **Study V**), the DNA extractions and assembly for single genes (*18S* and *COI*) caused problems. Standardized protocols used for *18S* and *COI* amplification in the molecular laboratory of the Leibniz Institute for the Analysis of Biodiversity Change (Hamburg), as well as a protocol used by Kolbasova et al. (2023) used for *COI* amplification specifically on priapulidans with Geller primer (jgLCO1490 and jgHCO2198; Geller et al 2013) were tried during this thesis, but without success (see **Study I** for *P. bicaudatus*). However, one modified protocol used for *CO1* amplification on *H. spinulosus* specimens (see **Study III** for PCR protocol) using Geller primers was successful on a few specimens.

Concentrations of extracted DNA differed between ethanol and RNA*later* preserved specimens. DNA concentrations of old museum-stored specimens preserved in ethanol were often not detectable (<0.5 ng/mL) or very low (<1 ng/mL). Fresh ethanol preserved specimens had in comparison higher DNA concentrations (2.6 to 123 ng/mL). Highest DNA concentrations were extracted from RNA*later* preserved specimens (76 to 371 ng/mL), but only a few specimens of *P. caudatus* and *H. spinulosus* were available. RNA*later* is a storage solution that is originally designed to stabilize and protect cellular RNA in unfrozen samples (tissue samples and whole organisms) by deactivating nucleases and keeping the RNA from degrading for up to eight months at 5 °C and one

month unrefrigerated (Gorokhova 2005). Similarly, DNA is also preserved in RNA*later* (Gorokhova and Kyle 2002).

For the *CO1* amplifications of **Study III**, an amplification was achieved from two out of four ethanol preserved *H. spinulosus* specimens (2.68 and 4.95 ng/mL), and one of two RNA*later* preserved specimens (149 ng/mL). The remaining two ethanol preserved specimens did not have detectable DNA concentrations, whereas the other RNA*later* preserved specimen had a DNA concentration of 79 ng/mL, but did not achieve a *COI* amplification.

As molecular analyses including priapulidan species are scarce, protocols are not yet well established for this taxon. Priapulida could benefit from reliable amplification protocols for single gene analyses, especially when only few specimens are available. Additionally, specimen preservation in RNA*later* is proposed for a higher extracted DNA concentration.

2.4. Conclusions and future research

The studies of this thesis were able to close knowledge gaps of long known macroscopic species of Priapulida. While the morphology of respective adult specimens is now documented quite well, postlarval stages still need to be examined in future studies. Potential future studies could give new insights into the development of morphological structures, as shown in this thesis for diagnostic characters of *Priapulopsis bicaudatus* (bipartite teeth and paired caudal appendage). Especially, postlarval stages of the small-sized *Halicryptus spinulosus* and large-sized *H. higginsi* depict an interesting research topic for the development of these morphologically similar species that exhibit enormous differences in their maximum adult body size.

As most macroscopic species are now described in detail, the morphological research should now focus on microscopic Priapulida. While *Meiopriapulus fijiensis* was reinvestigated in detail more recently, *Maccabeus* and rare *Tubiluchus* species (e.g., *T. arcticus*, *T. australensis*, *T. vanuatensis* and *T. remanei*) should undergo similarly standardized morphological reinvestigations. In particular, the previously neglected circumoral field of microscopic species requires detailed documentation for further comparisons.

Regarding larvae, several larval stages of *P. bicaudatus* were documented here in detail for the first time. However, loricate larval stages are similar among macroscopic priapulidans, most notably between *Priapulus* and *Priapulopsis*. Differences in the larval

morphology are vague or not evident, and the species are mostly assumed based on findings of adult specimens in the same area, as the development from loricate larva to postlarva has not yet been documented. Long term experiments documenting the full developmental line (from hatching larva to adult) would be benefitting for future species determinations of Priapulida.

Furthermore, the here generated first phylogenetic tree based on molecular and morphological data validates almost entirely previous proposed relationships. As not all priapulidan genera are represented with molecular data in the newly generated phylogenetic tree, further studies should focus on obtaining fresh material of the missing rare taxa *Acanthopriapulus* and *Maccabeus* for genomic analyses and validation of the here proposed relationships in Priapulida.

Ancestral state reconstructions of morphological characters on the newly generated phylogenetic tree propose an ancestrally microscopic body size and an internal fertilization mode in extant Priapulida, matching with the remaining Scalidophora. Findings of microscopic priapulidan fossils could validate this suggestion.

References

Adrianov, A.V., Malakhov, V.V., 1991. First findings of dwarf priapulids of the genus *Tubiluchus* (Priapulida, Tubiluchidae) in Oceania (New-Hebrides). Zoologicheskii Zhurnal, 70, 23-32. [In Russian]

Adrianov, A.V., Malakhov, V.V., 1996a. Priapulida: Structure, development, phylogeny, and classification. Moscow: KMK Scientific Press. [In Russian with English summary]

Adrianov, A.V., Malakhov, V.V., 1996b. The phylogeny, classification and zoogeography of the class Priapulida. II. Revision of the family Priapulidae and zoogeography of priapulids. Zoosystematica Rossica, 5, 1-6.

Adrianov, A.V., Malakhov, V.V., Chesunov, A.V., Tsetlin, A.B., 1989. A dwarf priapulid *Tubiluchus arcticus* sp. n. from the White Sea (Priapulomorpha, Tubiluchidae). Zoologicheskii Zhurnal 68, 126-131. [In Russian]

Adrianov, A.V., Malakhov, V.V., 2001a. Symmetry of priapulids (Priapulida). 1. Symmetry of adults. Journal of Morphology, 247(2) 99-110. https://doi.org/10.1002/1097-4687(200102)247:2<99::AID-JMOR1005>3.0.CO;2-0.

Adrianov, A.V., Malakhov, V.V., 2001b. Symmetry of priapulids (Priapulida). 2. Symmetry of larvae. Journal of Morphology, 247(2), 111-121. https://doi.org/10.1002/1097-4687(200102)247:2<111::AID-JMOR1006>3.0.CO;2-C.

Afzelius, B. A., Ferraguti, M., 1978. The spermatozoon of *Priapulus caudatus* Lamarck. Journal of Submicroscopic Cytology and Pathology, 10, 71-79.

Aguinaldo, A.M.A., Turbeville, J.M., Linford, L.S., Rivera, M.C., Garey, J.R., Raff, R. A., Lake, J.A., 1997. Evidence for a clade of nematodes, arthropods and other moulting animals. Nature, 387(6632), 489-493. https://doi.org/10.1038/387489a0.

Alberti, G., Storch, V., 1983. Fine structure of developing and mature spermatozoa in *Tubiluchus* (Priapulida, Tubiluchidae). Zoomorphology, 103, 219-227. https://doi.org/10.1007/BF00310479.

Alberti, G., Storch, V., 1986. Zur Ultrastruktur der Protonephridien von *Tubiluchus philippinensis* (Tubiluchidae, Priapulida). Zoologischer Anzeiger, 217(3-4), 259-271.

Apel, W., 1885. Beitrag zur Anatomie und Histologie des *Priapulus caudatus* (Lam.) und des *Halicryptus spinulosus* (v. Siebold). Zeitschrift für wissenschaftliche Zoologie, 42, 459-529.

Appeltans, W., Ahyong, S.T., Anderson, G., Angel, M.V., Artois, T., Bailly, N., ... & Costello, M.J., 2012. The magnitude of global marine species diversity. Current biology, 22(23), 2189-2202. https://www.doi.org/10.1016/j.cub.2012.09.036.

Bang-Berthelsen, I., Schmidt-Rhaesa, A., Kristensen, R.M., 2013. Loricifera. In: Schmidt-Rhaesa, A., editor. Handbook of Zoology: Nematomorpha, Priapulida, Kinorhyncha and Loricifera. Volume 1. Berlin: Walter de Gruyter, 349-378. https://doi.org/10.1515/9783110272536.349.

Borner, J., Rehm, P., Schill, R.O., Ebersberger, I., Burmester, T., 2014. A transcriptome approach to ecdysozoan phylogeny. Molecular Phylogenetics and Evolution, 80, 79-87. https://doi.org/10.1016/j.ympev.2014.08.001.

Brix, S., Bauernfeind, W., Brenke, N., Blazewicz, M., Borges, V., Buldt, K., Cannon, J., Díaz Agras, G., Fiege, D., Fiorentino, D., Haraldsdóttir, S., Hoffmann, S., Holst, S., Hüttmann, F., Jeskulke, K., Jennings, R., Kocot, K., Khodami, S., Lucas Rodriguez, Y., Martinez Arbizu, P., Meißner, K.,

Mikkelsen, N., Miller, M., Murray, A., Neumann, H., Ostmann, A., Riehl, T., Schnurr, S., Savavarsson, J., Yasuhara, M., 2012. Overflow, Circulation and Biodiversity. Cruise No. M85/3, August 27 - September 28, 2011, Reykjavik (Iceland) - Cuxhaven (Germany). METEOR-Berichte, M85/3, pp. 1-41. https://doi.org/10.2312/cr_m85_3.

Brix, S., 2013. IceAGE. Icelandic Marine Animals: Genetics and Ecology. Cruise No. POS456, IceAGE2, 20.07.2013-04.08.2013. Kiel (Germany) - Reykjavik (Iceland). Cruise Report POS 456. http://www.geomar.de/fileadmin/content/zentrum/ze/fs/Poseidon_Berichte_2013_PDF/POS456_Brix.pdf.

Butterfield, N.J., Harvey, T.H.P., 2012. Small carbonaceous fossils (SCFs): a new measure of early Paleozoic paleobiology. Geology, 40(1), 71-74. https://doi.org/10.1130/G32580.1.

Calloway, C.B., 1975. Morphology of the introvert and associated structures of the priapulid *Tubiluchus corallicola* from Bermuda. Marine Biology, 31, 161-174. https://doi.org/10.1007/BF00391628.

Campos, P., Gilbert, T.P., 2012. DNA Extraction from Formalin-Fixed Material In: Shapiro, B., Hofreiter, M., editors. Methods in Molecular Biology. Humana Press, Vol. 840, 81-85. https://doi.org/10.1007/978-1-61779-516-9_11.

Candia Carnevali, M.D., Ferraguti, M., 1979. Structure and ultrastructure of muscles in the priapulid *Halicryptus spinulosus*: functional and phylogenetic remarks. Journal of the Marine Biological Association of the United Kingdom, 59(3), 737-748. https://doi.org/10.1017/S0025315400045719.

Cannon, J.T., Vellutini, B.C., Smith, J., Ronquist, F., Jondelius, U., Hejnol, A., 2016. Xenacoelomorpha is the sister group to Nephrozoa. Nature, 530, 89-93. https://doi.org/10.1038/nature16520.

Cepeda, D., González-Casarrubios, A., Sánchez, N., Spedicato, A., Michaud, E., Zeppilli, D., 2022. Two new species of mud dragons (Scalidophora: Kinorhyncha) inhabiting a human-impacted mangrove from Mayotte (Southwestern Indian Ocean). Zoologischer Anzeiger, 301, 23-41. https://doi.org/10.1016/j.jcz.2022.09.001.

Conway Morris, S., Robison, R.A., 1986. Middle Cambrian priapulids and other soft-bodied fossils from Utah and Spain. University of Kansas Paleontological Contributions, 117, 1-22.

Cunningham, J.A., Liu, A.G., Bengtson, S., Donoghue, P.C., 2017. The origin of animals: can molecular clocks and the fossil record be reconciled?. BioEssays, 39(1), 1-12. https://doi.org/10.1002/bies.201600120.

Danielssen, D.C., 1869. To maerkelige Sodyr. Forhandlinger Ved de Skandinaviske Naturforskeres Möde (i Christiania fra den 4de til den 10de Juli 1868), 10, 541-542.

Danovaro, R., Dell'Anno, A., Pusceddu, A., Gambi, C., Heiner, I., Kristensen, R.M., 2010. The first metazoa living in permanently anoxic conditions. BMC biology, 8, 1-10. https://doi.org/10.1186/1741-7007-8-30.

De Guerne J., 1886. Sur les Gèphyriens de la famille des Priapulides recueillis par la mission de Cap horn. Comptes rendus hebdomadaires des séances de l'Académie des sciences, 103, 760-762. https://doi.org/10.5962/bhl.part.5842.

Dodsworth, S., 2015. Genome skimming for next-generation biodiversity analysis. Trends in Plant Science, 20, 525-527. https://doi.org/10.1016/j.tplants.2015.06.012.

References

Dong, X.-P., Donoghue, P.C.J., Cheng, H., Liu, J.-B., 2004. Fossil embryos from the middle and late Cambrian period of Hunan, south China. Nature, 427, 237-240. https://doi.org/10.1038/nature02215.

Dong, X.-P., Bengtson, S., Gostling, N.J., Cunningham, J.A., Harvey, T.H.P., Kouchinsky, A., Val'kov, A.K., Repetski, J.E., Repetski, J.E., Stampanoni, M., Marone, F., Donoghue, P.C.J., 2010. The anatomy, taphonomy, taxonomy and systematic affinity of *Markuelia*: Early Cambrian to Early Ordovician scalidophorans. Palaeontology, 53, 1291-1314. https://doi.org/10.1111/j.1475-4983.2010.01006.x.

Dong, X.-P., Donoghue, P.C., Cunningham, J.A., Liu, J.B., Cheng, H., 2005. The anatomy, affinity, and phylogenetic significance of *Markuelia*. Evolution and Development, 7(5), 468-482. https://doi.org/10.1111/j.1525-142X.2005.05050.x.

Dunn, C.W., Hejnol, A., Matus, D.Q., Pang, K., Browne, W.E., Smith, S.A., ... & Giribet, G., 2008. Broad phylogenomic sampling improves resolution of the animal tree of life. Nature, 452(7188), 745-749. https://doi.org/10.1038/nature06614.

Ehlers, E., 1862. Ueber die Gattung *Priapulus* Lam. Ein Beitrag zur Kenntnis der Gephyreen. Zeitschrift für wissenschaftliche Zoologie, 11, 205-252.

Elder, H.Y., Hunter, R.D., 1980. Burrowing of *Priapulus caudatus* (Vermes) and the significance of the direct peristaltic wave. Journal of Zoology, 191(3), 333-351. https://doi.org/10.1111/j.1469-7998.1980.tb01463.x.

Fänge, R., Mattisson, A., 1961. Function of the caudal appendage of *Priapulus caudatus*. Nature, 190, 1216-1217. https://doi.org/10.1038/1901216a0.

Ferraguti, M., Garbelli, C., 2006. The spermatozoon of a 'living fossil': *Tubiluchus troglodytes* (Priapulida). Tissue and Cell, 38(1), 1-6. https://doi.org/10.1016/j.tice.2005.05.001.

Franzén, A., 1977. Sperm structure with regard to fertilization biology and phylogenetics. Verhandlungen der Deutschen Zoologischen Gesellschaft 1977, 123-138.

Fu, C.N., Mo, Z.Q., Yang, J.B., Cai, J., Ye, L.J., Zou, J.Y., Qin, H.T., Zheng, W., Hollingsworth, P.M., Li, D.Z., Gao, L.M., 2022. Testing genome skimming for species discrimination in the large and taxonomically difficult genus *Rhododendron*. Molecular Ecology Resources, 22, 404-414. https://doi.org/10.1111/1755-0998.13479.

Geller, J., Meyer, C., Parker, M., Hawk, H., 2013. Redesign of PCR primers for mitochondrial cytochrome c oxidase subunit I for marine invertebrates and application in all-taxa biotic surveys. Molecular ecology resources, 13(5), 851-861. https://doi.org/10.1111/1755-0998.12138.

Giribet, G., Distel, D., Polz, M., Sterrer, W., Wheeler, W., 2000. Triploblastic relationships with emphasis on the acoelomates and the position of Gnathostomulida, Cycliophora, Plathelminthes, and Chaetognatha: a combined approach of 18S rDNA sequences and morphology. Systematic Biology, 49(3), 539-562. https://doi.org/10.1080/10635159950127385.

Giribet, G., Edgecombe, G.D., 2017. Current understanding of Ecdysozoa and its internal phylogenetic relationships. Integrative and Comparative Biology, 57, 455-466. https://doi.org/10.1093/icb/icx072.

References

Gorokhova, E., 2005. Effects of preservation and storage of microcrustaceans in RNAlater on RNA and DNA degradation. Limnology and Oceanography: Methods, 3(2), 143-148. https://doi.org/10.4319/lom.2005.3.143.

Gorokhova, E., Kyle, M., 2002. Analysis of nucleic acids in *Daphnia*: development of methods and ontogenetic variations in RNA-DNA content. Journal of plankton research, 24(5), 511-522. https://doi.org/10.1093/plankt/24.5.511.

Grzelak, K., Sørensen, M.V., 2022. *Echinoderes* (Kinorhyncha: Cyclorhagida) from the Hikurangi Margin, New Zealand. European journal of taxonomy, 844, 1-108. https://doi.org/10.5852/ejt.2022.844.1949.

Hammarsten, O.D., 1913. Beitrage zur Entwicklung von *Halicryptus spinulosus* (von Siebold). Zoologischer Anzeiger, 41, 501-505.

Hammarsten, O.D., 1915. Zur Entwicklungsgeschichte von *Halicryptus spinulosus* (von Siebold). Zeitschrift für wissenschaftliche Zoologie, 112, 527-571.

Hammond, R.A., 1970a. The burrowing of *Priapulus caudatus*. Journal of Zoology, 162(4), 469-480. https://doi.org/10.1111/j.1469-7998.1970.tb01281.x.

Hammond, R.A., 1970b. The surface of *Priapulus caudatus* (Lamarck, 1816). Zeitschrift für Morphologie der Tiere, 68, 225-268. https://doi.org/10.1007/BF00277505.

Han, J., Shu, D., Zhang, Z., Liu, J., 2004. The earliest-known ancestors of recent Priapulomorpha from the early Cambrian Chengjiang Lagerstätte. Chinese Science Bulletin, 49, 1860-1868. https://doi.org/10.1007/BF03183414.

Harvey, T.H.P., Dong, X.-P., Donoghue, P.C.J., 2010. Are palaeoscolecids ancestral ecdysozoans? Evolution & Development, 12, 177-200. https://doi.org/10.1111/j.1525-142X.2010.00403.x.

Harvey, T.H.P., Butterfield, N.J., 2017. Exceptionally preserved Cambrian loriciferans and the early animal invasion of the meiobenthos. Nature Ecology & Evolution, 1, 0022. https://doi.org/10.1038/s41559-016-0022.

Hejnol, A., Obst, M., Stamatakis, A., Ott, M., Rouse, G.W., Edgecombe, G.D., ... & Dunn, C.W. (2009). Assessing the root of bilaterian animals with scalable phylogenomic methods. Proceedings of the Royal Society B: Biological Sciences, 276(1677), 4261-4270. https://doi.org/10.1098/rspb.2009.0896.

Herranz, M., Stiller, J., Worsaae, K., Sørensen, M.V., 2022. Phylogenomic analyses of mud dragons (Kinorhyncha). Molecular Phylogenetics and Evolution, 168, 107375. https://doi.org/10.1016/j.ympev.2021.107375.

Higgins, R.P., Storch, V., 1991. Evidence for direct development in *Meiopriapulus fijiensis* (Priapulida). Transactions of the American Microscopical Society, 37-46. https://doi.org/10.2307/3226738.

Higgins, R.P., Storch, V., Shirley, T.C., 1993. Scanning and transmission electron microscopical observations on the larvae of *Priapulus caudatus* (Priapulida). Acta Zoologica, 74(4), 301-319. https://doi.org/10.1111/j.1463-6395.1993.tb01245.x.

Howard, R.J., Giacomelli, M., Lozano-Fernandez, J., Edgecombe, G.D., Fleming, J.F., Kristensen, R.M., ... & Pisani, D., 2022. The Ediacaran origin of Ecdysozoa: integrating fossil and phylogenomic data. Journal of the Geological Society, 179(4), jgs2021-107.

https://doi.org/10.1144/jgs2021-107.

Huang, D., Vannier, J., Chen, J., 2004. Recent Priapulidae and their Early Cambrian ancestors: comparisons and evolutionary significance. Geobios, 37(2), 217-228. https://doi.org/10.1016/j.geobios.2003.04.004.

Jamieson, A., 2015. The Hadal Zone: Life in the Deepest Oceans. Cambridge University Press.

Janssen, R., Wennberg, S.A., Budd, G.E., 2009. The hatching larva of the priapulid worm *Halicryptus spinulosus*. Frontiers in Zoology, 6, 1-7. https://doi.org/10.1186/1742-9994-6-8.

Jarvis, G.C., Marshall, D.J., 2023. Fertilization Mode Covaries with Body Size. The American Naturalist, 202(4), 448-457. https://doi.org/10.1086/725864.

Kirsteuer, E., 1976. Notes on Adult Morphology and Larval Development of *Tubiluchus corallicola* (Priapulida), Based on in vivo and Scanning Electron Microscopic Examinations of Specimens from Bermuda 1. Zoologica Scripta, 5(1-4), 239-255. https://doi.org/10.1111/j.1463-6409.1976.tb00706.x.

Kirsteuer, E., Van der Land, J., 1970. Some notes on *Tubiluchus corallicola* (Priapulida) from Barbados, West Indies. Marine Biology, 7(3), 230-238. https://doi.org/10.1007/BF00367493.

Kirsteuer, E., Rützler, K., 1973. Additional notes on *Tubiluchus corallicola* (Priapulida), based on scanning electron microscope observations. Marine Biology, 20, 78-87. https://doi.org/10.1007/BF00387678.

Kolbasova, G., Schmidt-Rhaesa, A., Syomin, V., Bredikhin, D., Morozov, T., Neretina, T., 2023. Cryptic species complex or an incomplete speciation? Phylogeographic analysis reveals an intricate Pleistocene history of *Priapulus caudatus* Lamarck, 1816. Zoologischer Anzeiger, 302, 113-130. https://doi.org/10.1016/j.jcz.2022.11.013.

Koren, J., Danielssen, D.C., 1877. Bidrag til de Norske gephyreers naturhistorie. In: Koren, J., Danielssen, D.C., editors. Fauna Littoralis Norvegiae, vol. 3, 111–151.

Kristensen, R.M., 1983. Loricifera, a new phylum with Aschelminthes characters from the meiobenthos. Zeitschrift für zoologische Systematik und Evolutionsforschung, 21(3), 163-180. https://doi.org/10.1111/j.1439-0469.1983.tb00285.x.

Laakkonen, H.M., Hardman, M., Strelkov, P., Väinölä, R., 2021. Cycles of trans-Arctic dispersal and vicariance, and diversification of the amphi-boreal marine fauna. Journal of Evolutionary Biology, 34(1), 73-96. https://doi.org/10.1111/jeb.13674.

Lamarck, J.B. de, 1816. Histoire naturelle des animaux sans vertébrés, 3: 1-586.

Lang, K., 1939. Über die Entwicklung von *Priapulus caudatus* LAM. Kungl. Fysiografiska Sällskapets I Lund Förhandlingar, 9, 80-87.

Lang, K., 1948. On the morphology of the larva of *Priapulus caudatus* Lam. Arkiv För Zoologi, 41(9), 1-9.

Lang, K., 1951. *Priapulus caudatus* Lam. and *Priapulus caudatus* forma *tuberculato-spinosus* Baird represent two different species. Arkiv För Zoologi, 2(11), 565-568.

Laumer, C., Bekkouche, N., Kerbl, A., Goetz, F., Neves, R., Sørensen, M., Kristensen, R., Hejnol, A., Dunn, C., Giribet, G., Worsaae, K., 2015. Spiralian phylogeny informs the evolution of

microscopic lineages. Current Biology, 25(15), 2000-2006. https://doi.org/10.1016/j.cub.2015.06.068.

Laumer, C.E., Fernández, R., Lemer, S., Combosch, D.J., Kocot, K.M., Riesgo, A., Andrade, S.C.S., Sterrer, W., Sørensen, M., Giribet, G., 2019. Revisiting metazoan phylogeny with genomic sampling of all phyla. Proceedings of the Royal Society B: Biological Sciences, 286, 20190831. https://doi.org/10.1016/j.cub.2015.06.068.

Le Bris, N., Gaill, F., 2007. How does the annelid *Alvinella pompejana* deal with an extreme hydrothermal environment?. Reviews in Environmental Science and Bio/Technology, 6, 197-221. https://doi.org/10.1007/s11157-006-9112-1.

Lemburg, C., 1995a. Ultrastructure of sense organs and receptor cells of the neck and lorica of the *Halicryptus spinulosus* larva (Priapulida). Microfauna Marina, 10, 7-30.

Lemburg, C., 1995b. Ultrastructure of the introvert and associated structures of the larvae of *Halicryptus spinulosus* (Priapulida). Zoomorphology, 115(1), 11-29. https://doi.org/10.1007/BF00397931.

Lemburg, C., 1999. Ultrastrukturelle Untersuchungen an den Larven von *Halicryptus spinulosus* und *Priapulus caudatus*: Hypothesen zur Phylogenie der Priapulida und deren Bedeutung für die Evolution der Nemathelminthes. Cuvillier.

Literman, R., Windsor, A.M., Bart Jr, H.L., Sage Hunter, E., Deeds, J.R., Handy, S.M., 2023. Using low-coverage whole genome sequencing (genome skimming) to delineate three introgressed species of buffalofish (*Ictiobus*). Molecular Phylogenetics and Evolution, 182, 107715. https://doi.org/10.1016/j.ympev.2023.107715.

Lord, A., Cunha, T.J., de Medeiros, B.A.S., Sato, S., Khost, D.E., Sackton, T.B., Giribet, G., 2023. Expanding on our knowledge of ecdysozoan genomes, a contiguous assembly of the meiofaunal priapulan *Tubiluchus corallicola*. Genome Biology and Evolution, 15, evad103. https://doi.org/10.1093/gbe/evad103.

Lüling, K.H., 1940. Über die Entwicklung des Urogenitalsystems der Priapuliden. Zeitschrift für wissenschaftliche Zoologie, 153, 136-180.

Makarova, A.A., Diakova, A.A., Chaika, S.Y., Polilov, A.A., 2022. Scaling of the Sense Organs of Insects. 2. Sensilla. Discussion. Conclusion. Entomological Review, 102(3), 323-346. https://doi.org/10.1134/S0013873822030058.

Malakhov, V.V., 1978. New representative of sedentary priapulid *Chaetostephanus cirratus* sp.n.. Zoologicheskii Zhurnal, 58, 1410-1412. [In Russian]

Mallatt, J., Winchell, C.J., 2002. Testing the new animal phylogeny: first use of combined large-subunit and small-subunit rRNA gene sequences to classify the protostomes. Molecular Biology and Evolution, 19(3), 289-301. https://doi.org/10.1093/oxfordjournals.molbev.a004082.

Marshall, D.J., Krug, P.J., Kupriyanova, E.K., Byrne, M., Emlet, R.B., 2012. The biogeography of marine invertebrate life histories. Annual Review of Ecology, Evolution, and Systematics, 43(1), 97-114. https://doi.org/10.1146/annurev-ecolsys-102710-145004.

Martín-Durán, J.M., Janssen, R., Wennberg, S., Budd, G.E., Hejnol, A., 2012. Deuterostomic development in the protostome *Priapulus caudatus*. Current Biology, 22, 2161-2166. https://doi.org/10.1016/j.cub.2012.09.037.

References

Martín-Durán, J.M., Wolff, G.H., Strausfeld, N.J., Hejnol, A., 2016. The larval nervous system of the penis worm *Priapulus caudatus* (Ecdysozoa). Philosophical Transactions of the Royal Society B: Biological Sciences, 371(1685), 20150050. https://doi.org/10.1098/rstb.2015.0050.

Mattisson, A., Fänge, R., 1973. Ultrastructure of erythrocytes and leucocytes of *Priapulus caudatus* (de Lamarck) (Priapulida). Journal of Morphology, 140(3), 367-379. https://doi.org/10.1002/jmor.1051400309.

Mattisson, A., Nilsson, S., Fänge, R., 1974. Light microscopical and ultrastructural organization of muscles of *Priapulus caudatus* (Priapulida) and their responses to drugs, with phylogenetic remarks. Zoologica Scripta, 3(5-6), 209-218. https://doi.org/10.1111/j.1463-6409.1974.tb00818.x.

Merriman, J.A., 1981. Cuticular structures of the priapulid *Halicryptus spinulosus*: A scanning electron microscopical study. Zoomorphology, 97, 285-295. https://doi.org/10.1007/BF00310281.

Moritz, K., 1972. Fine structure of integumental features in priapulids (*Halicryptus spinulosus* and *Priapulus caudatus*). Zeitschrift für Morphologie der Tiere, 72, 203-230. https://doi.org/10.1007/BF00391552.

Morse, M.P., 1981. *Meiopriapulus fijiensis* n. gen., n. sp.: an interstitial priapulid from coarse sand in Fiji. Transactions of the American Microscopical Society, 100(3), 239-252. https://doi.org/10.2307/3225549.

Neuhaus, B., 2013. Kinorhyncha (= Echinodera). In: Schmidt-Rhaesa, A., editor. Handbook of Zoology: Nematomorpha, Priapulida, Kinorhyncha and Loricifera. Volume 1. Berlin: Walter de Gruyter, 181-348. https://doi.org/10.1515/9783110272536.181.

Neuhaus, B., Higgins, R.P., 2002. Ultrastructure, biology, and phylogenetic relationships of Kinorhyncha. Integrative and Comparative Biology, 42(3), 619-632. https://doi.org/10.1093/icb/42.3.619.

Neves, R.C., Kristensen, R.M., Møbjerg, N., 2021. New records on the rich loriciferan fauna of Trezen ar Skoden (Roscoff, France): Description of two new species of *Nanaloricus* and the new genus *Scutiloricus*. Plos one, 16(5), e0250403. https://doi.org/10.1371/journal.pone.0250403.

Neves, R.C., Kristensen, R.M., Rocha-Olivares, A., Rivas, G., 2022. A first look at the biodiversity of Loricifera in the southern Gulf of Mexico. Frontiers in Marine Science, 9, 944795. https://doi.org/10.3389/fmars.2022.944795.

Nielsen, C., 2012. Animal evolution: interrelationships of the living phyla. 3rd ed. Oxford: Oxford University Press.

Nyholm, K. G., Bornö, C., 1969. Introductory studies of the oxygen intake of *Priapulus caudatus* Lam. Zoologiska Bidrag, 38, 262-264.

Oeschger, R., 1990. Long-term anaerobiosis in sublittoral marine invertebrates from the Western Baltic Sea: *Halicryptus spinulosus* (Priapulida), *Astarte borealis* and *Arctica islandica* (Bivalvia). Marine Ecology Progress Series, 59(1/2), 133-143. http://www.jstor.org/stable/24842429.

Oeschger, R., Janssen, H.H., 1991. Histological studies on *Halicryptus spinulosus* (Priapulida) with regard to environmental hydrogen sulfide resistance. Hydrobiologia, 222, 1-12. https://doi.org/10.1007/BF00017494.

Ockelmann, K.W., 1964. An improved detritus-sledge for collecting meiobenthos. Ophelia, 1(2), 217-222. https://doi.org/10.1080/00785326.1964.10416279.

References

Park, J.K., Rho, H.S., Kristensen, R.M., Kim, W., Giribet, G., 2006. First molecular data on the phylum Loricifera–an investigation into the phylogeny of Ecdysozoa with emphasis on the positions of Loricifera and Priapulida. Zoological Science, 23(11), 943-954. https://doi.org/10.2108/zsj.23.943.

Paulay, G., Holthuis, B.V., 1994. Biology and morphology of living *Meiopriapulus fijiensis* Morse (Priapulida). In: Wilson, W.H., Stricker, S.A., Shinn, G.L., editors, Reproduction and Development of Marine Invertebrates, 158-165. John Hopkins Press, London.

Paulay, G., 2024. World List of Priapulida. Priapulida. Accessed through: World Register of Marine Species at: https://marinespecies.org/aphia.php?p=taxdetails&id=101063 on 2024-10-18.

Peel, J.S., 2022. A priapulid larva from the middle Cambrian (Wuliuan Stage) of North Greenland (Laurentia). Bulletin of Geosciences, 97(4), 445-452. https://doi.org/10.3140/bull.geosci.1865.

Por, F.D., 1972. Priapulida from deep bottoms near Cyprus. Israel Journal of Zoology, 21(3-4), 525-528.

Por, F.D., Bromley, H.J., 1974. Morphology and anatomy of *Maccabeus tentaculatus* (Priapulida: Seticoronaria). Journal of Zoology, 173(2), 173-197. https://doi.org/10.1111/j.1469-7998.1974.tb03125.x.

Rogers, A. D., Miloslavich, P., Obura, D., Aburto-Oropreza, O., 2023. Marine Invertebrates. In: McLean, N., editor. The Living Planet. The State of the World's Wildlife. Cambridge University Press, 249-269.

Rothe, B.H., Schmidt-Rhaesa, A., Todaro, M.A., 2006. The general muscular architecture in *Tubiluchus troglodytes* (Priapulida). Meiofauna Marine, 15, 79-86.

Rothe, B.H., Schmidt-Rhaesa, A., 2010. Structure of the nervous system in *Tubiluchus troglodytes* (Priapulida). Invertebrate Biology, 129(1), 39-58. https://doi.org/10.1111/j.1744-7410.2010.00185.x.

Rucci, K.A., Neuhaus, B., Bulnes, V.N., 2022. A new species of *Echinoderes* (Kinorhyncha: Cyclorhagida: Echinoderidae) from the Argentinean continental shelf with notes on its postembryonic development and on subcuticular morphological characters unreported for Kinorhyncha. Zootaxa, 5099(1), 65-90. https://doi.org/10.11646/zootaxa.5099.1.3.

Salvini-Plawen, L. von, 1973. Ein neuer Priapulide mit Kleptocniden aus dem Adriatischen Meer. Marine Biology, 20, 165-169. https://doi.org/10.1007/BF00351455.

Salvini-Plawen, L. von, 1974. Zur Morphologie und Systematik der Priapulida: *Chaetostephanus praeposteriens*, der Vertreter einer neuen Ordnung Seticoronaria. Journal of Zoological Systematics and Evolutionary Research, 12(1), 31-54. https://doi.org/10.1111/j.1439-0469.1974.tb00156.x.

Sanders, H.L., Hessler, R.R., 1962. *Priapulus atlantisi* and *Priapulus profundus*. Two new species of Priapulids from bathyal and abyssal depths of the North Atlantic. Deep Sea Research and Oceanographic Abstracts, 9, 125-130. https://doi.org/10.1016/0011-7471(62)90004-9.

Scharff, R., 1885. On the skin and nervous system of *Priapulus* and *Halicryptus*. Quarterly Journal of Microscopical Science, 25, 193-213. https://doi.org/10.1242/jcs.s2-25.98.193.

References

Schmidt-Rhaesa, A., 2013. Priapulida. In: Schmidt-Rhaesa A., editor. Handbook of Zoology: Nematomorpha, Priapulida, Kinorhyncha and Loricifera. Volume 1. Berlin: Walter de Gruyter, 147-180. https://doi.org/10.1515/9783110272536.147.

Schmidt-Rhaesa, A., Bartolomaeus, T., Lemburg, C., Ehlers, U., Garey, J.R., 1998. The position of the Arthropoda in the phylogenetic system. Journal of Morphology, 238(3), 263-285. https://doi.org/10.1002/(SICI)1097-4687(199812)238:3<263::AID-JMOR1>3.0.CO;2-L.

Schmidt-Rhaesa, A., Cañete, J.I., Mutschke, E., 2022. New record and first description including SEM and μCT of the rare priapulid *Acanthopriapulus horridus* (Priapulida, Scalidophora). Zoologischer Anzeiger, 298, 1-9. https://doi.org/10.1016/j.jcz.2022.03.001.

Schmidt-Rhaesa, A., Freese, M., 2019. Microscopic priapulid larvae from Antarctica. Zoologischer Anzeiger, 282, 3-9. https://doi.org/10.1016/j.jcz.2019.06.001.

Schmidt-Rhaesa, A., Panpeng, S., Yamasaki, H., 2017. Two new species of *Tubiluchus* (Priapulida) from Japan. Zoologischer Anzeiger, 267, 155-167. https://doi.org/10.1016/j.jcz.2017.03.004.

Schmidt-Rhaesa, A., Rothe, B.H., Martínez, A.G., 2013. *Tubiluchus lemburgi*, a new species of meiobenthic Priapulida. Zoologischer Anzeiger, 253(2), 158-163. https://doi.org/10.1016/j.jcz.2013.08.004.

Schreiber, A., Eisinger, M., Rumohr, H., Storch, V., 1996. Icy heritage: ecological evolution of the postglacial Baltic Sea reflected in the allozymes of a living fossil, the priapulid *Halicryptus spinulosus*. Marine Biology, 125, 671-685. https://doi.org/10.1007/BF00349249.

Shao, T.Q., Wang, Q., Liu, Y.H., Qin, J.C., Zhang, Y.N., Liu, M.J., Shao, Y., Zhao, J.Y., Zhang, H.Q., 2020. A new scalidophoran animal from the Cambrian Fortunian Stage of South China and its implications for the origin and early evolution of Kinorhyncha. Precambrian Research, 349, 105616. https://doi.org/10.1016/j.precamres.2020.105616.

Shirley, T.C., 1990. Ecology of *Priapulus caudatus* Lamarck, 1816 (Priapulida) in an Alaskan subarctic ecosystem. Bulletin of Marine Science, 47(1), 149-158.

Shirley, T.C., Storch, V., 1999. *Halicryptus higginsi* n.sp. (Priapulida) – a giant new species from Barrow, Alaska. Invertebrate Biology, 118, 404-413. https://doi.org/10.2307/3227009.

Slater, B.J., Harvey, T.H., Guilbaud, R., Butterfield, N.J., 2017. A cryptic record of Burgess Shale-type diversity from the early Cambrian of Baltica. Palaeontology, 60(1), 117-140. https://doi.org/10.1111/pala.12273.

Smith, M.R., Harvey, T.H., Butterfield, N.J., 2015. The macro-and microfossil record of the Cambrian priapulid *Ottoia*. Palaeontology, 58(4), 705-721. https://doi.org/10.1111/pala.12168.

Sørensen, M.V., Grzelak, K., Kristensen, R.M., Herranz, M., 2022. First account on Loricifera from New Zealand: A new species of *Pliciloricus*, and a Shira larva with postlarva representing the new genus and species *Patuloricus tangaroa* gen. et sp. nov. Zoologischer Anzeiger, 299, 207-220. https://doi.org/10.1016/j.jcz.2022.06.004.

Sørensen, M.V., Hebsgaard, M.B., Heiner, I., Glenner, H., Willerslev, E., Kristensen, R.M., 2008. New Data from an Enigmatic Phylum: Evidence from molecular sequence data supports a sister group relationship between Loricifera and Nematomorpha. Journal of Zoological Systematics and Evolutionary Research, 46, 231-239. https://doi.org/10.1111/j.1439-0469.2008.00478.x.

References

Sørensen, M.V., Herranz, M., Grzelak, K., Shimabukuro, M., Kristensen, R.M., Zeppilli, D., 2023. Living on the edge–first survey of loriciferans along the Atacama Trench. European journal of taxonomy, 879, 162-187. https://doi.org/10.5852/ejt.2023.879.2169.

Sørensen, M.V., Rho, H S., Min, W.G., Kim, D., 2012. A new recording of the rare priapulid *Meiopriapulus fijiensis*, with comparative notes on juvenile and adult morphology. Zoologischer Anzeiger, 251(4), 364-371. https://doi.org/10.1016/j.jcz.2011.10.001.

Storch, V., Higgins, R.P., Morse, M.P., 1989. Ultrastructure of the body wall of *Meiopriapulus fijiensis* (Priapulida). Transactions of the American Microscopical Society, 319-331. https://doi.org/10.2307/3226262.

Storch, V., Higgins, R.P., Rumohr, H., 1990. Ultrastructure of introvert and pharynx of *Halicryptus spinulosus* (Priapulida). Journal of morphology, 206(2), 163-171. https://doi.org/10.1002/jmor.1052060203.

Storch, V., Higgins, R.P., Morse, M.P., 1989. Internal anatomy of *Meiopriapulus fijiensis* (Priapulida). Transactions of the American Microscopical Society, 245-261. https://doi.org/10.2307/3226343.

Storch, V., Higgins, R.P., 1991. Scanning and transmission electron microscopic observations on the larva of *Halicryptus spinulosus* (Priapulida). Journal of Morphology, 210(2), 175-194. https://doi.org/10.1002/jmor.1052100207.

Storch, V., Higgins, R.P., Malakhov, V.V., Adrianov, A.V., 1994. Microscopic anatomy and ultrastructure of the introvert of *Priapulus caudatus* and *P. tuberculatospinosus* (Priapulida). Journal of Morphology, 220, 281-293. https://doi.org/10.1002/jmor.1052200307.

Storch, V., Higgins, R.P., Anderson, P., Svavarsson, J., 1995. Scanning and transmission electron microscopic analyses of the introvert of *Priapulopsis australis* and *Priapulopsis bicaudatus* (Priapulida). Invertebrate Biology, 114, 64-72. https://doi.org/10.2307/3226954.

Straub, S.C.K., Parks, M., Weitemier, K., Fishbein, M., Cronn, R.C., Liston, A., 2012. Navigating the tip of the genomic iceberg: next-generation sequencing for plant systematics. American Journal of Botany, 99, 349-364. https://doi.org/10.3732/ajb.1100335.

Taite, M., Fernández-Álvarez, F.Á., Braid, H.E., Bush, S.L., Bolstad, K., Drewery, J., Mills, S., Strugnell, J.M., Vecchione, M., Villanueva, R., Voight, J.R., Allcock, A.L., 2023. Genome skimming elucidates the evolutionary history of Octopoda. Molecular Phylogenetics and Evolution, 182, 107729. https://doi.org/10.1016/j.ympev.2023.107729.

Théel, H.J., 1911. Priapulids and Sipunculids dredged by the Swedish Antarctic Expedition 1901–1903 and the phenomen of bipolarity. Kungl. Svenska Vetenskapsakademiens Handlingar, 47, 3–36.

Todaro, M.A., Shirley, T.C., 2003. A new meiobenthic priapulid (Priapulida, Tubiluchidae) from a Mediterranean submarine cave. Italian Journal of Zoology, 70(1), 79-87. https://doi.org/10.1080/11250000309356499.

Todaro, M.A., Telford, M.J., Lockyer, A.E., Littlewood, D.T.J., 2006. Interrelationships of the Gastrotricha and their place among the Metazoa inferred from 18S rRNA genes. Zoologica Scripta, 35(3), 251-259. https://doi.org/10.1111/j.1463-6409.2006.00228.x.

Tommasi, L.R., 1968. The Priapulida, a marine class of Aschelminthes new to Brazil. Cont. Inst. Oceanogr. Univ. Sao Paolo, Ser. Ocean. Biol., 13, 1-14.

References

Turk, K.A., Wehrmann, A., Laflamme, M., Darroch, S.A., 2024. Priapulid neoichnology, ecosystem engineering, and the Ediacaran–Cambrian transition. Palaeontology, 67(4), e12721. https://doi.org/10.1111/pala.12721.

Van der Land, J., 1968. A new aschelminth, probably related to the Priapulida. Zoologische Mededelingen, 42(22), 237-250.

Van der Land, J., 1970. Systematics, geography, and ecology of the Priapulida. Zoologische Verhandelingen, 112(1), 1-118.

Van der Land, J., 1972. *Priapulus* from the deep sea (Vermes, Priapulida). Zoologische Mededelingen, 47(27), 358-368.

Van der Land, J., 1982. A new species of *Tubiluchus* (Priapulida) from the Red Sea. Netherlands Journal of Zoology, 32, 324-335.

Van der Land, J., 1985. Two new species of *Tubiluchus* (Priapulida) from the Pacific Ocean. Proceedings of the Koninklijke Nederlandse Akademie van Wetenschappen, 88, 371-377.

Van Der Land, J., Nørrevang, A., 1985. Affinities and intraphyletic relationships of the Priapulida. In: Conway Morris, S., George, J.D., Gibson, R., Platt, H.M. (eds.), The origins and relationships of lower invertebrates. Clarendon Press, Oxford, 261-273.

Von Siebold, C.T., 1849. Beiträge zur Fauna Preussens. Neue Preuss. Provincialbl., 7, 184-185.

Walcott, C.D., 1911. Cambrian geology and paleontology II: No. 5. Middle Cambrian annelids. Smithsonian Institution, Washington DC.

Wennberg, S.A., Janssen, R., Budd, G.E., 2009. Hatching and earliest larval stages of the priapulid worm *Priapulus caudatus*. Invertebrate Biology, 128(2), 157-171. https://doi.org/10.1111/j.1744-7410.2008.00162.x.

Wernström, J.V., Slater, B.J., Sørensen, M.V., Crampton, D., Altenburger, A., 2023. Geometric morphometrics of macro-and meiofaunal priapulid pharyngeal teeth provides a proxy for studying Cambrian "tooth taxa". Zoomorphology, 142(4), 411-421. https://doi.org/10.1007/s00435-023-00617-4.

Wesenberg-Lund, E., 1930. Priapulidae and sipunculidae. The Danish Ingolf-Expedition 4, 1-44.

Westheide, W., 1990. *Meiopriapulus fijiensis* Morse (Priapulida) from south Adaman, another example of large-scale geographic distribution of interstitial marine meiofauna taxa. Proceedings of the Biological Society of Washington, 103(4), 784-788.

Willems, W.R., Curini-Galletti, M., Ferrero, T.J., Fontaneto, D., Heiner, I., Huys, R., Ivanenko, V.N., Kristensen, R.M., Kånneby, T., MacNaughton, M.O., Martínez Arbizu, P., Todaro, M.A., Sterrer, W., Jondelius, U., 2009. Meiofauna of the Koster-area, results from a workshop at the Sven Lovén Centre for Marine Sciences (Tjärnö, Sweden). Meiofauna marina, 17, 1-34.

Wills, M.A., 1998. Cambrian and Recent disparity: the picture from priapulids. Paleobiology, 24, 177-199. https://doi.org/10.1666/0094-8373(1998)024[0177:CARDTP]2.3.CO;2.

Wills, M.A., Gerber, S., Ruta, M., Hughes, M., 2012. The disparity of priapulid, archaeopriapulid and palaeoscolecid worms in the light of new data. Journal of Evolutionary Biology, 25(10), 2056-2076. https://doi.org/10.1111/j.1420-9101.2012.02586.x.

References

Worsaae, K., Vinther, J., Sørensen M.V., 2023. Evolution of Bilateria from a Meiofauna perspective - Miniaturization in the focus. In: Giere, O., Schratzberger, M., (Eds.). New Horizons in Meiobenthos Research. Springer, Cham, 1-31. https://doi.org/10.1007/978-3-031-21622-0_1.

WoRMS Editorial Board, 2024. World Register of Marine Species. Available from https://www.marinespecies.org at VLIZ. Accessed 2024-10-30. https://doi.org/10.14284/170.

Yamasaki, H., Fujimoto, S., Miyazaki, K., 2015. Phylogenetic position of Loricifera inferred from nearly complete 18S and 28S rRNA gene sequences. Zoological letters, 1, 1-9. https://doi.org/10.1186/s40851-015-0017-0.

Zhang, H., Xiao, S., Liu, Y., Yuan, X., Wan, B., Muscente, A.D., Shao, T., Gong, H., Cao, G., 2015. Armored kinorhynch-like scalidophoran animals from the early Cambrian. Scientific Reports, 5(1). https://doi.org/10.1038/srep16521.

Acknowledgements

I would like to express my gratitude to both my supervisors, Andreas Schmidt-Rhaesa and Katrine Worsaae, for giving me the opportunity to do my doctoral degree under their guidance. Your excellent expertise, support and advices during this thesis contributed significantly to the research topics of this thesis.

I would like to thank Marie Herberstein for serving as an examiner of this thesis.

Moreover, I am thankful for the German Research Foundation (Deutsche Forschungsgemeinschaft) for funding this research project to Andreas Schmidt-Rhaesa and Katrine Worsaae (SCHM 1278/20-1).

A special thanks goes to Karolin Engelkes and Lena Schwinger from the Morphology Lab of the LIB Hamburg, as well as Frank Friedrich and Elke Woelken from the Electron Microscopy Department of the University of Hamburg, for their essential help with the conducted morphological examinations during this thesis.

I want to thank María Herranz for the substantial guidance during the molecular work in the Worsaae Lab at the University of Copenhagen and for her help with the phylogenomic analyses.

I would also like to thank Gonzalo Giribet and Arianna Lord (Museum of Comparative Zoology, Harvard University) for their cooperation and essential contributions to the phylogenomic analyses.

I want to thank everybody, who provided specimens and essential support during field trips: Alejandro Martínez, Ekin Tilic, Katrin Iken, Anna J. Phillips, Glafira Kolbasova, Saskia Brix, Katherine A. Turk, Michelle Kelly, Sadie Mills, Richard Taylor, Ursula Schwarz and Frank Melzner. Without your help, this project would not have been possible.

I want to thank the whole Scalidophora community for their encouragement and support during this project. Especially, Martin V. Sørensen and María Herranz provided helpful information and images regarding Loricifera and Kinorhyncha. I am also grateful to Hiroshi Yamasaki for enabling me to participate in the VII. International Scalidophora Workshop in Japan.

Many thanks go to my working group, Helma Roggenbuck, Hilke Ruhberg, Herbert Jelinek and Andreas Schmidt-Rhaesa, as well as to former members Lenke Tödter, Katharina Ritt, Yander Luis Diez Garcia and Peter Smirnov. I am grateful for all of your support and I always enjoyed our Wednesday's meetings and the following visit of the Asia Lounge!

I am deeply grateful to my fellow colleagues, Melissa Aksoy, Katharina Gebauer, Jenni Lauschke, Lena Schwinger, Simon Bober, Markus Reinhardt and Thilo Weddehage, as well as my fellow PhD students, Elisa Becher, Eda Dönmez, Robin Saulnier Masson and Jesse Theilen for our insane amount of humorously lunch and coffee + sweets breaks!

A special thanks goes out to Peter for our movie nights with takeout food.

My biggest gratitude goes to my most important emotional supporters: my parents, Sonja and Holger, and my brother Tim. I am deeply thankful for all your motivation and encouragement!

Eidesstattliche Versicherung / Affidavit

Hiermit versichere ich an Eides statt, die vorliegende Dissertationsschrift selbst verfasst und keine anderen als die angegebenen Hilfsmittel und Quellen benutzt zu haben.
Sofern im Zuge der Erstellung der vorliegenden Dissertationsschrift generative Künstliche Intelligenz (gKI) basierte elektronische Hilfsmittel verwendet wurden, versichere ich, dass meine eigene Leistung im Vordergrund stand und dass eine vollständige Dokumentation aller verwendeten Hilfsmittel gemäß der Guten wissenschaftlichen Praxis vorliegt. Ich trage die Verantwortung für eventuell durch die gKI generierte fehlerhafte oder verzerrte Inhalte, fehlerhafte Referenzen, Verstöße gegen das Datenschutz- und Urheberrecht oder Plagiate.

I hereby declare and affirm that this doctoral dissertation is my own work and that I have not used any aids and sources other than those indicated.
If electronic resources based on generative artificial intelligence (gAI) were used in the course of writing this dissertation, I confirm that my own work was the main and value-adding contribution and that complete documentation of all resources used is available in accordance with good scientific practice. I am responsible for any erroneous or distorted content, incorrect references, violations of data protection and copyright law or plagiarism that may have been generated by the gAI.

Hamburg, den 17.02.2025

Unterschrift / Signature

Studies

JCZ: Zoologischer Anzeiger - A Journal of Comparative Zoology 302 (2023) 1–16

Contents lists available at ScienceDirect

Zoologischer Anzeiger

journal homepage: www.elsevier.com/locate/jcz

Morphology of larval and postlarval stages of *Priapulopsis bicaudatus* (Danielssen, 1869) (Priapulida) from the north atlantic ocean

Andreas Schmidt-Rhaesa *, Jan Raeker

Museum of Nature Hamburg - Zoology, Leibniz Institute for the Analysis of Biodiversity Change (LIB) and University Hamburg, Martin-Luther-King-Platz 3, 20146, Hamburg, Germany

ARTICLE INFO

Corresponding Editor: Maikon Di Domenico

Keywords:
Priapulida
Ecdysozoa
SEM
Larva
Lorica
Introvert
Caudal appendage

ABSTRACT

We investigated larvae, postlarval stages and one adult of the priapulid *Priapulopsis bicaudatus* (Danielssen, 1869) collected in different locations in the North Atlantic between 300 and 1000 m depth. The superficial sculpture of the lorica of larvae remains unchanged in the stages investigated. We confirm the presence of frontal and laterofrontal lorica plates and the presence of first ring pharyngeal teeth with a distinct bipartition on one side. In postlarval stages, the separation of one first ring tooth into two parts could be demonstrated. All observed teeth possess receptors called tooth receptors. The paired caudal appendage, characteristic for the species, grows asymmetrically during early development. Ringpapillae appear late in development. The scalid arrangement basically corresponds between larvae and postlarval stages and can be generalized for priapulids. Additionally, scalids anterior of the primary scalids are reported in postlarval stages.

1. Introduction

Two species of macrofaunal priapulids, *Priapulus caudatus* Lamarck, 1816 and *Priapulopsis bicaudatus* (Danielssen, 1869), occur widespread throughout the oceans of the Northern Hemisphere. The latter, *P. bicaudatus*, was discovered in the Varangerfjord in Northeastern Norway and described by Danielssen (1869) under the name *Priapulus bicaudatus* in very short form and without illustration. In two subsequent publications, Koren & Danielssen (1876, 1877) described the species in further detail, first in Norwegian (1876) and then in English (1877). The genus name was changed to *Priapulopsis* (Koren & Danielssen, 1876) and then to *Priapuloides* (Koren & Danielssen, 1877), but later authors returned to *Priapulus bicaudatus*, until Van der Land (1970) suggested to place the species into its own genus, for which he used Koren & Danielssen's proposed generic name, *Priapulopsis*.

The most evident difference between *P. caudatus* and *P. bicaudatus* is, as their epithets suggest, that *P. caudatus* has one and *P. bicaudatus* has two caudal appendages. Théel (1911) noted notorious differences concerning the pharyngeal teeth of the two species, which had been overseen despite being quite conspicuous. In all priapulids, at least the anterior pharyngeal teeth are arranged in rings with the constant number of 5 teeth per ring. Exceptionally, in *P. bicaudatus* the first ring contains 10 small teeth, from which Théel (1911) already suspected that they originated by a division of one tooth into two smaller ones. The teeth in the third ring are the largest. Wesenberg-Lund (1930) noted further differences in the structure of scalids, which consist of two parts in *P. bicaudatus* in contrast to a single part in *P. caudatus*. Van der Land (1970) assumed that these scalids were telescopic.

A second species of the genus *Priapulopsis*, *P. australis*, was described from the Southern Hemisphere by De Guerne (1886) (first as *Priapuloides australis*). This species also has a paired caudal appendage, telescopic scalids and 10 anterior pharyngeal teeth, which are much more reduced than in *P. bicaudatus* (De Guerne, 1886; 1891; Storch et al., 1995). A third species, *P. cnidephorus* was incompletely described on the basis of one postlarval specimen collected in the Mediterranean Sea (Von Salvini-Plawen, 1973) and has been since then regarded as questionable species.

Since its description, *P. bicaudatus* has been reported only from the Northern Hemisphere (very few exceptions are probably misidentification, see Van der Land, 1970), with most records concentrated in the northern Atlantic Ocean and the Barents Sea (see Van der Land, 1970; Sørensen & Murina, 2009). Few records from the Pacific coast of Japan (between 32°40′ and 38°52′N) are a notable exception (Satô, 1934; see Van der Land, 1970 for further references). Sanders & Hessler (1962) described specimens collected in the Northwestern Atlantic Ocean as a new species, *Priapulus atlantisi*, but these were later regarded as young,

* Corresponding author.
E-mail address: a.schmidt-rhaesa@leibniz-lib.de (A. Schmidt-Rhaesa).

https://doi.org/10.1016/j.jcz.2022.11.006
Received 11 July 2022; Received in revised form 4 November 2022; Accepted 8 November 2022
Available online 13 November 2022
0044-5231/

Table 1
Numbering and locations of the investigated specimens. ZMH = Zoological Museum Hamburg (final accession number); DZMB = Deutsches Zentrum für Marine Biodiversitätsforschung (primary number); exp. = expedition: IA = IceAGE, IA2 = IceAGE2; stat. = station number; tool means collecting gear, AGT = Agassiz trawl, BC = box corer, with analysed fraction of core (in cm), EBS = epibenthic sledge, µm value gives mesh size of sieve used for sieving the sediment; latitude, longitude and depth show start and end point when tool (AGT, EBS) was pulled; depth in meter.

ZMH #	DZMB #	# specimens	locality	exp.	stat.	Date (day – month – year)	tool	latitude	longitude	depth
V13477	22,730	1 Juvenil	North-East Iceland, Norwegian Sea	IA	1213	22.09.2011	AGT	66° 33.160′ N-66° 33.270′ N	012° 53.400′ W-012° 53.600′ W	318.2–318.4
V13478	28,635	14 Larvae	East Iceland, Norwegian Sea	IA	1216	22.09.2011	BC, 0–2 cm, 300 µm	66° 18.060′ N	012° 22.380′ W	730.8
V13479	29,006	1 Larva	Norwegian Sea	IA	1216	22.09.2011	BC, 0–2 cm, 500 µm	66° 18.060′ N	012° 22.380′ W	730.8
V13480	30,625	1 Larva	East Greenland, Denmark Strait	IA	1129	14.09.2011	BC, 0–2 cm, 300 µm	67° 38.770′ N	026° 44.780′ W	320.6
V13481	30,921	1 Larva	East Greenland, Denmark Strait	IA	1129	14.09.2011	BC, 2–5 cm, 300 µm	67° 38.770′ N	026° 44.780′ W	320.6
V13482	31,068	1 Juvenil	East Greenland, Denmark Strait	IA	1116	14.09.2011	BC, 0–2 cm, 500 µm	67° 12.820′ N	026° 16.310′ W	683.1
V13483	32,166	1 Larva	Faroe Island Ridge, middle	IA2	879	31.07.2013	EBS, 300 µm	63° 06.100′ N-63° 05.620′ N	008° 34.320′ W-008° 36.220′ W	510.9–500.6
V13484	34,080	1 Juvenil	Faroe Island Ridge, North	IA2	881	01.08.2013	EBS, 300 µm	63° 34.660′ N-63° 36.210′ N	007° 42.690′ W-007° 44.790′ W	1043.6–1051.8
V13485	34,103	1 Juvenil	Faroe Island Ridge, North	IA2	881	01.08.2013	EBS, 300 µm	63° 36.540′ N-63° 38.330′ N	007° 45.210′ W-007° 46.690′ W	1056.2–1076.8
V13486	39,077	3 Larvae	Norwegian Channel	IA2	868	25.07.2013	BC, 0–2 cm, 300 µm	62° 12.490′ N	000° 15.670′ E	669.4
V13487	39,195	1 Larva	Norwegian Channel	IA2	868	25.07.2013	BC, 0–2 cm, 500 µm	62° 12.490′ N	000° 15.670′ E	669.4
V13488	41,157	8 Larvae	Faröer Channel, East	IA2	873	28.07.2013	van Veen grab, whole grab, 300 µm	61° 46.520′ N	003° 52.510′ W	833.8
V13489	41,482	11 Larvae	Faroe Island Ridge, middle	IA2	879	31.07.2013	Shipek Grab, whole grab, 300 µm	63° 06.020′ N	008° 35.140′ W	505.9
V13490	42,303	1 Larva	Faroe Island Ridge, middle	IA2	882	02.08.2013	EBS, 300 µm	63° 25.040′ N-63° 25.920′ N	010° 58.200′ W-010° 57.980′ W	440.5–441.8
V13491	42,304	10 Juvenils	Faroe Island Ridge, middle	IA2	882	02.08.2013	EBS, 300 µm	63° 25.040′ N-63° 25.920′ N	010° 58.200′ W-010° 57.980′ W	440.5–441.8
V13492	42,534	1 Adult	Faroe Island Ridge, middle	IA2	882	02.08.2013	van Veen, whole grab, hand sorting	63° 25.010′ N	010° 58.800′ W	441.4
V13493	42,618	2 Larvae 39 Juvenils	Faroe Island Ridge, middle	IA2	882	02.08.2013	EBS, 300 µm	63° 25.040′ N-63° 25.920′ N	010° 58.200′ W-010° 57.980′ W	440.5
V13494	42,619	16 Larvae	Faroe Island Ridge, middle	IA2	882	02.08.2013	EBS, 300 µm	63° 25.040′ N-63° 25.920′ N	010° 58.200′ W-010° 57.980′ W	440.5–441.8
V13495	43,003	3 Larvae	Faroe Island Ridge, North	IA2	881	01.08.2013	van Veen, whole grab, 300 µm	63° 38.500′ N	007° 47.030′ W	1073.4
V13496	51,390	28 Larvae 1 Juvenil	East Iceland, Norwegian Sea	IA	1217	22.09.2011	BC, 0–7 cm, 300 µm	66° 18.060′ N	012° 22.400′ W	732.1
V13497	51,487	4 Larvae 5 Juvenils	East Iceland, Norwegian Sea	IA	1217	22.09.2011	BC, 0–7 cm, 500 µm	66° 18.060′ N	012° 22.400′ W	732.1
V13498	54,328	1 Juvenil	East Greenland, Denmark Strait	IA	1119	14.09.2011	EBS, hand sorting	67° 12.810′ N-67° 12.830′ N	026° 14.500′ W-026° 13.510′ W	696.9–706.4
V13499	55,690	2 Juvenils	East Iceland, Norwegian Sea	IA	1222	22.09.2011	EBS	66° 17.490′ N-66° 17.760′ N	012° 21.090′ W-012° 21.720′ W	610.8–674
V13500	55,790	3 Larvae	East Iceland, Norwegian Sea	IA	1219	22.09.2011	EBS, 300 µm	66° 17.340′ N-66° 17.550′ N	012° 20.820′ W-012° 21.300′ W	579.1–622.4
V13501	56,032	1 Larva	Norwegian Channel	IA2	868	25.07.2013	BC, 0–2 cm, 300 µm	62° 12.520′ N	000° 15.720′ E	669.4
V13502	56,553	1 Juvenil	Faroe Island Ridge, middle	IA2	882	02.08.2013	van Veen, whole grab, 300 µm	63° 25.030′ N	010° 58.730′ W	439.6

postlarval stages of *P. bicaudatus* (Van der Land, 1970). Sanders & Hessler (1962) were the only ones to describe the putative larva of *P. bicaudatus*. Nine larvae were found at the same site where the postlarval specimens were collected. According to the description by Sanders & Hessler (1962), these larvae resemble those of other macroscopic priapulids in having a lorica composed of larger dorsal and ventral plates and additional lateral plates, on the margin of which a pair of tubuli arises on each side of the body. However, the larvae of *P. bicaudatus* differ from all other described larvae of priapulids in having a set of small anterior plates and in possessing several bristles scattered on the lorica.

The few morphological investigations by Koren & Danielssen (1877), Théel (1911), Wesenberg-Lund (1930), Sanders & Hessler (1962) and Van der Land (1970) are complemented by a single ultrastructural analysis by Storch et al. (1995). This is, however, rather brief concerning *P. bicaudatus* and concentrates on the structure of the scalids and to a lesser extent on the pharyngeal teeth. It is our aim to give a more detailed ultrastructural description of several life history stages based on scanning electron microscopy.

Additionally, very little is known about the development from embryo to adult in priapulids in general. It was discovered quite recently (Janssen et al., 2009; Wennberg et al., 2009) that at least in *Priapulus*

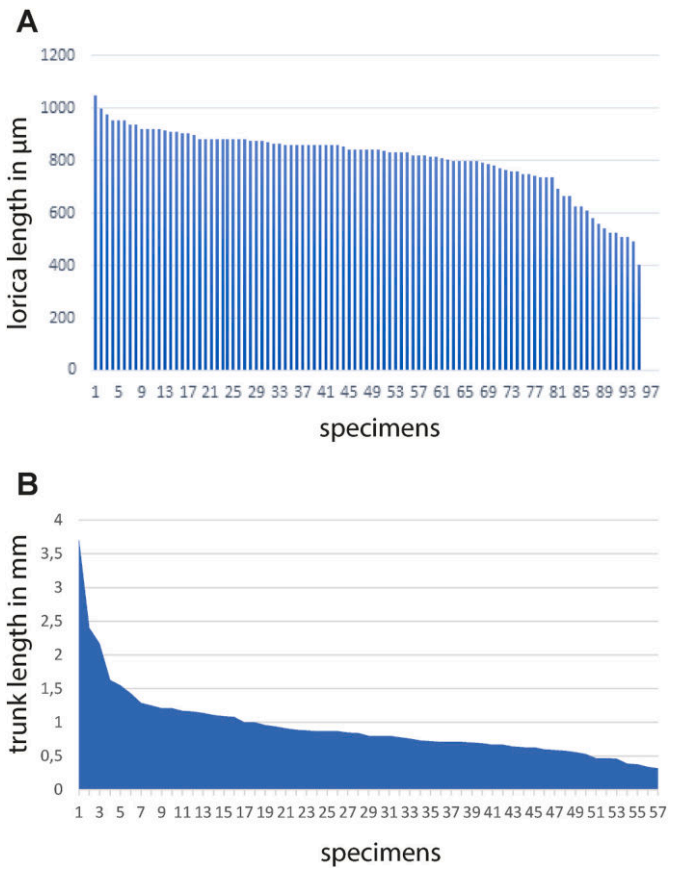

Fig. 1. Graphic representation of measurements. A. Lorica length in larvae, measured from light microscopical images. B. Trunk length in postlarval stages, the adult and the largest postlarval specimen (6.75 mm trunk length) were not included. Specimens (on x-axis) are ordered according to their length (longest to shortest).

caudatus and *Halicryptus spinulosus* hatching larvae do not possess a lorica. They molt into the loricate larva. Loricate larvae are known from most species, but it is only incompletely known how many larval stages are present and how the structure of the lorica changes during development. The larval development of *H. spinulosus* is quite well known (e.g. Hammarsten, 1913, Purasjoki, 1944; Storch & Higgins, 1991; Adrianov & Malakhov, 1996; Janssen et al., 2009). Higgins et al. (1993) investigated larval stages of *Priapulus caudatus* by documentation of a series with changing larval morphology, but from other species mostly only single stages are known. This fragmentary framework makes it quite challenging to identify newly found larvae (e.g. Schmidt-Rhaesa & Freese, 2019). The material investigated here includes larvae, postlarval and adult specimens and we have good arguments to assume that they all belong to *Priapulopsis bicaudatus*. It is the second aim of this investigation to describe the structural changes during development.

2. Material and methods

The specimens investigated were collected during the expeditions IceAGE (August 27 - September 28, 2011; Brix et al., 2012) and IceAGE2 (July 20 – August 4, 2013; Brix 2013) at different stations in the North Atlantic Ocean by different methods: Agassiz trawl, box corer, epibenthic sledge, Shipek grab and Van Veen grab. Sorting was done by hand or sieving. For details see Table 1.

In total, 99 larvae, 63 postlarval stages and one adult specimen were found. 95 larvae were documented with light microscopy, 57 were subsequently prepared for SEM. All 63 postlarval stages and the adult were documented with light microscopy, 30 postlarval stages and the adult were prepared for SEM. All specimens and SEM stubs are deposited in the Museum of Nature Hamburg, Leibniz Institute for the Analysis of Biodiversity Change (LIB), for accession numbers see Table 1.

All specimens were first photographed with a Keyence VHX-7000 digital light microscope using the stacking function for composed images of different focal layers. The adult was additionally photographed with an Olympus Stylus Tough camera. Several specimens were prepared for scanning electron microscopy (SEM). Specimens were dehydrated in series of ethanol dilutions in increasing concentrations, critical point dried in a Leica EM CPD300 and sputter coated with gold in a Leica EM ACE 600. Investigation took place with a LEO SEM 1524. The large specimen V13477 was cut in half before drying and the adult specimen V13492 was dissected and parts were prepared for SEM while the remaining pieces were stored in 70% ethanol.

Measurements were taken from scaled images of trunk, introvert and caudal appendage. During this process we discovered that the measurements from SEM images were consistently smaller those from light micrographs (see, e.g. Fig. 2A and B. Lorica length is, in the same specimen, 932 µm in the light microscopical image (A) and 820 µm in the SEM image (B), the width of the upper margin varies much less, it is 295 µm in A versus 280 µm in B). The calibration of scale bars was checked and found to be precise. Therefore, we assume a slight shrinkage during preparation for SEM. Additionally, most specimens fold more or less dramatically during SEM dehydration, which leads to additional problems in comparing measurements. Measurements from smaller structures were always made from SEM images. The total body length or the length of different body parts was usually reported from light microscographs.

Attempts to sequence the CO1 gene from larvae and postlarval stages remained unsuccessful for larvae despite trying different sets of primers.

3. Results

3.1. Larvae: lorica

The light micrographs were analyzed in search for size classes. The lorica length of the 95 larvae varies from 400 to 1055 µm, with a mean of 808.09 µm. A histogram of the measurements (Fig. 1A) shows that most loricae vary around the mean value. There is a steeper incline and decline towards the extreme values, but the sizes do not cluster in distinct size classes.

The lorica consists of large dorsal and ventral plates that are connected by six slender lateral plates (Fig. 2C–F). The lateral plates are folded in zig-zag and create 3 inner folding lines and two outer ridges (Fig. 2E and F). The outer ridges are more conspicuous than the inner folding lines. Three pairs of lateral plates are called, according to their position, sublateral or midlateral plates (Fig. 2E and F). We could not detect any differences in structure of the large lorica plates (one exception, see below), therefore we assume that dorsal and ventral plate are similar and we label them as dvp (dorsal/ventral plate) in the figures. Dorsal and ventral plates have a curved anterior margin (Fig. 2A–D); whereas their lateral margin is gently curved, first (starting from the anterior margin) inwards, then outwards, before the plates taper towards the narrower posterior margin (Fig. 2A and B). Some larvae appear thicker than others (Fig. 2C) due to the presence of an outfolding of the sublateral and midlateral plates (Fig. 2D). The dorsal/ventral plates are sculptured. With one exception (see below) the lorica substructure consists of few longitudinal ridges and multiple finer, perpendicular ridges, creating a pattern of rectangular compartments (Fig. 2B, D). There is one median longitudinal ridge, which is always the most prominent one and it reaches from the anterior to the posterior end (Fig. 2B, D). Two additional longitudinal ridges start from the anterior margin, but may become less obvious in the posterior region (Fig. 2B, D). We could not detect any structural differences in differently sized loricae. Only one lorica (larva 4 from V13478) had a different structure (Fig. 2G). Here the median ridge extends from the anterior to

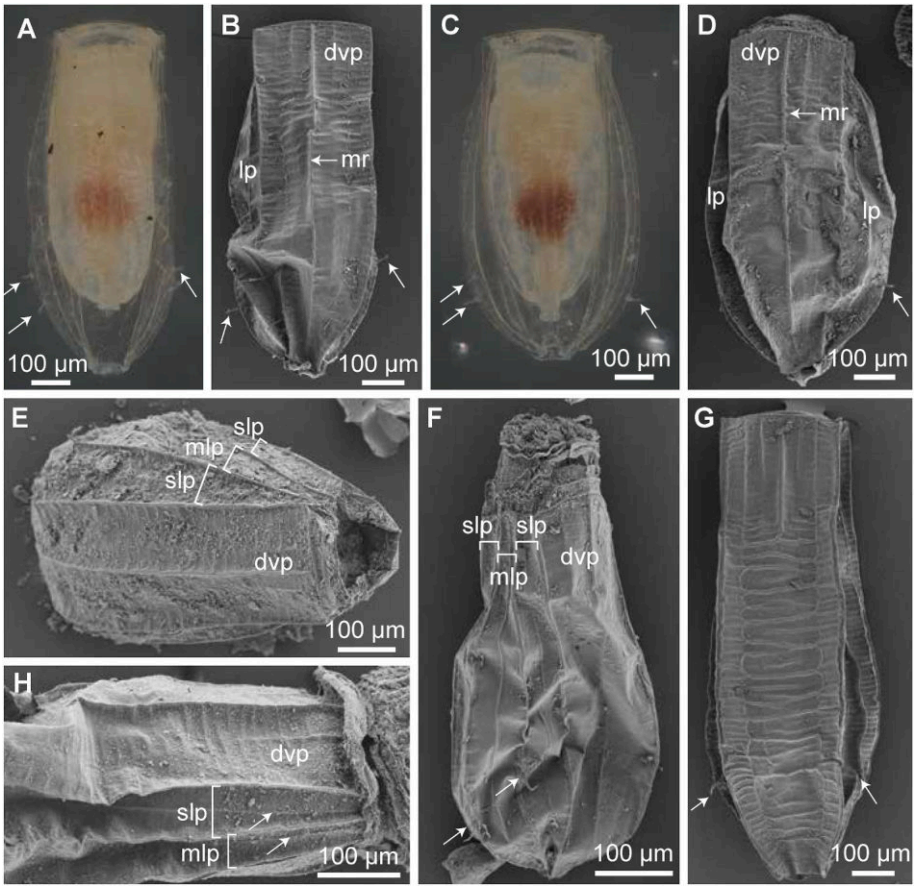

Fig. 2. Lorica structure. A, B. The same larva (29,006) imaged with light microscoy (A) and SEM (B). Note slight size differences and folding artifacts possibly due to preparation for SEM. Arrows indicate lateral tubuli (as in B-D, F and G). C, D. The broader and more oval appearance of some larvae is created by the outfolding of the lateral plates, as seen by SEM (D). E, F. Three pairs of lateral plates are present, named sublateral plates (slp) and midlateral plates (mlp). G. Structurally different lorica of specimen 28,635_4. H. Arrows indicate the inner folding edge between the two sublateral and the two midlateral plates. Further abbreviations: dvp = dorsal/ventral plate, mr = median ridge. A, C by light microscopy, B, D-H by SEM. A, B from V13479, C, D from larva 5 of V13478, E from larva 10 of V13494, F from larva 10 of V13478, H from larva 6 of V13488.

approximately one quarter of the lorica length. Two further pairs of longitudinal ridges are present, one of which fades out very soon, whereas the other, the most lateral one, runs to the posterior end. Together with the perpendicular ridges this creates a pattern of smaller lateral rectangles and large central rectangles. In addition, the perpendicular ridges in the median rectangles are irregular and partly incomplete (Fig. 2G). This larva measures 1055 µm in length and is therefore the largest larva in the sample.

Two tubuli per side are located at a level between 71 and 77% of the total lorica length, measured from anterior (Fig. 2A–D). They are situated on the ridges between sublateral and lateral plates (Fig. 2F). Each tubulus originates from a socket-like structure, the proximal part is composed of a series of ring-like structures and the distal part is a tube that becomes gradually thinner (Fig. 3A).

Anterior of the dorsal, ventral and lateral lorica plates are additional plates that act in closing the lorica. These plates were observed in very different stages of closure. There are two plates anterior of the dorsal and ventral ones, these are called frontal plates. Frontal plate 1 is trapezoid, almost as broad as the dorsal/ventral plate (Fig. 3B and C) and its lateral margins are oblique (Fig. 3B). The frontal plate 2 attaches at the frontal margin of frontal plate 1 and appears to be rectangular (Fig. 3B). Whereas frontal plate 1 lacks ornamentation, frontal plate 2 is subdivided by a median ridge (Fig. 3B). The margin between these two frontal plates is a very conspicuous ridge (Fig. 3B, C, E). During closure both frontal plates fold inwards, the dorsal and ventral plate approach each other and the gap between them is sealed by frontal plate 1 with the thick margins as the median structures (Fig. 3F). In some specimens, a pair of small laterofrontal plates seems to be present (Fig. 3C, E). Apparently no additional plates are present anterior of the lateral plates (Fig. 3E and F). During closure of the lorica, the anterior part of the lateral plates appears to be quite flexible and is compressed. In some cases this compressed anterior part artificially protrudes beyond the frontal margin of the lorica (Fig. 3D) and may be mistaken as an individual structure.

The transparent larvae allowed some observation of the internal structure using light microscopy, although these observations were limited by the opaque appearance of the fixed tissue. The body of some larvae occupies the lorica entirely (Fig. 4B and C), whereas in other larvae the body seems to be set off from the lorica and appears smaller than the lorica (Fig. 4A, H). In these last instances, the posterior end of the larval body is connected to the posterior end of the lorica by a funnel-like structure (Fig. 4A, D). A clear molt was observed in only one larva, where the larval body is detached from the lorica as described before, but in this case additionally a cuticular exuvia including the pharyngeal teeth is present in the anterior end of the larva (Fig. 4E). In some larvae the intestinal system was partly visible. In larvae with withdrawn introvert this consists of an anterior bulbous structure, likely the pharynx and a posterior bulbous structure, likely the midgut (Fig. 4F, H). From the midgut, a slender hindgut leads to the anus (Fig. 4F). In larvae with everted introvert, the thickening of the pharyngeal region is still present, but the remaining intestine is a straight tube (Fig. 4G).

3.2. *Larvae: introvert and pharyngeal teeth*

23 of the 57 larvae investigated by SEM had their introvert partly or fully everted. Due to the different extent of eversion, some characters could be observed only in few or single specimens.

The introvert is composed of three regions, a neck, the scalid region and the mouth cone (Figs. 5A and 6A). The neck is visible in only two larvae (larva 2 of V13489 and larva 1 of V13500), where the introvert is everted (Figs. 5A and 6A). In most larvae the introvert is less everted and only the scalid region is visible. The neck consists of a series of ring-

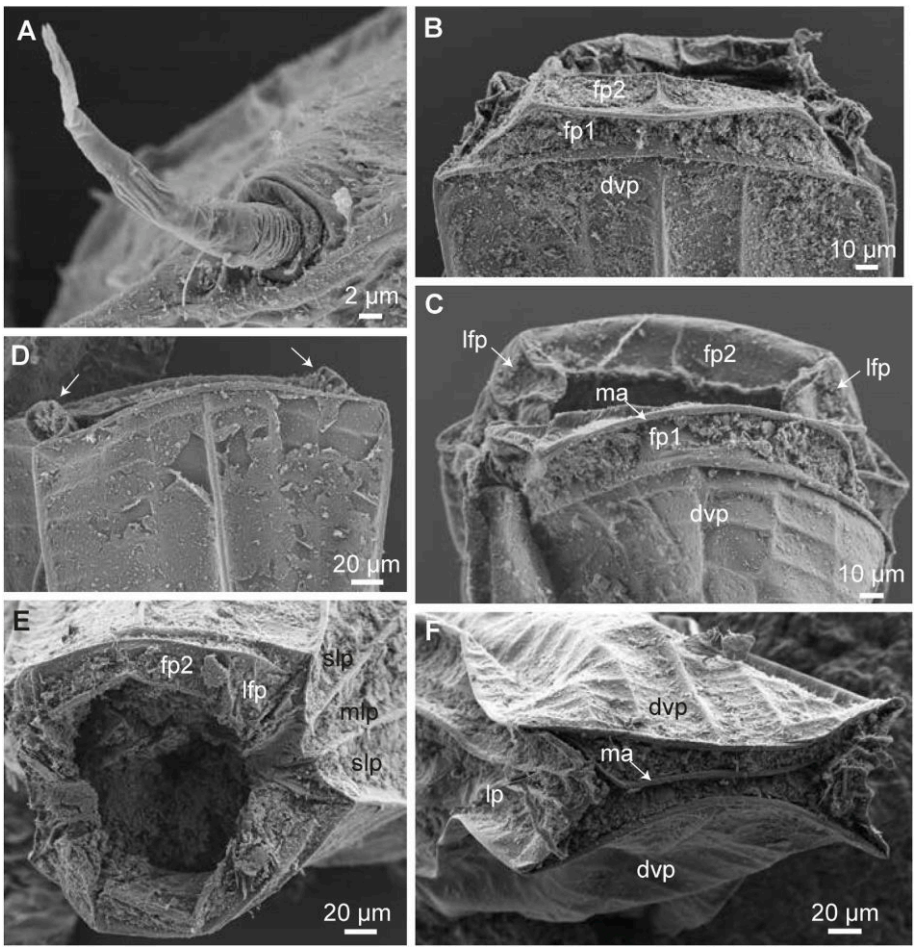

Fig. 3. Lorica: tubuli and frontal plates. A. Fine structure of a tubulus. B. Two frontal plates (fp1, fp2) are present frontal of the dorsal/ventral plate (dvp). C. A pair of laterofrontal plates (lfp) is visible in some specimens. The margin (ma) between frontal plates 1 and 2 is very prominent. D. The folded lateral plates may extend beyond the frontal margins in the closed lorica. E. Frontal view showing the frontal plate 2 and one laterofrontal plate. The sublateral (slp) and midlateral (mlp) plates do not have frontal plates. F. Frontal view on almost closed lorica, showing the prominent margin between the two frontal plates. All images by SEM. A from larva 10 of V13478, B from V13483, C from larva 2 of V13488, D-F from three different specimens of V13494.

folds, from which the posterior one is largest, followed by at least six smaller ones (Fig. 5A). The scalid region is densely covered by leaf-like scalids (in the following called "regular scalids") and an anterior ring of 8 primary scalids (Fig. 5A–C). The primary scalids are directed anteriorly, very slender and longer than the regular scalids (Fig. 5A–C). The regular scalids are mostly directed posteriorly and arranged in longitudinal rows of 6 or 7 scalids (Fig. 5D). In relation to the 8 primary scalids, the rows of the regular scalids are arranged in the following pattern: One row extends on a line exactly between two primary scalids and two rows are left and right of a virtual line extending from the primary scalids (Fig. 5C). The rows between the primary scalids start with a regular scalid that is more elongate and slender than the other regular scalids (Fig. 5B and C). The regular scalids in each row are arranged at different levels, but it was very difficult, if not impossible, to assign positions of scalids to comparable levels, i.e. into distinct rings.

The regular scalids are flat, leaf-like, triangular structures (Fig. 5D and E). The dorsal margin is broad and surrounding an inner triangular region (Fig. 5E). Both margin and triangle are finely granulated (Fig. 5E). The margin carries a pair of conical, tube-like structures with an apical opening (Fig. 5E). The distal region of the inner triangle carries a border of fringes. They overlap the broad margin and at the tip of the scalid and extend slightly over the edge of the scalid (Fig. 5E). The region between the scalids is structured by numerous circular and fewer longitudinal folds (Fig. 5D). The 8 anterior regular scalids from the rows between the primary scalids slightly differ in structure, as they are larger than the other regular scalids (Fig. 5B and C). A margin is absent, but the distal fringes are present.

The primary scalids are very long (about 43 µm) and slender. Their tip is curved, in some only slightly, in others strongly (Fig. 5A–C, F, G). The outer frontal side has a smooth surface, while the inner posterior side has a granulated surface (Fig. 5F and G). In the tip, the granulated region extends, the "granules" become larger (Fig. 5F and G) and partly form special arrangement patterns (Fig. 5G). The margin of the smooth region has spine-like fringes (Fig. 5G). On the "outer" side are irregular spines of different size (Fig. 5H).

The mouth cone opens in front of the primary scalids (Fig. 5A–C, 6A, B). In the maximally stretched larva V13500 it is 130 µm long (Fig. 6A). It consists of a frontal "ruff" and an area with smooth cuticle connecting the ruff with the scalid region. The ruff is structured mainly by longitudinal folds, sometimes also smaller circular ones (Figs. 5C and 6A). The ruff seems to be separated by a strong cuticular lamella (Fig. 5A). In some specimens, this lamella is the most frontal structure (Fig. 5C), therefore the ruff seems to be invaginable. No further structures (papillae, receptor structures etc.) are present on the mouth cone. Although termed "cone" here, the walls are only slightly inclined. The mouth cone surrounds a large circular mouth opening. In two specimens, pharyngeal teeth of the first two circles could be observed (Figs. 5B, 6A-F). The first ring is composed of 5 teeth (Fig. 6C). Each tooth appears from the outer side to be composed of two symmetrical parts (Fig. 6B–D), but on the inner side these parts are completely connected and appear as an oval structure with a smooth surface (Fig. 6C, E). On the frontal margin is a row of apical spines connecting both sides (Fig. 6D–F). Between the spines are two structures named here tooth receptors (Fig. 6E and F). They consist of a hemispherical base and an apical tube-like structure (Fig. 6E and F). Each tooth of the first ring is approximately 41 µm broad and 24 µm high, each of the bilateral parts measures 18.5 µm in width. Only one tooth of the second ring was observable (Fig. 6C), and this not in great detail.

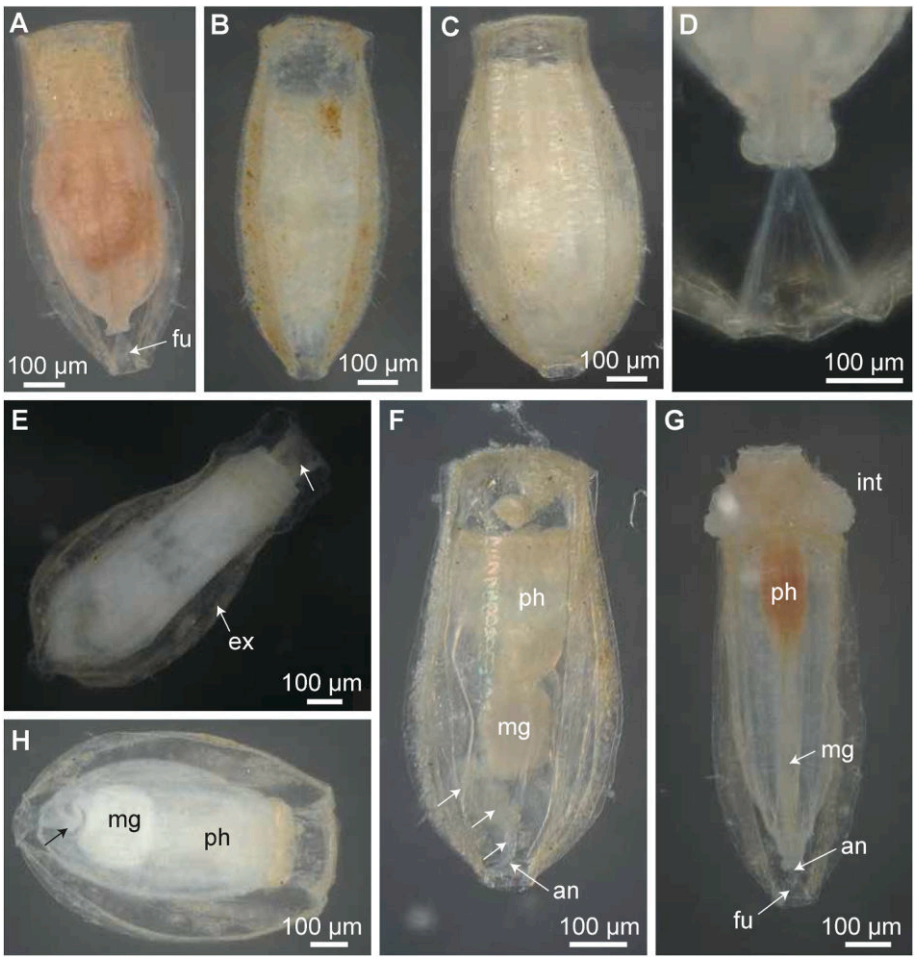

Fig. 4. Larvae, habitus and internal structure. A. Example of a specimen, where the larval body does not completely fill out the lorica volume. A funnel-shaped structure (fu) connects the putative anus with the posterior lorica margin. B, C. Examples of specimens, in which the larval body fills the lorica completely. D. Magnification of the funnel-structure. E. Larva in (putative) molt, ex = exuvia, recognizable by the molted scalids (arrow). F–H. Internal structure showing compartmentalization of the intestine in larvae with withdrawn introvert into a thicker pharyngeal region (ph), midgut (mg) and a more slender part (arrows), ending in the anus (an). In specimens with everted introvert, the intestine appears straight. All images by light microscopy. A, D from two different specimens of V13478, B from larva 1 of V13493, C from larva 3 of V13500, E from larva 1 of V13497, F from larva 12 of V13494, G from V13490, H from larva 1 of V13496.

3.2.1. Postlarval stages and adult

The trunk length of 57 specimens ranged from 0.3 mm to 3.7 mm, with a mean of 0.94 mm. There was one additional large specimen (6.75 mm trunk length) and the adult, which measures 47 mm in trunk length. The histogram of the measurements (Fig. 1B) shows that the majority of specimens ranges in size between around 0.3 and 1 mm and there are no size classes, but a gradual transition between body sizes. Few specimens represent larger sizes, but the number of specimens is too small to define size classes.

The introvert is in different degrees of eversion and the trunk musculature is in different stages of contraction, therefore the outer appearance of specimens differs on first view. In some specimens, the introvert is moderately everted (e.g. 7A, B), in others it is fully everted (Fig. 7C–G) and then often the anterior rings of pharyngeal teeth are visible on a mouth-cone-like structure (Fig. 7E and F). When the introvert is everted, the trunk (Fig. 7G) or parts of it (Fig. 7D–F) are contracted. One or two caudal appendages were observed, one of them is sometimes limited to a small bud (Fig. 7C, F). The adult specimen has its introvert partly everted (Fig. 7H) and two caudal appendages of similar size (Fig. 7I).

3.3. Trunk and caudal appendage(s)

The trunk surface is structured into rings that are separated by grooves, more evident in the adult than in younger stages. The trunk is covered densely by roundish structures, the tumuli (Fig. 8A, D). In some specimens, a longitudinal elevation was observed, probably marking the ventral midline (Fig. 8B and C). The elevation is also covered by tumuli (Fig. 8C). In one specimen (V13498), several papilliform structures were observed scattered throughout the trunk (Fig. 8E), each carrying several conical structures ending with one tube (Fig. 8F).

In the adult, there are three rings of elongated papillae (= ring-papillae) on the posterior rings (Fig. 8G and H). These reach 200 µm and are situated close together (Fig. 8H, I, K). They have a groove along the side facing anteriorly (Fig. 8I), that extends apically to a small depression (Fig. 8K). In the apical region there are several receptors composed of a semispherical base and one or two tubules (Fig. 8J). The surface of the posterior rings of the trunk contains fine longitudinal ridges (covered with tumuli). The edges of the grooves of the ringpapillae fan out and are continuous with these ridges (Fig. 8I). In the larger postlarval stages, ringpapillae are arranged in one to three rings as papillae (Fig. 8L and M), in some cases already containing the groove mentioned above (Fig. 8M). These papillae have few apical receptors (Fig. 8N).

Few specimens lack a caudal appendage, most species have one (Fig. 7A, B, D, E) and some specimens have two caudal appendages (Fig. 7C, G, H). When one caudal appendage is present, it is not in a central position, but slightly besides the center (Fig. 7A and B, 9A). When two caudal appendages are present, they are mostly unequal in length (Fig. 7F and G, 9B). Only in the adult (Fig. 7H and I), both caudal appendages are equally long. The anus is located between the two appendages (Fig. 9B). In some specimens, the caudal appendage is distinctly annulated (Figs. 7G and 9D), the annuli are ring-like thickenings. In shorter caudal appendages of smaller postlarval specimens the annulation is not very evident, but in some cases, there are repeated shallow grooves (Fig. 9C).

In the adult, the stem of the caudal appendages is equally thick and lateral structures, the vesicles, attach and cover the central stem almost completely (Fig. 7I). These vesicles are organized in rings, as is visible

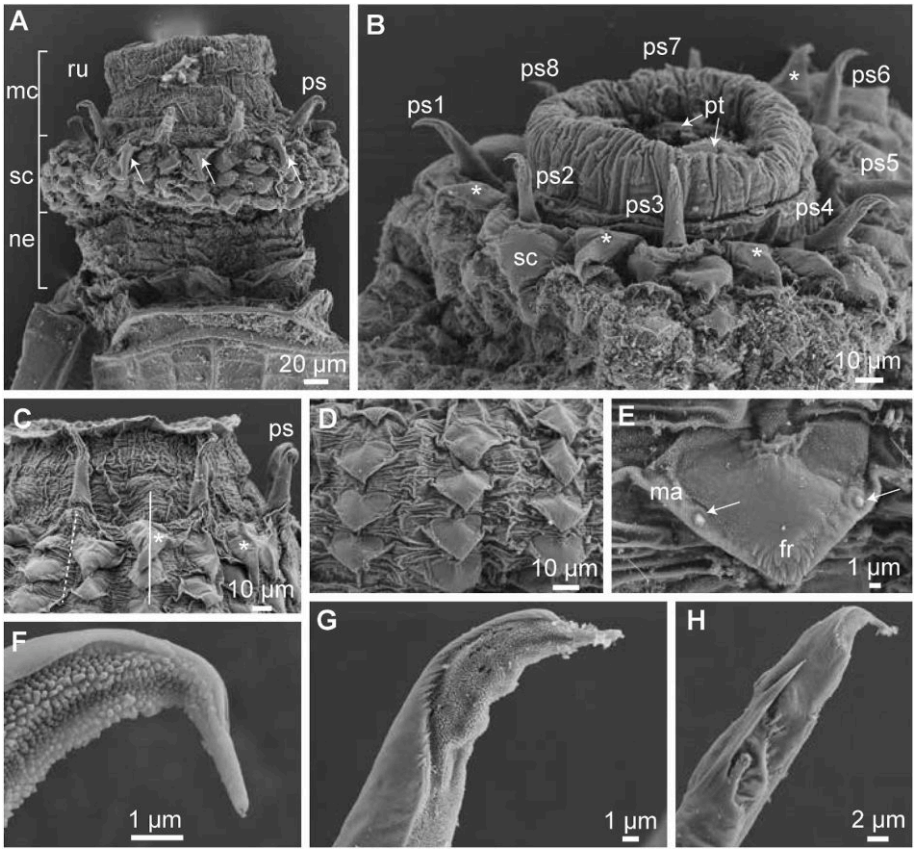

Fig. 5. Introvert of the larva. A. Fully everted introvert showing the division into neck (ne), scalid region (sc) and mouth cone (mc). The primary scalids (ps) are directed anteriorly, the ring 2-scalids are marked by an arrow. ru = ruff. B. Arrangement of the 8 primary scalids (ps1-ps8), the ring 2-scalids (asterisks) and the further scalids (sc). The edge of two pharyngeal teeth (pt) is visible. C. Magnification of the mouth cone and the primary scalids (ps). The dashed line indicates a virtual line, along which scalids are arranged on both sides. The white line marks a row of scalids between primary scalids, the asterisk marks the first, larger scalid in these rows. D. Scalids are arranged in longitudinal rows. E. The broad, leaf-like scalids are have a margin (ma), a pair of tube-like structures (arrows) and a fringe (fr). F. Magnification of the "inner" region of the apical end of a primary scalid. G. Side view on a primary scalid. H. Back side of a primary scalid with several spines. All images SEM. A from V13489, B, D-H from three different specimens of V13478, C V13495.

where vesicles broke off (Fig. 9 G). Postlarval stages lack vesicles, but rings of buds are present in the larger specimens, e.g. in the specimen with the strongly annulated appendage (Fig. 9D). Apically, each vesicle bud and each vesicle has several "spinulets", which are conical structures, ending with one (non-adult postlarval stages; Fig. 9F) or few (adult; Fig. 9J) tubes (Fig. 9E, F, H, I).

3.4. Scalids

The scalid arrangement, especially the pattern of the first scalids, is exposed only in few specimens with completely everted introvert. In the following description, we already use terms for certain scalids (e.g. "primary scalid") or their position ("ring 0", "ring 2"), which are explained in the discussion. To avoid confusion we find it helpful to use these terms already in the results section. In general, scalids are arranged in longitudinal rows except for different arrangement patterns of the most anterior scalids.

In the smallest stages, there is an anterior ring of large scalids (about 29 µm long) that are directed anteriorly when the introvert and the anterior pharyngeal teeth are fully everted (Fig. 10A). This ring is called here "ring 0". Ten scalids were counted in lateral view (Fig. 10A). All scalids are of equal size, position and distance to the neighboring scalids, except for a single smaller scalid in specimen 6-1 of V13493, which is anterior of the larger scalids (Fig. 10A). Posterior of the ring 0 is a 14–21 µm wide region without scalids (Fig. 10A). At the posterior margin of this region are slender scalids (= primary scalids) of up to 36 µm length (Fig. 10A). Five of the primary scalids are visible in lateral view (Fig. 10A). Posterior of the primary scalids are longitudinal rows of scalids. As in the larvae, the rows are aligned on virtual lines between the primary scalids and left and right of a line extending from the scalids (compare Fig. 5C). The rows that are positioned in the middle between two primary scalids start with a large scalid, which is more anterior than any other scalid, but still posterior of the primary scalids (Fig. 10A). These scalids are called here "ring 2 scalids". In the rows of scalids, series of differently sized scalids are present (Fig. 10A). These series consist mostly of three, sometimes of two scalids of decreasing size, followed by a new series (Fig. 10A). Between the scalids is a network of ridges (Fig. 10A). The scalids in neighboring rows are not strictly aligned, but the network makes it difficult to discover, whether there is a regular pattern in this. Towards the posterior region of the introvert, the series become smaller, first the third scalid in a series disappears and finally, in the posterior part of the introvert, only the first scalid remains (Fig. 11A).

The described pattern was well visible in the specimen 6-1 of V13493. In several other specimens the anterior scalids are in a grove that probably emerges from a slight retraction of the pharyngeal teeth region. This makes the observation of arrangement patterns difficult, but the visible patterns, at least of the smaller stages, confirm the observations from specimen 6-1 of V13493. In some specimens, dirt or suboptimal preservation in the scalid region makes observations difficult.

The arrangement pattern of scalids in the anterior region described above was also observed in larger postlarval stages. There is no region free of scalids separating the ring 0 scalids from the following ones. Irregularly distributed smaller scalids are present anterior of the ring 0 scalids (Fig. 10B). The primary scalids are still recognizable by their slender shape. The arrangement pattern of two scalid rows following each primary scalid and one scalid row following the ring 2-scalids is present, comparable to the younger stages (Fig. 10B).

The scalids themselves differ in structure, but all scalids are cone-shaped and have an apical or subapical region with receptors. In the smaller postlarval stages, the scalids are short and the receptor region is apically (Fig. 11B). Depending on scalid size, one to six receptors are present. The receptors consist of a semispherical base and a central tube (Fig. 11E). The receptors are surrounded by dense bristle-like structures (Fig. 11E). In larger specimens, the scalids become longer, more slender and are divided into a basal and a distal part (Fig. 11C–E). The distal

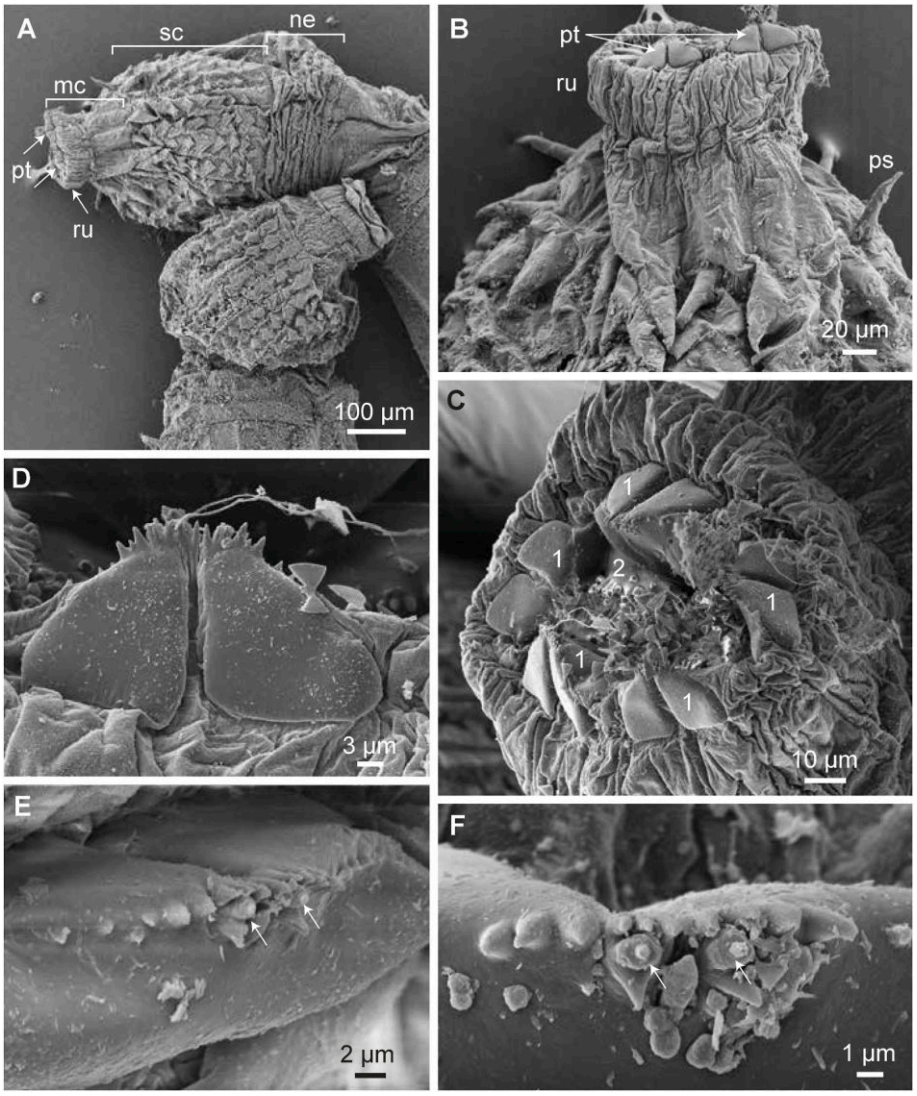

Fig. 6. Pharyngeal teeth in the larva. A. Frontal introvert with widely extended mouth cone (mc), showing teeth of the first ring (pt). B. Teeth (pt) from "outer" side, showing deep median groove. C. Almost frontal view on the first ring of teeth (labelled "1"), part of one tooth of the second ring ("2") is visible. D. Magnification of one tooth from the outer side. E, F. Magnification of the frontal margin with spines and tooth receptors (arrows). Note undivided inner side. Further abbreviations: ne = neck, ps = primary scalid, ru = ruff, sc = scalids. All images SEM, all from V13500.

part, existing of a slender stem with the apical region with receptors (Fig. 11E), is separated from the basal part by a groove and may be mobile in relation to the basal part (in the literature this is named "telescopic scalids"). The series consist of up to five scalids (Fig. 11C). The size of scalids in comparable positions in the series decreases from anterior to posterior. The scalids of ring 0 in the smallest specimens are more pointed than other scalids, but otherwise correspond in structure, having apical receptors.

In the adult, the arrangement pattern of the anterior scalids could not be observed, because the introvert is partly withdrawn. Scalids are visible in the longitudinal section anterior of the first pharyngeal teeth (Fig. 12D and E). All scalids have the same shape and consist of a basal and a long, slender apical part with an apical receptor region including more than 20 receptors per scalid (Fig. 11D).

3.5. Pharyngeal teeth

In most postlarval specimens, the anterior rows of the pharyngeal teeth are everted, showing the first three pentagons and in some cases also teeth of further pentagons (Fig. 12A and B). Teeth of the first pentagon show a development from one tooth to a divided tooth (Fig. 12C, F, G, J). In the smallest stages there are five broad and flat teeth (100–110 µm) (Fig. 12B and C). On their inner side they are more or less smooth, whereas on the outer side they have several furrows from the base to the apical ridge. The apical ridge is covered by a broad row of small cusps of different size, but without one being dominant. Between the cusps, partly surrounded by cusps, are some receptor structures (Fig. 12K). These consist of a spherical base and a distal tube with an open apex. These structures are abundant on pharyngeal teeth and are in the following named tooth receptor (see larva). In larger stages, a fine groove appears on the inner side of the teeth of the first pentagon (Fig. 12C, F). The larger the specimens are, the more distinct and broad is this groove (Fig. 12G) and in the largest stages and in the adult each tooth is divided completely into two teeth, which are clearly separated from each other (Fig. 12J). Each tooth is around 170 µm broad. In the withdrawn introvert of the adult, the first pentagon teeth direct horizontally into the pharyngeal lumen (Fig. 12D and E).

Teeth of the second pentagon are relatively similar in early stages and become distinct only in the largest stages. From the outer side the tooth of the younger stages is almost square and has a smooth surface (Fig. 13A). On the upper margin there is a row of spines (Fig. 13A). The central of these spines is larger, in younger stages this size difference is subtle, in older stages more pronounced (Fig. 13B). Often spines appear on the sides of the central spine (Fig. 13B). There are 4–6 lateral spines per side and the central spine can have one or two side spines. Few very tiny spines can be present (Fig. 13D). Tooth receptors are present irregularly on some spines (Fig. 13A, B, D). In the largest stages the central spine grows strongly in size and also the lateral spines (still 5 in

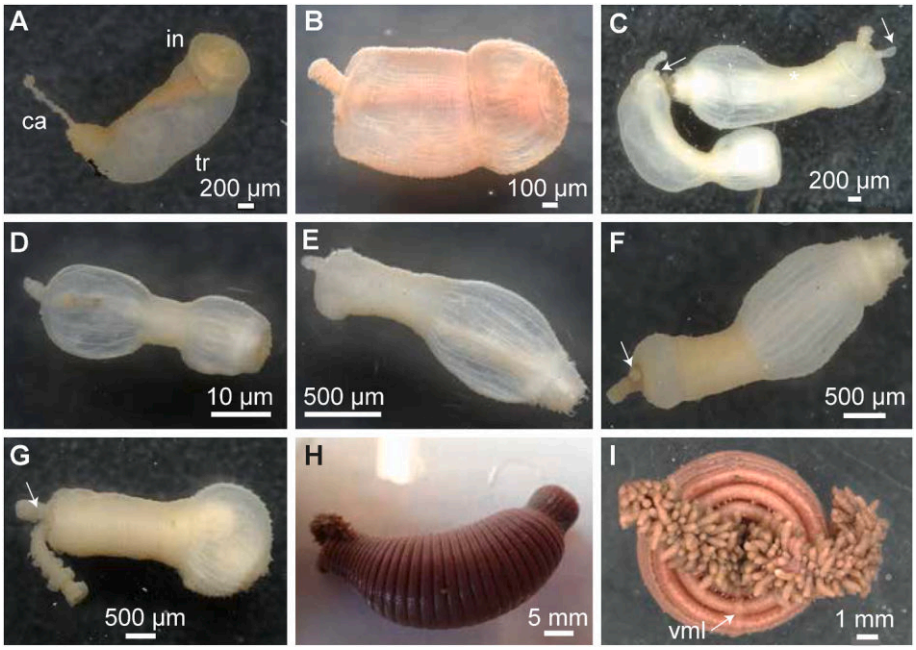

Fig. 7. Postlarval stages: general shape. A. Specimen V13482 with partly everted introvert (in), trunk (tr) and one caudal appendage (ca). B. Specimen V13491. C. Two specimens of V13497 with asymmetrical caudal appendages, the left one with a small bud (arrow), the right one with two equally long, but unequally thick appendages (arrow on the thinner appendage). D-G. Four different specimens from V13493 with differently everted introverts, different contraction stages of the trunk and different development of the caudal appendage. Arrows in F and G point at the smaller second appendage. Note segmented longer appendage in G. H. Adult specimen V13492 in overview. I. Posterior view, showing the paired caudal appendage. Note the structural change at the ventral midline (vml).

number) grow further (Fig. 13C). On the inner side, towards the mouth opening, there is a broad "cushion" as part of each second-ring tooth (Fig. 12A and B).

Teeth of the third pentagon are the largest in all stages. Their structure varies only slightly. In all cases the central spine is strongly pronounced and very long (Fig. 13E and F). There are three to five lateral spines and one pair of spines on the base of the central spine (Fig. 13E and F). In all stages except for the largest the outer side of the teeth is covered by small spines (Figs. 12B and 13F), these are very pronounced in teeth of younger stages and become less pronounced in older stages, until they disappear in the largest stage. On the inner side of all but the largest stage is a cushion-like structure that is slightly broader than the tooth itself (Figs. 12B and 13E). Tooth receptors are present (Fig. 13G).

In the adult the teeth of the first six rings have a very strong central spine and smaller lateral spines (Fig. 13H and I). Further behind, teeth become distinctly smaller, but still have a larger central and smaller lateral spines (Fig. 13L). Tooth receptors are irregularly present on all observed teeth (Fig. 13H–K, M, N).

4. Discussion

Priapulids develop by a series of consecutive stages through molts. The knowledge of this series is fragmentary for all species, which makes it difficult to assign larval and postlarval specimens to a certain species. Life stages are best known from *H. spinulosus* (e.g. Hammarsten, 1915; Purasjoki, 1944; Adrianov & Malakhov, 1996; Janssen et al., 2009). Even the development of the most popular species, *Priapulus caudatus*, is only incompletely known. Nevertheless, we are convinced that almost all specimens included in this investigation belong to *Priapulopsis bicaudatus*. The division of the pharyngeal teeth of the first ring is a unique character of the genus *Priapulopsis*, for which *P. bicaudatus* is the only species known in the Northern Hemisphere (Adrianov & Malakhov, 1996) (excluding here the questionable species *P. cnidephorus* Von Salvini-Plawen, 1973). As divided teeth, or at least teeth with a clear indication of subdivision, were found in larvae, postlarval stages and adults, we take this as a strong argument that all these stages belong to the same species, *P. bicaudatus*. Unfortunately, attempts to sequence the CO1 markers from both larvae and postlarval stages remained unsuccessful for larvae, therefore a molecular confirmation that both belong to the same species remains to be shown.

From the development of priapulids four morphologically differing stages are known: the hatching larva, the lorica larva, postlarval stages and the adult. Loricate larvae are known from all genera except the viviparous *Meiopriapulus* (Higgins & Storch, 1991). Hatching larvae are known only from *Priapulus caudatus* (Wennberg et al., 2009, probably Higgins et al., 1993) and *H. spinulosus* (Janssen et al., 2009). Postlarval stages are not known very well and the transition to adults seems to be gradual (see below).

For the following comparisons, we mainly concentrate on the species *Priapulus caudatus* and *Priapulopsis australis*. *Priapulus caudatus* co-occurs with *P. bicaudatus* in the Northern Hemisphere. *Priapulopsis australis* is congeneric, but occurs in the Southern Hemisphere. From other macroscopic species, either the larva is characteristic and cannot be confused with larvae of *Priapulus* and *Priapulopsis* (*Halicryptus* and *Maccabeus*) or larvae are unknown (*Acanthopriapulus horridus* Théel, 1911 and *Priapulus abyssorum* Menzies, 1959).

4.1. Larvae

In our material, we do not find hatching larva. With about 400 µm the smallest larva investigated is already far larger than the earliest lorica larvae described from *P. caudatus* by Wennberg et al. (2009), which are between 102 and 134 µm long. Although some authors identified different size classes (Purasjoki, 1944 for *H. spinulosus*, Shirley, 1990 for *P. caudatus*), this is not the case in our material. As the number of included specimens is comparably small (29) in Purasjoki (1944) and size classes were not further explained or defined in Shirley (1990), information about growth during priapulid larval development remains patchy.

Molting was observed by Wennberg et al. (2009) in *P. caudatus*. In our material, only one larva is clearly molting, but we suspect that those specimens where the larval body appeared smaller than the surrounding lorica were in a pre-molting state. Probably, the epidermis has detached from the cuticle and the larval body either was in a contracted state for shedding the exuvia or it contracted in reaction to the fixation. This interpretation is supported by the funnel-shaped structure connecting the anus with the lorica. We interpret this as the cuticular ectodermal hindgut connected with the lorica cuticle and therefore as a part of the molting process. This funnel was observed earlier, e.g. by Sanders &

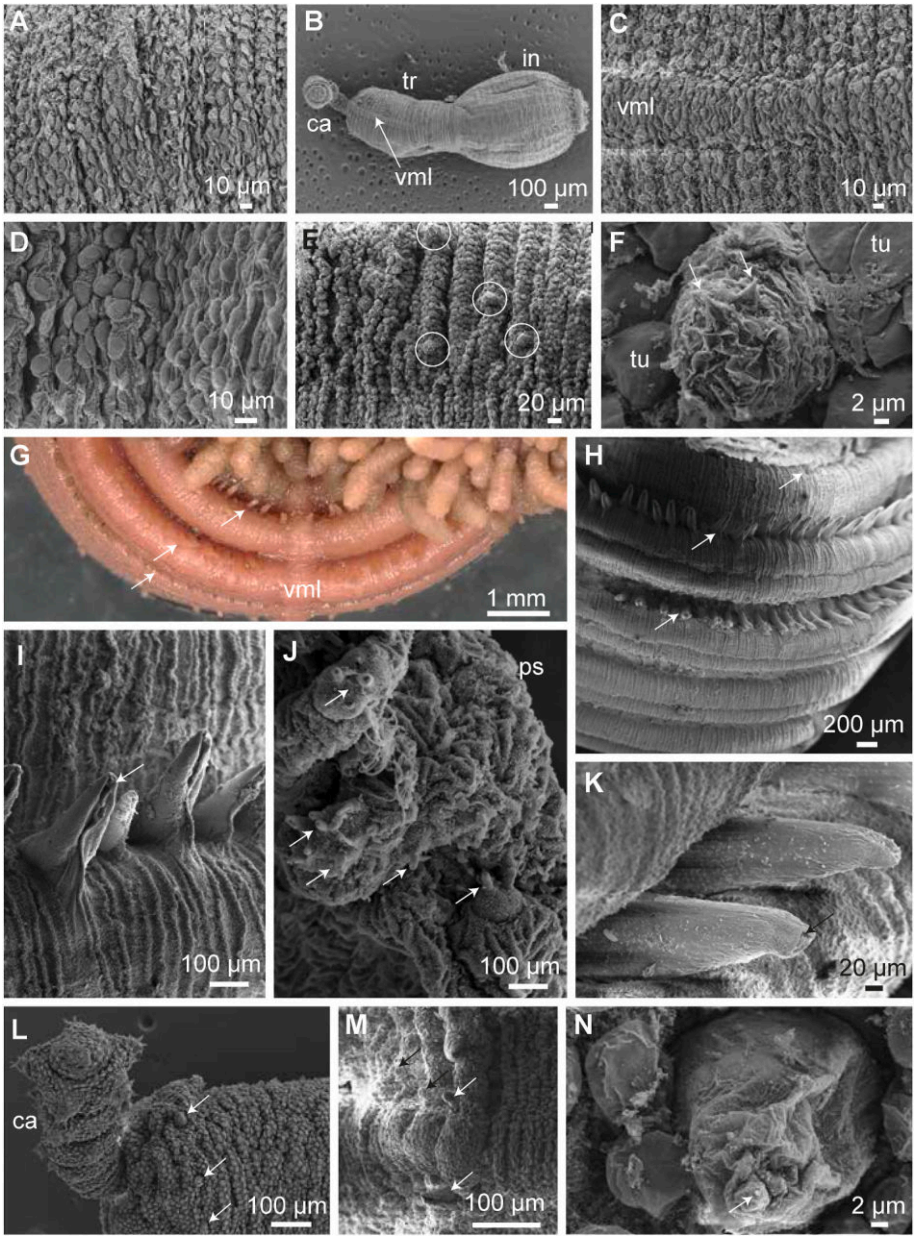

Fig. 8. Postlarval stages: trunk. A, D. The trunk is covered by tumuli. B, C. The ventral midline (vml) is elevated. E. In one specimen, scattered papillae (encircled) are present on the trunk. F. In magnification, these papillae have pointed receptors with an apical tubulus (arrows). G, H. Posterior end of the adult with three rings of ringpapillae (arrows). I. The ringpapillae have a frontal groove. The arrow indicates the region of receptors shown in J. J. Several receptors (arrows) are present apically on the ringpapillae. K. View on the caudal side of the ringpapillae from the third ring, the arrow indicates the region of receptors. L, M. Ringpapillae (arrows) are present in the larger postlarval stages. Note papilla with a groove at lower side of M. N. Magnification of ringpapilla with one apical receptor. Further abbreviations: ca = caudal appendage, in = introvert, tr = trunk, tu = tubuli. All images except G by SEM, A-C from V13484, D from V13502, E, F, M from V13498, G-K from V13492, L, N from specimen 9-2 of V13493.

Hessler (1962), who interpreted it as a muscle.

The construction of the lorica composed of large dorsal and ventral plates and a series of six lateral plates arranged in a zig-zag pattern is common for macroscopic priapulids (Adrianov & Malakhov, 1996). Sanders & Hessler (1962) describe three lateral plates for the larvae observed by them, but we assume that they overlooked the fine median folding line on each of these plates, so that their three plates represent the six lateral (ventrolateral and midlateral) plates. Adrianov & Malakhov (1996) published a figure (their Figs. 13.25–6) of a *P. bicaudatus* cross section, in which no lateral plates are recognizable.

The sculpturing of the dorsal and the ventral plate of the lorica is challenging to compare to patterns described so far, as these are few and partly inconsistent. This is complicated by the fact that the sculpture of the lorica may change during development, at least for *P. caudatus* (Higgins et al., 1993) and *P. tuberculatospinosus* (Schmidt-Rhaesa & Freese, 2019). In *P. bicaudatus*, such a change of sculpture seems to be absent, at least within the range of sizes investigated. The most important character is the longitudinal median ridge which extends along the entire lorica length. *Priapulopsis australis* is quite distinct in having paired plates creating a median zig-zag-line (Adrianov & Malakhov, 1996; Schmidt-Rhaesa & Freese, 2019). Larvae of (probably) *P. tuberculatospinosus* (Schmidt-Rhaesa & Freese, 2019) and some descriptions of the *P. caudatus* larva (Hammond, 1970; Adrianov & Malakhov, 1996) have a median ridge that is present only in the anterior part of the lorica. Older larvae of *P. caudatus* from the Eastern Pacific described by Higgins et al. (1993) do have a median ridge running along the entire lorica. This illustrates the necessity to describe the structural changes of priapulid larvae in different size stages. The single lorica observed with a median ridge only in the anterior part of the lorica may be the single case of being not *P. bicaudatus*, but rather *P. caudatus*. As it is the largest larva, it may, however, also represent a structural change of lorica sculpture during development of *P. bicaudatus*.

The larvae of *P. bicaudatus* described by Sanders & Hessler (1962) differ in having more anterior lorica plates than those described from other species. In *P. caudatus*, one plate attaches to the anterior margin of each the dorsal and the ventral plate (anterior plate: Lang 1948; accessory plate: Van der Land 1970; closing plate: Higgins et al., 1993 [the plate is drawn as one plate, but described as subdivided into four

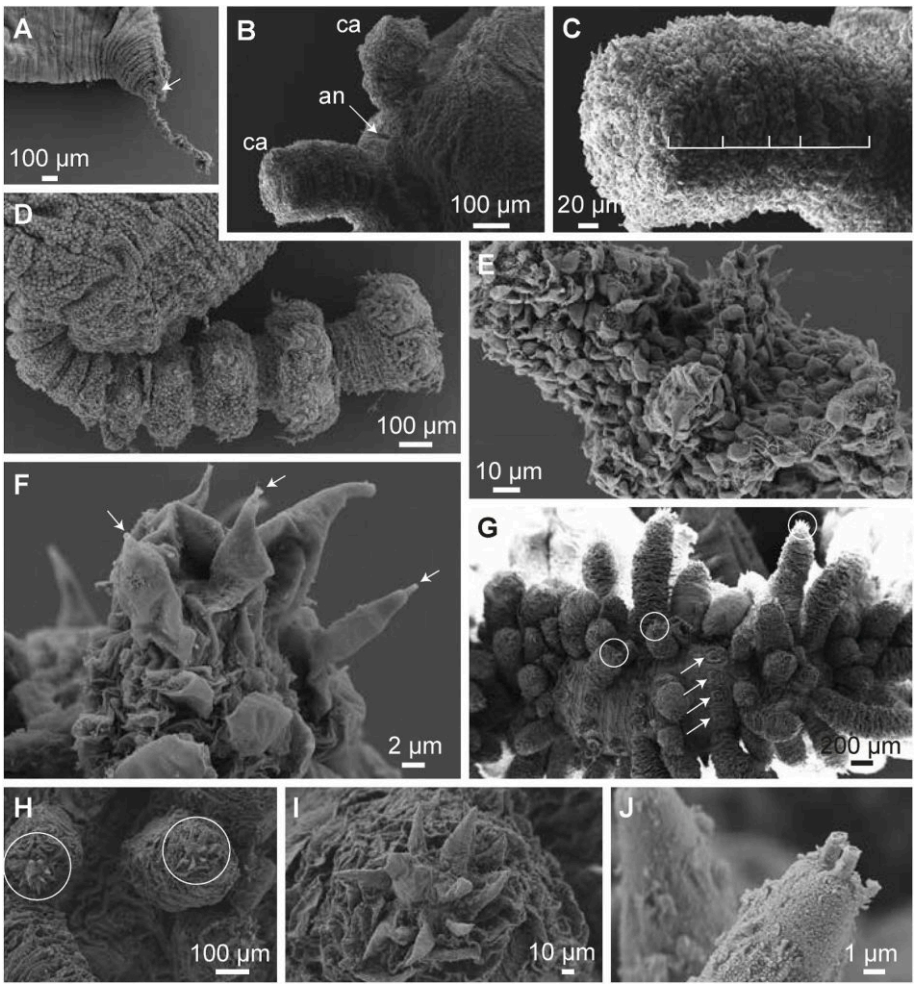

Fig. 9. Postlarval stages: caudal appendage. A. Many specimens have only one caudal appendage, the bud of the second (arrow) may be visible. B. The anus (an) is located between the two caudal appendages (ca). C. In short caudal appendages, an annulation is indicated. D. In some specimens, the caudal appendage is strongly annulated. E. Arranged in rings, vesicle buds with apical "spinulets" are present. F. The spinules end with one tube. G. In the adult, the stem of the caudal appendage is covered with vesicles. In places where these are broken off, their arrangement in rings becomes evident (arrows). Spinulets are present on the apex of the vesicles (circle). H, I. Magnification of the spinulets (encircled in H). J. In the adult, the apex contains 2–3 tubes. All images SEM, A, E, F from V13482, B, C from V13499, D from V13493, G-J from V13492.

plates]). In *P. bicaudatus*, Sanders & Hessler (1962) described four plates anterior of both dorsal and ventral plate that are confirmed here as frontal and laterofrontal plates. Additionally, they reported small plates anterior to the lateral plates, but this could not be confirmed by us and we assume that the lateral plates end frontally without additional plates.

The possession of four tubuli and their location on or close to the margins between midlateral and sublateral plates appears to be consistent among larvae in the genera *Priapulus* and *Priapulopsis*. Also the fine structure, with a base composed of ring-like structures and a tapering tubulus is consistent (e.g. Hammond, 1970; Higgins et al., 1993). The position of the tubuli in relation to the total lorica length varies and may help to distinguish species (Lang, 1951; Van der Land, 1970). Sanders & Hessler (1962) did not measure of the tubuli position, but drew them at around 80% of the lorica length (measured from anterior), therefore slightly further posterior than the values reported here (71–77%). Sanders & Hessler (1962) reported bristles on the lorica. Such bristles have never been reported for any other lorica. They constitute the only difference to the larvae reported here. A confirmation of this character would be helpful.

Fine structural descriptions of the larval introvert are very rare. Sanders & Hessler (1962) sketch the introvert of *P. bicaudatus*, but do not describe it in detail. Higgins et al. (1993), Adrianov & Malakhov (1996) and Wennberg et al. (2009) show SEM images from *P. caudatus*, Adrianov & Malakhov (1996) additionally show images from *Priapulopsis australis*. The subdivision into neck, scalid region and mouth cone is shared by all these species. Most authors do not include the neck as part of the introvert and only use this term to refer to the scalid region. The term "mouth cone" is used by most authors (Higgins et al., 1993; Adrianov & Malakhov, 1996). Whether or not it is homologous to conical structures between anterior scalids and the mouth opening in kinorhynchs and loriciferans is left open here.

The arrangement of scalids in priapulids is often shown in a "polar-coordinate mapping system", in which the position of each scalid is assigned to a certain ring and a certain sector around the mouth opening (for larvae of *P. caudatus* and *P. australis*: Higgins et al., 1993; Adrianov & Malakhov 1996; 2001a). Neither for larval not for adult *P. bicaudatus* such a mapping system has been made so far. For larvae of *P. caudatus* and *P. australis*, Higgins et al. (1993) and Adrianov & Malakhov (1996, 2001a) describe a first ring of 8 scalids they call primary or circumoral scalids. These are followed by a ring of scalids that are positioned between the primary scalids. In the ventral midline, these second-ring scalids are paired, therefore their number adds to 9 scalids. Higgins et al. (1993) did not recognize the paired ventral scalids and therefore assume 8 scalids in the second ring. The following scalids are aligned with the second-ring scalids as well as left and right of a virtual longitudinal line extending from the primary scalids. This adds to a number of 25 longitudinal rows. The scalids within the rows are postulated to belong to several rings, so that e.g. scalids of neighboring rows are not in the same rings. The total number of rings increases with age. Our investigation confirms the arrangement pattern of scalids for *P. bicaudatus* with the exception that we did not observe the putative ventral side and therefore can neither confirm nor exclude the presence of double second-ring scalids. What we find extremely difficult is the assignment of scalids to certain rings. The cuticular folds on the introvert show that scalids in neighboring rows are indeed not at the same level, but a clear assignment to certain rings is, especially in the anterior

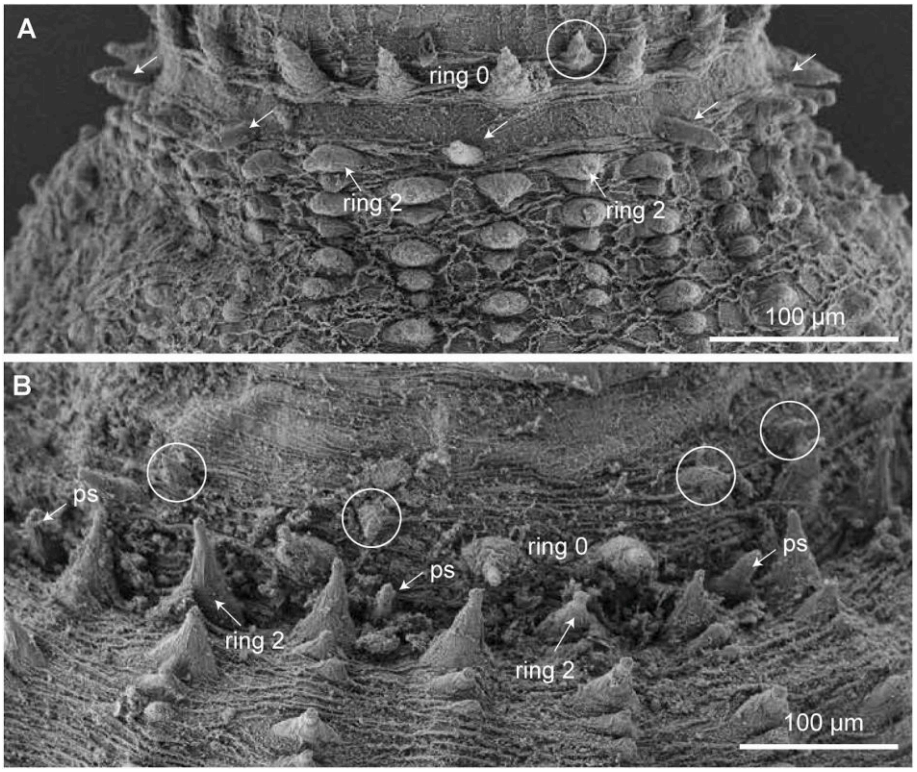

Fig. 10. Postlarval stages: Anterior scalid region. A. Young specimen 6-1 of V13493. Scalids of the frontal ring (ring 0) are directed anteriorly. One smaller tooth (encircled) is not in line with the others. Arrows point at primary scalids. Note one longitudinal row of scalids following each ring 2 scalid (ring 2) and two rows following each primary scalid. B. Older specimen 9-4 of V13493 with ring 0 scalids, several smaller scalids anterior of this ring (encircled), primary scalids (ps), ring 2 scalids (ring 2) and scalid rows.

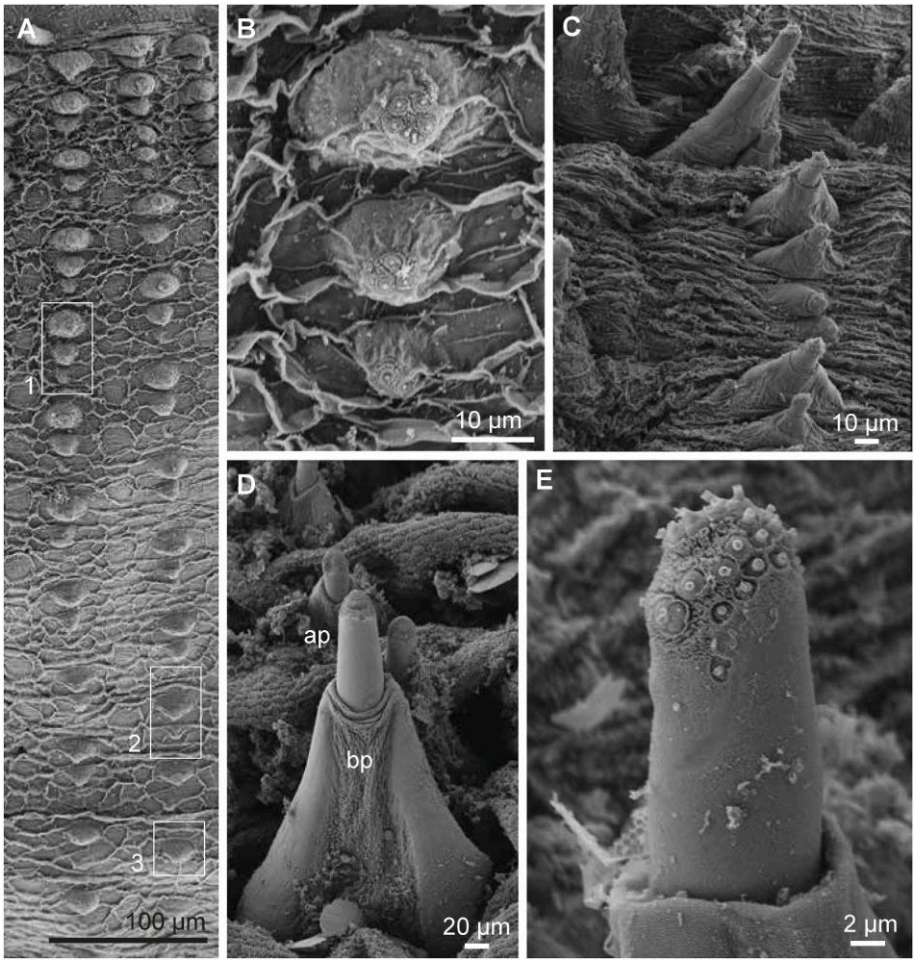

Fig. 11. Postlarval stages: scalids. A. Series of scalids in younger stages decrease in number from three scalids (rectangle 1) over two scalids (rectangle 2) to one scalid (rectangle 3). B. Magnification of one scalid series showing apical receptors. C. Telescopic scalids and larger series in older stages. D. Telescopic scalids, here from the adult V13492 are composed of a basal (bp) and an apical (ap) part. E. Receptors at the tip of the apical part. All images SEM, A, B from specimen 6-1 of V13493, C, E from specimen 9-1 of V13493.

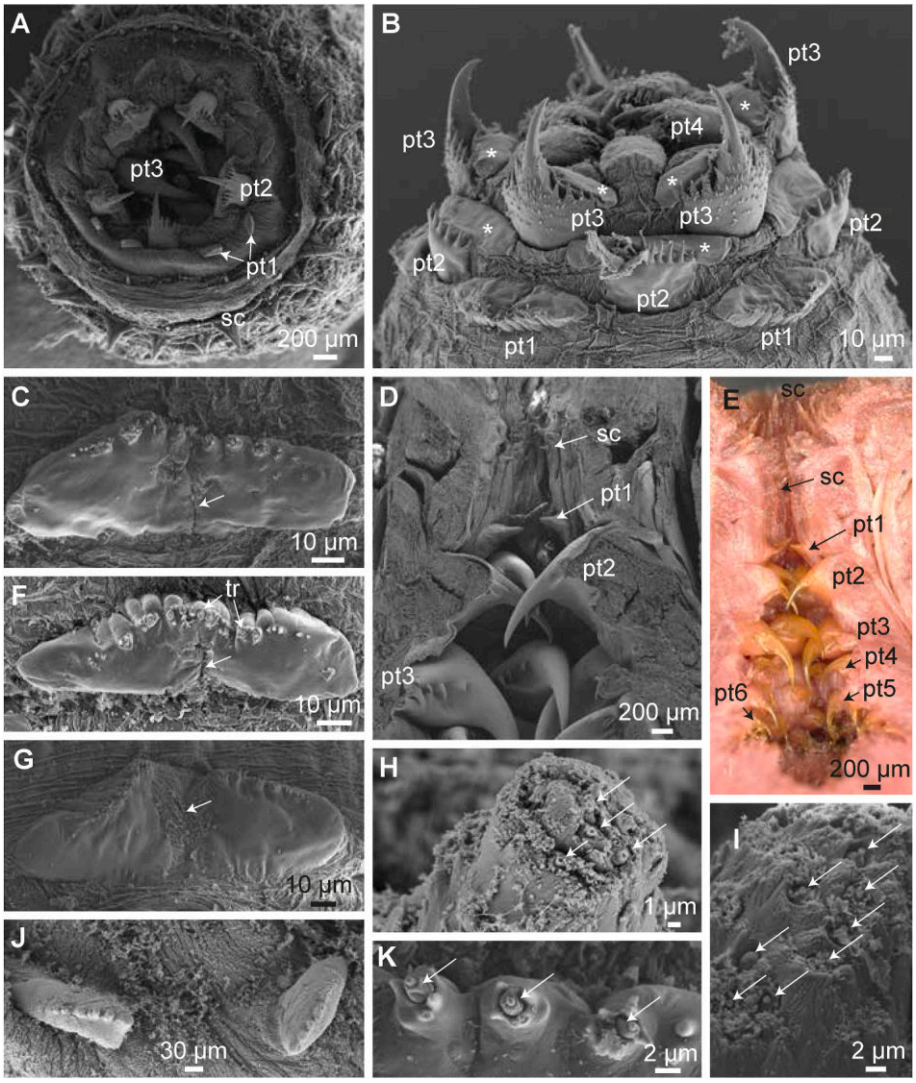

Fig. 12. Postlarval stages: pharyngeal teeth. A. Overview on everted anterior pharyngeal teeth in a late postlarval stage (V13477), showing three rings of pharyngeal teeth (pt1-3) and the beginning of the scalid region (sc). Note paired teeth in the first ring. B. Overview on everted introvert in a younger postlarval stage (specimen 6 of V13493) with pharyngeal tooth rings 1–4 visible (pt1-4). Asterisks mark the cushion-like base at the inner side of the teeth. C, F, G, J. First-ring pharyngeal tooth in stages of increasing size (C and F from the same specimen V13484, G from specimen 9-2 of V13493, J from V13477). Note the development from a fine median furrow to a broader groove to the complete separation of the tooth (arrows in C, F, G). D, E. Longitudinal section through the upper pharynx in the adult (V13492), showing teeth of different rings (pt1-pt6) and the first scalids (sc). Note the position of first-ring teeth and the largest size of third-ring scalids. H. Magnification of one of the cusps from the tooth shown in J with apical tooth receptors (arrows). I. Surface of one first-ring tooth in the adult (V13492) showing tooth receptors (arrows). K. Tooth receptors on the cusps of tooth shown in C. All images except E SEM.

region, very difficult.

The 8 primary scalids are the largest and most conspicuous (Higgins et al., 1993; Adrianov & Malakhov 1996; 2001a for *P. caudatus* and *P. australis*). According to these authors, the following scalids decrease gradually in size and become leaf-shaped in the 4th or 5th ring. This differs from the specimens reported here, in which the scalids still decrease in size, but only scalids of the second ring are elongate and the remaining ones are broad and leaf-like. This may distinguish *P. caudatus* from *P. bicaudatus*. The primary scalids documented in Higgins et al. (1993) and Adrianov & Malakhov (1996) are conspicuous, but never project so distinctly into a different direction (related to the other scalids) as in the specimens reported here. The anterior direction of the primary scalids is present also in the drawing of *P. bicaudatus* by Sanders & Hessler (1962). The fine structure of the primary scalids as described in this publication is very particular, insofar as the primary scalids documented by Higgins et al. (1993) and Adrianov & Malakhov (1996) are apically covered by fine bristles. The pair of lateral small tubuli described in this publication for the leaf-like scalids is also present in the leaf-like scalids of *P. caudatus* (Higgins et al., 1993; Adrianov & Malakhov, 1996), but probably not in *P. australis* (Fig. 13.24 F, G in Adrianov & Malakhov, 1996).

Pharyngeal teeth have so far not been demonstrated for the *P. bicaudatus* larva. Sanders & Hessler (1962) drew structures anterior of the primary scalids, but sketched those in the same way as the scalids. The morphology of the first-ring pharyngeal teeth documented here, with their distinct groove separating the upper side of the teeth into two halves is very characteristic and has not been described for any other larva before (Van der Land, 1970; Higgins et al., 1993; Adrianov & Malakhov, 1996; 2001a; Wennberg et al., 2009). The tooth receptors are documented here for the first time. By looking at published SEM images of *P. caudatus* larvae (Higgins et al., 1993; Adrianov & Malakhov, 1996) we suspect that further details will be revealed by using higher magnifications.

4.2. *Postlarval stages and adult*

There is a clear morphological difference between larval and postlarval stages in *P. bicaudatus*. We assume that a series of larval molts with gradual growth and development, one molt with metamorphosis from the larval to the postlarval phase and then again a series of molts with gradual growth and development from postlarval stages to the adult are present in the life cycle. We observed morphological changes during the development of postlarval stages (see below). Our material of older postlarval stages and adults is too scarce to recognize whether the transition between these stages is gradual or not. Although the term "postlarva" is used in the literature (e.g. Van der Land, 1996; Adrianov & Malakhov, 1996), such a stage has never been characterized or defined. Among the postlarval stages we do not recognize a particular stage, which would justify the term "postlarva" and therefore strongly encourage not to use this term for priapulids.

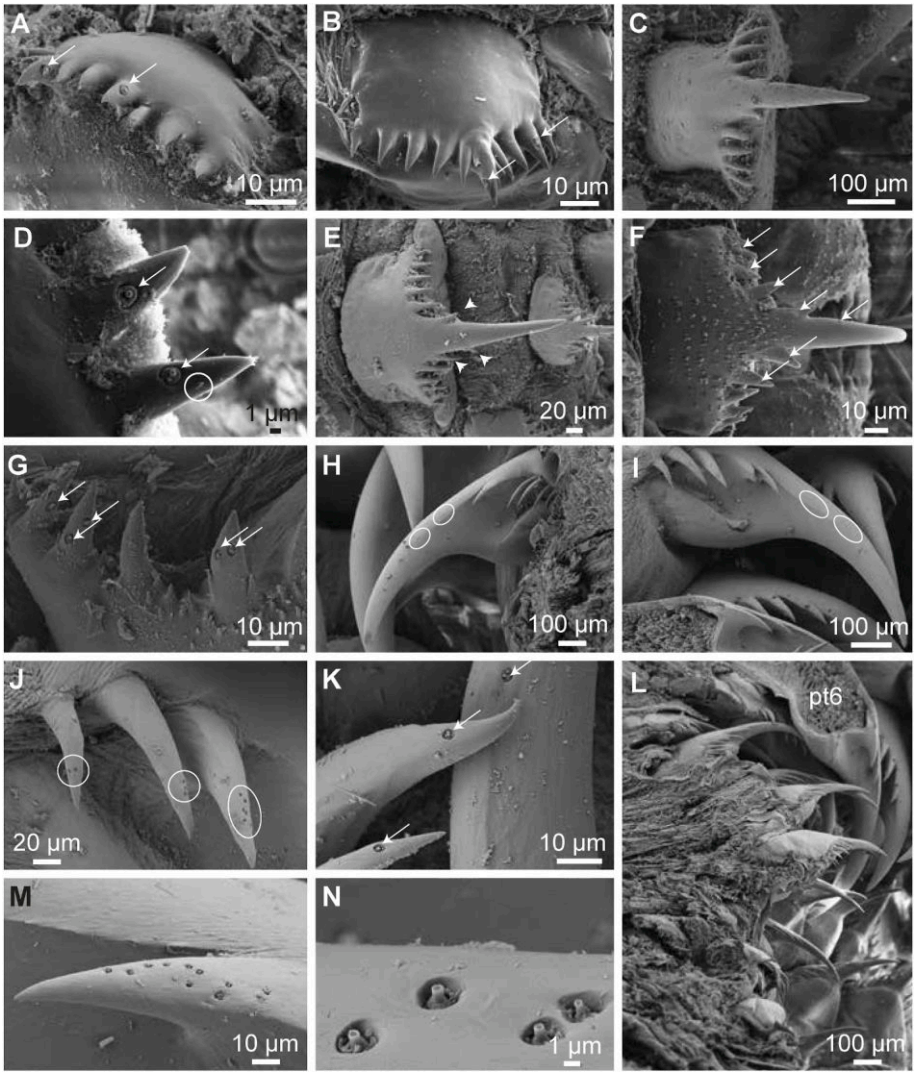

Fig. 13. Postlarval stages: Pharyngeal teeth of ring 2 (A–D), ring 3 (E–G) and tooth receptors. A-C show development of second-ring teeth in three specimens of different size, note different size of the central spine. Note also tooth receptors (arrows) on spines. D. Magnification of tooth receptors (arrows) and a small secondary spine (encircled). E, F. Third-ring tooth in two stages of different size with different intensity of back spines coverage. Arrowheads in E point at secondary spines, arrows in F at tooth receptors. G. Magnification of tooth receptors (arrows). H–N. Presence of tooth receptors (encircled or arrow) on different teeth from the adult (V13492), in ring 4 (H), 5 (I) and further. L. In the adult, posterior of tooth-ring 6 the pharyngeal teeth become distinctly smaller. All images SEM, A from specimen 8-4 of V13493, B, D from V13484, C from V13477, E fromV13498, F from V134482, G from V13499, H-L from V13492.

It may be the case that the proportions between trunk and introvert change between postlarval and adult stages and that earlier stages have a proportionally longer introvert. However, due to the ability to contract the trunk, measurements have to be interpreted cautiously. Most published records correspond to adults or very late postlarval stages. The specimens reported by Sanders & Hessler (1962) correspond well to the postlarval specimens reported by us. Therefore the synonymization of *P. atlantisi* with *P. bicaudatus* by Van der Land (1970) is correct.

Besides the covering with tumuli, the trunk is reported in some references to carry a number of papillae (Koren & Danielssen, 1877, Satô, 1934, see also Fig. 2 in Storch et al., 1995; but not Van der Land, 1970). We investigated only smaller pieces of the trunk surface, but did not find any papilla-like structures there. However, the presence of such structures in one postlarval stage warrants further investigation. In *Priapulus* species, the posterior trunk contains ringpapillae and posterior warts (Murina & Starobogatov, 1961; Van der Land, 1970). Posterior warts cover the posterior part and are lacking in *P. bicaudatus* and *P. australis* (De Guerne, 1891; Wesenberg-Lund, 1930). The ringpapillae in *P. caudatus* are irregularly distributed, semispherical structures (Van der Land, 1970), whereas in *P. bicaudatus* they consit of regularly arranged, elongate structures (Koren & Danielssen, 1877; Wesenberg-Lund, 1930; Van der Land, 1970). Only the number of rings with ringpapillae differs in the literature amongst three (this publication), five (Wesenberg-Lund, 1930) and six (Koren & Danielssen, 1877). In *P. australis*, five or six rings of pear-shaped ringpapillae are present (De Guerne, 1891). The presence (*Priapulus*) or absence (*Priapulopsis*) of posterior warts and the shape and arrangement of ringpapillae (conical, irregular in *Priapulus*, elongate or pear-shaped, regular in *Priapulopsis*) distinguished the genera *Priapulus* and *Priapulopsis*. As younger stages either lack ringpapillae or bear only a few simple papillae, the presence of ringpapillae is mostly a character defining adults. This is congruent with the absence of structures in the posterior part of the trunk reported by Sanders & Hessler (1962).

Our data show that the caudal appendage of *P. bicaudatus* develops asymmetrically over most of the postlarval development. Early stages have one appendage, which is not central, but slightly laterally displaced. The complete absence of a caudal appendage in few specimens is interpreted as being broken off and not a primary absence. As the appendage grows, it becomes metameric (in the literature usually termed "segmental"). This metameric character originates from the arrangement of vesicles in rings. In adults, both appendages are equally long and the dense covering of vesicles masks their arrangement in rings. Potential receptors, the "spinulets" (term by Van der Land, 1970), are present on the apical tip of the vesicles from very early stages on.

The asymmetrical development of the caudal appendage of *P. bicaudatus* has so far not been mentioned or figured. The specimens investigated by Sanders & Hessler (1962) already have a paired caudal appendage and size differences were not indicated. The few vesicles are arranged in metameric rings. The fine structure of caudal appendages of all species that have such an appendage has been superficially documented, perhaps with the exception of *A. horridus* (Schmidt-Rhaesa

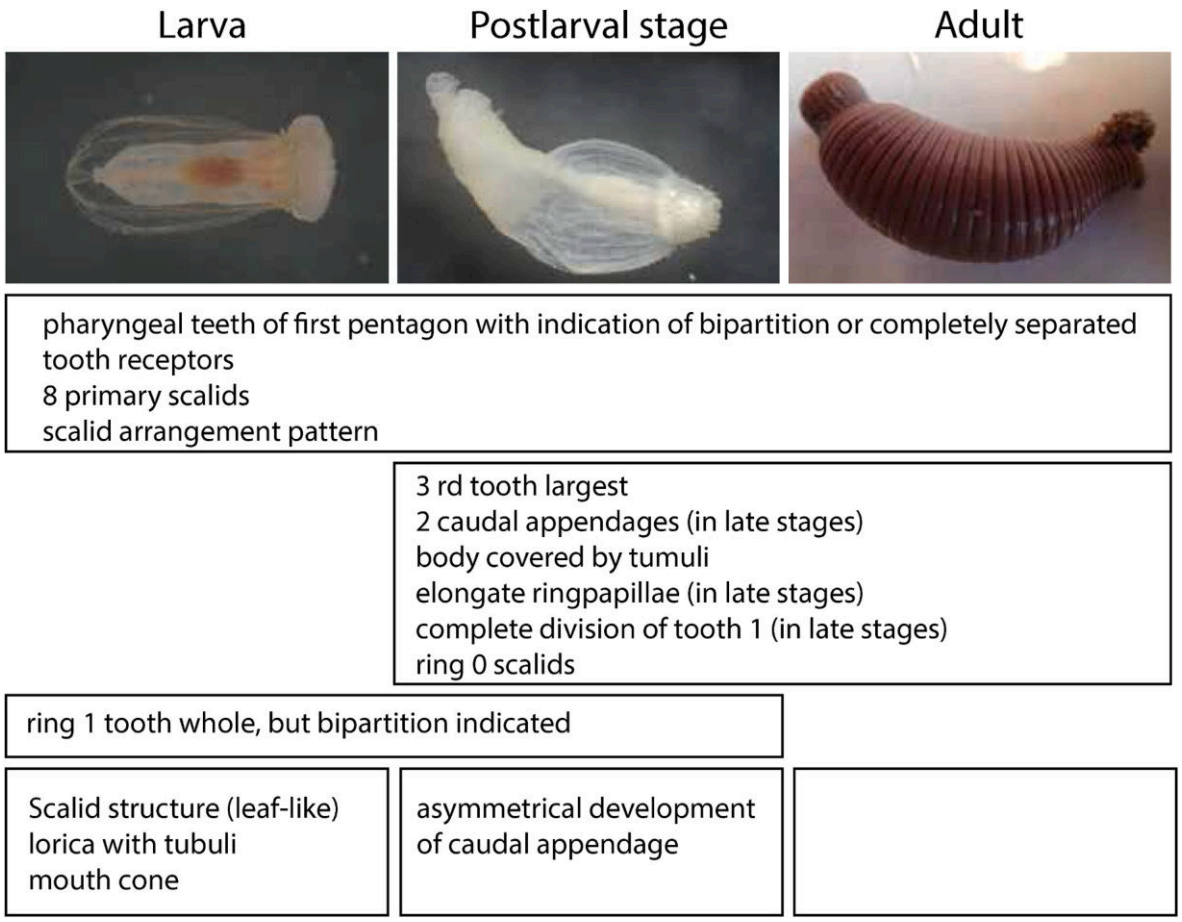

Fig. 14. Summary of characters occurring in different life stages of *Priapulopsis bicaudatus*.

et al., 2022). Spinulets on the vesicles are, besides *P. bicaudatus*, also present in *Priapulus* species (Murina & Starobogatov, 1961; Van der Land, 1970; Adrianov & Malakhov, 1996). A possible slight difference may be that the spinulets are concentrated on the tip in *Priapulopsis*, whereas in *Priapulus* they cover the entire vesicles (see Van der Land, 1970; Adrianov & Malakhov, 1996).

The general arrangement of scalids that is described above for larvae remains in adults (Adrianov & Malakhov, 2001b). Our data confirm this general arrangement in part, but probably more scalids are present in postlarval stages anterior of the primary scalids. Because we mainly observed the introvert laterally, scalids could not be counted completely. We hypothesize that the scalids named here "slender scalids" are the primary scalids and because five of them were observed, a total number of eight is likely, extrapolated over the entire circumference. Some authors use other names for these scalids: "circumoral scalids" (Adrianov & Malakhov, 1996) or "sensory spines" (Storch et al., 1994), both for *P. caudatus*. The further arrangement of teeth into 25 longitudinal rows is comparable to the larva and seems to be a conserved pattern. Different from the larvae is the presence of further scalids (or scalid-like structures) anterior of the primary scalids. These are present in the "ring 0" (as primary scalids are usually regarded as the first ring of sclids) described above and as single or few additional, irregularly distributed small scalids. To our knowledge, these structures have not been described before, but Storch et al. (1994) shows an unlabeled and undescribed scalid-like structures anterior to the primary scalids. Therefore we assume that such a ring 0 may be present in late postlarval stages and adults of at least *P. caudatus* and *P. bicaudatus*. In addition, there are small papillae called "buccal papillae" in *P. caudatus* between the ring 0-scalids and the pharyngeal teeth (Storch et al., 1994). Such papillae are also described from *P. australis* and *P. bicaudatus* (Storch et al., 1995). In our adult specimen, such buccal papillae were not recognized, but this may be due to the retracted state of the introvert.

For *P. bicaudatus*, Koren & Danielssen (1877) already counted 25 longitudinal rows of scalids, Wesenberg-Lund (1930) recognized that scalids are arranged in repeated series of decreasing size, Van der Land (1970) recognized that the scalids are composed of two parts that are assumed to be telescopic and Storch et al. (1995) documented the subapical receptors in the scalids. The number of reported scalids per series varies from 4 (this investigation) and 5 (Storch et al., 1995) to 6 (Sanders & Hessler, 1962); Adrianov & Malakhov (2001b) mention 4 to 7 scalids to be present.

The anterior pharyngeal teeth are visible in many specimens and might constitute the maximal eversion of the introvert. The exposure of the anterior pharyngeal teeth allows prey capture. Some images (e.g. page 132 in Adrianov & Malakhov, 1996) show the pharynx almost completely everted, allowing the documentation of most or all pharyngeal teeth. We assume that this is an artifact, probably caused by osmotic changes during fixation.

The first ring of pharyngeal teeth was overlooked in the first descriptions and recognized later (Théel, 1911). The gradual split of each tooth in the first ring into two teeth is documented here for the first time and confirms earlier assumptions (e.g. Théel, 1911) on the origin of the unusual number of 10 pharyngeal teeth in the first ring in *Priapulopsis*. As pharyngeal teeth function in prey capture and transport into the gut, the reason for the reduction of the first-ring teeth is a challenging question. As their position in the withdrawn introvert in adults is almost horizontal (see Fig. 12 D, E and also Storch et al., 1995), they might either be used to cut prey into smaller pieces or to close the pharyngeal region terminally.

The bipartition of pharyngeal teeth of the first ring has only been

observed in *P. bicaudatus* and *P. australis*. The larvae documented here already show a bipartition on one side of the teeth, supporting that larvae and postlarval stages investigated here are conspecific. However, as first ring pharyngeal teeth in young postlarval stages are still undivided, in larval teeth the bipartition appears stronger than in the subsequent, postlarval stages. Therefore, this development can hopefully be documented in further detail in the future.

We document further morphological changes in teeth during postlarval development, e.g. the growing of a central spine in the second-ring scalids. Quite surprising was the discovery of receptors on the teeth. Such receptors were figured by Storch et al. (1994) in *P. caudatus* on the first-ring teeth (called "cuticular tubules"). We show here, that such receptors are present on all investigated teeth of *P. bicaudatus*. Their presence in *P. caudatus* shows that this is not a unique character of *P. bicaudatus*, but it remains to be shown whether other species have tooth receptors on as many teeth as *P. bicaudatus*. The magnification of most teeth figured in the literature is too low to recognize these structures.

Although sampled in different locations, almost all specimens investigated here likely belong to *P. bicaudatus*, except for one larva with a different lorica structure. *Priapulopsis bicaudatus* seems to be the dominant priapulid species in the central northern North Atlantic Ocean in depths between 300 and 1000 m. This supports Van der Land's (1970) assumption that *P. bicaudatus* is predominant at greater depths (reports down to 2000 m), whereas *P. caudatus* is more common in coastal regions (not excluding the occurrence of *P. caudatus* in deeper waters and the occurrence of *P. bicaudatus* close to the coast.

In summary, we could show that larva, postlarval stages and the adult are connected through a number of common characters (Fig. 14). Some characters, such as the scalid pattern described above, including the presence of 8 primary scalids, are probably common characters among priapulids or at least macroscopic priapulids. The presence of tooth receptors throughout all investigated developmental stages is currently unique for *P. bicaudatus*, but their presence in adult *P. caudatus* shows that they may also be present in other priapulids. At least some indication of a bipartition of the first-ring teeth is characteristic for the genus *Priapulopsis*. A number of characters connects postlarval stages and adults, some of these characters, such as the occurrence of two caudal appendages, the complete division of the first ring teeth or the elongate ringpapillae develop in late postlarval stages. Larvae and (early) postlarval stages are connected by undivided first ring teeth, in which a bipartition is indicated in some way.

Declaration of competing interest

The authors declare that they have no known competing financial interests or personal relationships that could have appeared to influence the work reported in this paper.

Data availability

Data will be made available on request.

Acknowledgements

We thank the entire crew of the two IceAGE expeditions, the team of the DZMB (Deutsches Zentrum für Marine Biodiversitätsforschung) in Hamburg and especially Saskia Brix for making these interesting specimens available. We thank two reviewers for their intense and careful reading and their constructive comments and corrections.

References

Adrianov, A.V., Malakhov, V.V., 1996. Priapulida: Structure, Development, Phylogeny, and Classification. KMK Scientific Press, Moscow, p. 266.

Adrianov, A.V., Malakhov, V.V., 2001a. Symmetry of priapulids (Priapulida). 2. Symmetry of larvae. J. Morphol. 247, 111–121.

Adrianov, A.V., Malakhov, V.V., 2001b. Symmetry of priapulids (Priapulida). 1. Symmetry of adults. J. Morphol. 247, 99–110.

Brix, S., Bauernfeind, W., Brenke, N., Blazewicz, M., Borges, V., Buldt, K., Cannon, J., Díaz Agras, G., Fiege, D., Fiorentino, D., Haraldsdóttir, S., Hoffmann, S., Holst, S., Hüttmann, F., Jeskulke, K., Jennings, R., Kocot, K., Khodami, S., Lucas Rodriguez, Y., Martinez Arbizu, P., Meißner, K., Mikkelsen, N., Miller, M., Murray, A., Neumann, H., Ostmann, A., Riehl, T., Schnurr, S., Savavarsson, J., Yasuhara, M., 2012. Overflow, Circulation and Biodiversity. Cruise No. M85/3, August 27 - September 28, 2011, Reykjavik (Iceland) - Cuxhaven (Germany). METEOR-Berichte, M85/3, pp. 1–41. https://doi.org/10.2312/cr_m85_3.

Brix, S., 2013. IceAGE. Icelandic Marine Animals: Genetics and Ecology. Cruise No. POS456, IceAGE2, 20.07.2013-04.08.2013. Kiel (Germany) - Reykjavik (Iceland). Cruise Report POS 456. http://www.geomar.de/fileadmin/content/zentrum/ze/fs/Poseidon_Berichte_2013_PDF/POS456_Brix.pdf.

Danielssen, D.C., 1869. To mærkelige Sødyr. Forhandl. Skand. Naturforsk. Møde Christiania 1868, 541–542.

De Guerne, J., 1886. Sur les Géphyriens de la famille des Priapulides recueillis par la mission du Cap Horn. C.R. Acad. Sci. Paris 103, 760–762.

De Guerne, J., 1891. Priapulides. Mission scientifique du Cap Horn 83 (6), 3–20, 1882.

Hammarsten, O.D., 1915. Zur Entwicklungsgeschichte von *Halicryptus spinulosus* (von Siebold). Z. Wiss. Zool. 112, 527–571.

Hammond, R.A., 1970. The surface of *Priapulus caudatus* (Lamarck). Z. Morph. Tiere 68, 225–268.

Higgins, R.P., Storch, V., 1991. Evidence for the direct development in *Meiopriapulus fijiensis*. Trans. Am. Microsc. Soc. 110, 37–46.

Higgins, R.P., Storch, V., Shirley, T.C., 1993. Scanning and transmission electron microscopic observations on the larva of *Priapulus caudatus* (Priapulida). Acta Zool. 74, 301–319.

Janssen, R., Wennberg, S., Budd, G.E., 2009. The hatching larva of the priapulid worm *Halicryptus spinulosus*. Front. Zool. 6, 8. https://doi.org/10.1186/1742–9994–6–8.

Koren, J., Danielssen, D.C., 1876. Bidrag til de Norske gephyreers naturhistorie. Nyr Mag. Naturv. 21, 108–138.

Koren, J., Danielssen, D.C., 1877. Bidrag til de Norske gephyreers naturhistorie. In: Koren, J., Danielsse, D.C. (Eds.), Fauna Littoralis Norvegiae, vol. 3, pp. 111–151.

Lamarck, J.B. de, 1816. Historie naturelle des animaux sans verèbres 3, 1–586.

Lang, K., 1948. On the morphology of the larva of *Priapulus caudatus* Lam. Ark. Zool. 41A, 1–8.

Lang, K., 1951. *Priapulus caudatus* Lam. and *Priapulus caudatus* forma *tuberculato-spinosus* Baird represent two different species. Ark. Zool. 2, 565–568.

Menzies, R.J., 1959. *Priapulus abyssorum*, new species, the first abyssal priapulid. Nature 184, 1585–1586.

Murina, V.V., Starobogatov, J.J., 1961. Classification and zoogeography of priapuloidea. Trudy Inst. Okean. 46, 179–200.

Purasjoki, K.J., 1944. Beiträge zur Kenntniss der Entwicklung und Ökologie der *Halicryptus spinulosus*-Larve (Priapulida). Ann. Zool. Soc. Zool. Bot. Fenn. 9, 1–14.

Sanders, H.L., Hessler, R.R., 1962. *Priapulus atlantisi* and *Priapulus profundus*. Two new species of priapulids from bathyal and abyssal depth of the North Atlantic. Deep-Sea Res. 9, 125–130.

Satô, H., 1934. Report on the sipunculoidea, echiuroidea and priapuloidea collected by the sôyô-maru expedition of 1922-1930. Sci. Rep. Tôhoku Imp. Univ. 9, 1–32.

Schmidt-Rhaesa, A., Freese, M., 2019. Microscopic priapulid larvae from Antarctica. Zool. Anz. 282, 3–9.

Schmidt-Rhaesa, A., Cañete, J.I., Mutschke, E., 2022. New record and first description including SEM and μCT of the rare priapulid *Acanthopriapulus horridus* (Priapulida, Scalidophora). Zool. Anz. 298, 1–9.

Shirley, T.C., 1990. Ecology of *Priapulus caudatus* Lamarck, 1816 (priapulida) in an alaskan subarctic ecosystem. Bull. Mar. Sci. 47, 149-15.

Sørensen, J., Murina, V.V., 2009. The occurrence oft wo species of the family Priapulidae in Faroese waters. Fróðskaparrit Faroese Sci. J. 57, 149–158.

Storch, V., Higgins, R.P., 1991. Scanning and transmission electron microscopic observations on the larva of *Halicryptus spinulosus* (Priapulida). J. Morphol. 210, 175–194.

Storch, V., Higgins, R.P., Malakhov, V.V., Adrianov, A.V., 1994. Microscopic anatomy and ultrasructure of the introvert of *Priapulus caudatus* and *P. tuberculatospinosus* (Priapulida). J. Morphol. 220, 281–293.

Storch, V., Higgins, R.P., Anderson, P., Svavarsson, J., 1995. Scanning and transmission electron microscopic analysis of the introvert of *Priapulopsis australis* and *Priapulopsis bicaudatus* (Priapulida). Invertebr. Biol. 114, 64–72.

Théel, H., 1911. Priapulids and sipunculids dredged by the Swedish Antarctic Expedition 1901-1903 and the phenomenon of bipolarity. K. Sven. Vetenskapsakad. Handl. 47, 1–36.

Van der Land, J., 1970. Systematics, zoogeography, and ecology of the Priapulida. Zool. Verhandel. 112, 1–118.

Von Salvini-Plawen, L., 1973. Ein Priapulide mit Kleptocniden aus dem Adriatischen Meer. Mar. Biol. 20, 165–169.

Wesenberg-Lund, E., 1930. Priapulidae and sipunculidae. Danish Ingolf Exped 4, 1–44.

Wennberg, S.A., Janssen, R., Budd, G.E., 2009. Hatching and earliest larval stages of the priapulid worm *Priapulus caudatus*. Invertebr. Biol. 128, 157–171.

JCZ: Zoologischer Anzeiger - A Journal of Comparative Zoology 312 (2024) 135–152

Contents lists available at ScienceDirect

Zoologischer Anzeiger

journal homepage: www.elsevier.com/locate/jcz

New morphological structures of *Priapulus caudatus*, Lamarck 1816 (Priapulida) and analysis of homologous characters across macroscopic priapulids

Jan Raeker [a,*], Katrine Worsaae [b], Andreas Schmidt-Rhaesa [a]

[a] *Museum of Nature Hamburg - Zoology, Leibniz Institute for the Analysis of Biodiversity Change (LIB) and University Hamburg, Martin-Luther-King-Platz 3, 20146, Hamburg, Germany*
[b] *Marine Biological Section, Department of Biology, University of Copenhagen, Universitetsparken 4, 2100, Copenhagen Ø, Denmark*

ARTICLE INFO

Handling Editor: Maikon Di Domenico

Keywords:
Priapulida
Ecdysozoa
Priapulus caudatus
SEM
Histology
Homology

ABSTRACT

The macroscopic *Priapulus caudatus* Lamarck, 1816 is one of the most investigated priapulids, yet, the adult morphology warrants detailed characterization and analyses of potential priapulid homologies. Using light microscopy, scanning electron microscopy and histology, we examine adult specimens of *P. caudatus* from three localities in the Northeast Atlantic and the Arctic Oceans (Gullmarsfjord, North Sea, White Sea). Our examinations show ring papillae on the posterior trunk of *P. caudatus* for the first time in detail and describe previously overlooked structures on the circumoral field (hemispherical papillae, ring 0 scalids and circular folds). In addition, we add new information on pharyngeal teeth, scalids, trunk papillae, posterior warts, and on spinulets of the caudal appendage. The new collected data of *P. caudatus* allows us to compare structures across species of the macroscopic Priapulidae (*Acanthopriapulus*, *Priapulopsis*, *Priapulus*, *Halicryptus*) in detail and to build hypotheses on their homology within this clade.

1. Introduction

Priapulida contains 22 extant species of marine worms (Schmidt-Rhaesa and Raeker, in press), which can be divided into macroscopic and microscopic size classes (Schmidt-Rhaesa, 2013). Macroscopic priapulids form the family Priapulidae Gosse, 1855, which includes *Acanthopriapulus* van der Land, 1970 (one species), *Priapulopsis* Koren and Danielssen, 1875 (three species), *Priapulus* Lamarck, 1816 (three species) and *Halicryptus* von Siebold, 1849 (two species) (Van der Land, 1970). The former three genera constitute the group Megintroverta based on morphology (Lemburg, 1999). Shared characters among Megintroverta are a large introvert, scalid rows with scalid series, ring papillae on the posterior trunk and caudal appendage(s) with vesicles and spinulets (Lemburg, 1999). In contrast, *Halicryptus* has a short introvert, scalid rows without scalid series, a ring of flosculus-tubulus-complexes on posterior trunk and no caudal appendage (e.g. Van der Land, 1970; Raeker et al., 2024). Recent detailed investigations have decreased the knowledge gap in Priapulida morphology, describing new characters and fine-structures in a number of priapulid species (*Acanthopriapulus horridus* in Schmidt-Rhaesa et al., 2022; *Priapulopsis bicaudatus* in Schmidt-Rhaesa and Raeker, 2022; *Priapulopsis australis*, *Priapulopsis papillatus* and *P. tuberculatospinosus* in Schmidt-Rhaesa and Raeker, in press; *Halicryptus spinulosus* and *Halicryptus higginsi* in Raeker et al., 2024). Since the majority of characters show similarities among macroscopic priapulids, an analysis on potential homology of characters can be approached.

The most familiar priapulid is *Priapulus caudatus* Lamarck, 1816, the first species described in Priapulida (Van der Land, 1970). This species has a broad boreal distribution (see Van der Land, 1970; Adrianov and Malakhov, 1996b) with additional more southern records from Japan (Okuda, 1934), California (Light et al., 1954) and the Mediterranean (Guille and Laubier, 1965). Specimens from different localities do not distinctly differ morphologically, raising the question whether they represent one species. Recent molecular analyses of various populations of *P. caudatus* showed a diverse population structure within this species, but results were interpreted differently, as either more potential *Priapulus* species exist (Laakkonen et al., 2021) or an incomplete speciation took place (Kolbasova et al., 2023).

Besides having the most reported occurrences (Schmidt-Rhaesa, 2013), *Priapulus caudatus* represents the most investigated priapulid

* Corresponding author.
E-mail address: j.raeker@leibniz-lib.de (J. Raeker).

https://doi.org/10.1016/j.jcz.2024.08.005
Received 29 July 2024; Received in revised form 15 August 2024; Accepted 25 August 2024
Available online 26 August 2024

species. First detailed investigations of adult *P. caudatus* were provided by Ehlers (1862), Apel (1885) and Scharff (1885). First scanning electron microscopy (SEM) investigations were made by Hammond (1970a) on body surface structures and by Storch et al. (1994) on introvert associated structures in more detail. Adrianov and Malakhov (1996a) included postlarval stages and young adults in their SEM investigations. Each investigation added new information about the body organization of *P. caudatus*, but some structures have still been overlooked, neglected, or not documented in detail. Reinvestigating all characters of adult *P. caudatus* using advanced microscopy will help close these knowledge gaps.

In this study we examine morphological structures of adult *Priapulus caudatus* specimens from three localities (White Sea, Gullmarsfjord and North Sea) using light microscopy, scanning electron microscopy (SEM) and histology. The examined structures include pharyngeal teeth, circumoral field, scalids, trunk papillae, ring papillae, posterior warts and vesicles of the caudal appendage. Furthermore, we compare similar characters among Priapulidae and discuss their potential homology.

2. Material and methods

Adult specimens of *Priapulus caudatus* were collected at three localities between 2021 and 2023 (Table 1). Small and medium-sized adults were collected in the intertidal of the Kandalaksha Gulf in the White Sea, Russia by searching the mud by hand. Medium-sized specimens were collected in the Gullmarsfjord, Sweden by Agassiz trawl. Medium-sized and large specimens were collected in the German Bight near Helgoland in the North Sea, Germany by Van Veen Grab.

Specimens were photographed with a Keyence VHX-7000 digital light microscope. The introverts and caudal appendages were cut from the trunk and all three parts were prepared for SEM. Body parts were dehydrated in a series of increasing ethanol concentrations, critical point dried in a Leica EM CPD300, sputter coated with platinum in a Polaron SC7640 Sputter Coater and investigated with a LEO SEM 1524.

One specimen of *P. caudatus* from the White Sea was used for histological investigations. The whole specimen was dehydrated in a series of increasing alcohol concentrations, embedded in paraffin in sectioned in 10 µm thick sections using a Microm HM 340E rotatory microtome. Sections were Azan stained (20 min staining in nuclear fast red aluminium sulphate, 5 min differentiation in 5 % phosphotungstic acid, 14 min staining in aniline blue-orange G) and photographed using an Olympus SLIDEVIEW VS200 slide scanner. Image contrast and tone were adjusted with the auto contrast and auto tone options in Adobe Photoshop 2024.

3. Results

3.1. General external priapulid organization

All examined specimens have three main compartments: anterior introvert, trunk and caudal appendage (Fig. 1A). Total body lengths differed among specimens from same locality (Table 2). However, measurements of the body length should be viewed with caution, as living specimens were often significantly longer (including the caudal appendage) than in the fixed state.

Terminal on the introvert is the mouth opening with pharyngeal teeth that occur in pentaradial rings (Fig. 1B). Approximately the anterior six to seven rings have this pentaradial organization (Fig. 1B), whereas in the following rings the organization gets ambiguous. The teeth have a cuspidate appearance with a large median cusp and several smaller lateral cusps on each side of the median cusp (Fig. 1B and C).

On the surface of the introvert are conically-shaped scalids occurring in 25 longitudinal rows (Fig. 1B). The distance between scalid rows is similar except between the two rows lateral of the ventral midline being about the half of this distance (Fig. 1B). The anteriormost scalids, primary scalids, are organized in a ring of eight. Primary scalids do not line up with the following scalid rows constituting rings of 25 scalids; between two primary scalids are always three following rows, only between the two primary scalids next to the ventral midline are four scalid rows (Fig. 1B). Each scalid row consists of approximately ten scalid series, which each consist of four to eight scalids of decreasing sizes (Fig. 1D). In a single specimen, the number of scalids in a series can differ.

The trunk is annulated with 37–49 annuli throughout examined specimens from all localities (Table 2; Fig. 1A and E). One specimen from Gullmarsfjord had the highest number of annuli (49 annuli), but most specimens had 38, 40 or 42 annuli, independent of body length. On the surface of annuli are irregularly scattered trunk papillae (Fig. 1A and E). On the posteriormost two to four annuli of the posterior trunk are hemispherical to elongate papillae in one to three rings, the ring papillae (Fig. 1E). Occasionally, the rings of ring papillae are not completely closed (Fig. 1E). On the posteriormost trunk are numerous posterior warts (Fig. 1A and E). In many specimens, posterior warts were covered with dirt, concealing the fine structure (Fig. 1E).

The trunk terminates posterior in a caudal appendage, which consists of a stem and balloon-like structures, the vesicles (Fig. 1A,E,F). The stem is in large and older specimens often not visible due to the high number of vesicles (Fig. 1A,E,F). The surface of the vesicles holds irregularly conical structures, the spinulets (Fig. 1F).

3.2. SEM examinations

3.2.1. Pharyngeal teeth

The pharyngeal teeth differ slightly between *P. caudatus* from different localities and tooth rings within a single specimen (Fig. 2). In specimens from Gullmarsfjord and White Sea, the anterior six rings of cuspidate teeth with pentaradial organization were observable in detail, whereas only the first two rings could be examined in specimens from North Sea (Fig. 2). A lateral cut of the pharynx revealed the posterior teeth (Fig. 2O–Q).

The pharyngeal teeth have a curved base (Fig. 2A–F,M,N). Teeth of the first ring of the White Sea specimens have a straight base (Fig. 2G), but following rings are curved as well (Fig. 2H–L). All teeth, except the ones in the far posterior pharynx (see below), have a smooth cuticular surface (Fig. 2). Pores or receptor structures on the cuticle of teeth were not visible. The second to fourth rings usually contain the largest teeth, but this may differ between specimens, as occasionally the teeth of the second ring are the broadest of the anterior six rings (Figs. 1B and 3A). Additionally, teeth of the fourth ring often have longer median cusps compared to those of remaining rings, but this could be a perspective

Table 1
Sampling information of *Priapulus caudatus* specimens.

No. Of specimens	Locality	Coordinates	Sampling date	Depth [m]	Sampling tool
44	White Sea, Russia	66°92′7.37″N/33°05′7.61″E 66°33′10.83″N/33°06′27.13″E 66°33′7.38″N/33°06′56.35″E	17.-18. September 2021	0	Hand
3	Gullmarsfjord, Sweden	58°16′36.6″N/11°28′16.3″E	05. May 2023	~40	Agassiz trawl
10	German Bight, North Sea, Germany	54°3′19.86″N/7°56′47.52″E 54°3′21.36″N/7°56′49.8″E 54°3′22.74″N/7°56′51″E	22. June 2022	36.4	Van Veen Grab

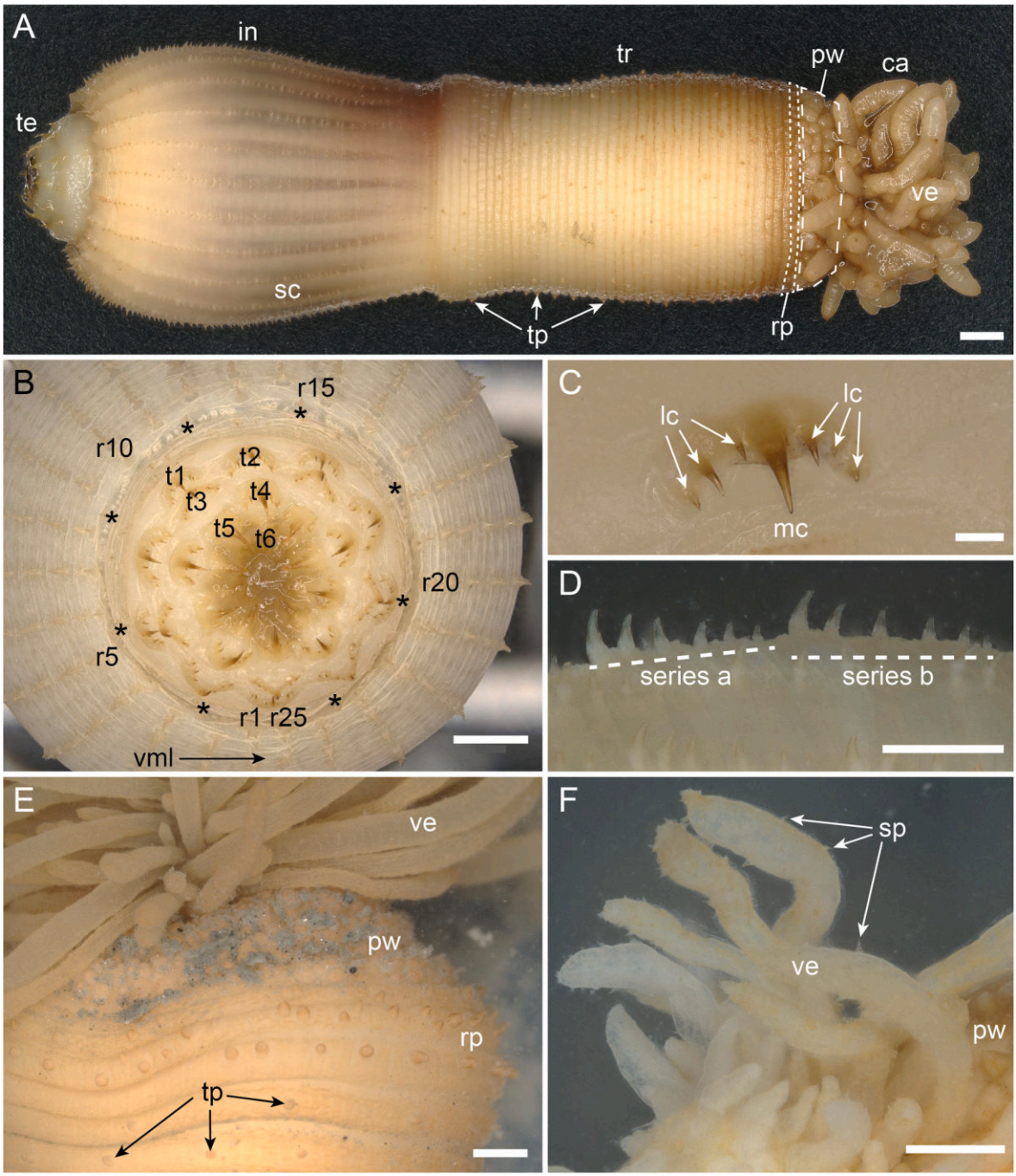

Fig. 1. General shape and morphological characters of adult *Priapulus caudatus* from the White Sea (A), Gullmarsfjord (B-D,F) and North Sea (E), light microscopical images. A. Habitus with arrangement in introvert (in) with pharyngeal teeth (te) and scalids (sc), trunk (tr) with trunk papillae (tp), ring papillae (rp) and posterior warts (pw) and caudal appendage (ca) with vesicles (ve). B. Frontal view of introvert with six pentaradial rings of teeth (t1-t6) and 25 rows of scalids (r1-r25). Asterisks (*) show position of primary scalids. C. Higher magnification of cuspidate tooth of the first ring with median cusp (mc) and lateral cusps (lc). D. Lateral view of scalid series. E. Posterior trunk with three rings of ring papillae and posterior warts on the last annulus. F. Higher magnification of vesicles with spinulets (sp). Further abbreviations: vml, ventral midline. Scale bars: A, B, E = 1 mm; C = 100 μm; D, F = 500 μm.

artefact (Fig. 3A).

In all specimens, a pronounced slightly bend median cusp is visible on the teeth, which seems to get larger in the anterior four to six rings (Fig. 2A–N), but loses its distinct appearance slightly (Fig. 2O and P) or completely (Fig. 2O–Q) in the posterior pharynx. Lateral on each side of the median cusp are lateral cusps (Fig. 2). The number of lateral cusps differs between localities and can differ within a single specimen and between each side of the median cusps (Table 2). Additionally, one or two small cusps can be present directly on the median cusp near the broad base of the tooth (e.g. Fig. 2A,B,G,H). Lateral cusps appear more pointy in the middle section of the pharynx (Fig. 2O and P).

Starting from approximately ring seven, the teeth decrease in size and the organization in rings becomes less distinct (Fig. 2O). The posteriormost pharynx, anterior to the midgut, is covered with smaller teeth appearing as cuticular protrusions (Fig. 2O–Q). The size transition of these two tooth appearances is abrupt in our material, without intermediate forms or a toothless gap in between them (Fig. 2O). The small posteriormost teeth have anteriorly a smooth cuticular surface, whereas

Table 2
Total body length, number of trunk annuli and lateral cusps per side of the median cusp on the pharyngeal teeth of *P. caudatus* from different localities. Abbreviations: scu, small cusp lateral on median cusp.

Locality	Gullmarsfjord	White Sea	North Sea
Total body length [mm]	25 - 40 (n = 3)	10 - 48 (n = 21)	17 - 80 (n = 10)
Number of trunk annuli	45 - 49 (n = 3)	37 - 42 (n = 21)	40 - 46 (n = 10)
Ring 1 teeth lateral cusps per side	3-5 (+1 scu)	4-5 (+2 scu)	3 (+2 scu)
Ring 2 teeth lateral cusps per side	3-4 (+1–2 scu)	4-6 (+1 scu)	3 (+1 scu)
Ring 3 teeth lateral cusps per side	2-3 (+1–2 scu)	3-5 (+1 scu)	–
Ring 4 teeth lateral cusps per side	2 (+1 scu)	4-7 (+1–2 scu)	–
Ring 5 teeth lateral cusps per side	2 (+1 scu)	3-4 (+2 scu)	–
Ring 6 teeth lateral cusps per side	2	2-3 (+2 scu)	–
Posterior teeth	–	5–7	–

the underside appears rough due to plate-like structures or folds on the cuticle (Fig. 2Q).

3.2.2. *Circumoral field*

The circumoral field represents the area between the first ring of teeth and the primary scalids around the mouth opening (Fig. 3A). Three structures were identified in this area: hemispherical papillae, ring 0 scalids and circular folds.

The hemispherical papillae are seemingly randomly scattered in a belt peripheral to the first ring of teeth (Fig. 3B and C). Their shape is hemispherical with a curved ridge that runs longitudinal to the body of the priapulid, and is mostly laterally flattened (Fig. 3C). Along the ridge are several receptors located (Fig. 3C). The receptors have a distinct circular base with a rough surface and a central, smooth surfaced tubular structure with five to seven apical finger-like cuticular protrusions (Fig. 3C and D). The ridge of hemispherical papillae is about 15–30 µm long.

In the middle region of the circumoral field occur the ring 0 scalids as conical structures organized in a ring, which look similar to scalids on the introvert, but smaller (Fig. 3A; 4A-C). Cuticular folds encircle the stem of ring 0 scalids (Fig. 4A). Ring 0 scalids can occur as pairs that stand close together (Fig. 4A) or slightly further apart (Fig. 4B), or they appear as single structures (Fig. 4C). In pairs, the anterior ring 0 scalid is often smaller (Fig. 4A), whereas they have the same size when being further apart (Fig. 4B). The tips of the ring 0 scalids have a subapical depression with a rough surface which is beset with several tubular receptor structures (Fig. 4D). In some specimens from the White Sea, the subapical depressions are extruded (Fig. 4E).

On the posterior circumoral field are distinct circular folds that appear approximately on the same level as the primary scalids (Fig. 3A; 4B,F,G). Circular folds occur mainly in small groups (Fig. 3A; 4F). The folds are not much elevated from the surface of the circumoral field and hold no other structures (Fig. 4B,F,G) We did not find any receptors on the circular folds (Fig. 4G).

3.2.3. *Scalids*

Primary scalids have a conical shape similar to the “normal” scalids occurring in the longitudinal scalid rows on the introvert, although with a slimmer stem (Fig. 5A and D). The tip of a primary scalid has a subapical depression with numerous tubular receptor structures and a distinct median fold (Fig. 5B). The tubular receptors appear as two types: one type with a smooth apical part of the tubulus and one with about five to ten finger-like protrusions on the apical part of the tubulus (Fig. 5C). In specimens from Helgoland, the subapical depression was extruded, showing the tubular receptor structures and hiding the median fold (Fig. 5C). Subapical depressions of the primary scalids point towards the posterior part of the specimens (Fig. 5D).

Scalids in the longitudinal rows decrease in size within a scalid series (Fig. 5D). Similar to primary scalids, the “normal” scalids have a subapical depression with numerous tubular receptor structures, but a median fold is missing (Fig. 5D–H). The tubular receptor structures appear as the same two types as on the tips of primary scalids (Fig. 5I). In contrast to primary scalids, the subapical depression of normal scalids point towards the anterior part of the specimens (Fig. 5D). Depressions in the cuticle of scalids containing one tubular receptor occur sometimes in specimens from the White Sea (Fig. 5E and G).

3.2.4. *Trunk structures*

Annuli of the trunk have a smooth (Fig. 6A) or slightly wrinkled (Fig. 6B) cuticular surface. Scattered on the annuli are structures called trunk papillae (Fig. 6A). The surface along the ventral midline is free of structures (Fig. 6B). Trunk papillae are elongate, slightly conical structures with a wrinkled surface (Fig. 6C–E). The tips of trunk papillae hold several tubular receptor structures (Fig. 6F and G). These receptors consist of a conical basal part and an apical tubulus with a smooth surface (Fig. 6H). About two to four receptors are connected to a broader basal part, forming a receptor unit (Fig. 6F–H). In specimens from Gullmarsfjord and the North Sea, several receptor units cover the tip of trunk papillae (Fig. 6F and G), whereas in specimens from the White Sea, occasionally only a single receptor unit appears on the tip (Fig. 6H).

On the posterior annuli are structures called ring papillae that appear in one to three rings, independent of body length. They have a smooth surface (Fig. 7). In specimens from Gullmarsfjord and some from the White Sea, ring papillae have a hemispherical shape (Fig. 7A,B,D), whereas specimens from the North Sea and some specimens from the White Sea have elongated ring papillae (Fig. 7C). Ring papillae do not occur in regular distances, as some papillae can be somewhat grouped together or single papillae appear outside of the organized ring (Fig. 7A and B). Hemispherical ring papillae have a subapical region that often faces towards the anterior of specimens (Fig. 7A and B). This region holds cuticular folds with tubular receptors, similar to the receptors of trunk papillae (Fig. 7D–F). Whether some receptors basally connect and form similar receptor units than in trunk papillae was not visible due to many cuticular folds and dirt.

The posterior trunk holds numerous posterior warts (Fig. 8), but the surface above the ventral midline is free of posterior warts. As in many examined specimens the posterior warts were covered in a dirt layer, only a few specimens from the White Sea and Gullmarsfjord could be examined. Posterior warts consist of several wart units that are separated by distinct trenches (Fig. 8A and B). Wart units again consist of several wart subunits that are also distinctly separated (Fig. 8C and D). Wart subunits hold apically about one to six tubes with a smooth surface (Fig. 8D–F). In one examined specimen from the White Sea, the tubes were collapsed, not showing distal openings (Fig. 8D), whereas in other specimens distal openings were visible (Fig. 8F).

3.2.5. *Vesicles*

The stem of the caudal appendage is beset with numerous vesicles in older specimens (Fig. 9A). Vesicles are elongate, balloon-like structures with irregularly scattered, conical spinulets (Fig. 9B and C). The surface of vesicles is rather smooth, but wrinkles and folds can be present due to partly deflation of vesicles (Fig. 9B and C). Apically accumulated spinulets occur on vesicles, forming a disorganized spinulet crown (Fig. 9B, D,E). Often, one to three large spinulets occur in the median area of the crown with about two to five tubular receptor structures with a smooth surface (Fig. 9E and F). Remaining spinulets on a vesicle hold apically one to three tubular receptor structures (Fig. 9G–I).

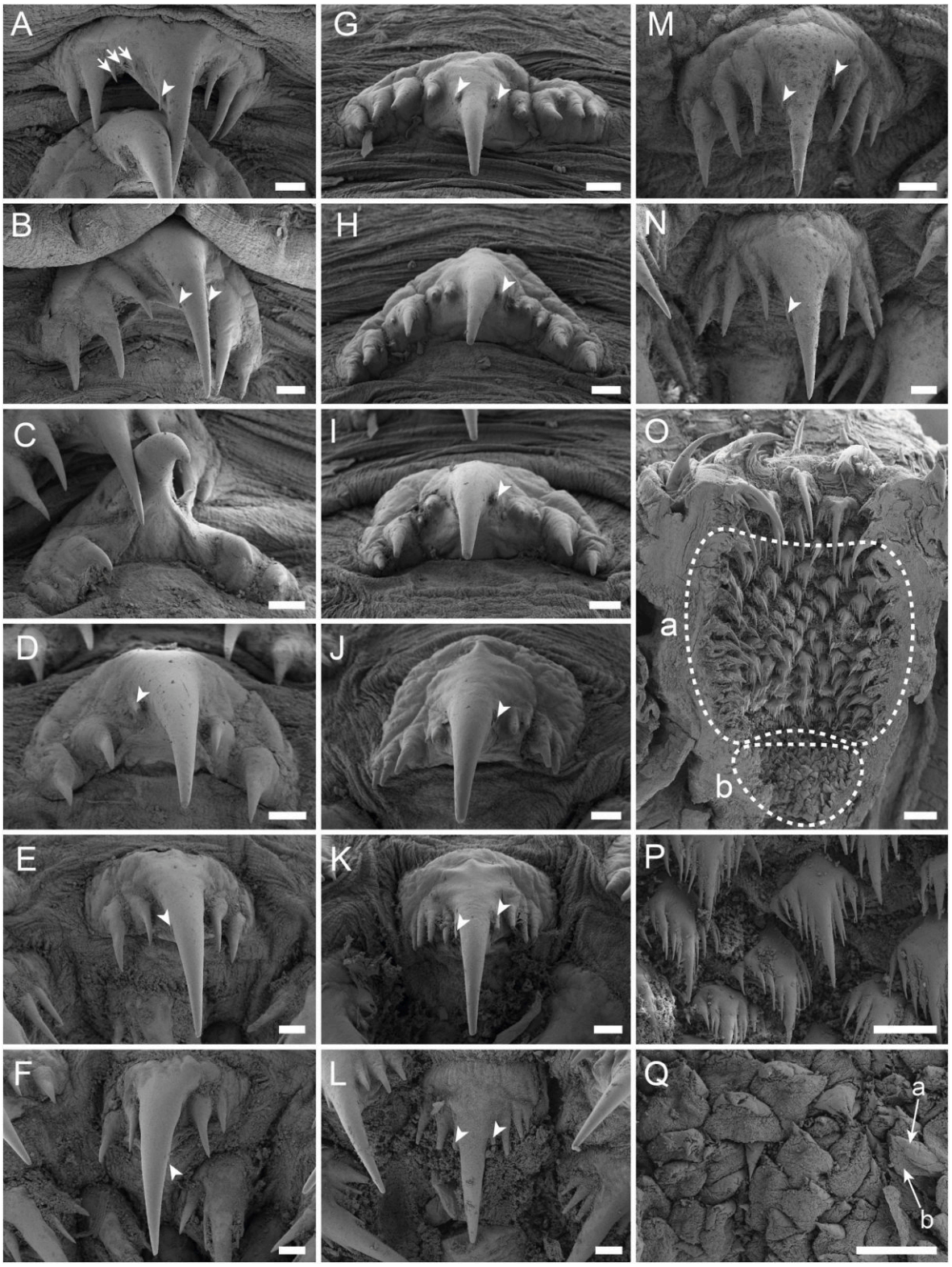

Fig. 2. Pharyngeal teeth, SEM images. A-F. Rings one to six of teeth of a specimen from the Gullmarsfjord. Small arrows in A show three small lateral cusps. G-L. Rings one to six of teeth of a specimen from the White Sea. M,N. Rings one and two of teeth of a specimen from the North Sea. O. Longitudinal cut of pharynx with less organized arrangement of teeth in the middle part of the pharynx (a) and small teeth in the posteriormost pharynx (b). P. Higher magnification of teeth in the middle part of the pharynx. Q. Higher magnification of small teeth in the posteriormost pharynx showing smooth (a) and rough (b) surfaces. Arrow heads show small cusps on the median cusp. Scale bars: A-F, M,N,P,Q = 100 μm; G-L = 50 μm, O = 200 μm.

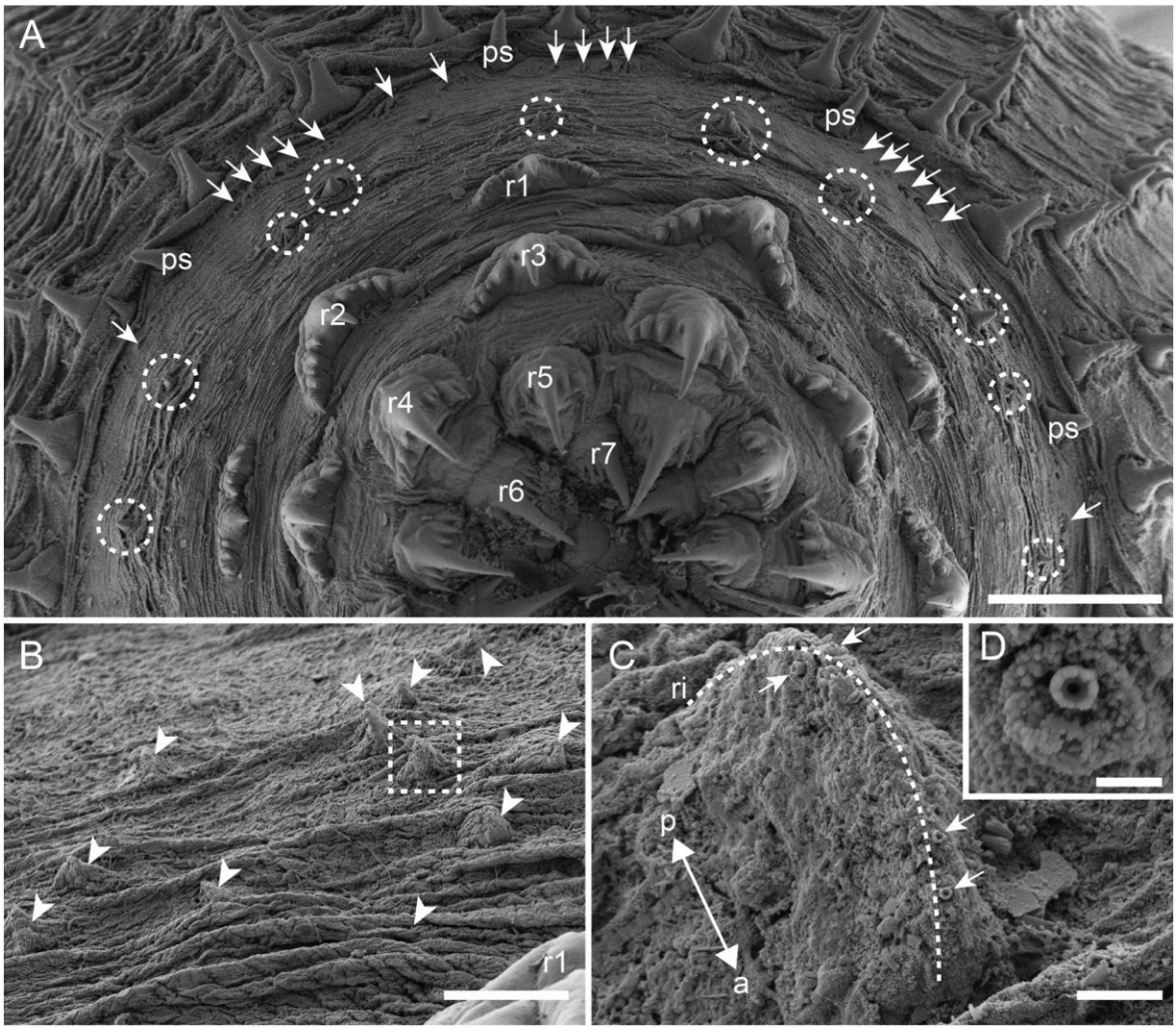

Fig. 3. Circumoral field and hemispherical papillae of specimens from the White Sea, SEM images. A. Terminal view on the introvert showing pharyngeal teeth (r1-r7) and circumoral field. Dotted circles show ring 0 scalids. Small arrows show circular folds. B. Area on the circumoral field between ring 0 scalids and first ring of teeth (r1) showing scattered hemispherical papillae (arrowheads). Dotted box shows C. C. Higher magnification of hemispherical papilla with receptor structures (arrows). Dotted line shows ridge (ri). Double arrow shows orientation of anterior (a) and posterior (p) of specimen. D. Higher magnification of receptor on hemispherical papilla. Further abbreviations: ps, primary scalid. Scale bars: A = 500 μm; B = 50 μm; C = 5 μm; D = 1 μm.

3.3. Histology

3.3.1. Introvert

The body wall of the introvert consists of a cuticle, circular musculature and 24 strands of longitudinal musculature that occur between the scalid rows (Fig. 10). Dependent on the contraction of the specimen, the midgut can occur on the same level as the introvert (Fig. 10). The pharyngeal bulb is encircled by several strands of muscles (Fig. 10). The eight longitudinal strands nearest to the pharynx are the long introvert retractors (Fig. 10). Each long introvert retractor has one short introvert retractor distally allocated, whereas the one in line with the ventral nerve chord has two short introvert retractors distally (Fig. 10). A potential split muscle strand can be excluded as no damage can be seen on these short introvert retractors. The long introvert retractors appear much thicker than the short introvert retractors (Fig. 10).

3.3.2. Posterior warts, caudal appendage and vesicles

Posterior warts of the last annulus of the trunk are occasionally thick und underlined by circular musculature (Fig. 11A). Externally, posterior warts are surfaced by a cuticle (Fig. 11A and B). Internally, they are filled with numerous large, longitudinally stretched glandular cells (Fig. 11A and B). Glandular cells reach into the tubuli on the surface of the posterior warts (Fig. 11A). Wart units and subunits are separated by cuticle (Fig. 11B).

The lumen of the stem of the caudal appendage expands the body cavity and coelomocytes occur within (Fig. 11C). The stem has a thin cuticle, one-layered epidermis, thin circular musculature and 15 strands of longitudinal musculature (Fig. 11C).

Vesicles are connected to the stem and further expand the body cavity, as they are open to the body cavity (Fig. 11C). Coelomocytes occur within vesicles (Fig. 11C–E). Vesicles consist of a thin cuticle and an epidermis, muscle layers are missing (Fig. 11C–E). Spinulets were not observable in the histological sections of the stem and vesicles.

3.4. Noteworthy observations

While examining specimens, some noteworthy observations were made that stand out compared to their “common” occurrence.

In at least one specimen from each the White Sea and Gullmarsfjord, abnormalities in the scalid rows were observed (Fig. 12A–C). In one case, one scalid row is slightly curved, resulting in a discontinuous scalid row, which overlaps with the following new “starting point” of the same scalid row (Fig. 12A) and another scalid row is strongly curved (Fig. 12B). In another specimen, three neighboured scalid rows are

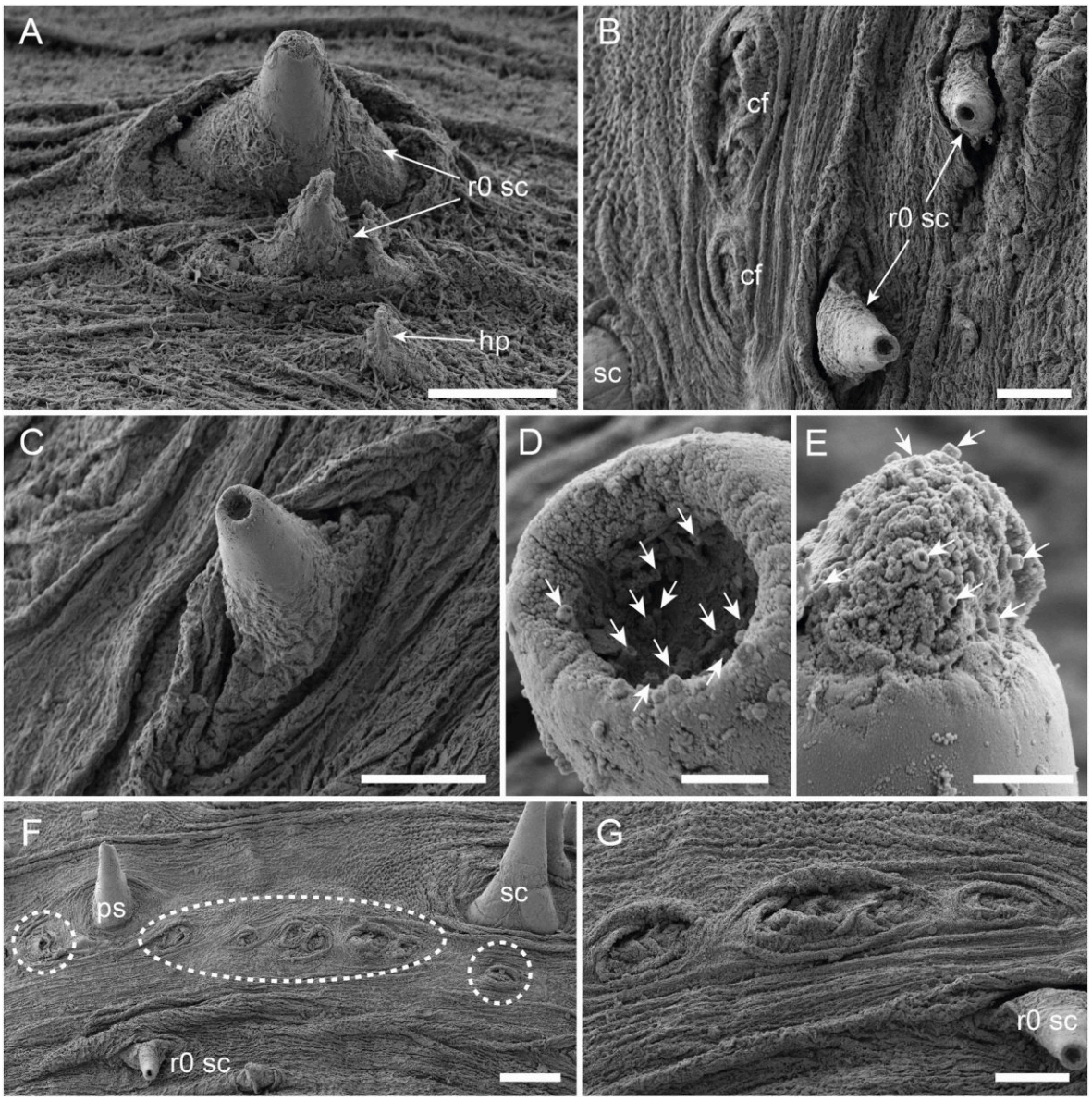

Fig. 4. Ring 0 scalids and circular folds on the circumoral field of specimens from the White Sea (A,D) and Gullmarsfjord (B,C,E-G), SEM images. A. Ring 0 scalids (r0 sc) as pair close together. B. Ring 0 scalids as pair further apart. C. Single ring 0 scalid. D, E. Examples of tips of ring 0 scalids with subapical depression (D) and with extruded subapical depression (E). Small arrows show tubular receptor structures. F. Higher magnification of posterior circumoral field. Dotted circles show circular folds (cf). G. Higher magnification of circular folds. Further abbreviations: hp, hemispherical papilla; ps, primary scalid; sc, scalids. Scale bars: A-C,G = 50 μm; E,D = 5 μm; F = 100 μm.

discontinued for about 100–150 μm on the same level before continuing the same scalid row (Fig. 12C).

One *P. caudatus* specimen from the White Sea has a single bipartite tooth in the first ring of teeth (Fig. 12D). The four remaining teeth of the first ring have the typical cuspidate tooth appearance. The bipartite tooth lacks the large median cusp, but a damaged tooth could be excluded due to an intact surface between both parts (Fig. 12D). One part of the tooth has three small cusps, whereas the other part has four small cusps (Fig. 12D). The bipartite tooth does not hold receptor structures (Fig. 12D).

The anterior trunk of one specimen from Gullmarsfjord has two scalids which are not aligned with scalid rows (Fig. 12E). Both scalids have the same appearance as the scalids of the introvert, including a subapical depression with several tubular receptor structures (Fig. 12E and F). The subapical depression is similar to the ones of the scalids on the introvert orientated towards the anterior part of the specimen.

The length of the caudal appendage of examined specimens differs highly. Especially in small adults between 1 and 2 cm in body length (excluding the tail), the appendage could be either short (Fig. 1A) or approximately the same length as the introvert and trunk (Fig. 12G and H). When the appendage is long, the stem on which the vesicles are attached is visible (Fig. 12G and H). On the anterior part of the stem, the vesicles are often bundled and occur in high numbers, whereas on the posterior part an organization of the vesicles in rings is visible (Fig. 12G–I). Sometimes the vesicle rings are further apart (Fig. 12H). Similar to the vesicles, the stem is beset with numerous spinulets (Fig. 12I). Spinulets on the stem were only visible in light micrographs, presumably due to dirt residues.

In addition, the colouration of *P. caudatus* differs between specimens and localities in our material. Specimens from Gullmarsfjord and North Sea are whitish to brown-yellowish and specimens from the White Sea are either whitish to yellowish or have a brown trunk and a brighter

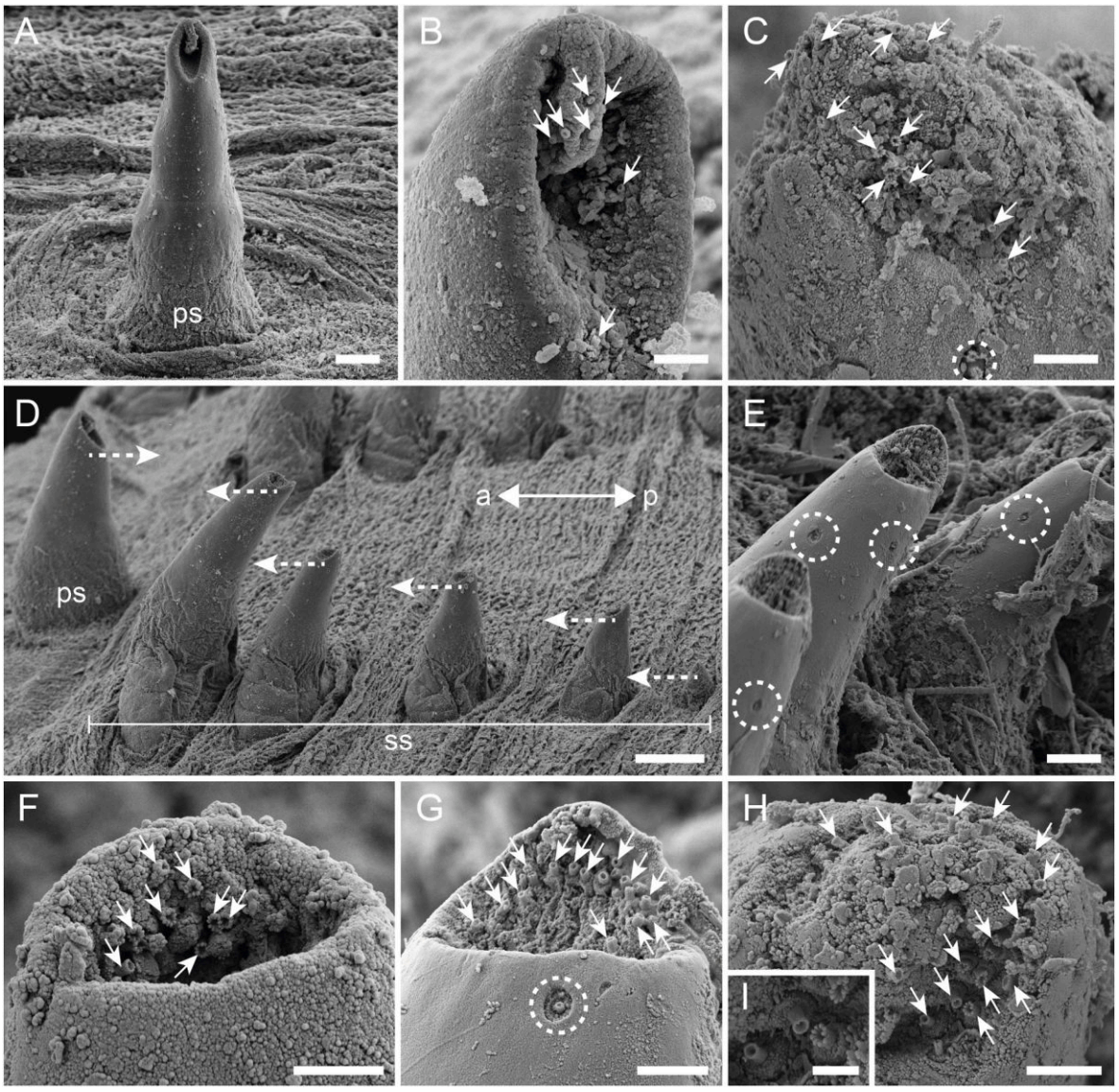

Fig. 5. Primary scalids and scalids of specimens from the Gullmarsfjord (A,B,D,F), North Sea (C,H) and White Sea (E,G), SEM images. Small arrows show tubular receptor structures in B,C,F-H. Dotted circles in C, E and G show depressions on the surface of primary scalids/scalids with one tubular receptor. A. Posterior view of primary scalid (ps). B, C. Examples of tips of primary scalids with subapical depression and distinct median fold (B) and extruded subapical depression without median fold (C). D. Lateral view of scalid series (ss). Double arrow shows orientation of anterior (a) and posterior (p) of specimen. Dotted arrows show orientation of subapical depressions of primary scalids (ps) and scalids. E. Frontal view of scalids. F, G, H. Examples of tips of scalids with subapical depression (F, G) and extruded subapical depression (H). I. Higher magnification of two types of tubular receptors in the subapical depression. Scale bars: A = 20 μm; B,C,F-H = 5 μm; D = 50 μm; E = 10 μm; I = 2 μm.

introvert (Fig. 1A; 12G,H).

4. Discussion

4.1. Verification of identified specimens

Five macroscopic priapulid species occur in the Northern Hemisphere: *Priapulus caudatus*, *Priapulus abyssorum* Menzies, 1959, *P. bicaudatus* Danielssen, 1869, *H. spinulosus* Von Siebold, 1849 and *H. higginsi* Shirley and Storch, 1999 (see Adrianov and Malakhov, 1996a; 1996b). One of the most distinct morphological characters among their genera is the number of caudal appendages in adult specimens. While *Halicryptus* has no caudal appendage and *Priapulopsis* has two appendages, *Priapulus* is the only macroscopic genus in the Northern Hemisphere with only one caudal appendage (Van der Land, 1970; Schmidt-Rhaesa, 2013). Due to the presence of a single caudal appendage in all our examined specimens, we confidently assign them all to *Priapulus*.

The holotype of *P. caudatus* does not exist, therefore, all described characters of this species were collected throughout several previous studies on different material. As *P. caudatus* does not have distinct unique traits, specimens are rather identified by a combination of traits overlapping with other species and excluding diagnostic characters of other macroscopic species. The other *Priapulus* species from the Northern Hemisphere, *P. abyssorum*, was only reported from abyssal to hadal depths of 3000–8000 m (Adrianov and Malakhov, 1996b). Nevertheless, it is still debateable, if *P. abyssorum* and other deep-sea priapulids represent separate species, as they lack unambiguous diagnostic characters (Van der Land, 1972). Proposed characteristics of *P. abyssorum* are the teeth of the first ring being smaller compared to those of the second ring, nine to ten scalids within a series, four to seven rings of ring papillae and the absence of posterior warts (Adrianov and Malakhov,

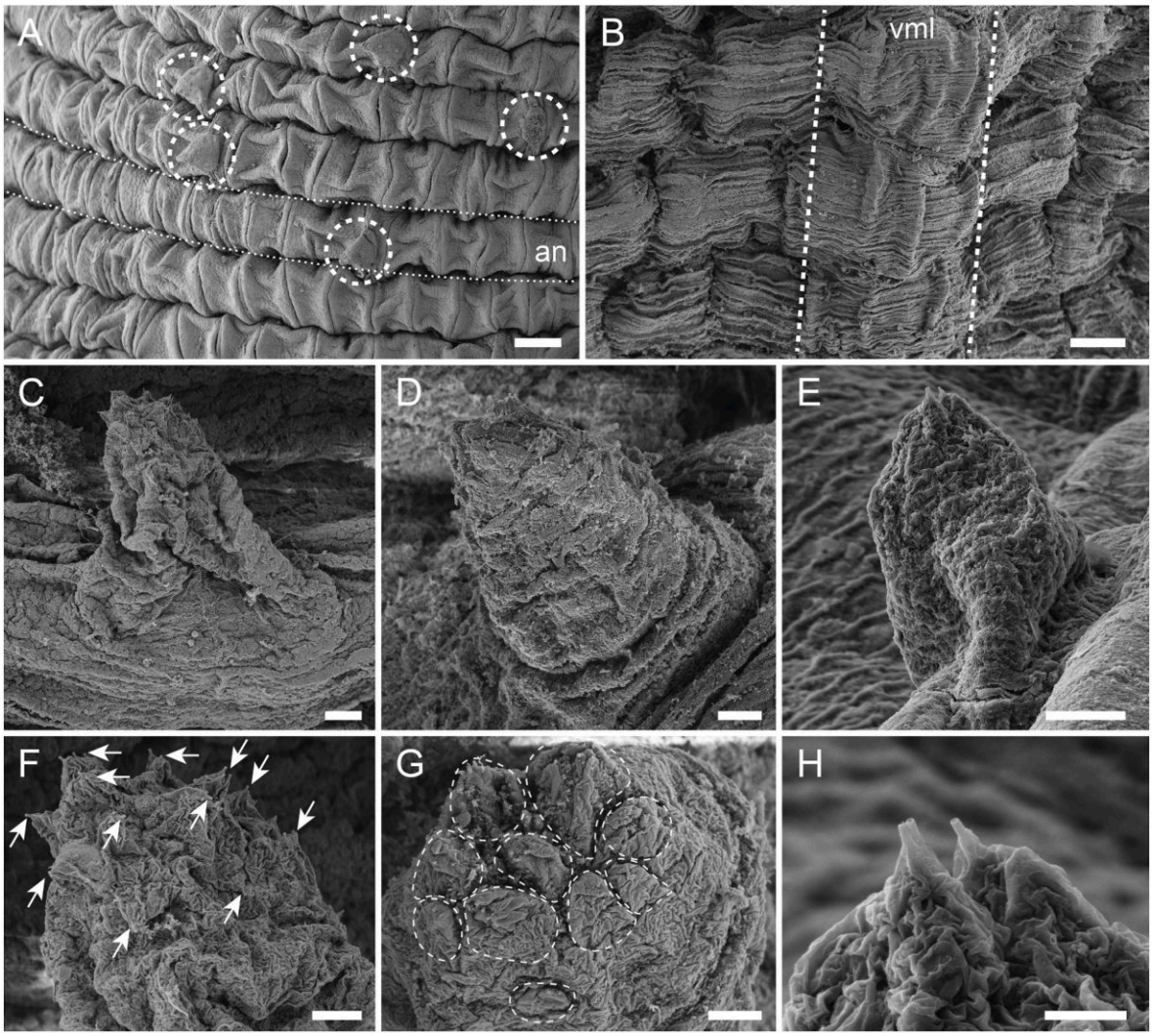

Fig. 6. Trunk and trunk papillae of specimens from the White Sea (A,E,H), Gullmarsfjord (B,C,F) and North Sea (D,G), SEM images. A. Trunk with annuli (an) and trunk papillae (dotted circles). B. Higher magnification of ventral midline (vml). C, D, E. Examples of trunk papillae. F, G, H. Examples of tips of trunk papillae. Small arrows in F show tubular receptors (H). Dotted areas in G show receptor units. Scale bars: A,B = 100 μm; C-E = 20 μm; F,G = 10 μm; H = 5 μm.

1996b). As our examined specimens were collected from up to 40 m depth and diagnostic characters are not congruent with those of *P. abyssorum*, we assign our specimens to *Priapulus caudatus*.

Priapulus caudatus has a broad distribution in the Northern Hemisphere (see Van der Land, 1970; Adrianov and Malakhov, 1996b). Two recent studies show a variable genetic population structure of *P. caudatus* from different localities, which are interpreted differently. Laakkonen et al. (2021) specify different *Priapulus* species across locations, whereas Kolbasova et al. (2023) argue for an incomplete speciation of *P. caudatus*. As interpretations are ambiguous, it remains unclear, if *Priapulus* specimens from different localities potentially represent more than one species. Specimens from different localities in our study did not show any variation in characters, except for minor details in specific structures (discussed below). Hence, we assign all our observed specimens to *P. caudatus*.

4.2. Morphological characters

In the following section we discuss the morphological characters of *P. caudatus* in the order of where they occur in a specimen from anterior to posterior.

Adult *P. caudatus* specimens have cuspidate pharyngeal teeth with a large median cusp and some small lateral cusps (e.g. Ehlers, 1862; Van der Land, 1970). The number of lateral cusps differs in various reports from two (Hammond, 1970a) to three (Ehlers, 1862) or up to six (Van der Land, 1970) per side of the median cusp in the anterior pentaradial rings of teeth. In postlarval stages, the median cusp is either missing or not yet distinctly developed and the number of lateral cusps can be higher (up to 16) than in adult specimens (e.g. Fig. 5 and 6 in Van der Land, 1970). The number of lateral cusps differs in our examined specimens slightly between specimens from different localities. The examined White Sea specimens have slightly more lateral cusps than specimens from Gullmarsfjord and North Sea. White Sea specimens were smaller than those of the other localities, which could display a younger age and support Van der Lands (1970) notification that the number of lateral cusps decreases with age.

In the congener from the Southern Hemisphere, *P. tuberculatospinosus* Baird, 1868, teeth of the first ring are distinctly smaller than in following rings (Van der Land, 1970) and hold tooth receptors ("cuticular tubules" in Storch et al., 1994). For adult *P. caudatus*, the surface of the teeth is described as smooth (Ehlers, 1862) and previous SEM studies (e.g. Storch et al., 1994; Adrianov and Malakhov, 1996a) do not report receptors on the teeth, which we can confirm here for all our investigated specimens of *P. caudatus*. Interestingly, larval stages of *P. caudatus* have in the first seven rings of teeth 1 to 12 receptor tubuli on the cusps (Lemburg, 1999). Whether tooth receptors are lost in development from

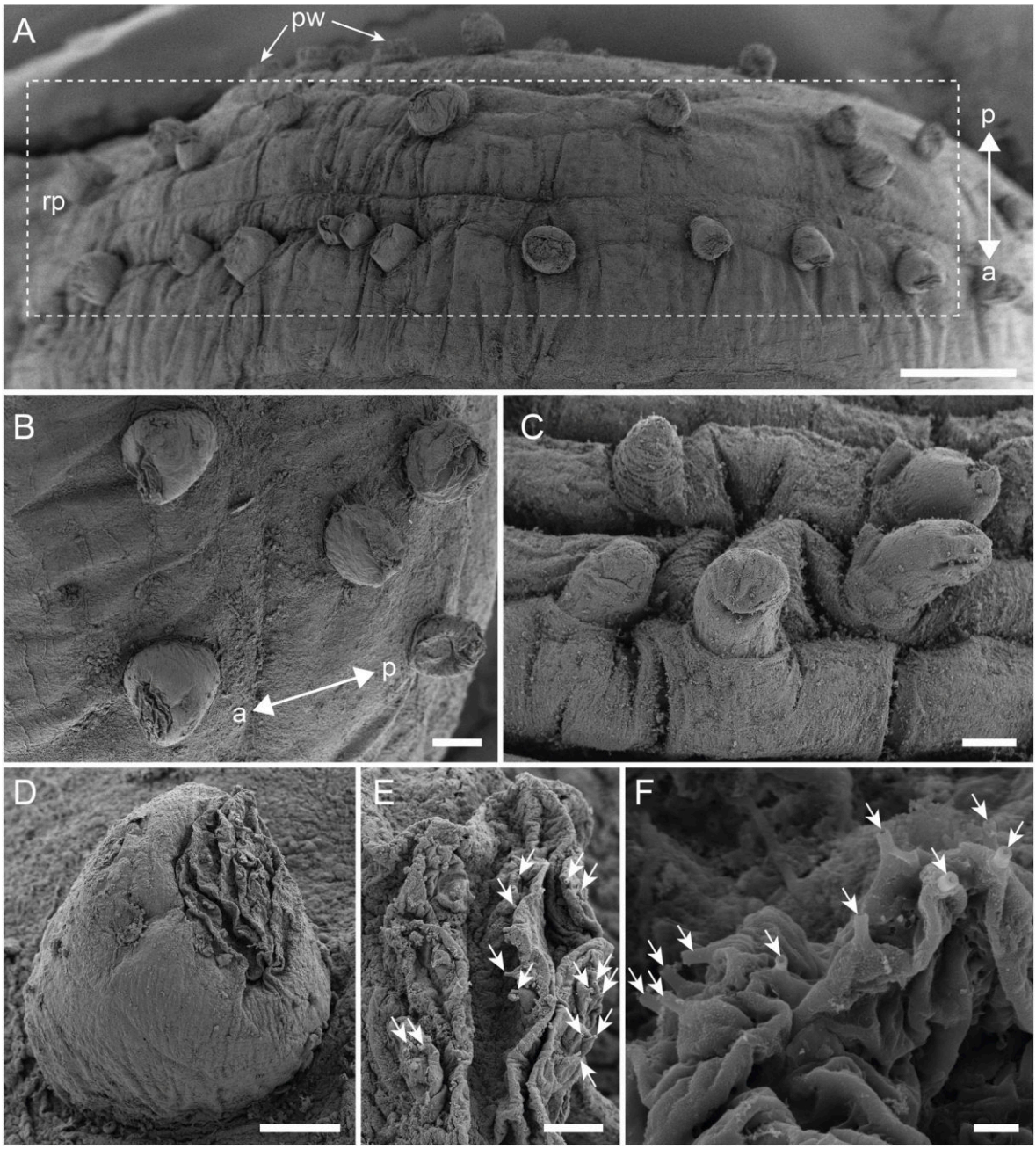

Fig. 7. Ring papillae of specimens from the Gullmarsfjord (A,B,D,E), North Sea (C) and White Sea (F), SEM images. Double arrow in A and B shows orientation of anterior (a) and posterior (p) of specimen A. Posterior end of trunk showing two rings of ring papillae (rp). B, C. Examples of hemispherical (B) and elongate (C) ring papillae. D. Higher magnification of hemispherical ring papilla. E. Magnification of subapical region with tubular receptor structures (small arrows). Higher magnification of tubular receptor structures (small arrows). Further abbreviations: pw, posterior warts. Scale bars: A = 500 μm; B,C = 100 μm; D = 50 μm; E = 10 μm; F = 2 μm.

larval to postlarval stages is unknown, as detailed information of postlarval stages of *P. caudatus* are lacking.

The size of teeth within one ring is reported to stay the same (e.g. Van der Land, 1970; Hammond, 1970a; Storch et al., 1994), which we can confirm here. Storch et al. (1994) report that the largest teeth of *P. caudatus* occur in the fourth ring, which we cannot fully support, as in our examined specimens the teeth of the second ring were often the broadest and the teeth of the fourth ring often had the longest median cusp. Tooth size is generally difficult to measure, because different angles and the curved shape make exact measurement difficult. Nevertheless, distinctly smaller teeth in the first ring compared to the second ring or two enlarged teeth within the fourth ring, as occurs in *P. tuberculatospinosus* (Van der Land, 1970) or bipartite teeth of the first ring in *Priapulopsis* species (e.g. Schmidt-Rhaesa and Raeker, 2022; Schmidt-Rhaesa and Raeker, in press), do not occur in *P. caudatus*. The one bipartite tooth in the first ring of a *P. caudatus* specimen from the White Sea (see Fig. 12D) may be an exception.

Main differences in size of teeth are visible when the pharynx is fully exposed. The teeth gradually decrease in size from the anterior to posterior pharynx (Ehlers, 1862; Van der Land, 1970), which we can confirm. Anterior teeth in pentaradial rings (approximately the first 5 to 7 rings) are the largest, whereas the size of teeth in the following middle section of the pharynx with a loose organization decreases slightly (e.g. Ehlers, 1862; Van der Land, 1970; Storch et al., 1994). Teeth of the

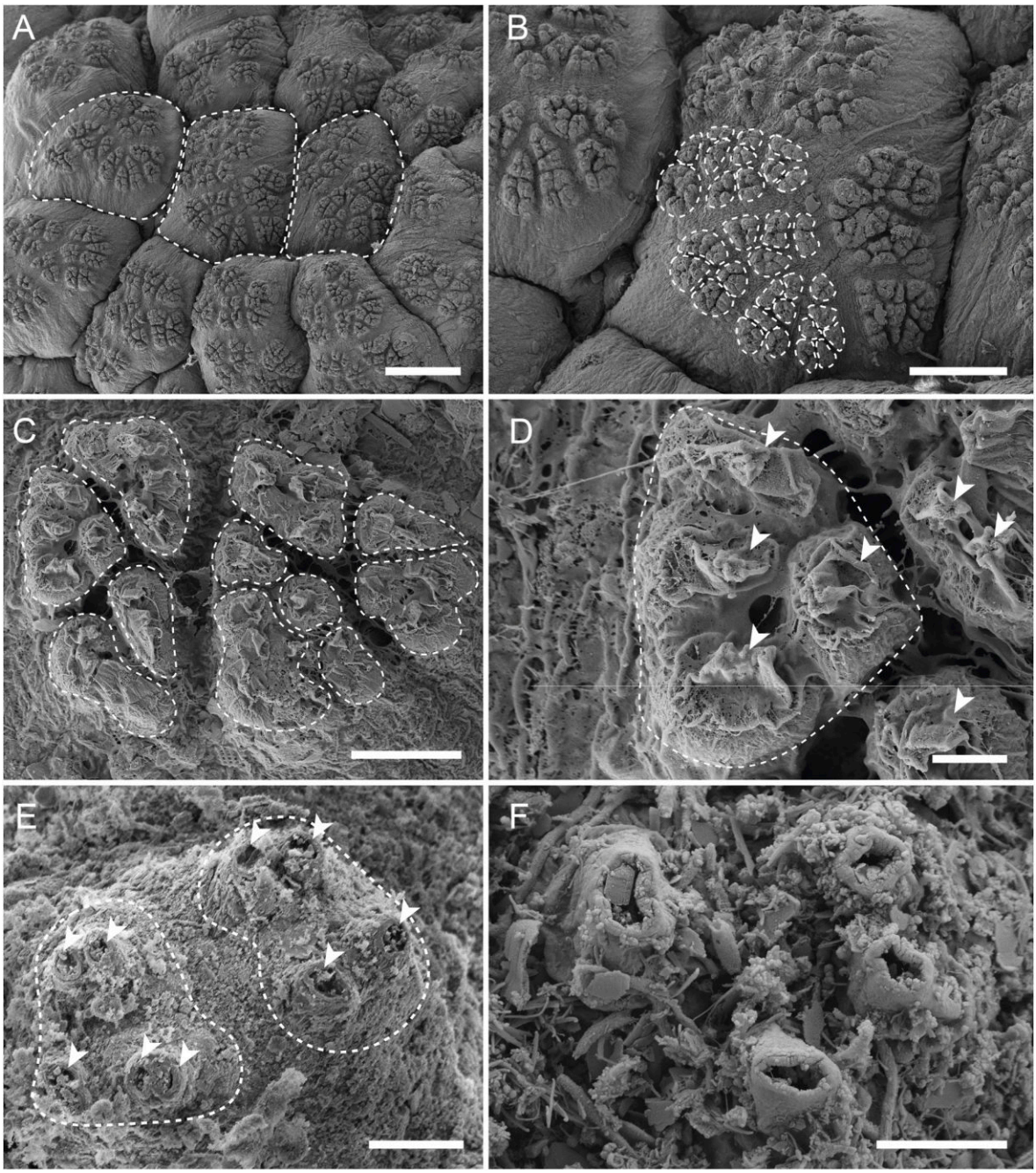

Fig. 8. Posterior warts on posterior trunk of specimens from the White Sea (A-D,F) and Gullmarsfjord (E), SEM images. A. Overview of posterior warts. Dotted areas show separation of the posterior warts. B. Higher magnification of posterior wart. Dotted areas show wart units. C. Higher magnification of wart units. Dotted areas show wart subunits. D. Higher magnification of wart subunit (dotted area) with collapsed tubes (arrowheads). Note the mucous-like structures between the tubes. E. Higher magnification of wart subunits (dotted areas) with tubes (arrowheads). F. Higher magnification of tubes of wart subunit. Scale bars: A = 200 μm; B = 100 μm; C,E = 20 μm; D,F = 5 μm.

posteriormost pharynx of *P. caudatus* are the smallest and occur as cuticular protrusions, but they are similar in shape and composition than those of *P. australis* (e.g. Fig. 3D in Schmidt-Rhaesa and Raeker, in press).

The circumoral field of Priapulida is here described as the region between the pharyngeal teeth and the primary scalids. Hammond (1970a) divided this region further into a circumoral region and a collar, which describes the ring-like elevation of the circular nerve-ring, when the introvert is slightly everted. Later, Adrianov and Malakhov (1996a) refer to this region only as circumoral field, which we adopt here, as the collar is not always visible, depending on the state of contraction of the introvert.

Cuticular structures on the circumoral field are either overlooked or named inconsistently in previous publications. They are often referred to as "buccal papillae" (e.g. Van der Land, 1970; Storch et al., 1994). Hammond (1970a) described these structures as "collar papillae", which include two types, conical and disc-like flattened papillae. Adrianov and Malakhov (1996a) report "buccal scalids" besides buccal papillae, although these seem to represent scalids, which are part of a scalid row (cf. their Fig. 3.8D). This study shows the occurrence of three types of cuticular structures on the circumoral field of *P. caudatus*.

The first type is represented by hemispherical papillae, which have a

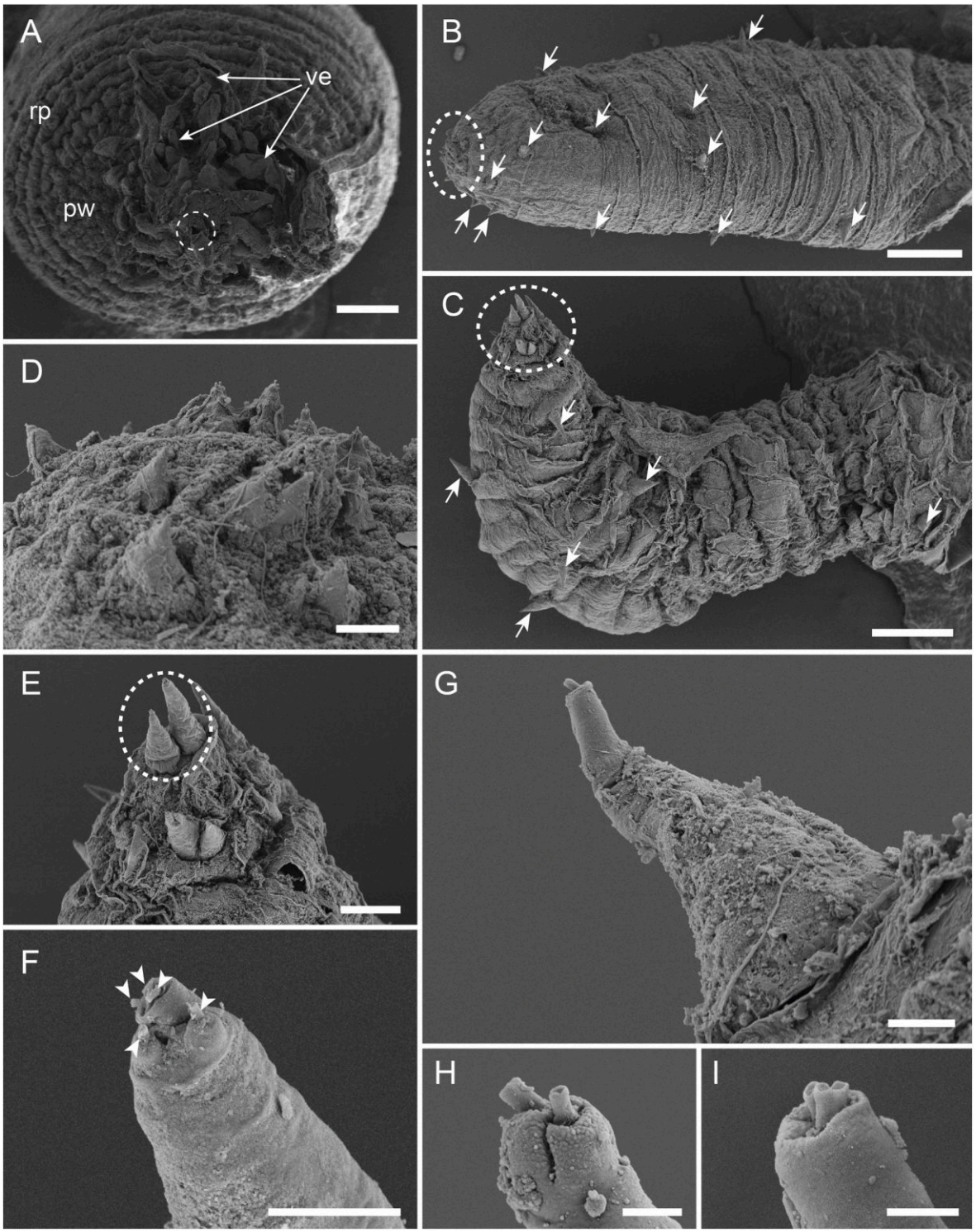

Fig. 9. Vesicles of the caudal appendage of specimens from the Gullmarsfjord (A,C,E,F), North Sea (B,D) and White Sea (G,H,I), SEM images. A. Caudal view on the caudal appendage with numerous vesicles (ve). Dotted circle shows hollow stem of the caudal appendage. B, C. Examples for vesicles with irregularly scattered spinulets (arrows) on the surface and apical spinulet crown (dotted circles). D. Higher magnification of spinulet crown with similar sized spinulets. E. Higher magnification of spinulet crown with large median spinulets (dotted circle). F. Higher magnification of the tip of a large spinulet with five tubular receptor structures (arrowheads). G, H, I. Examples for spinulets with one (G), two (H) and three (I) tubular receptor structures on the tip. Further abbreviations: pw, posterior warts; rp, ring papillae. Scale bars: A = 500 μm; B,C = 200 μm; D = 20 μm; E = 50 μm; F = 10 μm; G = 5 μm; H, I = 2 μm.

sensory function due to apical receptor tubuli and occur accumulated nearest to the teeth. Hemispherical papillae are laterally flattened, showing a distinct ridge which runs in anterior to posterior direction on the specimen. Recently, similar laterally flattened papillae with receptors on the circumoral field were figured for *P. tuberculatospinosus* and described as 'irregular structures' (e.g. Fig. 9A and B in Schmidt-Rhaesa and Raeker, in press). The hemispherical papillae could presumably be reported before in a previous study, as Hammond (1970a) described flattened, disc-like papillae on the circumoral field of *P. caudatus*, without providing any images.

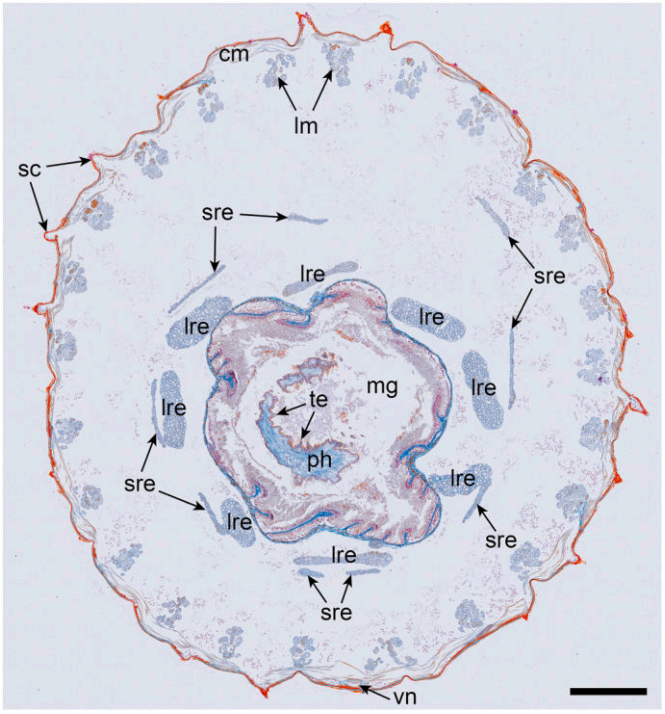

Fig. 10. Histological cross-section through the introvert of *P. caudatus* specimen from White Sea, light microscopic image. Posterior pharynx (ph) is slightly pushed into the midgut (mg). Note the 24 distinct longitudinal musculature strands (lm) lining the internal circular musculature (cm) of the introvert and the two short introvert retractors (sre) allocated to one long introvert retractor (lre) in line with the ventral nerve chord (vn). Further abbreviations: sc, scalid; te, teeth. Scale bar = 500 µm.

The second type are ring 0 scalids that are organized in a ring in the central part of the circumoral field. Ring 0 scalids of *P. caudatus* do not clearly align with posterior scalid rows. Due to subapical depressions with receptor tubuli, ring 0 scalids have a sensory function, which was previously shown by Adrianov and Malakhov (1996a). Probably, the "buccal papillae" of previous studies referred to ring 0 scalids, as these are the most prominent structures on the circumoral field and are already visible without higher magnifications. We chose the term ring 0 scalids, as these conical structures resemble small scalids and occur anterior of primary scalids, which were often referred to as the first ring of scalids (see Schmidt-Rhaesa and Raeker, 2022).

The third type of cuticular structures on the posterior circumoral field are circular folds. Circular folds have been visible in figures of previous studies (e.g. Fig. 2C in Hammond, 1970a, Fig. 16 in Storch et al., 1994), but were not described. The function of these circular folds remains unclear, as no receptor structures were visible. Developing structures can be excluded, as circular folds looked the same in adults of different sizes. Probably, circular folds represent rudimentary structures, but further investigations are needed to proof this assumption.

Between the circumoral field and the 25 scalid rows is a ring of eight primary scalids (previously described as "sensory spines" in Storch et al., 1994 or "circumoral scalid" in Adrianov and Malakhov, 1996a) that do not stand in line with the following longitudinal scalid rows. Primary scalids are organized in a distinct pattern, with three (or four in the part with the ventral midline) scalid rows between two primary scalids (Storch et al., 1994), which is present in other macroscopic priapulids as well (e.g. Schmidt-Rhaesa and Raeker, 2022; Schmidt-Rhaesa and Raeker, in press; Raeker et al., 2024). Sometimes, primary scalids are slightly smaller than normal scalids (Storch et al., 1994) and appear more slender due to the more narrow basal part, as we could show here. The sensory function of primary scalids due to receptor tubuli in a subapical depression was already reported by Storch et al. (1994) and Adrianov and Malakhov (1996a). A new observation is a distinct cuticular fold within the subapical depression of primary scalids, which is absent in remaining types of scalids. This fold could represent a dehydration artefact, as it is not visible when the surface of the subapical depression is extruded, and the natural appearance of the primary scalid tip is unknown. A further new observation are single lateral tubular receptors that are found occasionally. Additionally, the orientation of the subapical depression of primary scalids points towards the posterior part of the specimen.

Scalids in longitudinal rows are conical sensory structures with subapical depressions beset with receptor tubuli (e.g. Van der Land, 1970; Hammond, 1970a; Storch et al., 1994). Scalid rows consist of several scalid series that again consist of a varying number of scalids decreasing in size (Van der Land, 1970). The number of scalids varies mostly between five and six in a series in adults (e.g. Van der Land, 1970; Adrianov and Malakhov, 1996a; Schmidt-Rhaesa, 2013), but up to eight in large specimens or only three in postlarval stages (own observations) can occur. The receptors in the subapical depressions of scalids appear in two types (smooth and with apical cuticular protrusions), which were previously shown in images by Hammond (1970a) and Adrianov and Malakhov (1996a) and also appear in other macroscopic species (e.g. Storch et al., 1994 for *P. tuberculatospinosus*; Raeker et al., 2024 for *H. spinulosus*). A new report for scalids of *P. caudatus* in this study is the irregular occurrence of depressions on the lateral surface that contain a single tubular receptor. As these single receptors on scalids have only been found in specimens from the White Sea, this might reflect a specific character for specimens from this locality, but further material is needed to confirm this assumption. Another observation is the orientation of the subapical depressions of scalids towards the anterior of the specimen, oppositional to the ones of primary scalids. It is unknown, why both scalid types have their subapical depressions orientated differently, as both hold the same two types of receptor tubuli and presumably have the same function.

The introvert of Priapulida can be withdrawn by longitudinal musculature, the long and short introvert retractors (Schmidt-Rhaesa, 2013). While the number of long introvert retractors is always eight, the number of short introvert retractors of *P. caudatus* differs between 8 and 25 (summarized by Mattisson et al., 1974; Storch et al., 1994), probably due to division of muscle strands (Schmidt-Rhaesa, 2013). We examined nine short introvert retractors, from which seven are located directly next to a long introvert retractor and two are next to the remaining long introvert retractor, which is in line with the ventral nerve. As we only examined one specimen in histological cross sections and such high variation in number of short introvert retractors exist, we recommend to investigate the retractor musculature of priapulids in relation to total body length.

The trunk of macroscopic priapulids is annulated. The number of annuli is assumed to correspond with the number of circular muscles of the trunk (Van der Land, 1970). For *P. caudatus*, 40 to 50 annuli are reported, which we can confirm here. *Priapulus caudatus* seems to have a fixed number of annuli between 38 and 42, without distinct correlation to the body length. Interestingly, *Halicryptus* has nearly twice the amount of annuli in much smaller specimens (<1 cm) (Raeker et al., 2024). The reason of the varying number of annuli between related species remains unclear but does not seemingly relate to locality or size.

The annulated trunk of *P. caudatus* holds three structures: trunk papillae, ring papillae and posterior warts (Van der Land, 1970). Interestingly, Hammond (1970a) reported similar "papillae" as on the introvert (e.g. scalids) scattered on the trunk in specimens from the Gullmarsfjord, but without showing images. In this study, we only observed two scalids near the introvert on the trunk in a single specimen from the Gullmarsfjord. Eventually, scalids on the trunk could represent a character of specimens from this locality, but as these scalids were not reported more often, their occurrence tends to be exceptions.

Trunk papillae are scattered cuticular elevations on the entire trunk (Ehlers, 1862; Hammond, 1970a; Van der Land, 1970), but are absent on

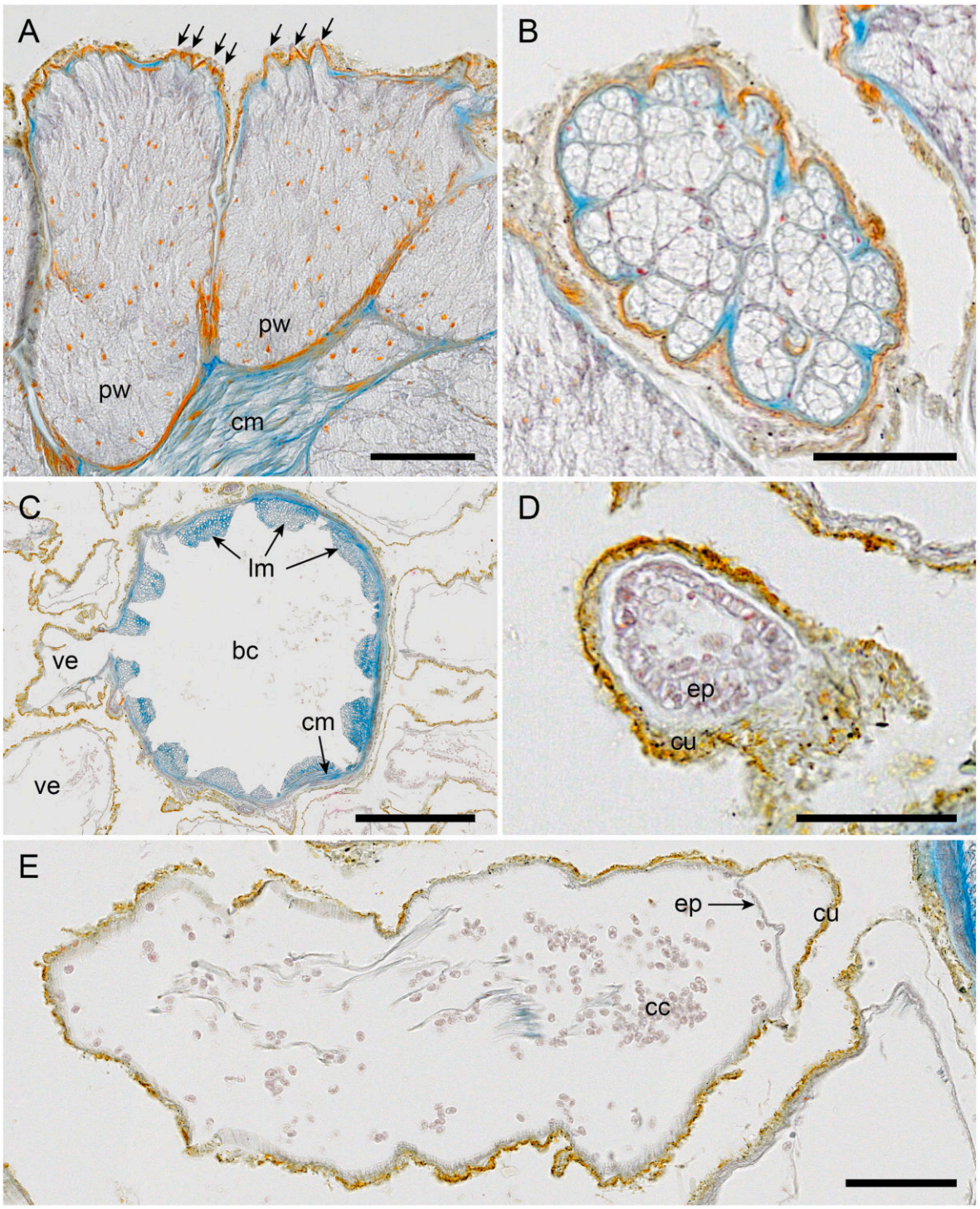

Fig. 11. Histological sections of posterior warts (A,B), caudal appendage (C) and vesicles (D,E) of *P. caudatus* specimen from the White Sea, light microscopic images. A. Longitudinal section of posterior warts (pw). Arrows show tubuli. B. Cross section of wart unit. C. Cross section of the stem of the caudal appendage. Note the connection of the lumen of the vesicle (ve) with the body cavity (bc). D. Cross section of the basal part of a vesicle. E. Longitudinal section of a vesicle with coelomocytes (cc) inside of the vesicle lumen. Further abbreviations: cm, circular musculature; cu, cuticle; ep, epidermis; lm, longitudinal musculature. Scale bars: A,E = 100 μm; B,D = 50 μm; C = 200 μm.

the surface along the ventral midline. Hammond (1970a) reported for trunk papillae a tip without apical openings, supposing trunk papillae are a developmental stage of scalids on the trunk. Adrianov and Malakhov (1996a) showed several tubular receptor structures on the tip, concluding a sensory function, which we confirm here. Additionally, we observed that some tubular receptors share a base and up to ten of these bases form the tip of a trunk papilla in large specimens. The function of trunk papillae remains unclear.

Ring papillae occur organized in one to seven rings on the posterior trunk of *Priapulus* species (Van der Land, 1970). *Priapulus caudatus* has one to three rings of ring papillae (Adrianov and Malakhov, 1996a), which we can confirm here. Whether the number of rings is conditioned by age is unclear, as large specimens from the North Sea had either two or three rings.

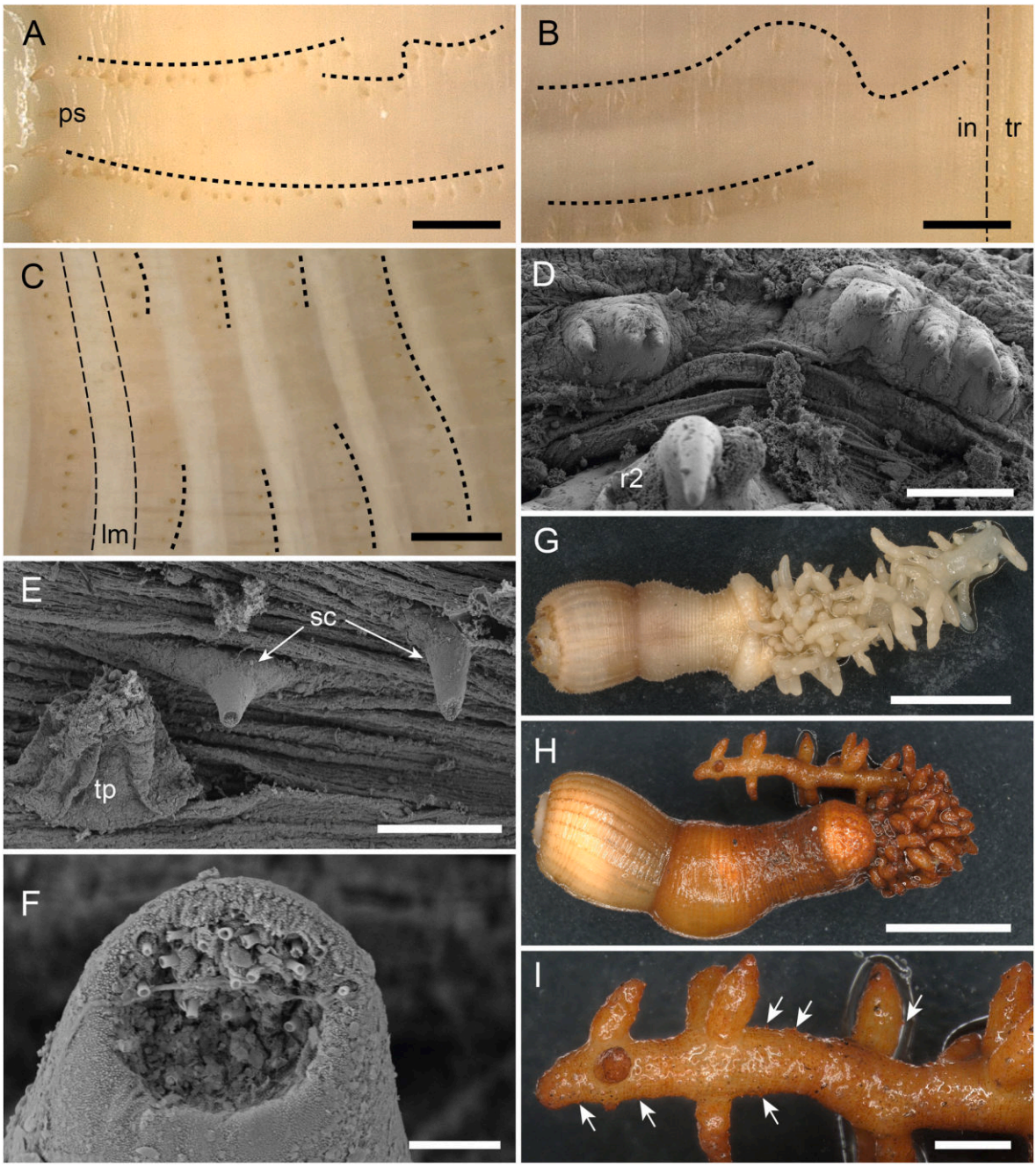

Fig. 12. Noteworthy observations of morphological characters of specimens from the White Sea (A,B,D,G-I) and Gullmarsfjord (C,E,F), light microscopic images (A-C,G-I) and SEM images (D–F). A-C. Abnormal organization of scalid rows (dotted lines) with curved rows (A,B) or discontinuous rows (C). Note the visible longitudinal muscles (lm) between scalid rows. D. Bipartite tooth of the first ring. E-F. Scalids (sc) next to a trunk papilla (tp) on the anterior trunk with typical subapical depression and tubular receptor structures on the tip (F). G-H. Examples for small adult specimens with long caudal appendage. Note the bundled vesicles on the anterior part of the caudal appendage and the more parted vesicles on the posterior part revealing the stem of the caudal appendage. I. Higher magnification of posterior part of the caudal appendage. Arrows show small structures on the stem. Further abbreviations: in, introvert; ps, primary scalid; tr, trunk. Scale bars: A,B = 500 μm; C,I = 1 mm; D,E = 100 μm; F = 5 μm; G,H = 5 mm.

For *P. caudatus*, ring papillae have not yet been shown by SEM. Van der Land (1970) illustrated them as hemispherical papillae and assumed a sensory function. We confirm the hemispherical appearance for small and medium-sized adult specimens, but large specimens occasionally have elongated ring papillae. In addition, we can confirm a sensory function, as a subapical region with tubular receptors facing anteriorly is present.

Posterior warts on the far posterior trunk are numerous in *P. caudatus*. Large, wart-like structures in *P. caudatus* and *P. tuberculatospinosus* (Van der Land, 1970) were first shown in detail by Hammond (1970a). Adrianov and Malakhov (1996a) later showed additional structures related to posterior warts ("pedicillate papillae" and "glandular papillae" in their Fig. 3.35B,C). These structures were observed in young *P. caudatus* specimens, but not in large specimens by Hammond (1970a) or in this study. Therefore, both papillae could represent posterior warts in development, as especially the glandular papillae have a similar appearance to posterior warts with distinct trenches separating units of openings (cf. Fig. 3.35B,F in Adrianov and Malakhov, 1996a). A comparison of postlarval stages, small adults and large adults of *P. caudatus* could clarify this assumption.

Ehlers (1862) assumed that posterior warts are glandular structures due to numerous apical tubes, which have been shown in detail much later (Hammond, 1970a; Adrianov and Malakhov, 1996a; Lemburg, 1999). The apical tubes seem to be fragile and can collapse, hiding the opening of the tubes (c.f. Fig. 3.35D in Adrianov and Malakhov, 1996a; this study). In addition, Hammond (1970a) reported diaphragm-like structures enclosing the tubes, which we have not found here in SEM images and histological sections on specimens with undamaged tubes. Scharff (1885) reported large secretory cells beneath the warts and that posterior warts were covered in sticky material, which we can both confirm. The function of posterior warts and their excretions remains unclear. As the warts are close to the caudal appendage, the mucous excretion could function as protective or lubricate layer of the vesicles, as the caudal appendage is often covered with mucus and dirt mixture (Hammond, 1970a; own observations). A second possible function could be the lining of the burrows in the mud with a mucous layer to keep them from collapsing as they remain in the mud (Turk et al., 2024), although reports of immediately collapsing burrows exist (Hammond, 1970b).

The caudal appendage of *Priapulus* consists of a stem and numerous vesicles (Van der Land, 1970). In postlarval stages and juveniles, vesicles are often absent, showing only the slightly annulated and with spinulets beset stem (Van der Land, 1970). We can confirm spinulets on the stem, as they are visible in light micrographs but covered by dirt in SEM images. Larger adults can hold up to 200 vesicles in different sizes that are connected with the body cavity, as direct transitions occur and the vesicles are filled with body fluid (Ehlers, 1862). According to Ehlers (1862), the vesicles are lined internally under the cuticle with a thin muscular layer, which we cannot confirm here, as only a one-layered epidermis underlines the cuticle. Spinulets, often accumulated on the tips of the vesicles, have been reported by Ehlers (1862) and shown in detail by Adrianov and Malakhov (1996a). In addition, the latter authors showed a large type of spinulet with three apical tubuli. Whether this larger spinulet is located centrally of the spinulet crown is unknown. Nevertheless, variations with different numbers of apical tubuli occur on the vesicles as shown in this study, but their function remains unclear.

4.3. Homologous characters of macroscopic Priapulida

Macroscopic priapulids are divided into four genera, *Acanthopriapulus*, *Priapulus*, *Priapulopsis* and *Halicryptus*. These four genera are summarized as Priapulidae (Van der Land, 1970), from which *Acanthopriapulus*, *Priapulus* and *Priapulopsis* form the Megintroverta (Lemburg, 1999). Adrianov and Malakhov (1995) classified *Halicryptus* within the invalid "Halicryptidae", as they seemingly misread Salvini-Plawens (1974) proposed subfamily "Halicryptinae" within Priapulidae. Later authors adapted the invalid family (e.g. Wills et al., 2012; Schmidt-Rhaesa, 2013; Giribet and Edgecombe, 2020; Wernström et al., 2023), as well as the World Register of Marine Species (WoRMS) (Paulay, 2024). We follow here the systematic proposed by Van der Land (1970) with *Halicryptus* within Priapulidae. As new findings in many species of Priapulidae were recently reported (*A. horridus* in Schmidt-Rhaesa et al., 2022; *P. bicaudatus* in Schmidt-Rhaesa and Raeker, 2022; *P. australis*, *P. papillatus* and *P. tuberculatospinosus* in Schmidt-Rhaesa and Raeker, in press; *H. spinulosus* and *H. higginsi* in Raeker et al., 2024; *P. caudatus* in this study) an analysis on the homology of adult characters can be approached (summarized in Table 3).

Cuspidate pharyngeal teeth represent homologous characters in Priapulidae. Differences occur in the number of lateral cusps of teeth (presumably affected by age, see Raeker et al., 2024), presence or absence of cuticular spinose projections on the surface and shape of the first ring teeth (small in *P. tuberculatospinosus*; bipartite in *Priapulopsis*). In some species (*P. tuberculatospinosus*; all *Priapulopsis* species), the teeth have an additional sensory function due to the presence of tooth receptors (Storch et al., 1994; Schmidt-Rhaesa and Raeker, 2022; Schmidt-Rhaesa and Raeker, in press).

Table 3
Overview of homologous characters of Priapulidae and Megintroverta.

	Priapulidae			
	Megintroverta			
	Acanthopriapulus	*Priapulopsis*	*Priapulus*	*Halicryptus*
Cuspidate pharyngeal teeth	+	+	+	+
Mouth papillae	–	–	?	?
Ring 0 scalids	?	+	+	?
Scalids	+	+	+	+
Trunk papillae	+	+*	+	?*
Ring papillae	+	+	+	?*
Posterior warts	+	–	+	–
Caudal appendage	+	+	+	–

Plus (+) represents reported characters. Dash (−) represents absent or not reported characters. Questionmarks (?) represent the presence of characters on similar position, but uncertainty, if they are homologous. Asterisks (*) show the presence of flosculi on characters.

Ring 0 scalids are on the central circumoral field and are reported for *P. bicaudatus* (Schmidt-Rhaesa and Raeker, 2022) and *P. caudatus* (this study). Indications for unlabelled ring 0 scalids are presumably given for *A. horridus* (cf. Fig. 3C in Schmidt-Rhaesa et al., 2022) and *P. tuberculatospinosus* (cf. Fig. 9 in Storch et al., 1994). Ring 0 scalids of *P. caudatus* and *P. bicaudatus* are both organized in a ring and resemble their respective scalids in the scalids rows, but differ in the ring pattern when compared to each other. In *P. bicaudatus*, ring 0 scalids seem to be standing in line with scalid rows (cf. Fig. 10A in Schmidt-Rhaesa and Raeker, 2022), whereas in *P. caudatus* they do not line up with scalid rows and occur sometimes as pairs. In comparison, *H. spinulosus* has three sizes of conical buccal papillae on the circumoral field, from which the large buccal papillae stand directly anterior of the primary scalids and are organized together with medium-sized buccal papillae in a loose ring (Raeker et al., 2024). Whether ring 0 scalids of *P. caudatus* and *P. bicaudatus* (and *A. horridus* and *P. tuberculatospinosus*) and large and medium-sized buccal papillae of *H. spinulosus* represent homologous structures is uncertain. Indications of homology lay within the position of these structures on the circumoral field and the presence of similar apical tubular receptors in *H. spinulosus* and *P. caudatus* (e.g. Raeker et al., 2024; this study).

Scalids are homologous structures in Priapulidae, as they form 25 longitudinal scalid rows on the introvert. In Megintroverta, the scalid rows consist of series made of conical scalids, whereas in *Halicryptus* they are single structures with triangularly flattened shape (Van der Land, 1970). Unique for *H. spinulosus* is an additional type of scalid (dentoscalids) in the posterior scalid row, which has two apical spines and is free of external receptors (e.g. Raeker et al., 2024), but contain receptor cells (Storch et al., 1990). Nevertheless, all investigated Priapulidae have the same two types of receptors in subapical depressions of scalids, assuming the same sensory function (e.g. Fig. 12 in Storch et al., 1994 for *P. tuberculatospinosus*; Fig. 3.27F in Adrianov and Malakhov, 1996a for *P. caudatus*; Fig. 3D in Schmidt-Rhaesa et al., 2022 for *A. horridus*; Fig. 5D–H in Raeker et al., 2024 for *H. spinulosus*). Similar to scalids in scalid rows, primary scalids are also homologous in Priapulidae, as their number is always eight and the pattern of scalid rows between primary scalids is the same.

Trunk papillae are scattered sensory structures on the trunk of Priapulidae. In Megintroverta they represent homologous structures, as their appearance is hemispherical to slightly elongate papillae with several apical tubular receptors (Schmidt-Rhaesa et al., 2022; Schmidt-Rhaesa and Raeker, 2022; Schmidt-Rhaesa and Raeker, in press; this study). Trunk papillae of *P. papillatus* stick out as they are organized in rings on the annuli and have one flower-shaped sensory structure (flosculus) among the apical receptors (Schmidt-Rhaesa and Raeker, in press). In contrary, small trunk papillae of *Halicryptus* appear as conical papillae, but apical tubular receptors are lacking, instead,

cuticular protrusions are present apically and numerous flosculi (sometimes also accessory papillae) encircle the median cone (Raeker et al., 2024). Due to this, a possible homology of small trunk papillae of *Halicryptus* to trunk papillae of Megintroverta is questionable.

Priapulidae have structures organized in one or more rings on the posterior trunk. In Megintroverta these are the ring papillae (Van der Land, 1970), whereas *Halicryptus* has one ring of flosculus-tubulus-complexes (Raeker et al., 2024). Ring papillae of Megintroverta have similar apical receptors (e.g. Schmidt-Rhaesa et al., 2022; Schmidt-Rhaesa and Raeker, 2022; this study). Differences between ring papillae of *Priapulus* and *Priapulopsis* occur in their shape and sequence. *Priapulus* has hemispherical ring papillae (large specimens can have elongate papillae) with an often unregularly pattern of papillae in their rings, whereas *Priapulopsis* has elongate ring papillae with a regular pattern (Schmidt-Rhaesa and Raeker, 2022; Schmidt-Rhaesa and Raeker, in press). Information on ring papillae of *Acanthopriapulus* is scarce, but their appearance is similar to those of *Priapulus* (cf. Fig. 6D in Schmidt-Rhaesa et al., 2022). In contrast, the flosculus-tubulus-complexes on the posterior trunk of *Halicryptus* are comparably much thinner in shape and they have a lateral flosculus (Raeker et al., 2024), which have not been reported for ring papillae of Megintroverta. We assume ring papillae of Megintroverta are homologous structures due to their position and similar apical receptors. Flosculus-tubulus-complexes of *Halicryptus* presumably are also homologous to ring papillae due to their position, but different receptors (e.g. flosculi) make this assumption uncertain.

Posterior warts on the posterior trunk are homologous in *P. caudatus*, *P. tuberculatospinosus* and *A. horridus*. Although posterior warts are reported to be absent in *A. horridus* (Van der Land, 1970), structures described as "groups of small ring papillae" (cf. Fig. 6D and E in Schmidt-Rhaesa et al., 2022) most likely represent posterior warts and not ring papillae, as their composition is similar to posterior warts described in this study (wart unit and subunit; apical tubes). As all reported specimens of *A. horridus* are under 25 mm in length (see Schmidt-Rhaesa et al., 2022), the posterior warts might not be well developed and could have been overlooked. *Priapulus abyssorum* has no reports of posterior warts, but they could be similarly not well developed, as the majority of reported specimens are only up to 30 mm in length (Adrianov and Malakhov, 1996b). One deep sea *Priapulus* specimen of about 53 mm length from the Pacific Ocean reported by Van der Land (1972) also lacked posterior warts, but it was not identified to species level with certainty. *Priapulopsis* and *Halicryptus* are lacking posterior warts (Schmidt-Rhaesa and Raeker, 2022; Raeker et al., 2024).

The distinct caudal appendage with vesicles in Megintroverta represents a homologous structure. *Acanthopriapulus* and *Priapulus* have both each one caudal appendage, whereas *Priapulopsis* has two appendages. The lumen of the appendage extends the body cavity (Van der Land, 1970), appears somewhat segmented and is internally layered with circular and longitudinal musculature (e.g. Schmidt-Rhaesa et al., 2022; Schmidt-Rhaesa and Raeker, 2022; this study). Minor differences occur on the surface of the vesicles, as net-like cuticular folds occur in *Priapulopsis* (e.g. Fig. 6A in Schmidt-Rhaesa and Raeker, in press), whereas the vesicles of *Acanthopriapulus* and *Priapulus* are either smooth or have wrinkles (e.g. Fig. 6 in Schmidt-Rhaesa et al., 2022, Fig. 9B and C in this study). Spinulets occur scattered on the whole vesicle and sometimes grouped as spinulet crown apically on the vesicles of Megintroverta. In addition, the posterior stem of *A. horridus* holds distinct spines (Schmidt-Rhaesa et al., 2022), which are lacking in other genera. The function of the caudal appendage is probably respiration, but there are also reports against this assumption (see summary by Van der Land, 1970). For *A. horridus*, an additional function as anchor-like structure (Van der Land, 1970) or defensive organ (Schmidt-Rhaesa et al., 2022) due to numerous spines is assumed.

We did not find possible homologous structures in other species/genera of Priapulidae from the following characters: hemispherical papillae of *P. caudatus* and *P. tuberculatospinosus*; circular folds of *P. caudatus*; mouth papillae of *H. spinulosus*; small buccal papillae, trunk tubuli and anal tubuli of *Halicryptus*.

There may be an exception for the five mouth papillae reported for adult *H. spinulosus* (see Raeker et al., 2024), as similar five "mouth cone papillae" are on the circumoral field of larval stages of *P. caudatus* (cf. Fig. 47 in Lemburg, 1999). Similar numbers and composition argue for a homologous structure, but the position on the circumoral field differs (posterior of each second ring tooth in adult *H. spinulosus*; one pair each dorso- and ventrolateral, one single papilla on left radius in *P. caudatus* larva). Surprisingly, adult *P. caudatus* do not have mouth cone papillae. This raises the question, whether mouth cone papillae are lost during development or represent presumably anlagen of ring 0 scalids.

The circular folds of *P. caudatus* may represent an apomorphic trait for this species. Further examinations on a higher number of specimens (including postlarval stages), and a reinvestigation of *P. abyssorum* due to the lack of detailed information on morphological characters of this species, is needed for verification.

5. Conclusions

Although *Priapulus caudatus* is a well examined species, this study shows that fine-structural investigations contribute to fill knowledge gaps, as previously shown for other macroscopic priapulids. We showed ring papillae for the first time in detail and described previously overlooked structures on the circumoral field (hemispherical papillae, ring 0 scalids and circular folds) of adult *P. caudatus*. Additionally, we added new observations on pharyngeal teeth (number of lateral cusps), scalids (lateral depressions with single receptors in the cuticle and orientation of subapical depressions), trunk papillae (composition), posterior warts (composition) and spinulets (varying number of apical receptors).

As new detailed information of morphological characters of Priapulidae were made available recently, we compared similar characters across species of Priapulidae and/or Megintroverta and discuss their potential homology based on their position and occurrence of similar receptors.

CRediT authorship contribution statement

Jan Raeker: Writing – review & editing, Writing – original draft, Visualization, Validation, Methodology, Investigation, Data curation, Conceptualization. **Katrine Worsaae:** Writing – review & editing, Supervision, Project administration, Funding acquisition, Conceptualization. **Andreas Schmidt-Rhaesa:** Writing – review & editing, Supervision, Resources, Project administration, Funding acquisition, Conceptualization.

Declaration of competing interest

The authors declare that they have no known competing financial interests or personal relationships that could have appeared to influence the work reported in this paper.

Data availability

Data will be made available on request.

Acknowledgements

We thank Katherine A. Turk (Vanderbilt University) for allocating us *Priapulus caudatus* specimens from the North Sea and Glafira Kolbasova (White Sea Biological Station, Lomonosov Moscow State University) for helping to collect specimens from the White Sea. Furthermore, we thank Elke Woelken (University of Hamburg) for providing essential help with the SEM and Karolin Engelkes and Lena Schwinger (Leibniz Institute for the Analysis of Biodiversity Change, Hamburg) for guidance in the morphology lab. This study was funded by the Deutsche

Forschungsgemeinschaft (DFG, Germany Research Foundation) with the grant number SCHM 1278/20-1 to Andreas Schmidt-Rhaesa.

References

Adrianov, A.V., Malakhov, V.V., 1995. The phylogeny and classification of the phylum Cephalorhyncha. Zoosystematica Ross. 3, 181–201.

Adrianov, A.V., Malakhov, V.V., 1996a. Priapulida: Structure, Development, Phylogeny, and Classification. KMK Scientific Press, Moscow [In Russian with English summary].

Adrianov, A.V., Malakhov, V.V., 1996b. The phylogeny, classification and zoogeography of the class Priapulida. II. Revision of the family Priapulidae and zoogeography of priapulids. Zoosyst. Rossica 5, 1–6.

Apel, W., 1885. Beitrag zur Anatomie und Histologie des *Priapulus caudatus* (Lam.) und des *Halicryptus spinulosus* (v. Siebold). Z. Wiss. Zool. 42, 459–529.

Ehlers, E., 1862. Ueber die Gattung *Priapulus* Lam. Ein Beitrag zur Kenntnis der Gephyreen. Z. Wiss. Zool. 11, 205–252.

Giribet, G., Edgecombe, G.D., 2020. The Invertebrate Tree of Life. Princeton University Press.

Guille, A., Laubier, L., 1965. Découverte de la classe des Priapuliens en Méditerranée. Comptes rendus Acad. Sci. Paris 261, 1125–1128.

Hammond, R.A., 1970a. The surface of *Priapulus caudatus* (Lamarck, 1816). Z. Morph. Tiere 68, 225–268. https://doi.org/10.1007/BF00277505.

Hammond, R.A., 1970b. The burrowing of *Priapulus caudatus*. J. Zool. Lond. 162, 469–480. https://doi.org/10.1111/j.1469-7998.1970.tb01281.x.

Kolbasova, G., Schmidt-Rhaesa, A., Syomin, V., Bredikhin, D., Morozov, T., Neretina, T., 2023. Cryptic species complex or an incomplete speciation? Phylogeographic analysis reveals an intricate Pleistocene history of *Priapulus caudatus* Lamarck, 1816. Zool. Anz. 302, 113–130. https://doi.org/10.1016/j.jcz.2022.11.013.

Laakkonen, H.M., Hardman, M., Strelkov, P., Väinölä, R., 2021. Cycles of trans-Arctic dispersal and vicariance, and diversification of the amphi-boreal marine fauna. J. Evol. Biol. 34, 73–96. https://doi.org/10.1111/jeb.13674.

Light, S.F., Smith, R.I., Pitelka, F.A., Abbott, D.P., Weesner, F.M., 1954. Intertidal Invertebrates of the Central California Coast. University of California Press, Berkeley.

Lemburg, C., 1999. Ultrastrukturelle Untersuchungen an den Larven von *Halicryptus spinulosus* und *Priapulus caudatus*. Hypothesen zur Phylogenie der Priapulida und deren Bedeutung für die Evolution der Nemathelminthes. Cuvillier, Göttingen.

Mattisson, A., Nilsson, S., Fänge, R., 1974. Light microscopical and ultrastuctural organization of muscles of *Priapulus caudatus* (Priapulida) and their responses to drugs, with phylogenetic remarks. Zool. Scripta 3, 209–218. https://doi.org/10.1111/j.1463-6409.1974.tb00818.x.

Okuda, S., 1934. Occurrence of *Priapulus caudatus* in northern Japan. Proceedings Imp. Acad. Tokyo 10 (2), 115–116. https://doi.org/10.2183/pjab1912.10.115.

Paulay, G., 2024. World list of Priapulida. Halicryptidae Salvini-Plawen, 1974. Accessed through: World Register of Marine Species at: https://www.marinespecies.org/aphia.php?p=taxdetails&id=1263710on2024-06-03.

Raeker, J., Worsaae, K., Schmidt-Rhaesa, A., 2024. David versus Goliath: an interspecific comparison between small-sized *Halicryptus spinulosus* and large-sized *Halicryptus higginsi* (Priapulida). Zool. Anz. https://doi.org/10.1016/j.jcz.2024.08.003.

Scharff, R., 1885. On the skin and nervous system of *Priapulus* and *Halicryptus*. Q. J. Microsc. Sci. 25, 193–213. https://doi.org/10.1242/jcs.s2-25.98.193.

Schmidt-Rhaesa, A., 2013. Priapulida. In: Schmidt-Rhaesa, A. (Ed.), Handbook of Zoology: Nematomorpha, Priapulida, Kinorhyncha and Loricifera, ume 1. Walter de Gruyter, Berlin, pp. 147–180.

Schmidt-Rhaesa, A., Cañete, J.I., Mutschke, E., 2022. New record and first description including SEM and μCT of the rare priapulid *Acanthopriapulus horridus* (Priapulida, Scalidophora). Zool. Anz. 298, 1–9. https://doi.org/10.1016/j.jcz.2022.03.001.

Schmidt-Rhaesa, A., Raeker, J., Review of the Priapulida of New Zealand with the description of a new species. N. Z. J. Zool.

Schmidt-Rhaesa, A., Raeker, J., 2022. Morphology of larval and postlarval stages of *Priapulopsis bicaudatus* (Danielssen, 1869) (Priapulida) from the North Atlantic ocean. Zool. Anz. 302, 1–16. https://doi.org/10.1016/j.jcz.2022.11.006.

Storch, V., Higgins, R.P., Rumohr, H., 1990. Ultrastructure of introvert and pharynx of *Halicryptus spinulosus* (Priapulida). J. Morphol. 203, 163–171. https://doi.org/10.1002/jmor.1052060203.

Storch, V., Higgins, R.P., Malakhov, V.V., Adrianov, A.V., 1994. Microscopic anatomy and ultrastructure of the introvert of *Priapulus caudatus* and *P. tuberculatospinosus* (Priapulida). J. Morphol. 220, 281–293. https://doi.org/10.1002/jmor.1052200307.

Turk, K.A., Wehrmann, A., Laflamme, M., Darroch, S.A.F., 2024. Priapulid neoichnology, ecosystem engineering, and the Ediacaran–Cambrian transition. Palaeontology 67, e12721. https://doi.org/10.1111/pala.12721.

Van der Land, J., 1970. Systematics, geography, and ecology of the Priapulida. Zool. Verhand. Leiden. 112, 1–118.

Van der Land, J., 1972. *Priapulus* from the deep sea (Vermes, Priapulida). Zool. Meded. 47, 358–368.

Wernström, J.V., Slater, B.J., Sørensen, M.V., Crampton, D., Altenburger, A., 2023. Geometric morphometrics of macro-and meiofaunal priapulid pharyngeal teeth provides a proxy for studying Cambrian "tooth taxa". Zoomorphology 142 (4), 411–421. https://doi.org/10.1007/s00435-023-00617-4.

Wills, M.A., Gerber, S., Ruta, M., Hughes, M., 2012. The disparity of priapulid, archaeopriapulid and palaeoscolecid worms in the light of new data. J. Evol. Biol. 25 (10), 2056–2076. https://doi.org/10.1111/j.1420-9101.2012.02586.x.

JCZ: Zoologischer Anzeiger - A Journal of Comparative Zoology 313 (2024) 1–20

Contents lists available at ScienceDirect

Zoologischer Anzeiger

journal homepage: www.elsevier.com/locate/jcz

David versus Goliath: An interspecific comparison between small-sized *Halicryptus spinulosus* and large-sized *Halicryptus higginsi* (Priapulida)

Jan Raeker [a,*], Katrine Worsaae [b], Andreas Schmidt-Rhaesa [a]

[a] *Museum of Nature Hamburg - Zoology, Leibniz Institute for the Analysis of Biodiversity Change (LIB) and University Hamburg, Martin-Luther-King-Platz 3, 20146 Hamburg, Germany*

[b] *Marine Biological Section, Department of Biology, University of Copenhagen, Universitetsparken 4, 2100 Copenhagen Ø, Denmark*

ARTICLE INFO

Handling Editor: Martin Vinther Sorensen

Keywords:
Priapulida
Halicryptus
Alaska
SEM
Histology
Body size

ABSTRACT

Halicryptus includes two priapulid species with highly different adult body sizes, small-sized *Halicryptus spinulosus* von Siebold, 1849 and large-sized *Halicryptus higginsi* Shirley and Storch, 1999. Due to ambiguity of diagnostic characters from juvenile to adult size and between species, a detailed morphological and molecular comparison is needed to resolve the distribution and characteristics of each species. We investigate an adult paratype specimen of *H. higginsi*, and young adult specimens of *H. spinulosus* from the Beaufort Sea and *H. spinulosus* from Kandalaksha Gulf, White Sea. Molecular analysis of the mitochondrial CO1 gene confirm the existence of two species of *Halicryptus*, a wide distribution of *H. spinulosus* across the Northern Hemisphere and the co-occurrence of both species in the Beaufort Sea. Our morphological analyses reveal undocumented characters for *Halicryptus*, such as the presence of three different sizes of buccal papillae, scattered small trunk papillae, and a loose ring of flosculus-tubulus-complexes on the posterior trunk. For both species, we revise characters, such as the number of long introvert retractors, pharynx protractors and lateral cusps of anterior teeth, and the maximum number of scalids in a row in *H. spinulosus*. We propose a total of ten reliable and potential diagnostic characters distinguishing the two species and revise the terminology of *Halicryptus*-specific characters due to inconsistency in the literature. In addition, we discuss the effect of body size on selected morphological traits.

1. Introduction

Priapulida is a morphologically conserved taxon of marine worms (Webster et al., 2006), yet containing only 22 described, extant species (Schmidt-Rhaesa and Raeker, in press). These occur in two different adult body size classes, macroscopic and microscopic (Schmidt-Rhaesa, 2013). Currently, nine extant species are of macroscopic adult size and separated in four genera (*Priapulus*, *Priapulopsis*, *Acanthopriapulus* and *Halicryptus*), and all priapulid fossil records also fall within this size class (e.g. Conway Morris and Robison, 1986; Huang et al., 2004; Hu et al., 2017). The remaining 13 species having microscopic sized adults of a few millimetres in length constitute three genera (*Tubiluchus*, *Meiopriapulus* and *Maccabeus*). *Halicryptus* holds the potential for an interesting comparison of morphological characters across vast size ranges - from the small-sized *Halicryptus spinulosus* von Siebold, 1849 with a maximum body length of 40 mm - to the largest priapulid *Halicryptus higginsi* Shirley and Storch, 1999 with a total body length up to 400 mm (Van der Land, 1970; Shirley and Storch, 1999).

Von Siebold (1849) discovered the first adult *Halicryptus* near Gdańsk, Poland, in the Baltic Sea and described them as *H. spinulosus*. The larval stages (soft-bodied hatching larvae and lorica-larvae) were described much later from the Baltic Sea (Hammarsten, 1913; 1915) or breeding experiments (Janssen et al., 2009). Multiple morphological investigations of *H. spinulosus* have since added to the original descriptions of adults (Apel, 1885; Scharff, 1885; Van der Land, 1970; Moritz, 1972; Candia Carnevali and Ferraguti, 1979; Merriman, 1981; Storch et al., 1990; Adrianov and Malakhov, 1996a) and larvae (Storch and Higgins, 1991; Lemburg, 1995). Interestingly, Merriman (1981) examined up to 200 mm long specimens of *H. spinulosus* from the Beaufort Sea near Point Barrow, Alaska, which extended the range of body size given by Van der Land (1970) for this otherwise small-sized species, and yielded inconsistencies in morphological characters, such as the absence of a certain type of scalids (dentoscalids) on the introvert or the presence of ring papillae and warts on the posterior trunk. Several additional North American records of *H. spinulosus* exist, all lacking morphological data, but some records included information on body

* Corresponding author.
E-mail address: j.raeker@leibniz-lib.de (J. Raeker).

https://doi.org/10.1016/j.jcz.2024.08.003
Received 11 April 2024; Received in revised form 23 July 2024; Accepted 21 August 2024
Available online 23 August 2024

sizes. MacGinitie (1955) reported large specimens of 70–170 mm from Eluitkak Pass near Point Barrow. Small specimens were found in Nuwuk Lake, Elson Lagoon and Sinclair Lake near Point Barrow by Holmquist (1963) and in the Labrador Sea near Nain by Carter (1966). Goldsmit et al. (2014) specimens were sampled near Churchill in the Hudson Bay, Canada, but lack information on body sizes.

Shirley and Storch (1999) later described the large-sized *H. higginsi* from Point Barrow, Alaska on adult specimens. Remarkable for adult *H. higginsi* is the enormous total body length (up to 40 cm), with specimens of about 20 cm body length being common (Shirley and Storch, 1999). Another diagnostic character of adult *H. higginsi* is the absence of dentoscalids on the introvert. This raised the question, whether Merriman (1981) and later authors in fact examined specimens of *H. higginsi* or whether both *Halicryptus* species occur in the Beaufort Sea. Shirley and Storch (1999) partially answered this question for MacGinitie's (1955) and Holmquist's (1963) material, mainly based on the sampling site and body size, suggesting that their examined specimens were presumably *H. higginsi*. A detailed study of small *Halicryptus* specimens from the Beaufort Sea near Point Barrow, Alaska could help answering the question, whether small specimens are juvenile *H. higginsi* specimens or whether both *Halicryptus* species coexist in these waters.

Halicryptus spinulosus is reported to have a wide circumpolar distribution on the Northern Hemisphere. Additional to the first records from the Baltic Sea and North America, specimens were also reported from the Barents Sea, around Iceland and on the east coast of Greenland (see summaries in Van der Land, 1970; Adrianov and Malakhov, 1996b). This widespread distribution raises the question of whether these records resemble a single species or a complex of cryptic species. However, the priapulid *Priapulus caudatus* have been shown to likely have a circumpolar distribution (Kolbasova et al., 2023).

In this study, we examined new material of small *Halicryptus* specimens collected in 2021 at two different locations near Point Barrow, Alaska and from Kandalaksha Bay, White Sea. We were also able to partially investigate one of the rare museum specimens of *H. higginsi* (Smithsonian Institution, National Museum of Natural History, Washington, DC). We aim to (1) test the species identity, a potential circumarctic distribution range of *H. spinulosus* and a potential geographical overlap with *H. higginsi*, by including both molecular data (generating new sequences and comparing mitochondrial CO1 from populations from east Siberia to Alaska) and morphological data (examining specimens using light microscopy, scanning electron microscopy and histology and comparing with published studies), (2) search for morphological differences and potential diagnostic characters of both species, (3) review the terminology of morphological characters due to inconsistency in the literature and (4) compare characters in relation to the adult body size of both species.

2. Material and methods

2.1. Specimens and morphological investigations

Adult *H. spinulosus* specimens from three different locations (one specimen from Elson Lagoon and five specimens from Jago Lagoon, Beaufort Sea, Alaska and eight specimens from the Kandalaksha Gulf, White Sea, Russia) were used for morphological investigations (Table 1; Fig. 1A). One *H. higginsi* paratype specimen (USNM No. 186062) from the original description by Shirley and Storch (1999) was loaned from the Smithsonian Institution, National Museum of Natural History, Washington, DC for comparison (Table 1). We use abbreviated codes for *H. spinulosus* specimens, but the species name for *H. higginsi* (see Table 1).

Before further preparation, all specimens were photographed and measured with a Keyence VHX-7000 digital light microscope. The introvert lengths were measured from anterior to posterior of the field of scalids, ignoring the projecting circumoral field and teeth if they were showing. Two *H. spinulosus* from Jago Lagoon, one from Elson Lagoon, two *H. spinulosus* from the White Sea and small parts of the body wall of *H. higginsi* were prepared for scanning electron microscopy (SEM). Specimens were dehydrated in a series of increasing ethanol concentrations. The introvert of the *H. spinulosus* from the Elson Lagoon was longitudinally cut to make the teeth accessible due to the deeply inverted pharynx. The material was critical point dried in a Leica EM CPD300, sputter coated with platinum in a Polaron SC7640 Sputter Coater and investigated with a LEO SEM 1524.

For histology, two whole specimens of *H. spinulosus* (one from Jago Lagoon and one from the White Sea) and the introvert, the posterior trunk end and two short trunk sections of *H. higginsi* were dehydrated in a series of increasing ethanol concentrations and embedded in paraffin. The specimens and body parts were sectioned in 7–10 µm thick sections using a Microm HM 340E rotatory microtome. Sections were Azan stained (20 min staining in nuclear fast red aluminium sulphate, 5 min differentiation in 5 % phosphotungstic acid, 14 min staining in aniline blue-orange G) and photographed using an Olympus SLIDEVIEW VS200 slide scanner.

From histological cross sections of three body regions (posterior introvert, approximately half of body length and posterior trunk), we measured the thickness of body wall layers (cuticle, epidermis, circular/longitudinal musculature) of the broadest and narrowest body wall part

Table 1
Halicryptus specimens investigated in this study with sampling location, date, used methods, total body lengths (mm), introvert lengths (mm) and introvert length relative to total body length (%). Abbreviations: A, Alaska; HIST, histology; LM, light microscopy; MOL, molecular analysis; *SEM*, scanning electron microscopy; W, White Sea.

Species	Specimen	Sampling location	Date (day -month - year)	Methods	Total body length	Introvert length	Introvert length to body length relation
H. spinulosus	A1	Jago Lagoon, Beaufort Sea	01.08.2021	LM, SEM, MOL	5.59	0.88	15.7
H. spinulosus	A2	Jago Lagoon, Beaufort Sea	01.08.2021	LM, SEM, MOL	5.37	0.52	9.6
H. spinulosus	A3	Elson Lagoon, Beaufort Sea	01.08.2021	LM, SEM	6.2	0.85	13.7
H. spinulosus	A4	Jago Lagoon, Beaufort Sea	01.08.2021	LM, HIST	4.91	0.61	10.7
H. spinulosus	A5	Jago Lagoon, Beaufort Sea	01.08.2021	LM, MOL	4.16	0.52	12.5
H. spinulosus	A6	Jago Lagoon, Beaufort Sea	01.08.2021	LM, MOL	2.89	0.38	13.3
H. spinulosus	W1	Kandalaksha Gulf, White Sea	17.09.2021	LM, SEM	10.96	1.53	13.9
H. spinulosus	W2	Kandalaksha Gulf, White Sea	17.09.2021	LM, SEM	10.67	1.5	14
H. spinulosus	W3	Kandalaksha Gulf, White Sea	17.09.2021	LM, HIST	16.75	–	–
H. spinulosus	W4	Kandalaksha Gulf, White Sea	17.09.2021	LM	6.43	0.72	11.2
H. spinulosus	W5	Kandalaksha Gulf, White Sea	17.09.2021	LM	23.15	0.86	3.7
H. spinulosus	W6	Kandalaksha Gulf, White Sea	17.09.2021	LM	4.64	0.43	9.1
H. spinulosus	W7	Kandalaksha Gulf, White Sea	17.09.2021	LM, MOL	5.09	0.65	12.8
H. spinulosus	W8	Kandalaksha Gulf, White Sea	17.09.2021	LM, MOL	6.35	–	–
H. higginsi	–	Intertidal zone near Point Barrow, Beaufort Sea	22.09.1993	LM, SEM, HIST, MOL	~200	2.14	10.7

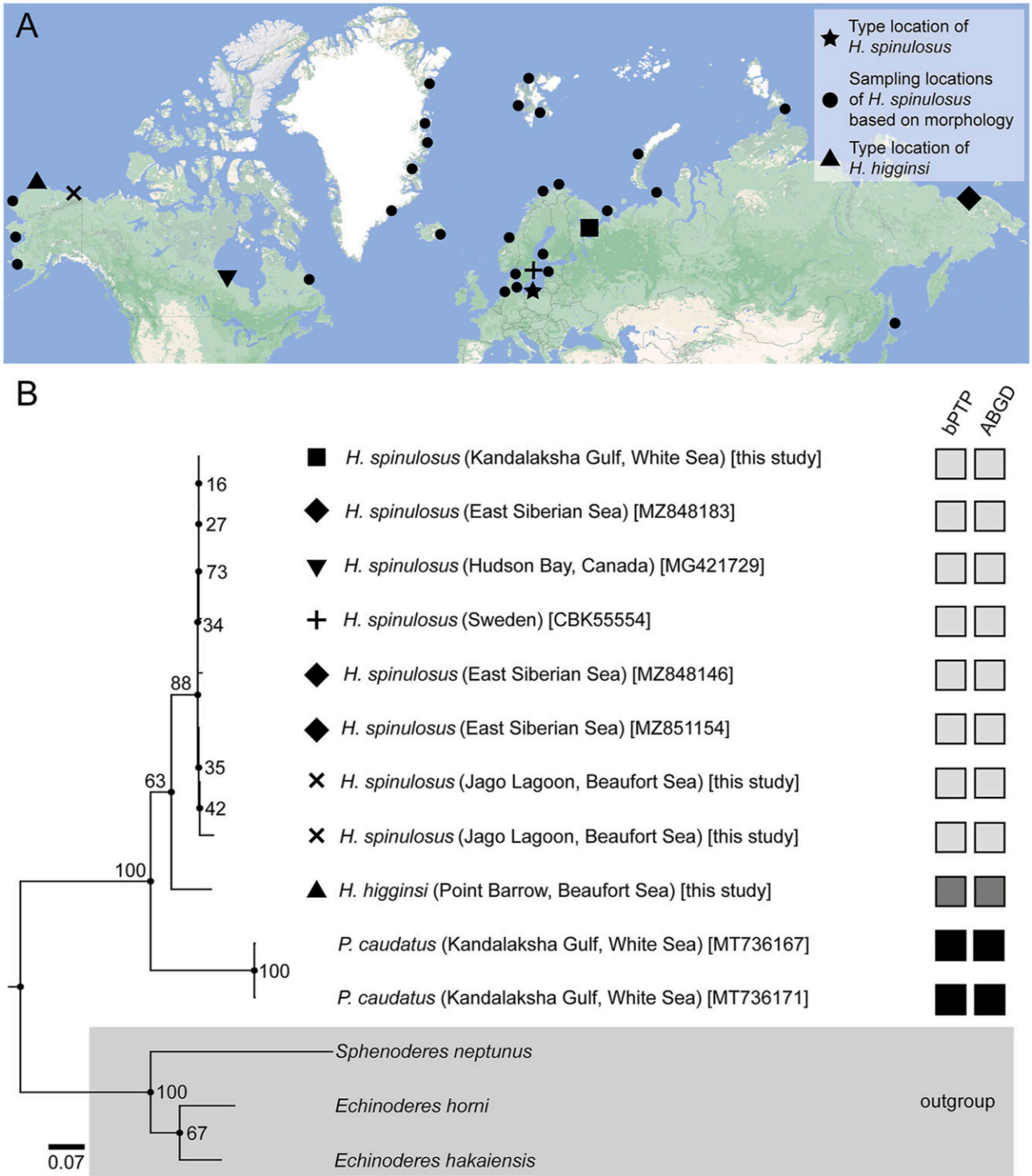

Fig. 1. Sampling locations and phylogenetic tree of *Halicryptus*. A. Sampling locations of as *H. spinulosus* identified specimens based on morphology (dots) (see Adrianov and Malakhov, 1996b). Star shows type location of *H. spinulosus*. Upright triangle shows type location of *H. higginsi*. Other geometric shapes show sampling locations of *H. spinulosus* specimens used in molecular analysis (see B for annotation). B. Maximum-likelihood phylogenetic tree of *Halicryptus* specimens inferred from a 525 bp fragment of mitochondrial CO1 gene nucleotide sequences. Nodes show ultrafast bootstrap values. Species delimitation results for bPTP and ABGD tests for each specimen are shown in squares with different grey scales. Different grey scales show each an individual species. Map source: Google Maps.

and put them in relation to the diameter of the respective cross section (Fig. 2). Measurements of the thickness of the body wall layers are displayed in Supplementary Table 1, whereas the relation of the thickness of the layers to the diameter of the cross section are shown in Supplementary Table 2.

2.2. Molecular methods and analyses

For molecular analyses, DNA of four *H. spinulosus* specimens from Jago Lagoon, Alaska and two specimens from Kandalaksha Gulf, White Sea were extracted by using the QIAGEN Blood and Tissue Extraction Kit on body wall tissue following the manufacturer's instructions. The

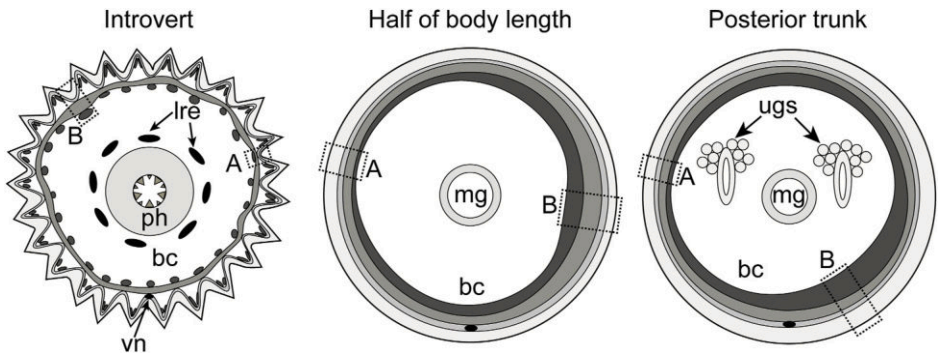

Fig. 2. Schemes of histological sections of the introvert region, approximately half of body length and posterior trunk with their respective narrowest (box A) and broadest (box B) body wall part. Differences in body wall thickness are hyperbolic. Different grey scales show the body wall layers, from external to internal: cuticle, epidermis, circular musculature and longitudinal musculature. Abbreviations: bc, body cavity; mg, mid gut; ph, pharyngeal bulb; vn, ventral nerve cord.

mitochondrial gene CO1 was amplified by polymerase chain reaction (PCR) using the primer pair jgHCO2198 and jgLCO1490 (Geller et al., 2013). The following thermo-cycler program was used: 94 °C/180 s, (94 °C/40 s, 45 °C/40 s, 72 °C/60 s; 37 cycles), 72 °C/600 s. PCR amplicons were checked using gel-electrophoresis. Positively tested amplicons (two from Jago Lagoon, one from the White Sea) were sequenced by Macrogen Europe (Netherlands).

For *H. higginsi*, DNA was extracted by using the same extraction kit from body wall tissue and gonads following the manufacturer's instructions. The DNA library was prepared for sequencing using the Kapa HyperPlus Kit (3 min enzymatic fragmentation time). Sequencing was done at the Bauer Core Facility at Harvard University on an Illumina NovaSeq 6000 S4 with 150 bp paired end reads. Adaptors of the raw reads were trimmed with Trimmomatic v0.39 (Bolger et al., 2014) and the mitochondrial genome was assembled with NOVOPlasty v4.3.3 (Dierckxsens et al., 2017) using the *H. spinulosus* mitochondrial genome (NCBI ID: NC_020030.1) as seed sequence. The mitochondrial CO1 gene fragment was filtered from aligning the assembled mitochondrial genome of *H. higginsi* to CO1 sequences of *H. spinulosus*.

The newly generated CO1 gene sequences and publicly available CO1 sequences of additional *H. spinulosus* specimens from three locations (see Fig. 1A), two *Priapulus caudatus* and three outgroup Kinorhyncha (Table 2) were aligned in MEGA X (Kumar et al., 2018) with the MUSCLE option (Edgar, 2004) using default settings. Conserved positions were analysed with Gblocks 0.91b (Dereeper et al., 2008), resulting in a final length of 525 bp for the mitochondrial CO1 gene. A maximum-likelihood tree was generated with IQ-Tree2 (Minh et al., 2020) using the automated model selection with ModelFinder (Kalyaanamoorthy et al., 2017) and 1000 ultrafast bootstrap replicates with UFBoot2 (Hoang et al., 2018). The generated tree file was rooted at the outgroup and edited with FigTree v1.44.

To further test the species identity of terminals included in the maximum-likelihood tree, species delimitation analyses were performed. A Poisson-Tree-Process (bPTP) analysis (Zhang et al., 2013) was done on the webserver (https://species.h-its.org/ptp) with default settings (100.000 Markov chain Monte Carlo generations). A second approach was done with the Automated Barcode Gap Discovery (ABGD) analysis (Puillandre et al., 2012) on the webserver (https://bioinfo.mnhn.fr/abi/public/abgd/abgdweb.html) with default settings.

3. Results

3.1. Molecular analysis

The maximum-likelihood phylogenetic tree inferred by 525 bp fragments of the mitochondrial CO1 gene of *Halicryptus* specimens shows a monophyletic clade of all included *Halicryptus* specimens (new generated and publicly available), though with moderate bootstrap support (Fig. 1B). The *H. higginsi* specimen is the sister-taxon of a *H. spinulosus* cluster, which shows low internal resolution and very short branch lengths. The results of the species delimitation tests (bPTP and ABGD) both support that *H. spinulosus* and *H. higginsi* are separate species (Fig. 1B).

3.2. Morphological analysis

While comparing previous morphological studies of *Halicryptus*, we noticed that some *Halicryptus* related characters have various terms given by different authors, although describing the same structures. We propose for these characters one definite term, which can be either new

Table 2
Newly generated and publicly available CO1 sequences used for molecular analysis with sampling location and GenBank accession number.

Species	Sampling location	GenBank accession number
Newly generated sequences:		
Halicryptus spinulosus (A1)	Jago Lagoon, Beaufort Sea	PQ032568
Halicryptus spinulosus (A2)	Jago Lagoon, Beaufort Sea	PQ032569
Halicryptus spinulosus (W7)	Kandalaksha Gulf, White Sea	PQ032570
Halicryptus higginsi	Intertidal zone near Point Barrow, Beaufort Sea	PQ032571
Publicly available sequences:		
Halicryptus spinulosus	Gordon Point, Hudson Bay, Canada	MG421729
Halicryptus spinulosus	Chaunskaya Bay, East Siberian Sea	MZ848146
Halicryptus spinulosus	Chaunskaya Bay, East Siberian Sea	MZ848183
Halicryptus spinulosus	Chaunskaya Bay, East Siberian Sea	MZ851154
Halicryptus spinulosus	Sweden	CBK55554
Priapulus caudatus	Kandalaksha Gulf, White Sea	MT736167
Priapulus caudatus	Kandalaksha Gulf, White Sea	MT736171
Echinoderes horni	Yucatan, Mexico	OP617670
Echinoderes hakaiensis	Kwakshua Channel, Canada	KY550656
Sphenoderes neptunus	Gulf of Naples, Italy	MW031146

Table 3
Overview of new proposed terminology for *Halicryptus* specific characters and their respective old terminology.

New terminology	Old terminology	Publication
Anal tubulus	spike	Scharff (1885)
	seta	Van der Land (1970)
	anal seta	Merriman (1981), Lemburg (1999)
	caudal spine	Adrianov and Malakhov (1996a)
Flosculus-tubulus-complex (end of scalid row) (Lemburg, 1999)	rudimentary scalid	Van der Land (1970)
	developing scalid	Adrianov and Malakhov (1996a)
Mouth papilla	rudimental tooth	Adrianov and Malakhov (1996a)
	rudimentäre Mundpapille [Ger.]	Lemburg (1999)
Peg-like ring papilla	ring papilla	Merriman (1981)
Small trunk papilla	posterior wart; anal papilla	Merriman (1981)
	"Irregularly arranged oval structures"	Shirley and Storch (1999)
Trunk tubulus (Storch et al. 1990)	Hornspitze [Ger.]	Von Siebold (1849)
	Spitze [Ger.]	Ehlers (1862)
	spike	Scharff (1885)
	abdominal seta	Van der Land (1970)
	secretory tubulus	Shirley and Storch (1999)

or the most appropriate given by previous authors (see Table 3). For justification of the proposed term, see respective part in the discussion, as we are using the new terminology in the following results.

3.2.1. *General external priapulid organization*

All investigated specimens exhibit the typical external macroscopic priapulid morphology of postlarval stages and adults with terminal mouth opening and anus, an eversible introvert with longitudinal scalid rows and an annulated cylindrical trunk (Fig. 3). A caudal appendage is not present. Though there are no criteria to distinguish postlarval stages from adults by their external morphology, the *H. spinulosus* specimens from Alaska most likely represent young adults due to the presence of gonads and their short total body length, whereas the specimens from the White Sea and the *H. higginsi* specimen are older adults.

3.2.2. *Body length and introvert length to total body length relation*

Total body length measurements vary slightly within and across populations but differ distinctly between the two species of *Halicryptus* examined, whereas relative measurements of the introvert length overlap between species (Table 1). Some examined *H. spinulosus* specimens from the White Sea are considerably larger (up to 21.15 mm) than specimens from Alaska (max. 6.2 mm), while the *H. higginsi* specimen is about 200 mm long (Table 1, Fig. 3). The introvert length differs slightly between *H. spinulosus* populations but falls relative to the body length within a similar range (Table 1). *Halicryptus higginsi* has the longest introvert, yet this is comparatively short relative to the body length (Table 1).

3.2.3. *Pharyngeal teeth and circumoral field*

The pharynx of all examined specimens is armed with cuspidate pharyngeal teeth, which occur in rings that are composed of five teeth in the anterior rings (Fig. 4A,D-F). The *H. spinulosus* specimens A1, W1 and W2 have their introverts strongly everted (Fig. 3A,E,F), showing the circumoral field and the teeth of the first three to five rings (Fig. 4A,D,E). In *H. higginsi*, only the first and second ring of teeth are visible in the light micrographs (Fig. 4F). All observed teeth have the same morphology with a large median cusp and small lateral cusps on each side of the median cusp (Fig. 4A–F). The number of lateral cusps varies between specimens and can vary within one ring of a specimen (Table 4; Fig. 4A–F). Whenever asymmetrical patterns of lateral cusps are present, no indication (= broken base) is present that cusps may have broken off, the cuticle is smooth. The teeth of the second and third ring are the largest, while the ones from the first ring are slightly smaller in all *H. spinulosus* specimens (Fig. 4A,D,E). In *H. higginsi*, the teeth of the second ring appear larger than the ones from the first ring (Fig. 4F). Some teeth show cut-off cusps, revealing an interior view with a thick cuticle (Fig. 4C). The surface of the cuticle of the teeth is smooth, but small pores are visible on the concave underside of the teeth (Fig. 4G).

Close to each of the five teeth of the second ring in *H. spinulosus* specimen A1, at about the level of the teeth of the first ring, there is one small conical papilla (Fig. 4A,H,I). These papillae are about 12 μm in length and have up to three observable small tubular structures on the apical part (Fig. 4H and I). We also observed some of these small papillae in specimens from the White Sea, which are slightly larger with 18 μm in length (Fig. 4E). We could find these structures neither in specimen A3 nor in *H. higginsi*.

The region between the pharyngeal teeth and the first scalids is called here circumoral field. On the middle part of the circumoral field of *H. spinulosus* specimen A1, situated in register with the teeth of the first ring, are five bulbous structures with a diameter between 76 and 120 μm and a height between 50 and 63 μm (Fig. 4A). Sensory structures were not observed on these bulbous structures. *Halicryptus spinulosus* specimen A2 also shows similar bulbous structures with widths between 67 and 97 μm directly on the closed mouth opening (Fig. 5A), but their position relative to the pharyngeal teeth could not be investigated in this specimen. In *H. spinulosus* specimens A3, W1, W2 and *H. higginsi*, these bulbous structures are not visible.

On the posterior part of the circumoral field is an area with numerous buccal papillae (Fig. 3A,E,F; 5A,B). Buccal papillae occur in three different sizes (Fig. 5A–C,E,G). Absolute measurements of buccal papillae differ slightly between *H. spinulosus* specimens, whereas measurements in *H. higginsi* are comparable larger (Table 4). Most posterior are eight large buccal papillae in all examined specimens, which are directly anterior of the eight primary scalids (for primary scalids see below) (Fig. 5A–C). In *H. higginsi,* one large buccal papilla next to the ventral midline is considerably larger (Fig. 5B). Large buccal papillae consist of a triangularly flattened basal part, which is covered with numerous tiny spine-like structures (Fig. 5C). Sometimes, these tiny spines seem to be arranged in lines. Apical to the base is the cone-like tip, which is not as densely covered with the tiny spines as the base (Fig. 5C). Occasionally, the tip bends slightly. On this bent part, with a median groove and cuticular folds, numerous small tubular structures are visible (Fig. 5D). In *H. higginsi*, we could not observe the tip in light micrographs, but the tiny spines on the surface of the buccal papillae are visible on higher magnifications.

Anterior of the large buccal papillae, towards the mouth opening, are medium-sized buccal papillae, which are organized loosely in a ring (Fig. 5A,B,E). This loose ring consists of about 16 medium-sized buccal papillae, which look similar to the large buccal papillae (Fig. 5E and F).

Small buccal papillae seem to be randomly arranged in between the medium-sized buccal papillae (Fig. 5A and B). It seems that when the pharynx is inverted, some small buccal papillae form a loose ring on a cuticular fold occurring on about the same level as the large buccal papillae (Fig. 5A). We counted about 16 small buccal papillae on that

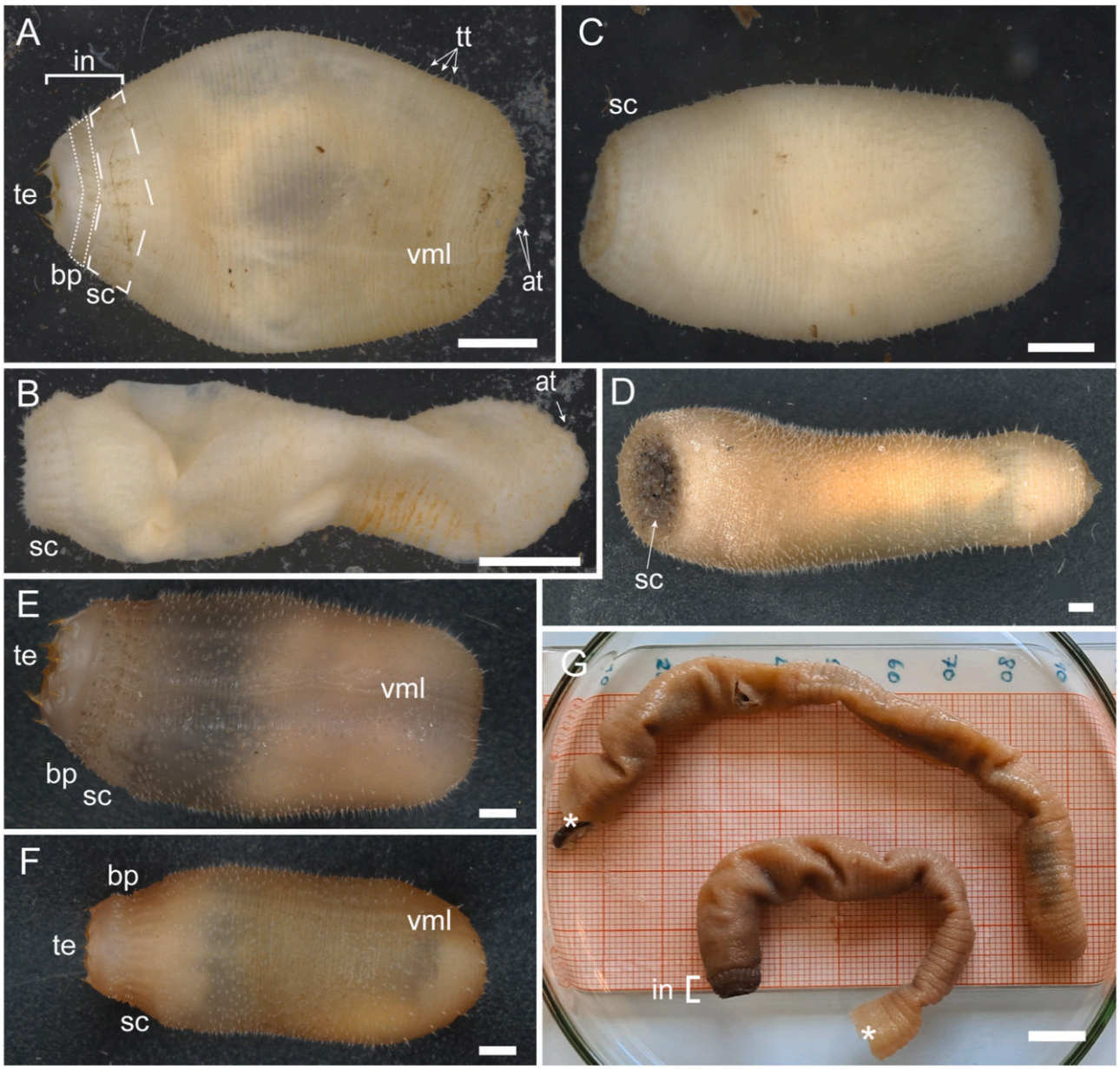

Fig. 3. Habitus of examined *Halicryptus* specimens, light microscopical images. A. *Halicryptus spinulosus* from Jago Lagoon, Alaska with everted pharynx (specimen A1). Dotted box shows area of buccal papillae (bp), dashed box shows scalids (sc). B. *Halicryptus spinulosus* from Jago Lagoon, Alaska with inverted pharynx (specimen A2). C. *Halicryptus spinulosus* from Elson Lagoon, Alaska (specimen A3). D. *Halicryptus spinulosus* from Kandalaksha Gulf, White Sea (specimen W3) used for histology. E. *Halicryptus spinulosus* from Kandalaksha Gulf, White Sea (specimen W1). F. *Halicryptus spinulosus* from Kandalaksha Gulf, White Sea (specimen W2). G. *Halicryptus higginsi*, paratype USNM No. 186062 from Point Barrow, Alaska. The asterisks (*) mark the part where the specimen was accidentally divided. Abbreviations: at, anal tubuli; in, introvert; te, pharyngeal teeth; tt, trunk tubuli; vml, ventral midline. Scale bars: A-F = 1 mm; G = 1 cm.

ring, but the exact number is hard to count. The total amount of all small buccal papillae is similar in *H. spinulosus* specimens from Alaska, while *H. higginsi* has more (Table 4). In *H. spinulosus* from the White Sea the introvert was not ideally everted to count the small buccal papillae (Fig. 4D and E). Small buccal papillae have the same morphology as large and medium-sized buccal papillae with about five small tubular structures on the tips (Fig. 5G and H).

3.2.4. Scalids

The introvert of all investigated priapulids is covered with 25 longitudinal rows of scalids (Fig. 5B; 6A-C). The gap width between two rows is always the same except between the two scalid rows on each side of the ventral midline, where the gap is about half of the usual width (Fig. 4E).

The number of scalids in each row differs between specimens and both species (Table 4). In *H. spinulosus* specimen W2, the number of scalids differs strongly (5–13 scalids), but only one scalid row lateral of the ventral midline has five scalids. Scalids can differ slightly in size within a row, but repeated series with decreasing scalid sizes as in e.g. *Priapulus* species are missing (Fig. 6A–C). Instead, the morphology of the scalids differs within a row.

The first three to four (Alaska specimens) or three to seven (White Sea specimens) scalids of a row have a broad and triangularly flattened base with a conical tip (Fig. 6A and B). The surface is smooth, but the lateral sides are dentate (Fig. 6A). The tips have subapical depressions, in which several tubular structures are present (Fig. 6D). These tubular structures appear to have two different shapes (Fig. 6D), either a smooth or a dented surface around the terminal opening (Fig. 6D inlay). We

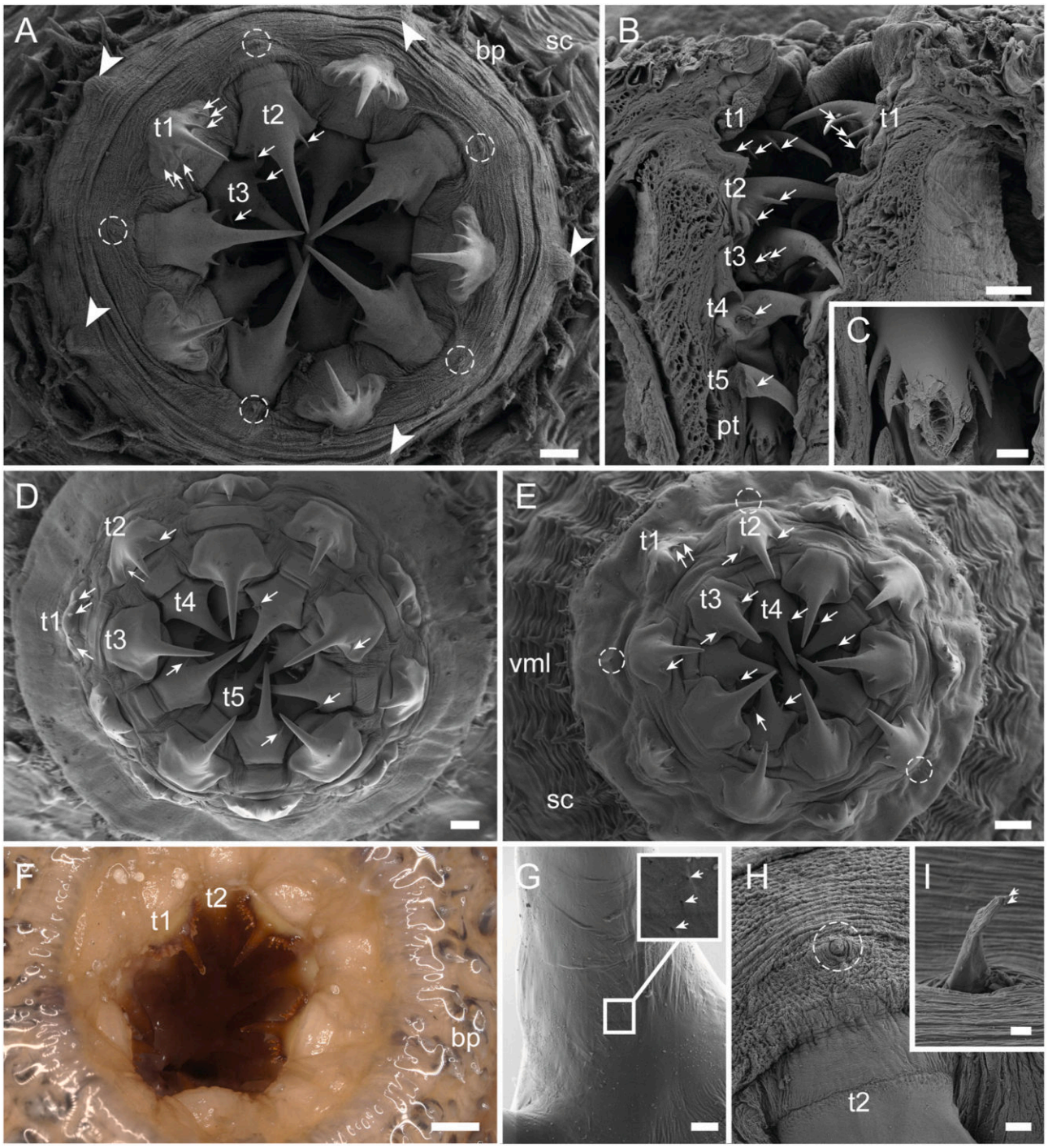

Fig. 4. Pharyngeal teeth, SEM images (A-E, G-I) and light microscopical image (F). A. Frontal view of the introvert of *H. spinulosus* specimen A1 showing the first three rings of pharyngeal teeth (t1-3). Small arrows show lateral cusps of the teeth. Big arrowheads show bulbous structures located behind the teeth of ring 1. Dotted circles show small papillae behind the teeth of ring 2. B. Longitudinal cut of the pharynx of *H. spinulosus* specimen A3, showing teeth of rings 1–5 (t1-5) and further posterior teeth (pt). Arrows show lateral cusps of the teeth. C. Higher magnification of posterior tooth of *H. spinulosus* specimen A3 with broken central cusp. D. Frontal view of the introvert of *H. spinulosus* specimen W1, showing the first five rings of teeth (t1-5). Arrows show lateral cusps of the teeth. E. Frontal view of the introvert of *H. spinulosus* specimen W2 showing the first four rings of teeth (t1-4). Arrows show lateral cusps of the teeth. Dotted circles show mouth papillae located behind the teeth of ring 2. F. Frontal view of the introvert of *H. higginsi*, showing the first two rings of teeth (t1-2). G. Concave underside of a tooth of the first ring from *H. spinulosus* specimen A1 with several pores on the surface. Inlay shows higher magnification of pores (arrows). H. Higher magnification of mouth papilla (dotted circle) located behind a tooth of ring 2 (t2). I. Lateral view of mouth papilla. Arrows show two tubular structures on the tip. Further abbreviations: bp, buccal papillae; sc, scalids; vml, ventral midline. Scale bars: A, B = 100 μm; C, H = 20 μm; D, E = 200 μm; F = 500 μm; I, G = 5 μm.

could not observe the scalid tips of *H. higginsi* in the light micrographs.

The following one to three scalids, the dentoscalids, of *H. spinulosus* specimens from Alaska (Elson Lagoon and Jago Lagoon) and the White Sea differ in shape compared to anterior scalids. They have the same broad, triangularly base with a dentate margin, but the tip consists of two spines, arranged in a crescent-like formation (Fig. 6A,B,E,F). These spines have a smooth surface without sensory structures. Anterior of the two spines in specimens from Alaska is a cuticular fold visible, which is

Table 4
Numbers and sizes of morphological structures of examined *Halicryptus* specimens. Order of structures respectively to the appearance in the results section. Abbreviations: Pt, posterior teeth; R1-5, teeth ring 1–5.

Specimen	*H. spinulosus* (Alaska)			*H. spinulosus* (White Sea)		*H. higginsi*
	A1	A2	A3	W1	W2	
Number of lateral cusps on teeth	**R1**: 3 per side; **R2**: 1 per side	–	**R1**: 3 per side; **R2**: 2 per side; **R3**: 2 per side; **Pt**: 3 per side	**R1**: 1 per side or 2 on one side and 1 on the other side; **R2**: four teeth with 1 cusp per side and one tooth without cusps; **R3**: two teeth with 1 cusp on one side, three teeth without cusps; **R4**: four teeth with 1 cusp, one tooth without cusps; **R5**: 1 per side or 2 on one side and 1 on the other side	**R1**: 2 per side; **R2**: three teeth with 1 cusp per side, one tooth with just 1 cusp and one tooth without cusps; **R3**: four teeth with 1 cusp per side and one tooth without cusps; **R4**: two teeth with 1 cusp per side, two teeth with only 1 cusp and one tooth without cusps **R5**: 2 per side	**R1**: 6–8 per side; **R2**: without cusps
Number and size of large buccal papillae	8; 102–147 µm	8; 66–78 µm	–	8; –	8; 137–214 µm	8; 460–680 µm (one large buccal papillae with 970 µm)
Number and size of medium-sized buccal papillae	about 16; 105–127 µm	about 16; 53–61 µm	–	–	-; 80–197 µm	about 16; 470–570 µm
Number and size of small buccal papillae	about 54; 40–72 µm	about 51; 15–34 µm	–	–	-; 39–63 µm	about 84; 166–380 µm
Number of scalids in a row	6–8	5–7	–	4–8	5–13	9–12
Number of trunk annuli	79	77	77	84	78	145
Size of trunk tubuli; mean size (relative size to body length)	87–200 µm; mean 150 µm (2.68 %)	76–107 µm; mean 97 µm (1,81 %)	176–204 µm; mean 190 µm (3,06 %)	210–317 µm; mean 272 µm (2.48 %)	154–217 µm; mean 190 µm (1.78 %)	388–837 µm; mean 506 µm (0.27 %)
Size of anal tubuli (relative size to body length)	303 µm (5.42 %)	150 µm (2.8 %)	120 µm (1.94 %)	294 µm (2.21 %)	325 µm (3.04 %)	229 µm (0.11 %)

absent in White Sea specimens (Fig. 6E and F). Dentoscalids can alternate with normal scalids in specimens from the White Sea (Fig. 6A). We did not find dentoscalids in *H. higginsi* (Fig. 6C). Instead, all scalids have a similar shape and one to four scalids in the posterior part of a row are slightly smaller and have a blunter tip than anterior scalids of *H. higginsi* (Fig. 6C).

The posteriormost scalid of a row of *H. spinulosus* can either be a "normal" scalid or a dentoscalid (Fig. 6A and B). When it is a "normal" scalid, the lateral margin can be smooth (Fig. 6A) or dentate and the size can be smaller than the previous scalids in the row (Fig. 6B).

A scalid row of *H. spinulosus* is completed with a significantly smaller structure, the flosculus-tubulus-complex (Fig. 6A). The flosculus-tubulus-complex is situated in a small cuticular fold, it is distinctly smaller than the scalids and does not have a scalid-like shape (Fig. 6A). Due to dirt or hidden in the cuticular fold, the flosculus-tubulus-complex could not be investigated in detail.

Between buccal papillae and the scalids rows are eight primary scalids, occurring directly posterior of the eight large buccal papillae (Fig. 5A–C; 6G). Primary scalids are not in line with the following scalid rows, instead they are located between two rows (Fig. 5A and B). Between the two primary scalids that occur lateral of the ventral midline are four scalid rows, otherwise there are three scalid rows between two primary scalids. Primary scalids are about the same size as the following scalids and share the same morphology (Fig. 6G). In *H. spinulosus*, the tips of primary scalids are slightly bent anteriorly, featuring a similar groove with cuticular folds and two different shaped tubulus types as on the tips of the normal scalids (Fig. 6H). The number of the tubuli on the tips of the primary scalids is higher than on the normal scalids, especially on the lateral area of the tip (Fig. 6H). The cuticle of the tip of primary scalids has a net-like surface (Fig. 6H). The tips of primary scalids in light micrographs of *H. higginsi* could not be investigated due to insufficient magnification.

3.2.5. Trunk

The trunk of all examined specimens is annulated and holds several types of sensory and secretory structures (Fig. 3; 7–9). *Halicryptus spinulosus* from both locations have roughly the same number of annuli, while *H. higginsi* has almost the double number of annuli, that also appear much broader (Table 4; Fig. 3; 7A).

The trunk carries numerous pointed structures, the trunk tubuli, which seem to occur randomly placed on the annuli, but never or rarely on the body surface above the ventral midline (Fig. 3A–G; 7A-C). Trunk tubuli consist of a broad conical base (Fig. 7C) and a thin tapering tip, which can be as long as the base. The tips of trunk tubuli are flattened and have an opening (Fig. 7D). The size of trunk tubuli differs slightly between *H. spinulosus* specimens, whereas the ones from *H. higginsi* are considerably larger (Table 4). Relative to the total body length, trunk tubuli of *H. higginsi* are about ten times smaller than the ones of *H. spinulosus* (Table 4).

On the posterior trunk of *H. spinulosus* specimens from Alaska and the White Sea occur numerous small trunk papillae, ranging from about 15 to 25 µm in length and 50–100 µm in diameter (Fig. 8A–C). Whether these papillae are organized in rings or randomly placed is not observable from our material. These papillae also occur irregularly on the remaining trunk. The shape of these papillae is conical (Fig. 8B). The tip has numerous cuticular protrusions (Fig. 8B). At the level of about half the length of the papillae are up to ten flosculus-shaped structures (Fig. 8B–D), which we call accessory flosculi here. They have numerous cuticular protrusions, which seem to be organized in rings around a central opening (Fig. 8D). Occasionally, additional smaller accessory papillae with finger-like cuticular protrusions around a terminal opening can be present on these small papillae (Fig. 8C and D).

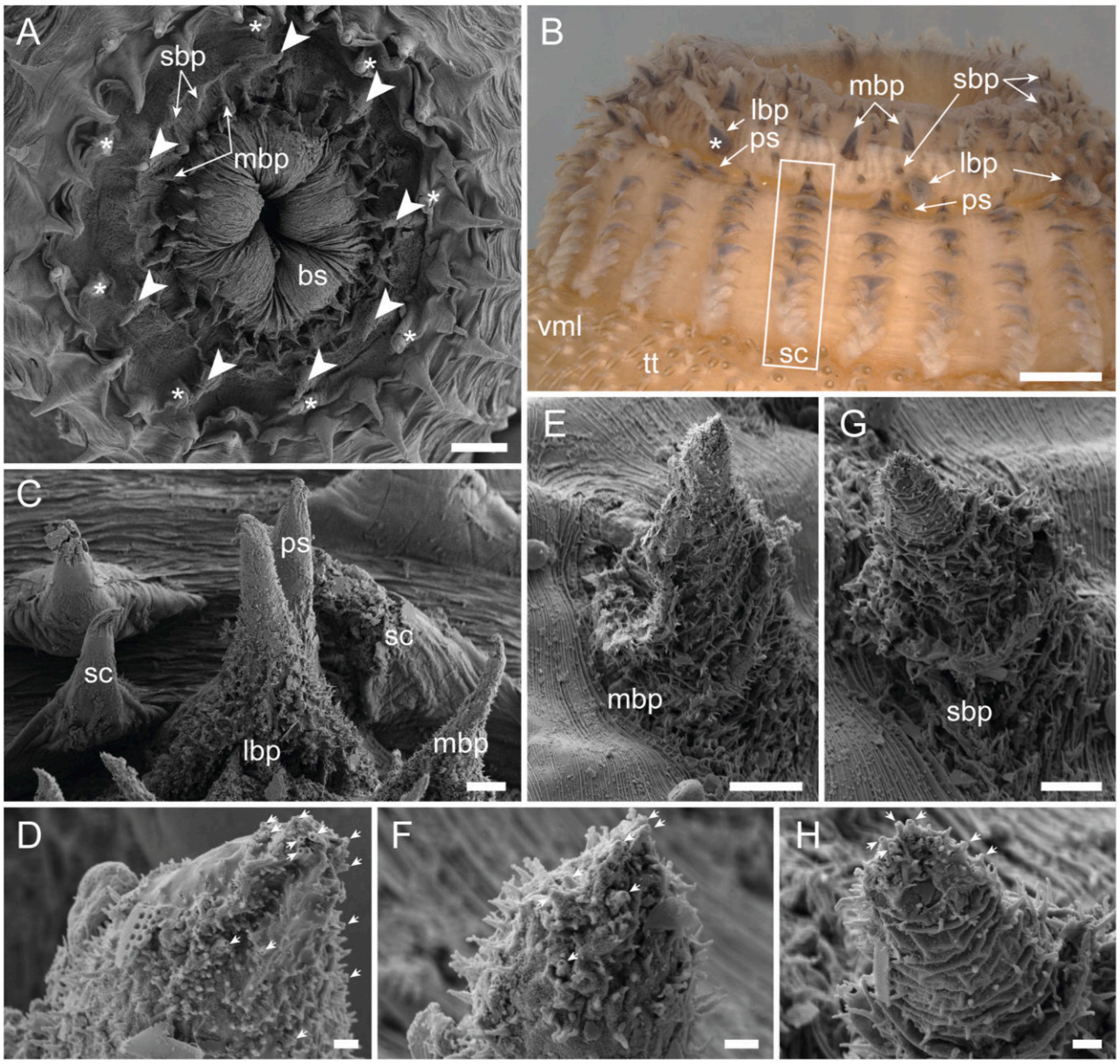

Fig. 5. Buccal papillae, SEM images (A, C-H) and light microscopical image (B). A. Frontal view of the introvert of *H. spinulosus* specimen A1 showing bulbous structures (bs) around the mouth opening. Arrowheads show the 8 large buccal papillae. The asterisks (*) mark the 8 primary scalids. B. Lateral view of the introvert of *H. higginsi*. Box shows a row of scalids (sc). The asterisk shows enlarged large buccal papilla (lbp). C. Large buccal papilla standing in line with primary scalid (ps) between two rows of scalids. D. Tip of large buccal papilla with tubular structures (arrows). E. Higher magnification of medium-sized buccal papilla (mbp). F. Tip of medium-sized papilla with tubular structures (arrows). G. Higher magnification of small buccal papilla (smp). H. Tip of small buccal papilla with tubular structures (arrows). Further abbreviations: tt, trunk tubuli; vml, ventral midline. Scale bars: A = 100 µm; B = 1 mm; C, E = 20 µm; D, F, H = 2 µm; G = 10 µm.

Further posterior on the last annulus occurs another type of small papilla, the flosculus-tubulus-complex. Several flosculus-tubulus-complexes seem to be organized in a loose ring (Fig. 8A; 9A). These papillae have a broad, narrow base and a long thin apical part that terminates in a tip with about five finger-like protrusions (Fig. 9A). A central opening was not distinctly visible. At about the same level as the beginning of the thin apical part occurs one flosculus, which is similar as the ones from the small trunk papillae (see above) with cuticular protrusions around a central opening (Fig. 9A).

In *H. higginsi*, similar small trunk papillae as in *H. spinulosus* are found all over the trunk surface (Fig. 9B). Whether these small papillae are also more accumulated on the posterior trunk is not observable in the examined specimen. The small trunk papillae are about 20–30 µm in length and 60–110 µm in diameter and are bordered by a cuticular fold (Fig. 9B). The tip of the projecting conical structure has numerous cuticular protrusions, similar to *H. spinulosus*, but the protrusions also occur downwards the cone (Fig. 9C). An opening on the tip was not visible. Around the basal part, we observed flosculi with the same appearance than in the congener (Fig. 9B).

Additionally, we observed in *H. higginsi* small papillae on the posterior trunk that seem to be organized in a ring (Fig. 9D). Whether these small papillae correspond to the flosculus-tubulus-complexes on the posterior trunk of *H. spinulosus* remains unclear. Furthermore, anterior of these structures in *H. higginsi* are similar conical structures as the trunk tubuli but without the tapering tip, giving them a blunt appearance (Fig. 9D). Dorsally, the blunt cones seem to be arranged in lines or half rings (Fig. 9D), whereas ventrally this arrangement is ambiguous (Fig. 7A).

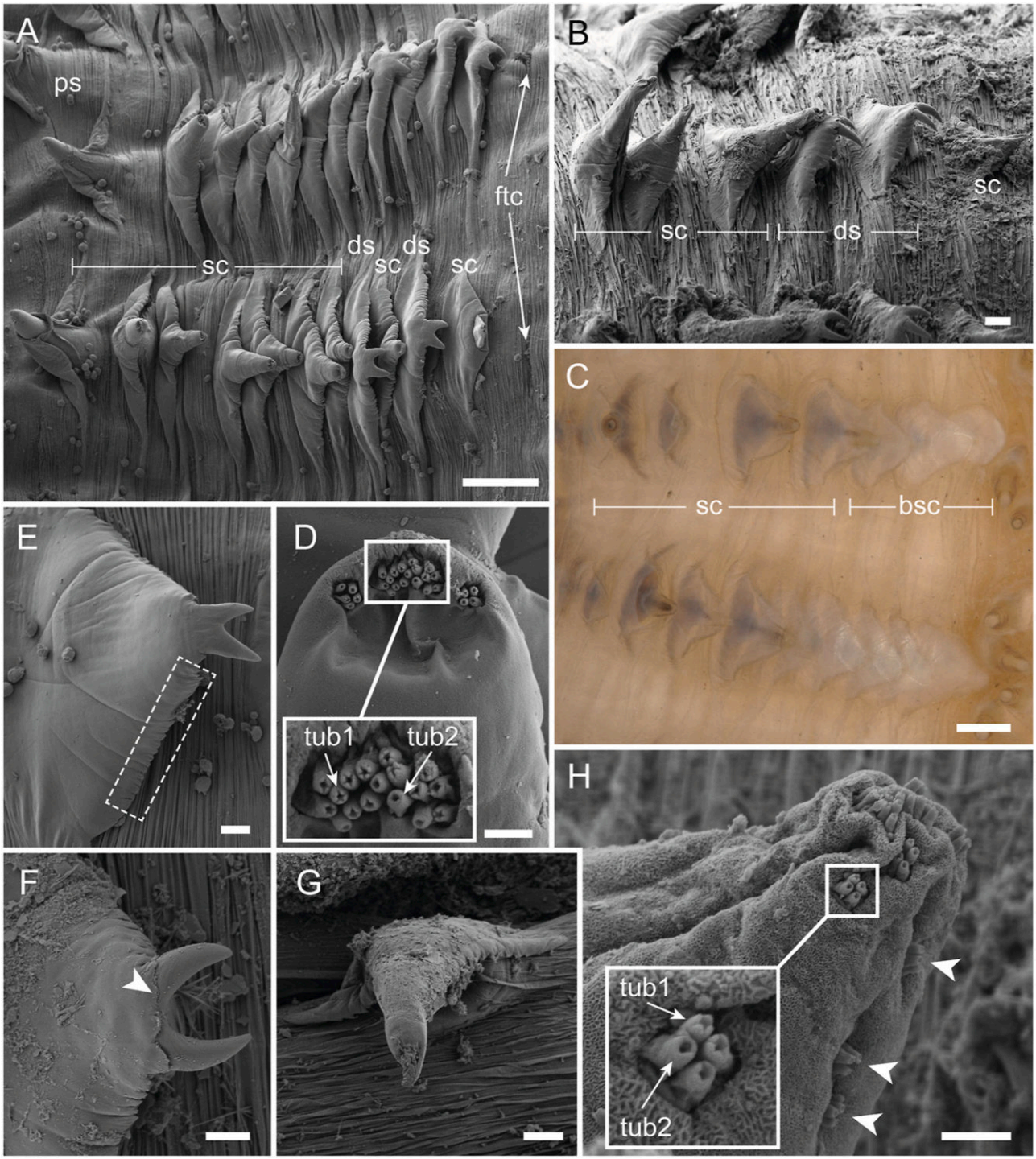

Fig. 6. Scalids, SEM images (A, B, D-H) and light microscopical image (C). A. Scalid rows of *H. spinulosus* specimen W2 with normal scalids (sc), dentoscalids (ds) and flosculus-tubulus-complex (ftc). B. Scalid row of *H. spinulosus* specimen A1 with normal scalids and dentoscalids. C. Scalid rows of *H. higginsi* with scalids and blunt scalids (bsc). D. Tip of a normal scalid of *H. spinulosus* with apical and lateral grooves filled with tubular structures. Inlay shows higher magnification of the apical groove filled with tubular structures with dented margin (tub1) and smooth margin (tub2). E. Dentoscalid of *H. spinulosus* specimen W2. Dotted box shows dented lateral margin. F. Dentoscalid of *H. spinulosus* specimen A1. Arrowhead shows cuticular fold anterior of the apical spines. G. Primary scalid of *H. spinulosus* specimen A1. H. Tip of primary scalid of *H. spinulosus* specimen W2 with apical and lateral (arrowheads) groups of tubular structures. Inlay shows higher magnification of a lateral group of tubular structures with dented and smooth margin. Further abbreviations: ps, primary scalid. Scale bars: A = 100 μm; B, E, G = 20 μm; C = 250 μm; D, H = 4 μm; F = 20 μm.

3.2.6. *Anal tubuli*

Lateral of the anus of *H. spinulosus* and *H. higginsi* are two distinct anal tubuli (Fig. 3A and B; 8A; 9D; 10A). Absolute and relative measurements of anal tubuli differ slightly between *H. spinulosus* specimens (Table 4). In *H. higginsi*, the relation of the size of anal tubuli compared to the total body length is smaller than in *H. spinulosus* (Table 4).

In *H. spinulosus*, the anal tubuli have a broad wrinkled base that extends into a smooth conical apical part with lateral grouped openings in the cuticle and paired tubular structures in grooves (Fig. 10A–C). The tip of the anal tubuli has several subapical tubular structures (Fig. 10D).

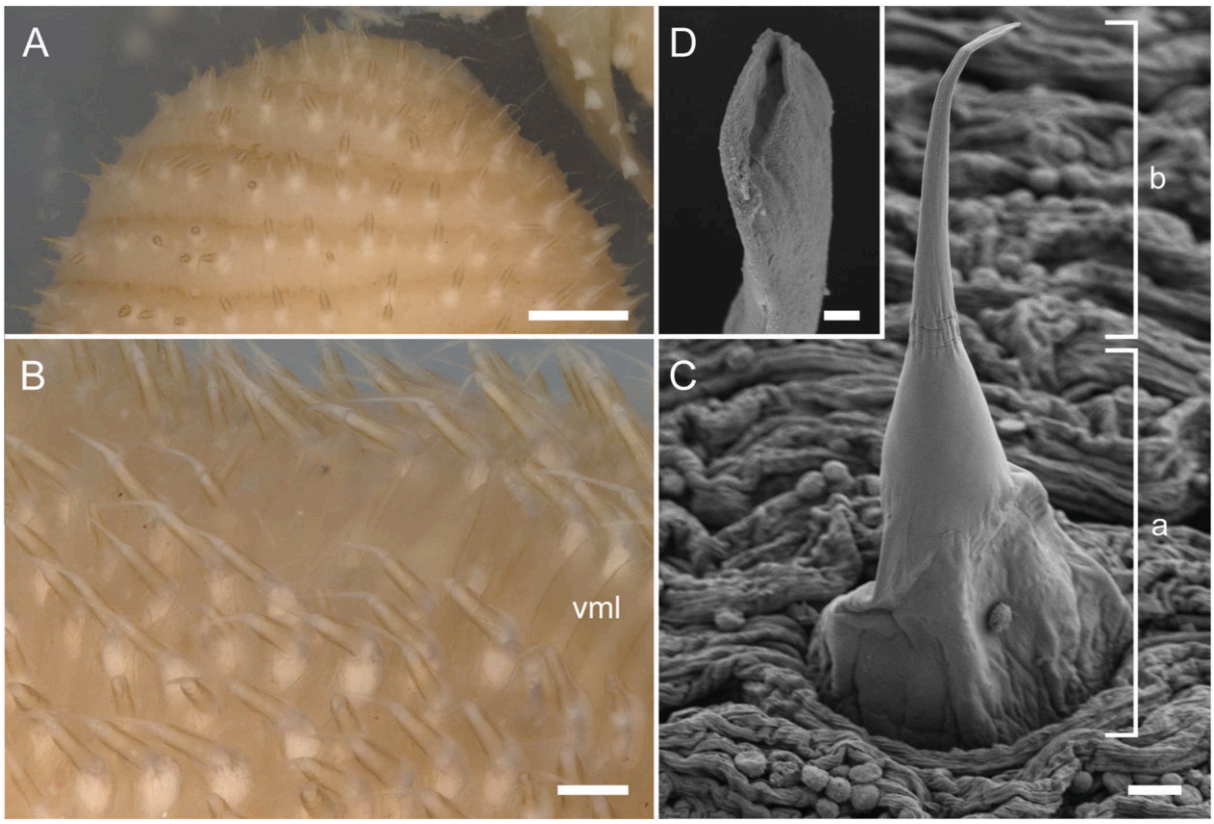

Fig. 7. Trunk tubuli, light microscopical images (A, B) and SEM images (C, D). A. Dorsal view of posterior trunk end of *H. higginsi* showing irregular organization of trunk tubuli. B. Ventral midline (vml) and trunk tubuli of *H. higginsi*. C. Trunk tubulus of *H. spinulosus* specimen W1 with conical base (a) and thin tapering tip (b). D. Tip of a trunk tubulus of *H. higginsi* with terminal slit-like opening. Scale bars: A = 1 mm; B = 250 μm; C = 20 μm; D = 1 μm.

Along the stem of the anal tubuli are several structures that resemble the flosculus-tubulus-complexes on the last annulus (Fig. 10E). In specimen W1 are four larger conical papillae connected to the base of the anal tubuli, which we only observed in this specimen (Fig. 10A). These papillae differ in their appearance and can appear with an accessory papilla and flosculus or can only have a hand-like tip with three to four accessory papillae (Fig. 10F and G). The anal tubuli of *H. higginsi* do not have a pointy appearance like the ones from *H. spinulosus*, instead they are blunt and look more like the blunt cones on the posterior part of the trunk (see above) (Fig. 9D). The fine structure could not be investigated in *H. higginsi*.

3.3. Histology

3.3.1. Body wall

The body wall consists of four layers: cuticle, single-layered epidermis, circular musculature and longitudinal musculature (Fig. 11; 12A,B inlays). Only in the introvert the continuous longitudinal musculature layer is missing and 25 distinctly separated strands of longitudinal muscles below the circular musculature layer are present (Fig. 12A). In different regions of the trunk, the composition of the body wall does not change (Fig. 11D–I). The cuticle is composed of two differently stained layers (Fig. 11; 12A,B inlays).

The thickness of body wall layers differs between species and body parts (Fig. 2; 11; Supplementary Table 1), especially the thickness of muscle layers (Fig. 11D–I; Supplementary Table 1) and the internal part of the cuticle of *H. spinulosus* specimen W3 and *H. higginsi* (Fig. 11B,C,E, F,H,I; Supplementary Table 1). In small *H. spinulosus* specimen A4 the musculature layers appear very thin, whereas in *H. higginsi* this layer is much more pronounced and the cuticle occasionally reaches deep into the circular musculature (Fig. 12A and B). In large *H. spinulosus* specimen W3, the musculature layers resemble those of *H. higginsi* (Fig. 11B,C,E,F,H,I). Relations of the total body wall thickness in the broadest and narrowest region to the diameter of the cross section on the other hand are almost identical between *H. higginsi* and *H. spinulosus* specimen W3 (Supplementary Table 2). In contrast, relations of the total body wall thickness to the diameter of the cross section in *H. spinulosus* specimen A4 are about two to three times smaller (Supplementary Table 2).

The epidermis, circular musculature and sometimes the longitudinal musculature of *H. spinulosus* specimen A4 are similarly stained as the external cuticle, which sometimes blurs the borders between layers and makes measurements less exact than in other specimens (Fig. 11A,D,G; 12A inlay).

3.3.2. Anterior body region

Histological cross-sections of the anterior body parts of *H. spinulosus* and *H. higginsi* show the pharynx with a strong muscle bulb and an inner cuticular lining with pharyngeal teeth (Fig. 12A and B). Between pharynx and body wall are diverse retractor muscles. All retractor muscles are very flat and broad in cross section (Fig. 12A and B). Six longitudinal muscles, the pharynx protractors, are located directly around the pharynx bulb. In *H. spinulosus*, the protractors seem to be of different size, whereas in *H. higginsi* they are of equal size. Further into the body cavity are eight long and nine short introvert retractors in *H. spinulosus* (Fig. 12A). In the anterior pharyngeal region, the eight long and eight short introvert retractors seem to stand in pairs, whereas one short retractor stands alone (Fig. 12A). In *H. higginsi*, only the eight long introvert retractors could be assigned with certainty in the posterior pharynx (Fig. 12B). The short introvert retractors are nearest to the body wall and connect to it at approximately the transition of the introvert to the trunk and can already be absent when looking at the posterior

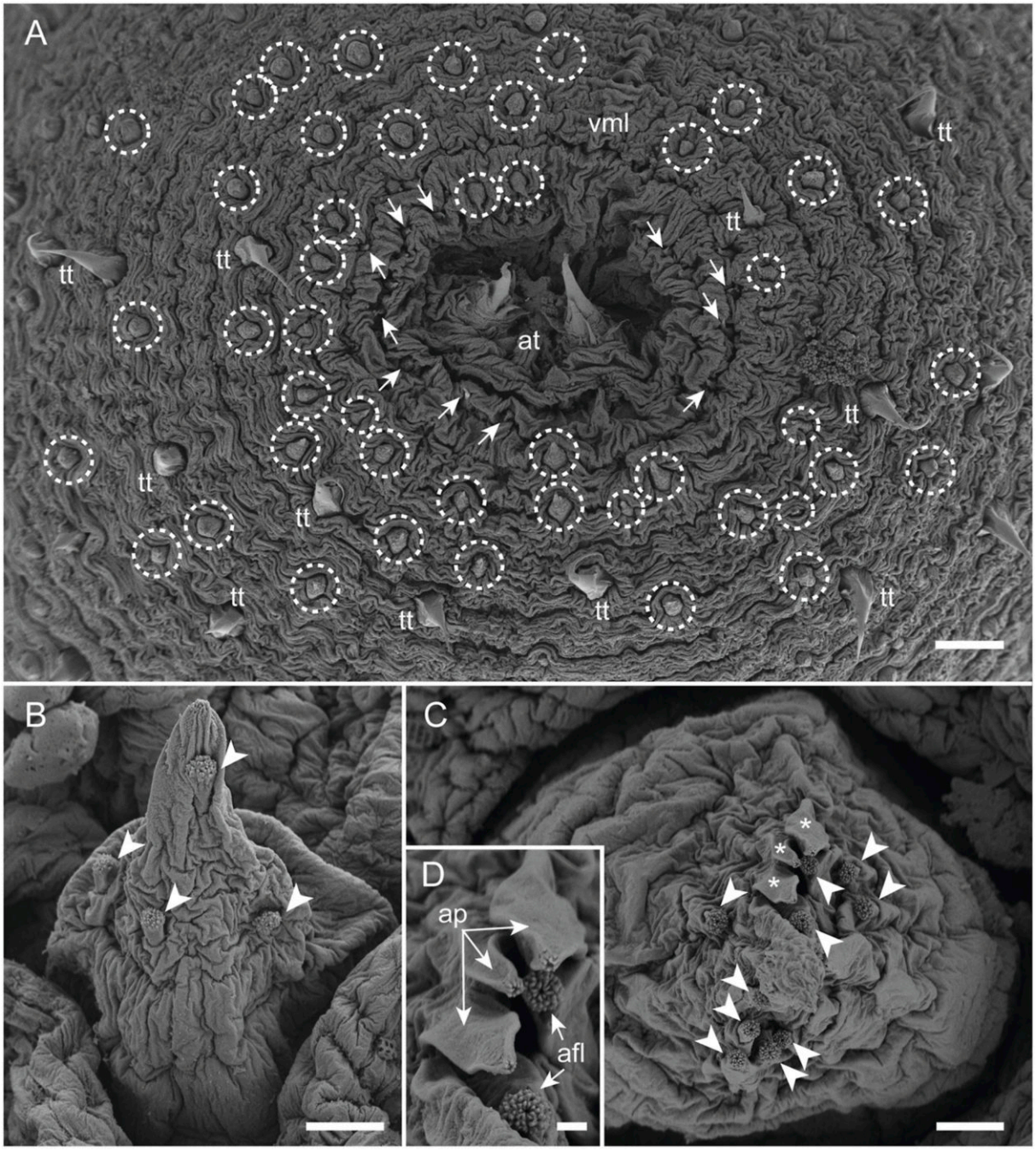

Fig. 8. Posterior end of the trunk of *H. spinulosus* specimen W1, SEM images. A. Frontal view of posterior trunk end showing various structures: anal tubuli (at), trunk tubuli (tt), small trunk papillae (dotted circles) and flosculus-tubulus-complexes on the last annulus arranged in a loose ring (arrows). B Small trunk papilla on posterior trunk. Arrowheads show accessory flosculi. C. Another small trunk papilla with more accessory flosculi (arrowheads) and accessory papillae (asterisks). D. Higher magnification of accessory papillae (ap) and accessory flosculi (afl). Further abbreviations: vml, ventral midline. Scale bars: A = 200 μm; B, C = 10 μm; D = 1 μm.

pharynx (Fig. 12B). Long introvert retractors are much longer and reach far into the trunk. The mid gut connects to the pharynx (Fig. 12B).

3.3.3. *Posterior trunk region*

Sections through the posterior body region show the urogenital system and gonads in different degrees of development. The *H. spinulosus* specimen W3 has male gonads (Fig. 13A and B), whereas specimen A4 and *H. higginsi* both have female gonads (Fig. 13C and F). Male gonads are composed of many seminal follicles that connect to seminal ducts which again are connected to the urogenital ducts (Fig. 13A and B). Female gonads are composed of oocytes that connect to the ovary sack, which leads to the urogenital duct (Fig. 13C–F). The gonads are connected by a thin mesenterium to the body wall (Fig. 13A–C). The body cavity is very spacious in both species.

3.4. *Additional remarks on gonads*

All specimens examined in this study have paired gonads, which were revealed either by preparation for SEM, in histological sections (see above) or sometimes by showing through the semi-transparent trunk (Fig. 3D–F).

The oviferous gonads of the *H. higginsi* specimen are extremely long

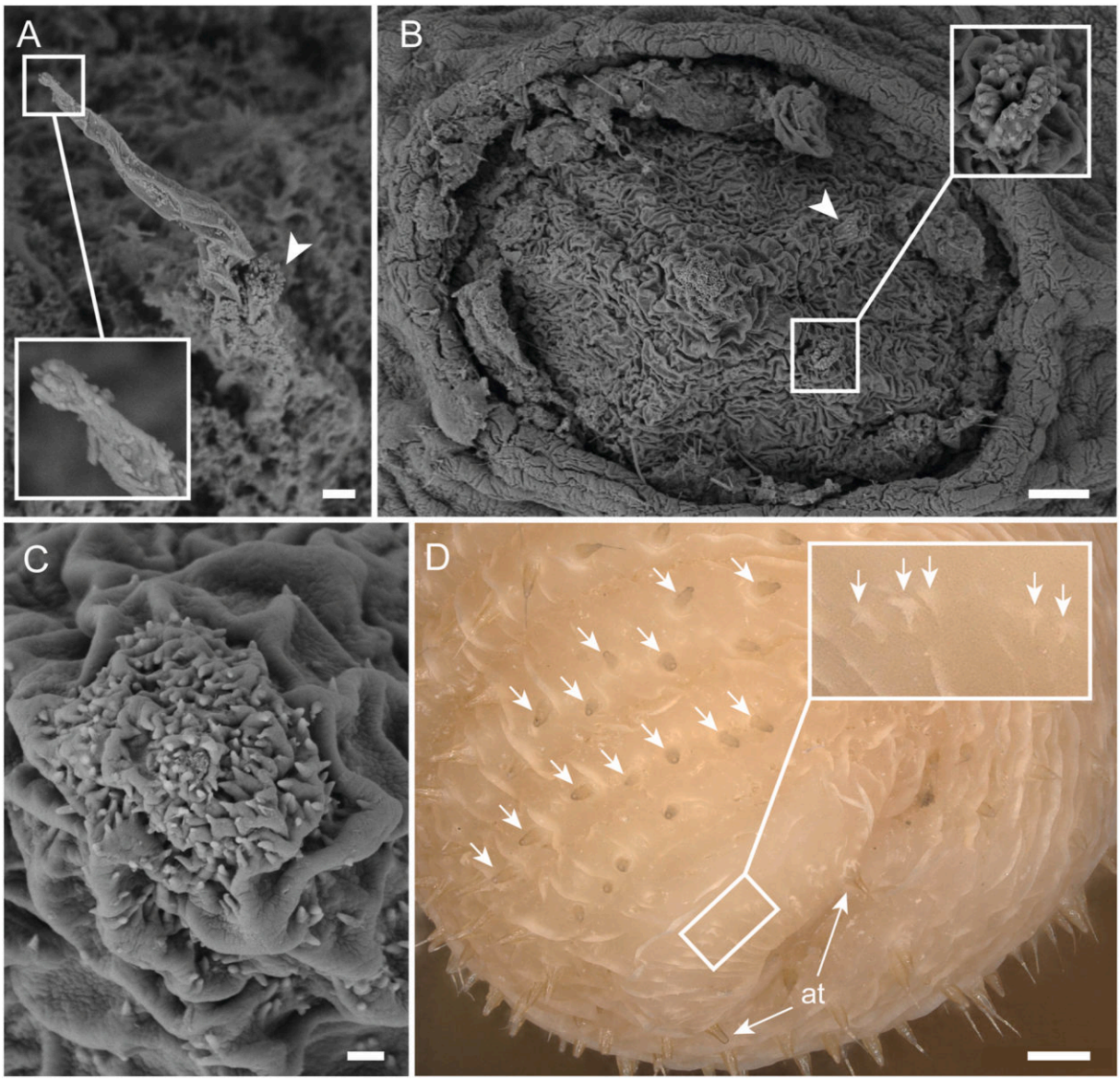

Fig. 9. Structures on the trunk, SEM images (A–C) and light microscopical image (D). A. Flosculus-tubulus-complex on the last annulus arranged in a loose ring of *H. spinulosus* specimen A1. Arrowhead shows accessory flosculus. Inlay shows higher magnification of the tip with 5 finger-like protrusions. B. Small trunk papilla of *H. higginsi*. Inlay and arrowhead show accessory flosculi. C. Higher magnification of the tip of a small trunk papilla of *H. higginsi* with numerous cuticular protrusions. D. Posterior trunk end of *H. higginsi* with anus between the anal tubuli (at). Arrows show blunt papillae arranged in lines. Inlay shows higher magnification of a part of the last annulus with small papillae (vertical arrows). Scale bars: A = 2 μm; B = 10 μm; C = 1 μm; D = 500 μm.

and almost fill out the whole body cavity up to the introvert. Thus, eggs can be detached and appear nearly everywhere in the body cavity (Fig. 12B).

3.5. Diagnostic characters of Halicryptus species

We analysed previous morphological studies of *Halicryptus* specimens and compared their reports with our new collected data to identify reliable and potential diagnostic characters of *H. spinulosus* and *H. higginsi* (see Table 5).

Reliable identified diagnostic characters are: (1) total body length of mature adults, (2) number of trunk annuli of mature adults, (3) presence/absence of dentoscalids, (4) scalids with subapical or lateral depressions, (5) position of largest teeth, and (6) distribution of cuticular protrusions on the cone of small trunk papillae (Table 5).

Potential diagnostic characters are: (7) presence/absence of circular structures on border of introvert to trunk, (8) presence/absence of peg-like ring papillae on posterior trunk, (9) size indication of trunk tubuli compared to total body length and (10) size indication of anal tubuli compared to total body length (Table 5). These potential diagnostic characters need further investigations to be justified as diagnostic.

4. Discussion

4.1. Distribution of Halicryptus

Our results confirm that there are two species in *Halicryptus*, one with a very regional distribution (*H. higginsi* around Point Barrow, Alaska) and one with a very broad, circumpolar distribution (*H. spinulosus*). Investigations of allozymes of different *H. spinulosus* populations from the Baltic Sea, White Sea and Iceland also revealed a broad distribution of this species (Schreiber et al., 1996). Our maximum-likelihood tree shows a poorly resolved cluster of *H. spinulosus* specimens from different locations. This cluster includes specimens from the Baltic Sea, Beaufort

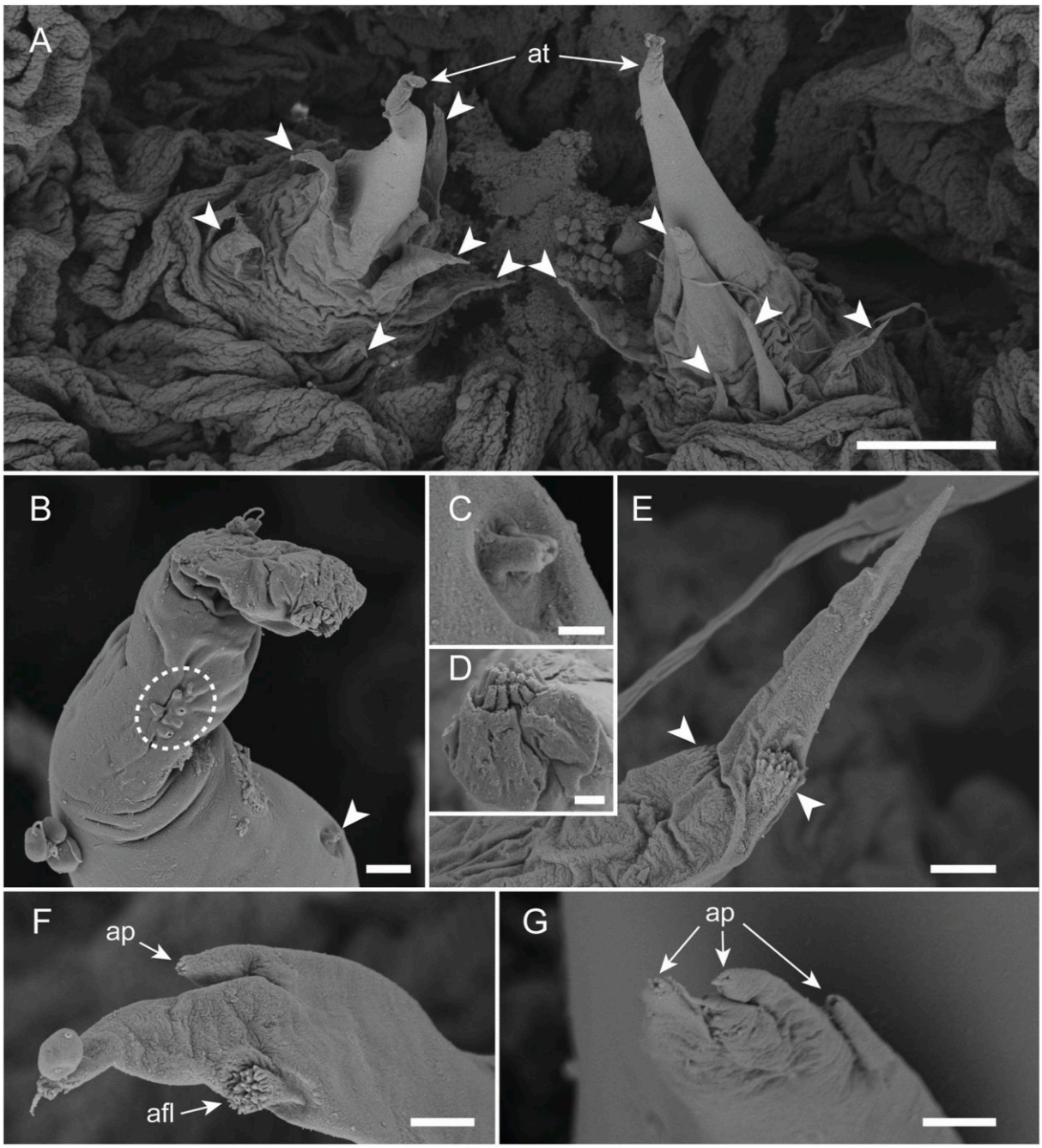

Fig. 10. Anal tubuli of *H. spinulosus* from the White Sea (specimen W1), SEM images. A. Overview of anal tubuli (at) with surrounding papillae (arrowheads). B. Tip of anal tubulus. Dotted circle shows group of openings on the cuticle. Arrowhead shows lateral paired tubular structures. C. Higher magnification of lateral paired tubular structures. D. Tip of anal tubulus with apical group of tubular structures. E. Small papilla surrounding the base of anal tubulus. Arrowheads show accessory flosculi. F. Papilla connected with the base of an anal tubulus with accessory flosculus (afl) and accessory papilla (ap). G. Another type of papilla connected with the base of an anal tubulus with apical accessory papilla. Scale bars: A = 100 μm; B, E-G = 4 μm; C = 1 μm; D = 2 μm.

Sea, White Sea, East Siberian Sea and Hudson Bay, revealing a widespread distribution of this species almost across the whole Northern Hemisphere. Van der Land (1970) showed a similar distribution of specimens identified as *H. spinulosus* from previous studies based on morphological data and mapped additional locations around Spitsbergen, north coast of Norway, Iceland, east coast of Greenland, southern Kara Sea, Labrador Sea and the Beaufort Sea. The latter two represent the findings of Carter (1966), MacGinitie (1955) and Holmquist (1963), from which the report of MacGinitie (1955) probably represents *H. higginsi*, due to the large body size. Adrianov and Malakhov (1996b) added a few new locations on the west coast of Alaska, the White Sea and south-east coast of Japan. A recent study by Kolbasova et al. (2023) revealed a similar broad northern distribution of macroscopic *P. caudatus*. Although analyses of the mitochondrial CO1 gene of intertidal and subtidal populations of *P. caudatus* show different genotypes pointing towards the presence of cryptic species, analyses of nuclear genes are not congruent, indicating a potential incomplete speciation (Kolbasova et al., 2023). As the molecular analysis in this study was only performed with a 525 bp fragment of the mitochondrial CO1 gene, we highly recommend conducting additional analysis with more genes and more samples.

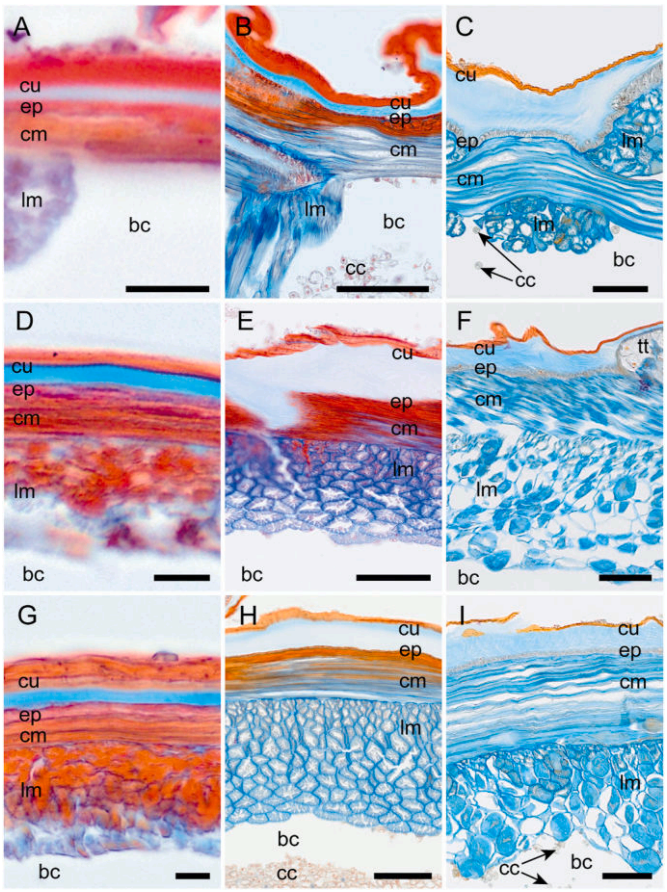

Fig. 11. Histological cross sections (Azan-stained) of the body wall of *H. spinulosus* specimens A4 (A, D, G) and W3 (B, E, H) and *H. higginsi* (C, F, I), light microscopical images. A-C. Body wall of introvert. D-F. Body wall of approximately the middle of the specimen. G-I. Body wall of posterior end of the specimen. Abbreviations: bc, body cavity; cc, coelomocytes; cm, circular musculature; cu, cuticle; ep, epidermis; lm, longitudinal musculature; tt, trunk tubulus. Scale bars: A, D, G = 10 µm; B, C, E, F, H, I = 100 µm.

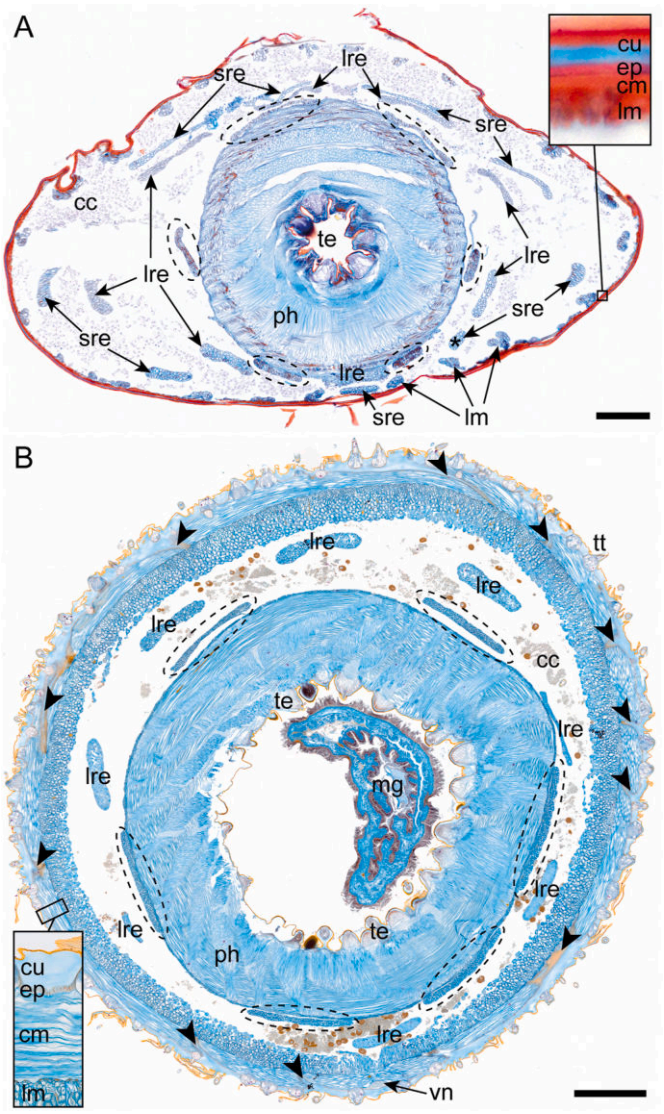

Fig. 12. Histological cross-sections (Azan-stained) of the pharynx, light microscopical images. Dotted ellipses show 6 pharynx protractors. A. Posterior part of the pharynx (ph) of *H. spinulosus* from Alaska. Inlay shows higher magnification of the body wall with two layered cuticle (cu), epidermis (ep), circular musculature (cm) and longitudinal musculature (lm). The asterisk (*) shows a short introvert retractor (sre) which is not paired with a long introvert retractor (lre). B. Far posterior part of the pharynx of *H. higginsi* with slightly into the pharynx pushed mid gut (mg). Arrowheads show deeply into the ring musculature drawn cuticle. Inlay shows higher magnification of the body wall with two layered cuticle, epidermis, circular musculature and longitudinal musculature. Further abbreviations: cc, coelomocytes; te, pharyngeal teeth; tt, trunk tubulus; vn, ventral nerve cord. Scale bars: A = 200 µm; B = 1000 µm.

4.2. Morphological characters and revised terminology

There are comparably few investigations on the external structure, especially the fine structure, of *Halicryptus*. As the terminology of *Halicryptus*-specific structures differs significantly between publications, we regard it helpful to review the literature in detail and suggest a clear terminology for these structures (see Table 3).

Priapulida are divided into two adult size classes, macroscopic (several centimetres) and microscopic (few millimetres) (Schmidt-Rhaesa, 2013). Although *Halicryptus* is of macroscopic adult size, both species (*H. spinulosus* max. 4 cm; *H. higginsi* max. 38.5 cm) differ significantly in mature adult size (Van der Land, 1970; Shirley and Storch, 1999). For *H. higginsi*, only large adults (>20 cm) are certainly reported. Shirley and Storch (1999) report alleged postlarval stages of 1.5 mm length of *H. higginsi*, but without providing morphological data. As all small specimens from Alaska examined in this study represent *H. spinulosus*, morphological information of small-sized *H. higginsi* specimens are still lacking.

According to Shirley and Storch (1999), the introvert length to total body length relation differs between both *Halicryptus* species. Shirley and Storch (1999) specified an introvert length of about 2 % of the total body length in *H. higginsi*, whereas in the specimens of Merriman (1981) the relation is about 10 %. Van der Land (1970) also states an introvert length to total body length relation of 10 % in *H. spinulosus*. Our *H. spinulosus* specimens deviate slightly from Van der Lands data. In addition, the introvert-body length relation of our investigated *H. higginsi* specimen is five times higher than specified by Shirley and Storch (1999), although it represents a paratype of their investigated material. Although *Halicryptus* has much lower introvert length to total body length relation than other macroscopic priapulids, we do not recommend using this relative measure as a species-specific diagnostic character due to the high contractibility of priapulids.

The pharynx of priapulids is armed with cuticular pharyngeal teeth. The teeth of *H. spinulosus* are arranged in pentaradial rings (Von Siebold, 1849) and were described in detail by Ehlers (1862). The teeth have the typical cuspidate teeth appearance of macroscopic priapulids with a large median cusp and smaller lateral cusps. In Ehlers' specimens, the amount of lateral cusps is two, whereas Scharff (1885) describes three to

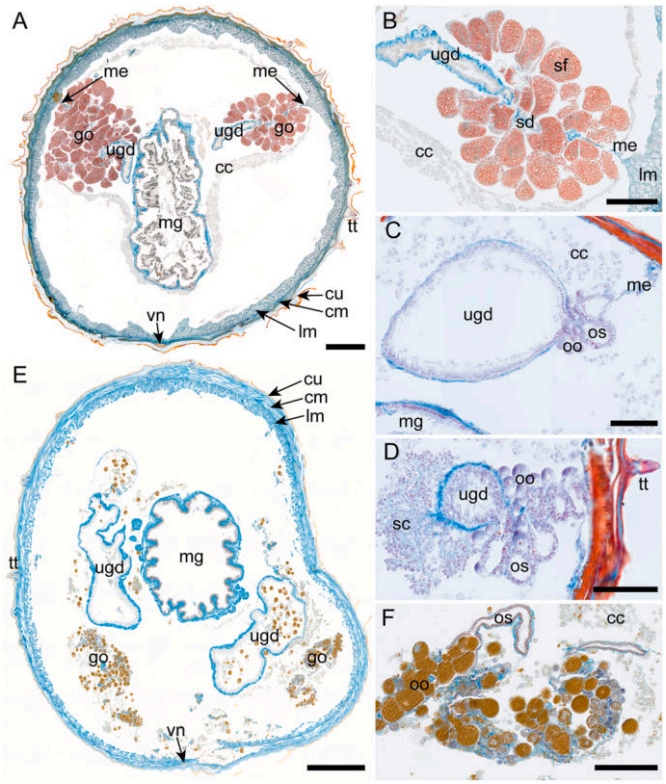

Fig. 13. Histological cross-sections (Azan-stained) of the posterior trunk and gonads of *H. spinulosus* specimen W3 from the White Sea (A,B), *H. spinulosus* specimen A4 from Alaska (C,D) and *H. higginsi* (E,F), light microscopical images. A. Overview of a cross-section with mid gut (mg), gonads (go) and urogenital ducts (ugd). B. Higher magnification of male gonads with seminal follicles (sf), seminal canals (sd) and urogenital duct. C. Posterior part of the urogenital system with female gonads. D. Anterior part of the urogenital system (app. 200 µm further anterior than C) with solenocyte tree (sc). E. Overview of a cross section with mid gut, urogenital ducts and gonads. F. Higher magnification of female gonads with oocytes in an ovary sack (os). Further abbreviations: cc, coelomocytes; cm, circular musculature; cu, cuticle; lm, longitudinal musculature; me, mesenterium; tt, trunk tubulus; vn, ventral nerve cord. Scale bars: A = 500 µm; B = 250 µm; C, D = 100 µm; E = 1000 µm; F = 200 µm.

four cusps. Van der Land (1970) gives a range between 0 and 12 lateral cusps and reports the biggest teeth in the second and third ring. Additionally, Van der Land states that large specimens from Novaya Zemlya (Arctic Ocean) and Alaska only have two lateral cusps in the first ring of teeth and no lateral cusps in the following three rings. Merriman (1981) showed the first SEM images of *Halicryptus* teeth with four to five lateral cusps on a tooth of the second ring. Later, Storch et al. (1990) showed also teeth with several "accessory spines" on the first four rings of teeth. Adrianov and Malakhov (1996a) also illustrated four to five lateral cusps on the first two rings of teeth of a juvenile specimen, but giving no information on adults. Unfortunately, not all previous studies report the total body length or developmental stage (juvenile or adult) of the investigated specimens. It appears from ours and Van der Land (1970) observations that the number of lateral cusps decreases with age. Currently this remains an assumption, as too few specimens were investigated.

Tubular tooth receptors were described on the pharyngeal teeth of some priapulid species, especially lateral on the median cusp or on the smaller lateral cusps (e.g. Storch et al. (1994) for *Priapulus tuberculatospinosus* and Schmidt-Rhaesa and Raeker (2022) for *Priapulopsis bicaudatus*). For *Halicryptus*, such receptors have not been reported yet and our investigations confirm the absence of tooth receptors in this species. We have observed pores on the cuticle of the concave underside of the teeth, which has not yet been reported for the teeth of priapulids.

At the same level of the first ring of teeth occur five small papillae directly located posterior of the teeth of the second ring of *H. spinulosus*. These structures have first been described as "rudimentary" structures (teeth or papillae) by other authors (see Table 3). Since our investigation also revealed these structures as conical papillae with apical tubuli, we agree with the terminology introduced by Lemburg (1999). We suggest omitting the prefix "rudimentary", because there is no indication why they should be rudimentary structures. The mouth papillae have not yet been reported for other adult priapulid species than *H. spinulosus*.

On the circumoral field of *Halicryptus*, between the pharyngeal teeth and primary scalids (see below), are numerous papilliform structures in different sizes. These structures are indicated as "buccal papillae" by Van der Land (1970), which have the same appearance as scalids. Later, Merriman (1981) described buccal papillae as curved truncated cones, showing also SEM images presumably of *H. higginsi*. Storch et al. (1990) described them for *H. spinulosus* as conical with tiny cuticular protrusions on the surface and indicated a sensory function due to an apical pore and tubular structures. The cuticular protrusions and apical tubuli have also been shown by Adrianov and Malakhov (1996a) and Lemburg (1999), but no apical pore was shown or mentioned, similar to our material. In *H. higginsi*, we observed a rough surface, tending to the presence of cuticular protrusions. Buccal papillae have been reported for other macroscopic species although these papillae do not correspond in terms of quantity and structure with the buccal papillae described for *Halicryptus* (e.g. Storch et al., 1994; 1995).

Different sizes of buccal papillae were first mentioned by Shirley and Storch (1999) for *H. higginsi*. Lemburg (1999) showed a new characteristic in describing eight "primary buccal papillae" in *H. spinulosus* that are located directly anterior of the eight primary scalids, but giving no further information on their size. Here, we describe for the first time three different size types of buccal papillae for *H. spinulosus* and *H. higginsi*. The eight large buccal papillae have a distinctly recognizable size and are about the same size as the primary scalids in *H. spinulosus*. The slightly smaller medium-sized buccal papillae are located slightly further anterior and are loosely arranged in a ring of about 16 papillae. The numerous small buccal papillae are about half the size of the medium-sized ones and are randomly scattered in between them. Additionally, they seem to occur on a level with the large buccal papillae, building a ring of about 16 small buccal papillae, which can be seen more distinctly when the introvert is inverted. One enlarged large buccal papilla next to the ventral midline of the examined *H. higginsi* specimen most likely resembles an artefact and it was not observed in any other specimens or species before. We recommend further investigation on more material, especially in the arrangement and number of the medium-sized and small buccal papillae.

Located directly anterior of a scalid row (see below) or sometimes on the same level as the anteriormost scalids are primary scalids. All macroscopic priapulids have eight primary scalids that have the same arrangement between the scalid rows as described here for *Halicryptus* (see results). Primary scalids of our examined *H. spinulosus* and *H. higginsi* specimens look similar to the anterior scalids of a scalid row, differing from the primary scalids shown in Adrianov and Malakhov (1996a), where they feature more conical papillae (cf. their Fig. 3.24B). Either they show the large buccal papillae, which is most likely due to the cuticular protrusions on the surface, or the structure of primary scalids can differ between specimens or life stages. Nevertheless, these structures have small tubular sensory structures apical, which we also observed in our material.

On the surface of the introvert of all macroscopic priapulids are 25 longitudinal rows of scalids (Schmidt-Rhaesa, 2013). Von Siebold (1849) comprised the number of scalid rows of *H. spinulosus* first as 15, which was corrected by Ehlers (1862) to 25, which we can confirm for all examined specimens.

Scalid rows of *H. spinulosus* consist of different types of scalids: one type representing blunt-tipped, triangularly flattened scalids with a dentate lateral margin ("normal scalids"), the other looking similar, but

Table 5
Morphological characters of adult *H. spinulosus* and *H. higginsi*. Data combined from previous studies by Van der Land (1970), Storch et al. (1990), Adrianov and Malakhov (1996a) and Lemburg (1999) for *H. spinulosus* and Merriman (1981) and Shirley and Storch (1999) for *H. higginsi*. Asterisks (*) represent identical results with previous studies or results that fall within the stated range. Dashes (–) represent not collected data or not investigated character. Italic characters show new observations and differences to previous studies. Bold characters show diagnostic characters of adult specimens. Terminology was adapted to our new proposed terminology.

Character	*H. spinulosus* (prev. studies)	*H. spinulosus* (this study)	*H. higginsi* (prev. studies)	*H. higginsi* (this study)
Diagnostic characters:				
Total body length of mature adults (Fig. 3)	**< 40 mm**	*	**> 40 mm (max. 385 mm)**	*
Number of trunk annuli of mature adults	**< 100**	*	**> 100 (max. 180)**	*
Dentoscalids in scalid rows (Fig. 6A,B,E,F)	**present**	*	**absent**	*
Subapical depression on scalid tip (Fig. 6D)	**present**	*	**absent (lateral groups of tubuli present)**	-
Position of largest teeth (Fig. 4D)	**2nd and 3rd ring**	*	**3rd and 4th ring**	-
Cuticular protrusions on cone of small trunk papilla (Fig. 8B and C; 9C)	-	***accumulated on the tip of the cone***	-	***accumulated on the tip and scattered downwards the cone***
Circular structures on border of introvert to trunk	-	***absent***	**present**	***not visible***
Peg-like ring papillae on posterior trunk (Fig. 9D)	**absent**	*	**present**	*
Size indication of trunk tubuli	-	***> 0.5 % of total body length***	-	***< 0.5 % of total body length***
Size indication of anal tubuli	**2 large anal tubuli (compared to body length)**	**** (>0.2 % of total body length)***	**2 small anal tubuli (compared to body length)**	**** (<0.2 % of total body length)***
Morphological characters with validated or updated attributes:				
Introvert to body length relation	~10 %	*4-15 %*	2–10 %	*~11 %*
Introvert retractors/pharynx protractors (Fig. 12)	7-10 long introvert retractors and 10 short introvert retractors; 2 sets of 8 pharyngeal protractors	*8 long and 9 short introvert retractors; 6 pharyngeal protractors*	9 long retractors; 5 pharyngeal protractors	*8 long introvert retractors; 6 pharyngeal protractors*
Number of scalids in row (Fig. 6A–C)	max. 10	*up to 13 in large specimens (including dentoscalids and flosculus-tubulus-complex)*	max. 13	* (including up to 5 blunt scalids)
Series of scalids in rows (Fig. 6A–C)	absent	*	absent	*
Flosculus-tubulus-complex on posterior end of scalid row (Fig. 6A)	present	*	–	–
Mouth papillae posterior of 2nd ring teeth (Fig. 4A–H,I)	present	*	–	–
Cuspidate teeth in pentagonal rings (Fig. 4A–F)	present	*	present	*
Number of lateral cusps on anterior teeth rings (Fig. 4A–F)	up to 4 per side; in large specimens sometimes devoid in 2nd to 4th ring	*small specimens with up to 4* per *side in anterior rings; large specimens with irregular amounts (0–2)* per *ring*	up to 6 per side in 1st ring (usually 4); 2nd and 3rd ring with 0–5 per side; 4th usually without lateral cusps	*6-8* per *side in* 1st *ring; 2nd ring without lateral cusps*
Small trunk papillae (Fig. 8B and C; 8B)	absent	*present*	present	*
Flosculus-tubulus-complexes scattered on trunk	present	*absent*	–	–
Flosculus-tubulus-complexes arranged in a ring on posterior trunk (Fig. 8A; 9D)	absent	*present*	–	*present*

with two apical prongs ("dentoscalids") (cf. Fig. 11 in Scharff, 1885). We can confirm both types for our examined *H. spinulosus* specimens. Adrianov and Malakhov (1996a) showed a subtype of dentoscalids with just one spine (cf. their Fig. 3.25B), which we did not find in our material. Dentoscalids are reported to be absent in *H. higginsi* and the posterior scalids have a more blunt appearance (Shirley and Storch, 1999), which we can also confirm. Whether the blunt scalids of *H. higginsi* represent a different type of scalids remains unclear. Therefore, we conclude that the presence of dentoscalids is a diagnostic character for *H. spinulosus*.

In addition to the two types of scalids, a small structure completes the posterior end of a scalid row in *H. spinulosus*, the flosculus-tubulus-complex. Before Lemburg (1999) introduced this term, this structure was considered as developing or rudimentary scalid by other authors (see Table 3). This structure is composed of a tubulus and a flosculus (cf. Fig. 3.25C in Adrianov and Malakhov, 1996a). We adapt the term "flosculus-tubulus-complex" for the small structure at the posterior end of a scalid row due to the presence of flosculi, which are not present in the fully developed scalids and we believe these are not just lost during development. In addition, we do not consider that these structures represent rudimentary structures, as there is no indication for this.

Flosculus-tubulus-complexes are not described for *H. higginsi*, but additional circular structures were described posterior of a scalid row on the border of the introvert to the trunk, which were presumed to be rudimentary scalids (cf. Fig. 3 in Shirley and Storch, 1999). We consider that these structures do not resemble scalids, as they are not directly part of a scalid row and due to their location. Additionally, we think these are not rudimentary structures, but could rather resemble a diagnostic character for *H. higginsi*, as these are not present in *H. spinulosus*. In our examined specimen, these circular structures were not visible due to a

slightly inverted introvert.

The number and arrangement of scalids in a scalid row differs between previous reports. Scharff (1885) illustrated a scalid row with two scalids followed by three dentoscalids, giving a total number of five scalids in a row for *H. spinulosus*, which was later increased to ten by Van der Land (1970). Van der Land illustrated first five scalids, then an alternation of a dentoscalid and a normal scalid, followed by two dentoscalids and completed the row with one "rudimentary scalid" (=flosculus-tubulus-complex, see above). Some of our examined specimens from the White Sea hold up to 13 scalids in a row (including dentoscalids and flosculus-tubulus-complex), which increases the previously described maximum number of scalids in a row from 10 to 13 for *H. spinulosus*. Additionally, an alternation of scalids and dentoscalids was only observed in specimens from the White Sea. This alternation could either represent a morphological difference between the populations or a potential indication of age. More material is needed to proof these assumptions. For *H. higginsi*, the maximum number of scalids in a row differs between 7 (Merriman, 1981) and 13 (Shirley and Storch, 1999), which we can confirm in our examined specimen. As the number of scalids in a row overlap between *H. spinulosus* and *H. higginsi*, we do not think it resembles a diagnostic character for species, but rather for age.

Scalid rows consist of several scalid series in decreasing sizes in other macroscopic priapulid genera, whereas in *H. spinulosus* such series are not present (Van der Land, 1970; Schmidt-Rhaesa, 2013). The size of the posterior scalids is unclear in *H. higginsi*, as they can be either slightly larger (Merriman, 1981) or smaller (Shirley and Storch, 1999) than the anterior scalids, but distinct series are not present. We can confirm the absence of scalid series in both species and slightly smaller posterior scalids in a row in *H. higginsi*, agreeing with Shirley and Storch (1999).

Scalid tips of *H. spinulosus* have a subapical depression with numerous small smooth tubuli and tubuli with a dented apical margin as sensory structures that are arranged in one large median and smaller lateral groups (see Fig. 3.23D in Adrianov and Malakhov, 1996a). In *H. higginsi*, the scalid tips do not have one large subapical depression, but small depressions with a small number of distally open tubuli lateral on the scalid (Shirley and Storch, 1999). The scalid tips of all our *H. spinulosus* specimens match with the description of Adrianov and Malakhov (1996a).

Dentoscalids of *H. spinulosus* have a smooth surface without any sensory structures on them but they are still considered as sensory organs due to containing receptor cells (Storch et al., 1990). We confirm the absence of sensory organs on the dentoscalids in our *H. spinulosus* specimens. The *H. spinulosus* specimens from Alaska have a cuticular fold anterior of the crescent-formed spines, which could be an indication of the start of a moult. Adrianov and Malakhov (1996a) also show a similar fold on the dentoscalids of their young *H. spinulosus* specimens (cf. their Fig. 3.25A,B).

The trunk of postlarval and adult macroscopic priapulids is annulated (Van der Land, 1970). Up to 100 annuli are reported for large *H. spinulosus* (Van der Land, 1970), whereas large *H. higginsi* have up to 172 annuli (Shirley and Storch, 1999). Thus, we consider the number of annuli as diagnostic characters for large specimens. Whether small-sized *H. higginsi* differ in number of annuli compared to same sized *H. spinulosus* is unknown.

The annuli of *Halicryptus* are beset with numerous pointed structures, the trunk tubuli. In previous studies, these structures were termed as setae or spines (see Table 3). Although having a spine-like appearance, we suggest using the term "trunk tubuli" introduced by Storch et al. (1990) due to an apical opening. We also consider linking "trunk" to the term to clarify the location of these structures rather than the function (e.g. "secretory" in Shirley and Storch, 1999). The composition of the trunk tubuli with a conical tapering base and a thin pointed apical part was mentioned by Ehlers (1862), sketched by Scharff (1885) for *H. spinulosus* and later shown by Merriman (1981) in SEM images for presumably *H. higginsi*. Scharff (1885) also showed the internal cellular composition of the trunk tubuli which was confirmed in detail by Moritz (1972), who also showed secretory cells in the trunk tubuli indicating a secretory function of these structures. All of our investigated specimens have numerous, randomly distributed trunk tubuli on the trunk with the described composition and an apical opening.

The trunk was first stated to be devoid of papillae or warts besides the trunk tubuli (Van der Land, 1970). Merriman (1981) described three structures on the posterior trunk, posterior warts, ring papillae and anal papillae, for *Halicryptus*. The terms "posterior warts" and "ring papillae" are also used in other genera, therefore it is important to review their possible homology.

The first structures described by Merriman (1981) are the posterior warts, that are situated in depressions in the integument and have "columnar features" at the base (cf. their Fig. 12). These structures resemble our here described small conical trunk papillae with accessory flosculi. Since these structures do not have a similar appearance than the ultrastructurally rarely shown posterior warts of *P. caudatus* or *P. tuberculatospinosus* and appear scattered on the whole trunk, we recommend using "small trunk papillae" instead. Shirley and Storch (1999) mentioned irregularly arranged oval structures on the trunk surface of *H. higginsi*, which we could show here in detail. Since these oval structures and the small trunk papillae of *H. spinulosus* are similar, we assume that they are the same structure.

The second structure described by Merriman (1981), the ring papillae, are peg-like structures, which have a similar appearance than trunk tubuli with an absent tapering apical part. Merriman shows two images of these ring papillae with one of them showing peg-like, blunt structures, whereas the other one clearly shows trunk tubuli with a strongly bent apical part (cf. Figs. 10 and 11 in Merriman, 1981). Whether these peg-like structures show ring papillae or damaged trunk tubuli is unclear. In our *H. spinulosus* material, we did not observe such structures. Interestingly, in *H. higginsi* we observed on light micrographs similar blunt structures building lines or rings on the posterior trunk, which seem not to represent damaged trunk tubuli. Since Merriman (1981) presumably already investigated *H. higginsi* specimens, this species could hold peg-like ring papillae, whereas in *H. spinulosus* this character is absent. Further investigation of these peg-like ring papillae is recommended, including a comparison with the bulbous-formed ring papillae of *Acanthopriapulus*, *Priapulopsis* and *Priapulus*.

The third structure described by Merriman (1981), the anal papillae, are scattered among the small trunk papillae and are composed of several round structures located in depressions. We have not observed such structures in our specimens. The anal papillae could resemble a variant of the small trunk papillae that can occur in different compositions as we showed here.

Additionally, we observed a loose ring of small papillae composed of a tubular structure with one or two accessory flosculi on the last annulus in both species. Similar papillae surrounding the two anal tubuli (see below) have already been shown by Adrianov and Malakhov (1996a) and by Lemburg (1999), who termed them as flosculus-tubulus-complex, like the structures at the end of a scalid row, due to their composition. Unlike Lemburg (1999), we did not find the flosculus-tubulus-complexes on the middle and anterior parts of the trunk. In contrast, Lemburg did not mention the arrangement in a loose ring on the posterior trunk. We conclude that *H. spinulosus* have at least two more structures on the trunk than previously assumed, the flosculus-tubulus-complexes and the small trunk papillae (see above) that occur in different variants. In *H. higginsi*, the peg-like ring papillae can represent an additional third structure.

The trunk terminates posterior with two anal tubuli lateral of the anus (Scharff, 1885). These structures were described before as spikes or setae by other authors (see Table 3). We suggest using the term "anal tubuli" instead, due to the apical tubular structures and lateral openings on the surface, implying a sensory or secretory function. Compared to the trunk tubuli, the two anal tubuli are more distinct and larger in *H. spinulosus* (Scharff, 1885; Van der Land, 1970), whereas in *H. higginsi*

they are smaller (Merriman, 1981; Shirley and Storch, 1999), which we can also confirm here. The conical structures around the stem of an anal tubulus have been sketched (Van der Land, 1970) and briefly shown by SEM (Adrianov and Malakhov, 1996a; Lemburg, 1999) before. Lemburg (1999) described them as small accessory setae. Since these structures have a similar appearance as flosculus-tubulus-complexes on the last annulus (see above), we assume they are similar structures. Additionally, Lemburg (1999) described one large accessory seta lateral on an anal tubulus with one lateral flosculus in a postlarval stage. We found similar large conical papillae directly connected with an anal tubulus in one adult specimen, but in different types. As the number and shape of these accessory structures differ between developmental stages, we recommend further investigations.

The inversion and eversion movement of the introvert is involved in the forward movement and burrowing of priapulids (Hammond, 1970). This introvert movement is performed by a complex musculature armature including long and short retractor muscles. The reported numbers of these retractors is variable. Van der Land (1970) first described 7–10 long retractors for *H. spinulosus*, which was later revised to eight by Candia Carnevali and Ferraguti (1979). In both studies, the number of short introvert retractors is described between 10 and 12. For larvae of *H. spinulosus*, Lemburg (1999) described eight long and nine short introvert retractors and six pharynx protractors, which numbers we can confirm here also for adult specimens. Shirley and Storch (1999) described nine long retractors and five protractors around the pharynx bulb for *H. higginsi* but gave no information on short retractor muscles. We found eight instead of nine previously described long introvert retractors and six instead of five pharynx protractors in *H. higginsi*. Especially in histological sections of the anterior pharynx, we often find it difficult to assign specific muscles to their specific function. In addition, parts of tissue (e.g. cross sections of isolated muscle strands) can be lost during the sectioning and staining process. We recommend further investigations using µCT scans as recent approaches in priapulids showed feasible results (Schmidt-Rhaesa et al., 2022; Wernström et al., 2023).

4.3. Effect of body size on characters of Halicryptus

The evolution of body size in Priapulida, containing both microscopic and macroscopic groups, is still debated (Worsaae et al., 2023). *Halicryptus* offers an interesting case in this respect, due to the vast intrageneric size span from the maximum four centimetre long *H. spinulosus* to the ten times larger *H. higginsi*. As both species differ in maximum body length, it is questioned how development and growth of body size affect the distribution and relative measures of morphological structures, complicating correct identification.

A larger body size affects randomly distributed structures on *Halicryptus*, as the number of small buccal papillae and trunk tubuli increase during development. Size-wise, trunk tubuli and anal tubuli seem to grow during development of *H. spinulosus*, though do seemingly not show systematic allometric growth relative to body size. In contrast, large specimens of *H. higginsi* have a comparable much lower relation of trunk tubuli and anal tubuli size to the body length than large *H. spinulosus* specimens. The relation of body wall thickness to total body length also increases in the development of *H. spinulosus* and reaches similar relations as large *H. higginsi*. Some other attributes, like the number of primary scalids, scalid rows, large- and medium-sized buccal papillae and anal tubuli, are not affected by body size and keep a fixed number throughout development of *H. spinulosus*. Similar observations were made in various types of sensory organs of insects, as some types correlate in number, size and/or composition with body size, whereas other types are not affected (Makarova et al., 2022). A recent study on geometric morphometrics of pharyngeal teeth of Priapulida by Wernström et al. (2023) shows both *Halicryptus* species within a similar morphospace regardless of size, indicating a potential allometric growth relative to body size of their teeth. An extensive analysis of homologous sensory organs across microscopic and macroscopic priapulan species would be beneficial to further inform on allometric growth in Priapulida.

5. Conclusions

We can confirm that *Halicryptus* contains two species, *H. spinulosus* and *H. higginsi*. While *H. spinulosus* exhibits a wide distribution around the Arctic Ocean including its various margin seas, *H. higginsi* seems to have a local distribution within the Beaufort Sea near Point Barrow and co-exists there with *H. spinulosus*. Moreover, we validate that prior studies containing large specimens from Alaska by MacGinitie (1955) and Merriman (1981) were of *H. higginsi*, and not *H. spinulosus* as originally reported. Holmquist (1963) and Carter (1966) did not provide sufficient information for us to classify their specimens to species.

Additionally, we revise the occurrence and terminology of morphological characters of *Halicryptus* (Table 3) and we propose six reliable diagnostic characters between both *Halicryptus* species and four potential diagnostic characters that need further investigations to be validated (Table 5).

Lastly, we show that few morphological characters of *Halicryptus* are potentially affected in their numbers by growing body size and that sizes of structures in relation to the total body length tend to decrease with a larger body size.

CRediT authorship contribution statement

Jan Raeker: Writing – review & editing, Writing – original draft, Visualization, Validation, Methodology, Investigation, Formal analysis, Data curation, Conceptualization. **Katrine Worsaae:** Writing – review & editing, Validation, Supervision, Project administration, Funding acquisition, Conceptualization. **Andreas Schmidt-Rhaesa:** Writing – review & editing, Validation, Supervision, Project administration, Methodology, Funding acquisition, Conceptualization.

Declaration of competing interest

The authors declare that they have no known competing financial interests or personal relationships that could have appeared to influence the work reported in this paper.

Data availability

Data will be made available on request.

Acknowledgements

We thank Katrin Iken (College of Fisheries and Ocean Sciences, University of Alaska Fairbanks) for providing *Halicryptus spinulosus* specimens from Alaska. We also thank Anna J. Phillips (Smithsonian Institution, Natural Museum of Natural History, Washington, DC) for entrusting us a *Halicryptus higginsi* specimen (USNM No. 186062) for this study. We thank Arianna Lord and Gonzalo Giribet (Museum of Comparative Zoology, Harvard University) for providing molecular data of *H. higginsi*. Furthermore, we thank Elke Woelken (University of Hamburg) for essential help with the SEM, and Karolin Engelkes and Lena Schwinger (Leibniz Institute for the Analysis of Biodiversity Change, Hamburg) for guidance in the morphology lab. This study was funded by the Deutsche Forschungsgemeinschaft (DFG, Germany Research Foundation) with the grant number SCHM 1278/20-1 to Andreas Schmidt-Rhaesa.

Appendix A. Supplementary data

Supplementary data to this article can be found online at https://doi.org/10.1016/j.jcz.2024.08.003.

References

Adrianov, A.V., Malakhov, V.V., 1996a. Priapulida: Structure, Development, Phylogeny, and Classification. KMK Scientific Press, Moscow [In Russian with English summary].

Adrianov, A.V., Malakhov, V.V., 1996b. The phylogeny, classification and zoogeography of the class Priapulida. II. Revision of the family Priapulidae and zoogeography of priapulids. Zoosyst. Rossica 5, 1–6.

Apel, W., 1885. Beitrag zur Anatomie und Histologie des *Priapulus caudatus* (Lam.) und des *Halicryptus spinulosus* (v. Siebold). Z. Wiss. Zool. 42, 459–529.

Bolger, A.M., Lohse, M., Usadel, B., 2014. Trimmomatic: a flexible trimmer for Illumina sequence data. Bioinformatics. https://doi.org/10.1093/bioinformatics/btu170 btu170.

Candia Carnevali, M.D., Ferraguti, M., 1979. Structure and ultrastructure of the muscles in the priapulid *Halicryptus spinulosus*. Functional and phylogenetic remarks. J. Mar. Biol. Assoc. U. K. 59, 737–744. https://doi.org/10.1017/S0025315400045719.

Carter, J.C.H., 1966. A relict priapulid from northern Labrador. Nature 211, 438–439. https://doi.org/10.1038/211438a0.

Conway Morris, S., Robison, R.A., 1986. Middle Cambrian priapulids and other soft-bodied fossils from Utah and Spain. Univ. Kans. Paleontol. Contrib. 117, 1–22.

Dereeper, A., Guignon, V., Blanc, G., Audic, S., Buffet, S., Chevenet, F., Dufayard, J., Guindon, S., Lefort, V., Lescot, M., 2008. Phylogeny.fr: robust phylogenetic analysis for the non-specialist. Nucleic Acids Res. 36, W465–W469. https://doi.org/10.1093/nar/gkn180.

Dierckxsens, N., Mardulyn, P., Smits, G., 2017. NOVOPlasty: de novo assembly of organelle genomes from whole genome data. Nucleic Acids Res. 45, e18. https://doi.org/10.1093/nar/gkw955.

Edgar, R.C., 2004. MUSCLE: multiple sequence alignment with high accuracy and high throughput. Nucleic Acids Res. 32 (5), 1792–1797. https://doi.org/10.1093/nar/gkh340.

Ehlers, E., 1862. Ueber *Halicryptus spinulosus* (v. Sieb.). Z. Wiss. Zool. 11, 401–413.

Geller, J., Meyer, C., Parker, M., Hawk, H., 2013. Redesign of PCR primers for mitochondrial cytochrome c oxidase subunit I for marine invertebrates and application in all-taxa biotic surveys. Mol. Ecol. Res. 13 (5), 851–861. https://doi.org/10.1111/1755-0998.12138.

Goldsmit, J., Howland, K.L., Archambault, P., 2014. Establishing a baseline for early detection of non-indigenous species in ports of the Canadian Arctic. Aquat. Invasions 9, 327–342. https://doi.org/10.3391/ai.2014.9.3.08.

Hammarsten, O.D., 1913. Beiträge zur Entwicklung von *Halicryptus spinulosus* (von Siebold). Zool. Anz. 41, 501–505.

Hammarsten, O.D., 1915. Zur Entwicklungsgeschichte von *Halicryptus spinulosus* (von Siebold). Z. Wiss. Zool. 112, 527–571.

Hammond, R.A., 1970. The burrowing of *Priapulus caudatus*. J. Zool. Lond. 162, 469–480. https://doi.org/10.1111/j.1469-7998.1970.tb01281.x.

Hoang, D.T., Chernomor, O., von Haeseler, A., Minh, B.Q., Vinh, L.S., 2018. UFBoot2: improving the ultrafast bootstrap approximation. Mol. Biol. Evol. 35, 518–522. https://doi.org/10.1093/molbev/msx281.

Holmquist, C., 1963. Some notes on *Mysis relicta* and its relatives in northern Alaska. Arctic 16, 109–128.

Hu, S.X., Zhu, M.Y., Zhao, F.C., Steiner, M., 2017. A crown group priapulid from the early Cambrian Guanshan Lagerstätte. Geol. Mag. 154, 1329–1333. https://doi.org/10.1017/s0016756817000191x.

Huang, D., Vannier, J., Chen, J., 2004. Recent Priapulidae and their Early Cambrian ancestors: comparison and evolutionary significance. Geobios 37, 217–228. https://doi.org/10.1016/j.geobios.2003.04.004.

Janssen, R., Wennberg, S., Budd, G.E., 2009. The hatching larva of the priapulid worm *Halicryptus spinulosus*. Front. Zool. 6, 8. https://doi.org/10.1186/1742-9994-6-8.

Kalyaanamoorthy, S., Minh, B.Q., Wong, T.K.F., Von Haeseler, A., Jermiin, L.S., 2017. ModelFinder: fast model selection for accurate phylogenetic estimates. Nat. Methods 14, 587–589. https://doi.org/10.1038/nmeth.4285.

Kolbasova, G., Schmidt-Rhaesa, A., Syomin, V., Bredikhin, D., Morozov, T., Neretina, T., 2023. Cryptic species complex or an incomplete speciation? Phylogeographic analysis reveals an intricate Pleistocene history of *Priapulus caudatus* Lamarck, 1816. Zool. Anz. 302, 113–130. https://doi.org/10.1016/j.jcz.2022.11.013.

Kumar, S., Stecher, G., Li, M., Knyaz, C., Tamura, K., 2018. Mega X: molecular evolutionary genetics analysis across computing platforms. Mol. Biol. Evol. 35 (6), 1547–1549. https://doi.org/10.1093/molbev/msy096.

Lemburg, C., 1995. Ultrastructure of sense organs and receptor cells of the neck and lorica of the *Halicryptus spinulosus* larva (Priapulida). Microfauna Mar. 10, 7–30. https://doi.org/10.1007/BF00397931.

Lemburg, C., 1999. Ultrastrukturelle Untersuchungen an den Larven von *Halicryptus spinulosus* und *Priapulus caudatus*. Hypothesen zur Phylogenie der Priapulida und deren Bedeutung für die Evolution der Nemathelminthes. Cuvillier, Göttingen.

Makarova, A.A., Diakova, A.A., Chaika, S.Y., Polilov, A.A., 2022. Scaling of the sense organs of insects. 2. Sensilla. Discussion. Conclusion. Entomol. Rev. 102, 323–346. https://doi.org/10.1134/S0013873822030058.

MacGinitie, G.E., 1955. Distribution and ecology of the marine invertebrates of Point Barrow, Alaska. Smithsonian Misc. Collect. 128, 1–201.

Merriman, J.A., 1981. Cuticular structures of the priapulid *Halicryptus spinulosus*: a scanning electron microscopical study. Zoomorphology 97, 285–295. https://doi.org/10.1007/BF00310281.

Minh, B.Q., Schmidt, H.A., Chernomor, O., Schrempf, D., Woodhams, M.D., von Haeseler, A., Lanfear, R., 2020. IQ-TREE 2: new models and efficient methods for phylogenetic inference in the genomic era. Mol. Biol. Evol. 37, 1530–1534. https://doi.org/10.1093/molbev/msaa015.

Moritz, K., 1972. Zur Feinstruktur integumentaler Bildungen bei Priapuliden (*Halicryptus spinulosus* und *Priapulus caudatus*). Z. Morph. Tiere 72, 203–230. https://doi.org/10.1007/BF00391552.

Puillandre, N., Lambert, A., Brouillet, S., Achaz, G., 2012. ABGD, automatic barcode gap discovery for primary species delimitation. Mol. Ecol. 21 (8), 1864–1877. https://doi.org/10.1111/j.1365-294X.2011.05239.x.

Scharff, R., 1885. On the skin and nervous system of *Priapulus* and *Halicryptus*. Q. J. Microsc. Sci. 25, 193–213. https://doi.org/10.1242/jcs.s2-25.98.193.

Schmidt-Rhaesa, A., 2013. Priapulida. In: Schmidt-Rhaesa, A. (Ed.), Handbook of Zoology: Nematomorpha, Priapulida, Kinorhyncha and Loricifera, vol. 1. Walter de Gruyter, Berlin, pp. 147–180.

Schmidt-Rhaesa, A., Cañete, J.I., Mutschke, E., 2022. New record and first description including SEM and μCT of the rare priapulid *Acanthopriapulus horridus* (Priapulida, Scalidophora). Zool. Anz. 298, 1–9. https://doi.org/10.1016/j.jcz.2022.03.001.

Schmidt-Rhaesa, A., Raeker, J., 2022. Morphology of larval and postlarval stages of *Priapulopsis bicaudatus* (Danielssen, 1869) (Priapulida) from the north Atlantic ocean. Zool. Anz. 302, 1–16. https://doi.org/10.1016/j.jcz.2022.11.006.

Schmidt-Rhaesa, A., Raeker, J., Review of the Priapulida of New Zealand with the description of a new species. N. Z. J. Zool.

Schreiber, A., Eisinger, M., Rumohr, H., Storch, V., 1996. Icy heritage: ecological evolution of the postglacial Baltic Sea reflected in the allozymes of a living fossil, the priapulid *Halicryptus spinulosus*. Mar. Biol. 125, 671–685. https://doi.org/10.1007/BF00349249.

Shirley, T.C., Storch, V., 1999. *Halicryptus higginsi* n.sp. (Priapulida) - a giant new species from Barrow, Alaska. Invertebr. Biol. 118, 404–413. https://doi.org/10.2307/3227009.

Storch, V., Higgins, R.P., Rumohr, H., 1990. Ultrastructure of introvert and pharynx of *Halicryptus spinulosus* (Priapulida). J. Morphol. 203, 163–171. https://doi.org/10.1002/jmor.1052060203.

Storch, V., Higgins, R.P., 1991. Scanning and transmission electron microscopic observations on the larva of *Halicryptus spinulosus* (Priapulida). J. Morphol. 210, 175–194. https://doi.org/10.1002/jmor.1052100207.

Storch, V., Higgins, R.P., Malakhov, V.V., Adrianov, A.V., 1994. Microscopic anatomy and ultrastructure of the introvert of *Priapulus caudatus* and *P. tuberculatospinosus* (Priapulida). J. Morphol. 220, 281–293. https://doi.org/10.1002/jmor.1052200307.

Storch, V., Higgins, R.P., Anderson, P., Svavarsson, J., 1995. Scanning and transmission electron microscopic analyses of the introvert of *Priapulopsis australis* and *Priapulopsis bicaudatus* (Priapulida). Invertebr. Biol. 114, 64–72. https://doi.org/10.2307/3226954.

Van der Land, J., 1970. Systematics, geography, and ecology of the Priapulida. Zool. Verhand. Leiden. 112, 1–118.

Von Siebold, C.T., 1849. Beiträge zur Fauna Preussens. Neue Preuss. Provincialbl. 7, 184–185.

Webster, B.L., Copley, R.R., Jenner, R.A., Mackenzie-Dodds, J.A., Bourlat, S.J., Rota-Stabelli, O., Littlewood, D.T.J., Telford, M.J., 2006. Mitogenomics and phylogenomics reveal priapulid worms as extant models for the ancestral Ecdysozoan. Evol. Dev. 8, 502–510. https://doi.org/10.1111/j.1525-142X.2006.00123.x.

Wernström, J.V., Slater, B.J., Sørensen, M.V., Crampton, D., Altenburger, A., 2023. Geometric morphometrics of macro-and meiofaunal priapulid pharyngeal teeth provides a proxy for studying Cambrian "tooth taxa". Zoomorphology 142 (4), 411–421. https://doi.org/10.1007/s00435-023-00617-4.

Worsaae, K., Vinther, J., Sørensen, M.V., 2023. Evolution of Bilateria from a Meiofauna perspective - Miniaturization in the focus. In: Giere, O., Schratzberger, M. (Eds.), New Horizons in Meiobenthos Research. Springer, Cham, pp. 1–31. https://doi.org/10.1007/978-3-031-21622-0_1.

Zhang, J., Kapli, P., Pavlidis, P., Stamatakis, A., 2013. A general species delimitation method with applications to phylogenetic placements. Bioinformatics 29 (22), 2869–2876. https://doi.org/10.1093/bioinformatics/btt499.

NEW ZEALAND JOURNAL OF ZOOLOGY
https://doi.org/10.1080/03014223.2023.2278738

Taylor & Francis
Taylor & Francis Group

RESEARCH ARTICLE

Review of the Priapulida of New Zealand with the description of a new species

Andreas Schmidt-Rhaesa and Jan Raeker

Museum of Nature Hamburg - Zoology, Leibniz Institute for the Analysis of Biodiversity Change (LIB) and University Hamburg, Hamburg, Germany

ABSTRACT

The number of priapulid species occurring in the waters around New Zealand is uncertain, as up to four species were reported and three of them declared as doubtful. Our investigation of 28 specimens from the NIWA collection (Auckland, New Zealand) document three species. Three specimens of *Priapulus tuberculatospinosus* come from circum-antarctic waters. Around New Zealand, *Priapulopsis australis* is most abundant, less abundant is *Priapulus tuberculatospinosus*. Two specimens are described here as a new species, *Priapulopsis papillatus sp. nov.*, as they deviate in several characters from the other species. These characters are the shape of the first ring teeth, presence of large, abundant and regularly arranged trunk papillae, a peculiar surface structure of the trunk and peculiarities in the posterior ringpapillae. All species are described by scanning electron microscopy and several new observations are reported. In addition to postlarval and adult specimens, 15 larval specimens are reported. The larvae resemble very much the previously described larvae of *Priapulopsis bicaudatus* and therefore likely belong to the genus *Priapulopsis*.

ARTICLE HISTORY
Received 30 August 2023
Accepted 27 October 2023
First Published Online 12 September 2024

HANDLING EDITOR
Rob Cruickshank

KEYWORDS
Priapulida; Ecdysozoa; new species; New Zealand; SEM; larva; lorica; introvert; caudal appendage

Introduction

Although having only 21 extant species, priapulids are nevertheless diverse in body size (from a few millimeters to about 40 cm), lifestyles and modes of reproduction (Schmidt-Rhaesa 2013). The eight macroscopic species occur in cool or temperate waters, while the 13 smaller, meiobenthic species occur predominantly in tropical and subtropical regions. While the genus *Halicryptus* occurs only in the Northern Hemisphere and the genus *Acanthopriapulus* only in the Southern Hemisphere, the genera *Priapulus* and *Priapulopsis* both have species on each hemisphere (Van der Land 1970).

Different opinions exist on how many species exist in New Zealand. In total, four species were mentioned in the literature, but, depending on the source, some of these were regarded as invalid records. However, the number of references dealing with New Zealand priapulids is low (Benham 1932; Dell 1955; Hurley 1962; Estcourt 1967; Storch et al. 1995; Adrianov and Malakhov 1996; Van der Land 2010).

CONTACT Andreas Schmidt-Rhaesa a.schmidt-rhaesa@leibniz-lib.de

So far the most certain New Zealand priapulid species is *Priapulopsis australis* (De Guerne 1886), a species described by De Guerne (1886) from South America (for more records and locations see Murina and Starobogatov 1961; Van der Land 1970). From New Zealand this species was reported by Hurley (1962) from Hawke Bay at 53–58.5 m depth, by Estcourt (1967) from Marlborough Sounds, by Storch et al. (1995) from Pauatahanui Inlet near Wellington at 3 m depth and by Adrianov and Malakhov (2001a, 2001b) from Bay of Plenty (North Island) at unknown depths. Van der Land (2010) investigated specimens from the NIWA (National Institute of Water and Atmospheric Research) collection (Auckland, New Zealand), concluding that all specimens were *P. australis*, being collected at a depth range of 2–1,190 m. He also mentioned a new record of one specimen from 38°S, 178° W at 1,195 m depth.

Priapulus tuberculatospinosus (Baird, 1868) was reported by Benham (1932) from Islington Bay at 15 m depth and by Dell (1955) from Hicks Bay at 110 m depth and off Cape Campbell at 73 m depth, but Van der Land (2010) assumed that these two records were in fact *Priapulopsis australis*. According to him, *P. tuberculatospinosus* was absent from New Zealand. Two further species records are regarded as valid by Van der Land (2010), but are critically reviewed by Schmidt-Rhaesa (in press). Murina and Starobogatov (1961) reported one specimen from Hikurangi Trench, east of Cape Palliser (41°29´7 S/177°38´5 E), from 3013 m depth, to be *Priapulus abyssorum* (Menzies 1959) (as *P. tuberculatospinosus abyssorum*). Probably, this represented a postlarval specimen lacking characters to assign it to a certain species (Van der Land 2010). *Acanthopriapulus horridus* (Théel 1911) was reported from New Zealand by Adrianov and Malakhov (1996). The images given in this publication were not convincing and do not correspond with the description of the species (Théel 1911; see also Schmidt-Rhaesa et al. 2022). Due to these doubts, the New Zealand records of *Priapulus abyssorum* and *Acanthopriapulus horridus* are regarded as questionable.

There are almost no data on developmental stages from New Zealand priapulids. Priapulids have four morphologically differing developmental stages. An early hatching larva has been shown in *Priapulus caudatus* and *Halicryptus spinulosus* (see Janssen et al. 2009; Wennberg et al. 2009), but it is unknown whether the other priapulid species also possess such a larva. The hatching larva develops into a loricate larva, in which the trunk cuticle forms stiff protective plates called a lorica. This larva grows through molting. After losing the lorica, specimens grow through several postlarval stages to the adult. The conclusion that certain larvae, postlarval stages and/or adults belong to the same species is mostly made just by their geographic co-occurrence.

From New Zealand, larvae were reported only once by Adrianov and Malakhov (1996) as larvae of *P. australis*. They had a characteristic sculpture on the lorica in the form of a median zig-zag-band. They looked different from larvae of *P. tuberculatospinosus* (see Lang 1951) and therefore an assignment to *P. australis* appeared plausible.

Van der Land (1970) listed a number of characters, in which the two genera *Priapulus* and *Priapulopsis* differed. One was the number of the caudal appendages, which was one in *Priapulus* and two in *Priapulopsis*. Recently, Schmidt-Rhaesa and Raeker (2023) showed that the paired caudal appendage of *Priapulopsis bicaudatus* grew asymmetrically, with one branch developing later than the other. Another difference was that *Priapulopsis* species had 10 pharyngeal teeth or tooth rudiments in the first ring, while *Priapulus* species had the 'usual' five teeth. Schmidt-Rhaesa and Raeker (2023) showed

that in *P. bicaudatus* a separation of one tooth into two teeth occurred gradually during development. A bipartition of each first-ring tooth was indicated in any observed stage from the larva on, but a complete separation occurred only in late postlarval stages. Further differences between the two genera were that the trunk cuticle was covered with structures called tumuli in *Priapulopsis*, while the surface was smooth in *Priapulus*. In the caudal end of the trunk, there were so-called ring papillae and posterior warts in *Priapulus*; in *Priapulopsis* posterior warts were absent.

We investigated material from the NIWA collection and were able to confirm the occurrence of *Priapulus tuberculatospinosus* and *Priapulopsis australis* in New Zealand and to extend their description in several aspects. Furthermore, two specimens deviated from these two species in some respects and we regard the differences to be fundamental enough to assume that they represent an undescribed species.

In each of the two genera, *Priapulus* and *Priapulopsis*, three species have been described so far. In both genera, there is one species with a broad distribution on the northern hemisphere (*Priapulus caudatus* (Lamarck, 1816) and *Priapulopsis bicaudatus* (Danielssen, 1868)) and one with a broad distribution on the southern hemisphere (*Priapulus tuberculatospinosus* and *Priapulopsis australis*). Additionally, there is one deep sea species in the genus *Priapulus*, *P. abyssorum* and one species in the genus *Priapulopsis*, *P. cnidephorus* (Von Salvini-Plawen, 1973). Because the description of the last species is based on a single juvenile specimen, it is generally regarded as invalid. Therefore, the comparison of the southern species described here is made primarily with their northern counterparts.

Material and methods

From the 128 specimens of the NIWA collection labelled as Priapulida, 80 specimens were investigated. From these, 28 (35%) turned out to be priapulids, 27 were sipunculids and 25 other non-priapulid worms. For catalogue numbers, sampling location and sampling gear see Table 1. Priapulids investigated here come from waters around New Zealand with the exception of three specimens (21401, 21402 and 21406), which come from circumantarctic waters, but are included here because they are NIWA material and supplement the description of *Priapulus tuberculatospinosus*. In addition to the NIWA specimens, three additional specimens, which were collected by Richard Taylor, were included in the investigation. These specimens are housed in the Museum of Nature Hamburg, Leibniz Institute for the Analysis of Biodiversity Change (LIB) under the catalogue numbers ZMH V13672-13674. For collection data see Table 1. In the following, NIWA collection specimens are given with their catalogue number, while the LIB catalogue number includes the acronym 'ZMH'.

All specimens were investigated and photographed with a Keyence VHX-7000 digital microscope using the stacking function for composed images of different focal layers. Several specimens were prepared for scanning electron microscopy (SEM; see Table 1). Specimens were dehydrated in an increasing ethanol series, critically point dried (with a Leica EM CPD300) and sputtered with platinum. Investigation took place with a LEO SEM 1524. Larvae and small specimens were investigated as complete animals, larger specimens were dissected and investigated in parts. In some specimens, the pharynx was cut longitudinally to reveal the pharyngeal teeth. Measurements were taken directly from

Table 1. Summary of catalogue numbers, identification, number of specimens per vial, whether specimens were used for SEM, location, depth and collecting gear. Sample numbers refer to specimens from the NIWA collection, ZMH numbers refer to specimens from the LIB collection.

Catalogue no.	Species	SEM	Location	Date day/month/year	Depth	Gear
21401	*Priapulus tuberculatospinosus*	–	−66.91283, 163.22749	04/03/2004	70–78 m	epibenthic sledge
21402	*Priapulus tuberculatospinosus*	+	−66.36467, 162.57617	05/03/2004	942 m	Van Veen grab
21406	*Priapulus tuberculatospinosus*	+	−65.49050, 161.05083	07/03/2004	759 m	Van Veen grab
63408	*Priapulopsis papillatus* nov. spec.	+	−41.55433, 175.82683, Hikurangi Margin	19/04/2010	917–945 m	beam trawl
63448	*Priapulopsis papillatus* nov. spec.	+	−41.5195, 175.80683, Hikurangi Margin	05/03/2004	723–746 m	beam trawl
72034	*Priapulopsis australis*	+	−41.44717, 175.022, Wairarapa Canyon	16/02/2011	168–260 m	rock dredge
124155	*Priapulopsis australis*	–	−42.47958, 173.57842	15/09/2017	847 m	Van Veen grab
125356	*Priapulopsis australis*; 2 specimens	+/–	−37.48117, 176.90517	15/11/2004	422–520 m	epibenthic sledge
149775	*Priapulopsis australis*	–	−41.04170, 174.22170	12/12/1983	32 m	not provided
149776	*Priapulopsis australis*	+	−41.10170, 174.17999	11/12/1983	34 m	not provided
157060	*Priapulopsis australis*	+	−41.26417, 174.83367, Harbour Basin, Wellington Harbour	14/09/1999	20 m	Van Veen grab
157948	?	–	−41.2731, 174.7949, ~0.5 km ENE of Aotea Quay east, Wellington Harbour	21/11/2020	20 m	corer, diver macrobenthic
157949	?	–	−41.2604, 174.8142, ~1.5 km SSE of Ngauranga Stream mouth, Wellington Harbour	25/11/2020	20 m	corer, diver macrobenthic
157950	*Priapulopsis australis*; 2 specimens	+/+	−41.2652, 174.7923, ~0.5 km ENE of Aotea Quay west, Wellington Harbour	26/11/2020	16 m	corer, diver macrobenthic
162905	?	–	−41.0583, 174.28329	07/12/1983	0 m	not provided
162907	*Priapulopsis australis*	–	−41.215, 174.0483	10/12/1983	2 m	diver with SCUBA
162918	*Priapulopsis australis*; 2 specimens	–	−41.1067, 173.92171	15/12/1983	19 m	not provided
162922	*Priapulopsis australis*	–	−41.0417, 173.9817	15/12/1983	23 m	not provided
162925	4 larvae	+	−42.635, 173.6608	11/12/1982	120 m	not provided
162926	1 larva	+	−40.9967, 171.8067	07/02/1983	127 m	box corer
162930	? (fragments)	–	−41.09999, 174.8833	04/02/1975	0 m	not provided
162936	*Priapulopsis australis*	+	−42.3833, 173.80	12/12/1982	50 m	not provided
162937	*Priapulopsis australis*; 3 specimens + 1 spec.?	+/−/−/−	−42.3833, 173.80	12/12/1982	50 m	not provided
162940	*Priapulus tuberculatospinosus*; 2 specimens	+/–	−50.7883, 166.05499	08/05/1963	59 m	trawl, Agassiz
162978	3 larvae	+	−42.63499, 173.6608	11/12/1982	120 m	not provided
162981	3 larvae	+	−42.6517, 173.6817	14/12/1982	380 m	not provided
162982	*Priapulopsis australis*	–	−42.455, 173.8017	20/12/1982	300 m	not provided
162989	4 larvae	+	−42.380, 173.888	13/12/1982	77 m	not provided
ZMH V13672	*Priapulopsis australis*	+	5 km north of Cape Rodney (Leigh, northeast New Zealand), muddy sand	24/11/2020	52 m	not provided
ZMH V13673	*Priapulopsis australis*	–	5 km north of Cape Rodney (Leigh, northeast New Zealand), muddy sand	24/11/2020	52 m	not provided
ZMH V13674	*Priapulus tuberculatospinosus*	+	5 km north of Cape Rodney (Leigh, northeast New Zealand), muddy sand	24/11/2020	52 m	not provided

specimens or from digital images. It has to be noted that priapulids contract strongly during fixation. Own observations showed a contraction to about 40% of length in life. Therefore, measurements only refer to the conserved state of the specimens. Measurements of larvae differed with both methods, with measurements from SEM images being consistently smaller than measurements from light microscopical images. This is likely due to some folding and compression during the dehydration process (see also Schmidt-Rhaesa and Raeker 2023 for a similar observation).

Not each specimen yielded the full set of characters due to different reasons. Most importantly, due to the state of introvert eversion, pharyngeal teeth and anterior scalids could not be observed in several specimens. Some specimens were injured or lacked certain body parts. SEM was made selectively on a subset of specimens (see Table 1).

Most specimens were originally fixed in formalin and later transferred to ethanol. Therefore, no genetic analyses were made.

Results

The 28 catalogue numbers from the NIWA collection included a total of 15 larval and 30 postlarval/adult specimens. They included the two species *Priapulopsis australis* and *Priapulus tuberculatospinosus* and two specimens are described here as a new species. The specimens investigated were collected at a depth range of 0–945 m.

We regard it as helpful to start with a brief overview of priapulid external morphology to introduce the terms used in the text. The pharyngeal teeth are arranged in rings of five teeth (pentagons), at least in the anterior rings (e.g. Figures 2D and 8A). In the posterior region of the pharynx, a larger number of smaller teeth are present and symmetrical patterns are not present or not easy to recognise (e.g. Figure 3A). In the first pentagon each tooth can be divided into two small teeth, giving a total of 10 small teeth in the first ring (e.g. Figure 2A). Teeth in the anterior rings are cuspidate, with one central cusp and several lateral cusps (e.g. Figure 2A). The size of the teeth differs between rings and exceptionally also within a ring. Exact measurements of teeth are extremely difficult, because they are slightly curved and different angles of observation alter measurements. The width of the tooth base can be measured more reliably, but the size of a tooth depends on the length of the central cusp and the width is not necessarily proportional to the cusp length. Despite these restrictions, size differences are usually quite obvious from images. Teeth may have tooth receptors, these are oval openings with a tube-like structure in the centre (e.g. Figure 2F). The largest teeth may have tiny cuticular spines on the outer side (e.g. Figure 2E).

The introvert is covered by scalids (e.g. Figure 7E and F). Scalids are conical or elongate. Sometimes they are composed of a basal and an apical part that appear to be telescopically movable (e.g. Figure 12B). Scalids are arranged in 25 longitudinal rows. Scalids within these rows differ in size and form subsets of decreasing size called series (e.g. Figure 7E). Series can follow each other directly (e.g. Figure 8H) or are separated by a gap (e.g. Figure 4B). Usually, scalids are arranged in a certain pattern. The anteriormost ring of scalids is composed of eight primary scalids. The 25 rows of scalids are arranged in a pattern, where two rows are present behind each primary scalid (to both sides of a virtual line extending from the primary scalid) and one row is present

between the primary scalids (e.g. Figure 15I). On the ventral side, one additional row is present. Usually, the pattern of scalid arrangement is best observed in larvae and younger specimens and is often difficult to observe in larger specimens when the introvert is partly inverted. We found some differences also in the fine structure of the surface of the introvert. Sometimes there are further structures between the scalids and the first pharyngeal teeth, their homology and terminology is unclear, but often they are called buccal papillae.

The trunk is structured into rings called annuli (e.g. Figure 1A). The surface is either smooth or covered by tumuli, which are tiny roundish elevations (e.g. Figure 5A). In a number of specimens trunk papillae are present on the annuli (e.g. Figure 5A). These are hemispherical structures, apically covered by receptors. The term 'receptor' is applied here to structures composed of a basis and an apical tube (e.g. Figure 5C). The number of trunk papillae differs strongly, from being absent, via few, to abundant. In the posterior end, ring papillae and/or posterior warts can be present. Ring papillae are arranged in 1–5 rings, which are elongate in structure (e.g. Figure 5E and H). Posterior warts are hemispherical structures and cover the caudal region around the attachment of the caudal appendage densely (e.g. Figure 7I).

The caudal appendage is composed of a central stem and laterally branching vesicles (e.g. Figure 1A). One or two appendages are present: when two are present, they may be so close together that they are difficult to recognise as two. The vesicles have a differing surface structure and carry receptors which are called spinulets (e.g. Figure 6A). The vesicles are thin-walled and often shrink during dehydration, making observation of the fine structure challenging.

Five specimens could not be identified with certainty: 157948, 157949, 162905, 162930 and specimen 4 of 162937. Specimens 157948 and 157949 are small (trunk length 2.7 and 2.4 mm, respectively) specimens with an unclear number of caudal appendages and no pharyngeal teeth visible. Specimen 162905 is larger, with a 24 mm trunk length, but the posterior end is missing and the introvert is not everted far enough to observe the pharyngeal teeth. Number 162930 contains several fragments from an unknown number of specimens, and specimen 4 of 162937 is only the posterior trunk with the caudal appendage. Posterior warts or ring papillae were not observed and there appears to be a single caudal appendage. The three other specimens in lot 162937 were identified as *P. australis* (see below).

Priapulopsis australis

(Figures 1–6, Table 2)

Catalogue numbers: 72034, 124155, 125356 (two specimens), 149775, 149776, 157060, 157950 (two specimens), 162907, 162918 (two specimens), 162922, 162936, 162937 (three specimens), 162982, ZMH V 13672, ZMH V13673.

Specimens were collected in a wide range of water depth, from 2–847 m (see Table 1).

Specimens ranged in length between 4.2–42 mm trunk length (Table 2). The smaller specimens likely represent postlarval (juvenile) stages, but no criterion from the external morphology can be named to recognise when specimens are adult. The introvert is everted to a varying extent (Figure 1A, C, E and G), making the observation of pharyngeal teeth possible in only some specimens.

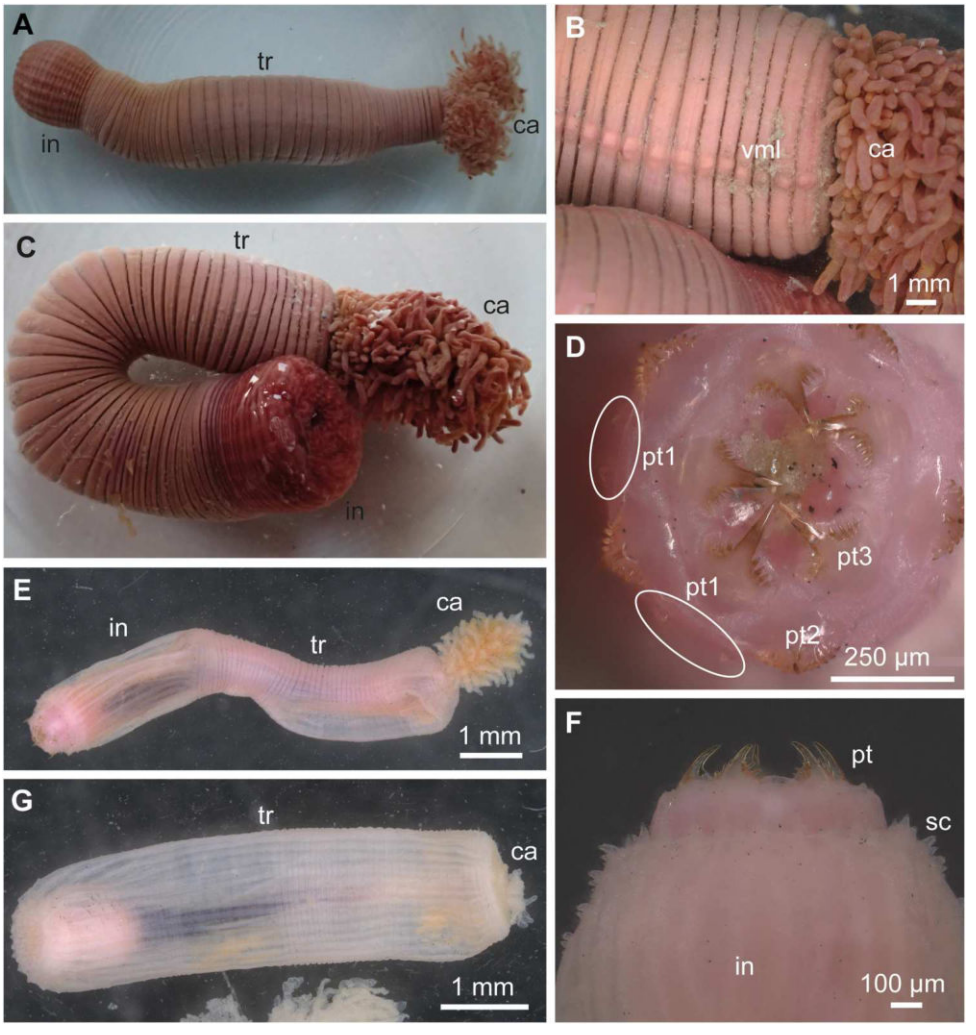

Figure 1. *Priapulopsis australis*, light microscopical images. **A,** Specimen 149775 with division into introvert (in), trunk (tr) and two caudal appendages (ca). **B,** Elevated ventral midline (vml) and attachment of the caudal appendage in specimen 72034. **C,** Specimen 72034 with largely withdrawn introvert. **D,** View on the three rings of pharyngeal teeth (pt) in specimen 157950-2, the small teeth of the first ring (pt1) are encircled. **E,** Specimen 157950-1. **F,** Lateral view on the pharyngeal teeth and scalids (sc) in specimen 157950-2. **G,** Strongly contracted specimen 157060 with very short caudal appendage.

Introvert: Up to three pentagons could be observed in strongly everted introverts (Figures 1D and F and 2A and D). The 10 teeth of the first ring are small and do not have a central cusp (Figures 1D and 2A, B and D). Instead, they are semicircular structures and the upper margin is covered with numerous (more than 12) small cusps and, between them, tooth receptors (Figure 2B). In the observed first-ring teeth the lateral cusps have a pointed tip, while the central ones were often not pointed (Figure 2B). The second-ring teeth have a large central cusp and 4–5 lateral cusps (Figure 2A, C and D). On the inner side, there is a cushion-like structure that is closely attached

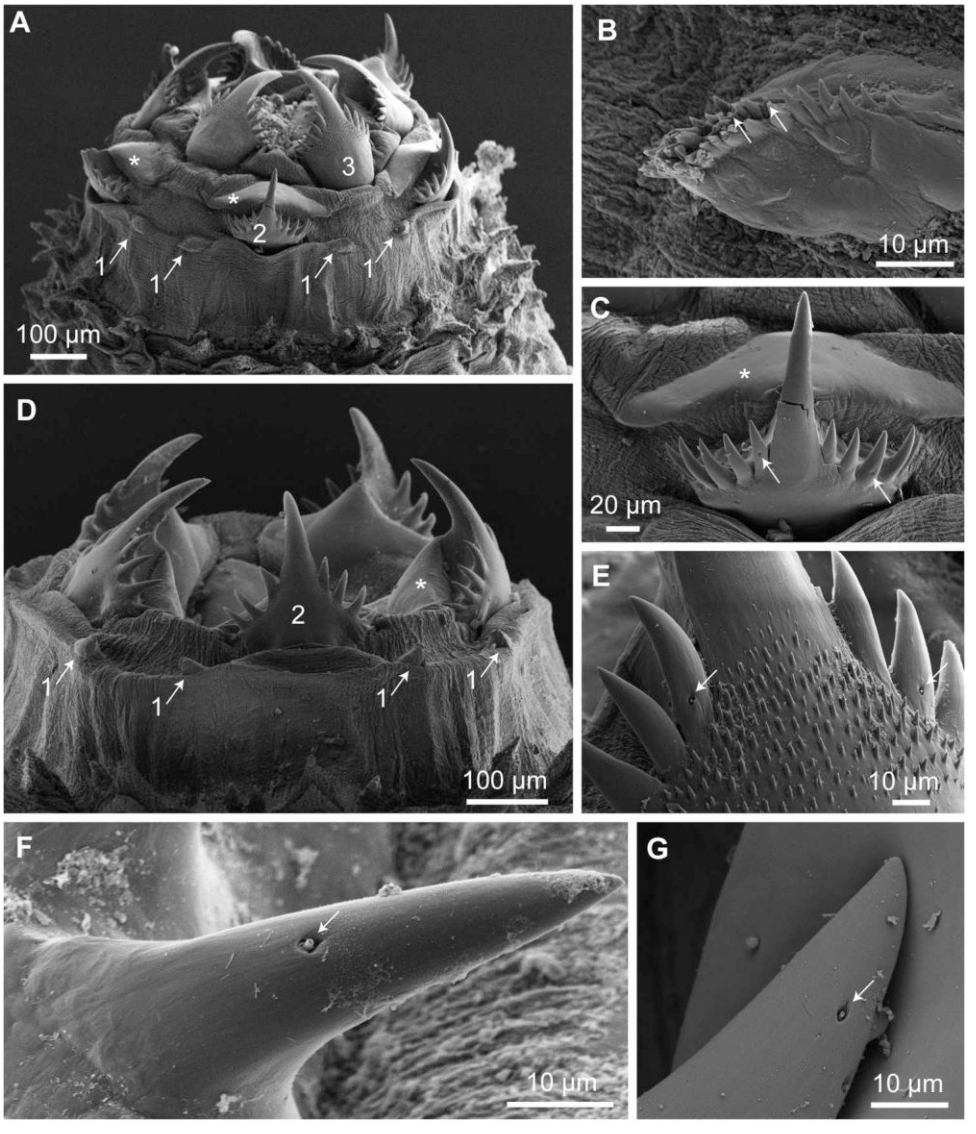

Figure 2. *Priapulopsis australis*, SEM of pharyngeal teeth. **A,** Lateral view on pharyngeal teeth of rings 1–3. The asterisk marks the cushion-like structure close to the second ring teeth. **B,** First-ring tooth, arrows point at tooth receptors. **C,** Second-ring tooth, arrows point at receptors, the asterisk marks the cushion-like structure. **D,** Teeth in specimen 157950-1, labelling as in A. **E,** The outside of third-ring teeth is covered with small cuticular spinose projections, arrows point at receptors. **F, G,** Magnification of receptors (arrows) on different cusps. A, B, C, E from 157950-2, D, F from 157950-1, G, from 125356.

to the teeth in one specimen (157950-1; Figure 2D), while it is detached from the teeth in another specimen (157950-2; Figure 2C). The third-ring teeth are the largest, they have a central and five lateral cusps (Figure 2A) and the outer side is covered with short cuticular spinose projections (Figure 2E). Tooth receptors are scattered on the teeth (Figure 2C and E–G).

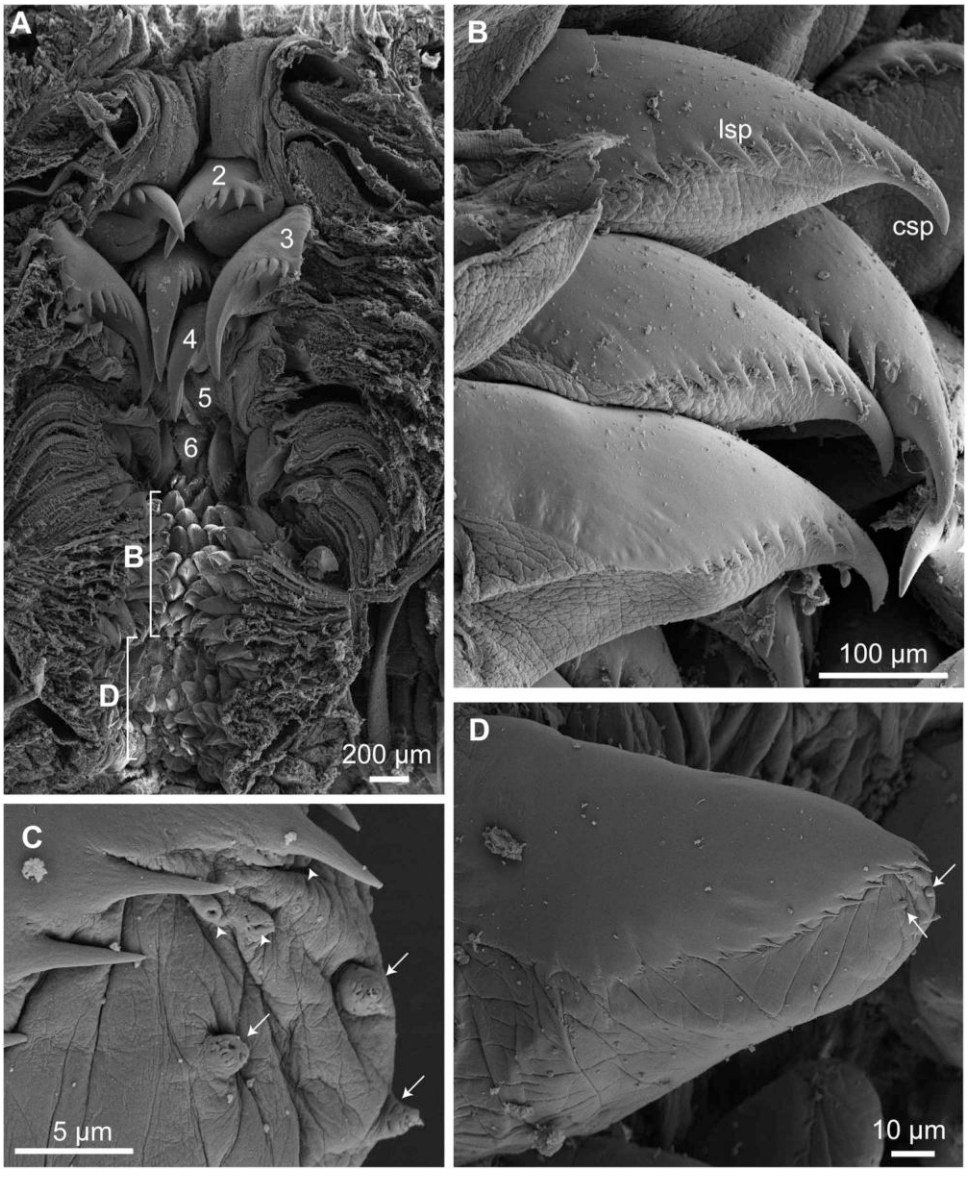

Figure 3. *Priapulopsis australis*, SEM of pharyngeal teeth. **A,** Longitudinal cut through pharynx of specimen 125356, showing teeth of rings 2–6, followed by smaller teeth (labelled B) and papilliform teeth (labelled D). The letters refer to the figure where these structures are magnified. **B,** Small teeth from the region labelled 'B' in A, showing a small central cusp (csp) and several lateral cusps (lsp). **C,** Openings on the tip of posterior, papilliform teeth in the form of tubes (arrowheads) or small papillae (arrows). **D,** Papilliform tooth from the region labelled 'D' in A. Papillae are marked by arrowheads. All images from specimen 125356.

The teeth further posterior could be observed in longitudinal sections through the pharynx of specimen 125356 and 162936 (Figure 3A). The first ring of 10 small teeth could not be observed and are likely hidden in folds. Pharyngeal teeth of rings 2–4 are very large, with teeth in ring 3 being the largest (Figure 3A). The large teeth have a

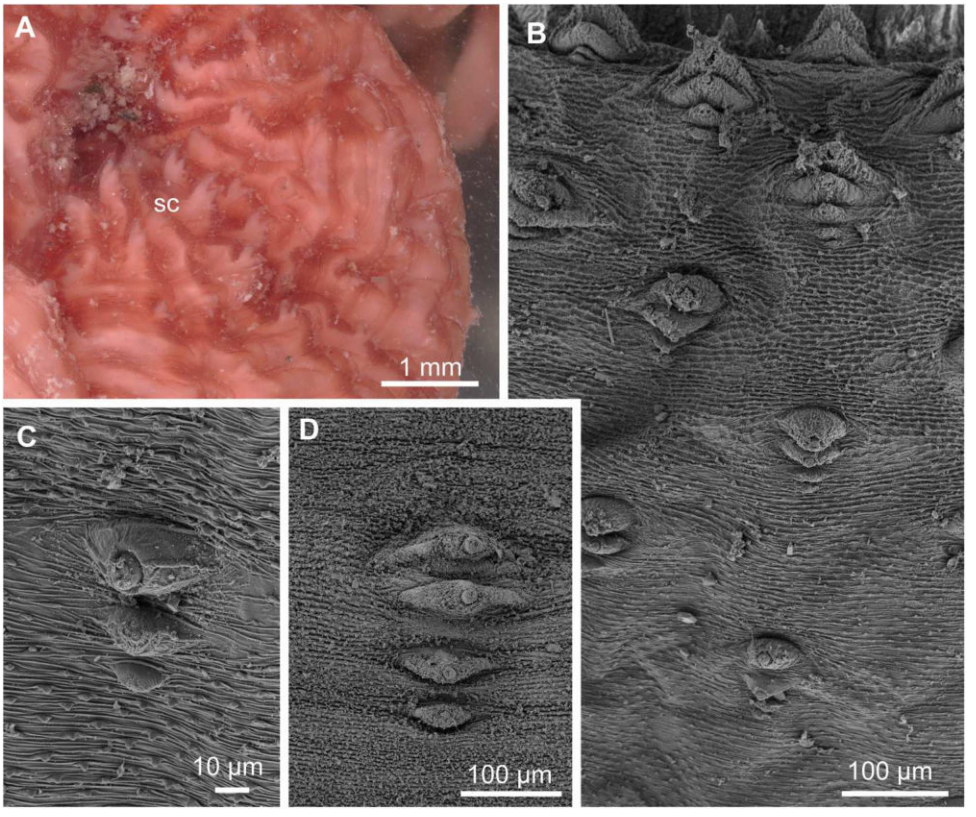

Figure 4. *Priapulopsis australis*, scalids. **A,** Light microscopical image of specimen 72034, in which scalid series (sc) appear to be fused basally. **B,** Introvert of specimen 157950-1, showing the wide spacing of scalid series. **C, D,** Scalid series in two specimens (157950-1 in C, ZMH V13672 in D), showing scalid structure and the cuticle between scalids. B–D by SEM.

strong central cusp and five lateral cusps. Teeth of rings 5 and 6 are distinctly smaller than the previous ones. They are followed by a region of even smaller teeth of the same structure. Teeth are compact and the central cusp is less dominant than in the previous teeth, being only slightly larger than the five (125356) or up to eight (162936) lateral cusps (Figure 3B). The anterior, largest of these teeth (rings 5 and 6) may be arranged in pentagons, but the following teeth are arranged very densely and if they are still arranged in rings these contain more than five teeth per ring. Following this region are widely spaced teeth that superficially look like papillae but have a line with numerous minute cusps separating an upper part with smooth surface from a lower part, which is structured by fine lines (Figure 3A and D). In the lower part, close to the tip, are some pore-like openings, either on the tip of small tubes or on small papillae (Figure 3C and D).

In all observed specimens, scalids are grouped into series and the series are separated from each other by ring-like gaps. By light microscopical investigation, it sometimes appears as if scalids of a series are basally fused (Figure 4A), but this was not observed by SEM investigation (Figure 4B–D). Scalids are broad conical structures (Figure 4C and D). Within a series, the first scalid is always the largest one and scalid size in

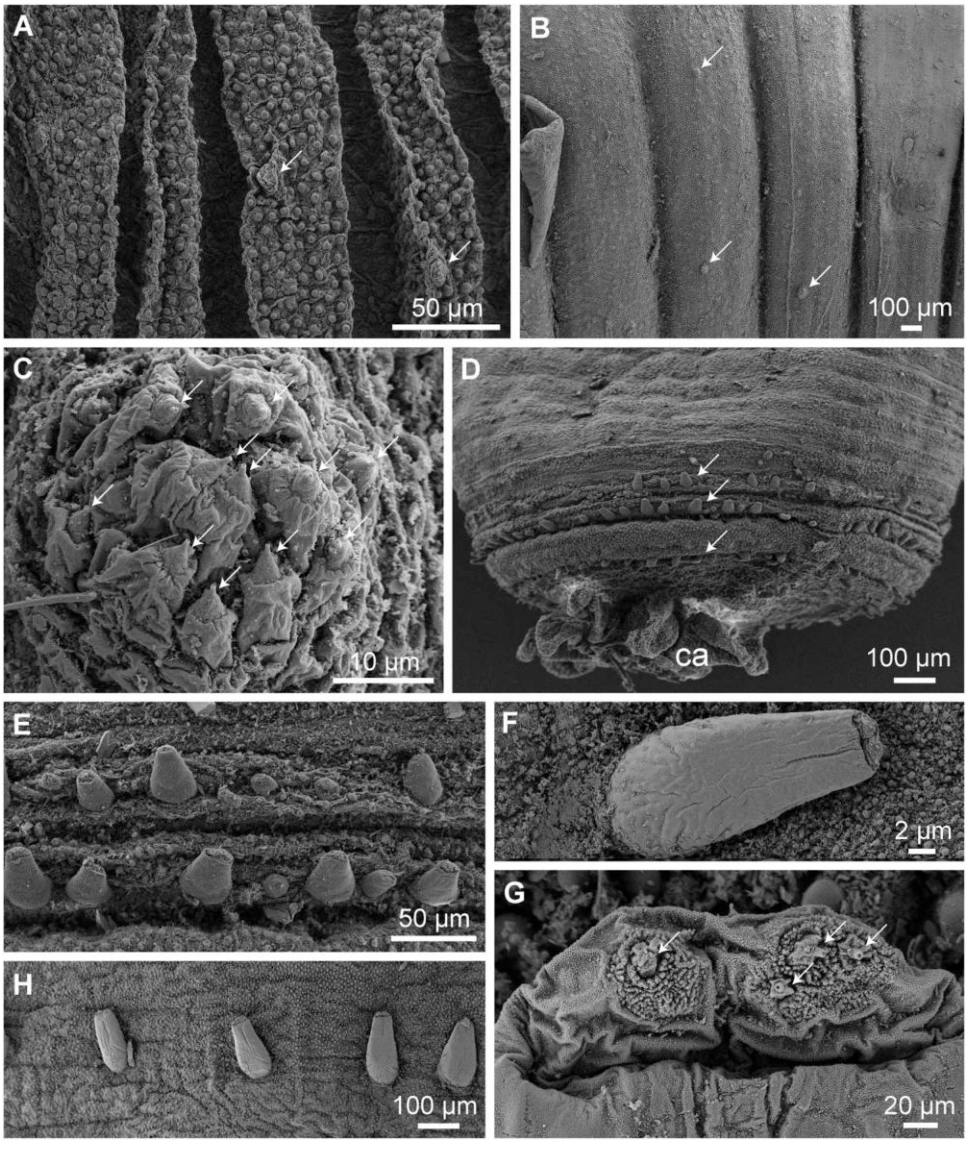

Figure 5. *Priapulopsis australis*, trunk. **A, B,** Trunk annuli are covered by tumuli and scattered trunk papillae (arrows). **C,** Fine structure of a trunk papilla with several receptors (arrows). **D,** In the posterior region, anterior of the caudal appendage (ca), there are rings of ringpapillae (arrows). **E, F, H,** Higher magnifications of ring papillae. **G,** Apical tip of a ringpapilla with receptors (arrows). All images by SEM. A from 157950-2, B, C from 125356, D, E from 157060, F–H from ZMH V13672.

general decreases from anterior to posterior (Figure 4B). Larger scalids are composed of a basal part and an apical tip, which is apically covered by receptors (Figure 4C and D). In the anteriormost scalids, this tip is elongate (Figure 4B), but in most scalids it is shorter (Figure 4C and D). The cuticle between scalids is structured by fine traverse lines and abundant small papilliform elevations (Figure 4C and D). No structures were observed between scalids and pharyngeal teeth (Figure 2A and D).

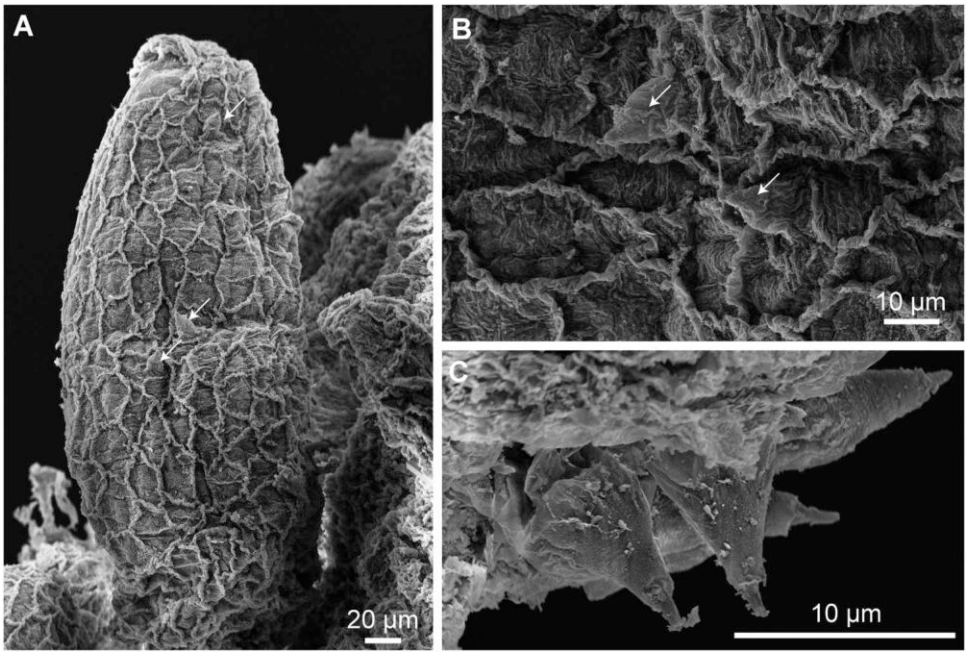

Figure 6. *Priapulopsis australis*, caudal appendage. **A,** One vesicle with net-like surface structure and scattered spinulets (arrows). **B,** Higher magnification of surface structure and spinulets (arrows). **C,** Higher magnification of spinulets. All images by SEM. A, B from 157950, C from 162937.

Trunk: The trunk is annulated, 29–49 annuli were counted. The ventral midline is elevated (Figure 1B). The surface is densely covered with tumuli (Figure 5A and B). Trunk papillae were observed in several specimens, these are scattered, not very abundant and of different size (Figure 5A and B). In some specimens, trunk papillae are very small and were only discovered by SEM (Figure 5B), in others they are larger and already evident by light microscopical investigation. Trunk papillae are hemispherical elevations, their apical surface is covered with conical structures bearing a receptor on top (Figure 5C).

In the posterior end, up to four rings of ringpapillae are present (Figure 5D). Sometimes the rings are arranged a bit irregularly, including lateral gaps, and the ringpapillae are of different size (Figure 5E), sometimes they are arranged very regularly (Figure 5H). The individual ringpapillae are elongate structures of around 120 µm length. They attach on the posterior margin of an annulus and are directed anteriorly (Figure 5E, F and H). The surface is finely granulated and, on the tip, they contain an area with receptors (Figure 5G). Posterior warts were not observed.

Caudal appendage: The caudal appendage is paired in most specimens (Figure 1A), but sometimes only one appendage is visible (Figure 1C and E). In some of these cases, two branches are close together and appear as one. In some specimens (see Table 2), especially those with short caudal appendages, even close examination could only reveal one appendage. When two appendages are present, one is often developed much stronger than the other (see Table 2). For example, in specimen 162918-2 the appendages are 10 and 3.5 mm long and in specimen 162937-2 they are 1.4 and

Table 2. Measurements in *Priapulopsis australis*. Number of trunk rings is the counted number of visible rings. Additional rings might be present, but difficult to observe. The introvert length refers to the visible part of the introvert, i.e. to the degree of introvert eversion and is therefore not the total introvert length. The extension '–1' etc. is used when more than one specimen occurs under one catalogue number. 'withdr.' = withdrawn.

						Caudal appendage		
Catalogue no.	Trunk length [mm]	Number of trunk rings	Trunk papillae	Introvert length [mm]	Number of visible rings of pharyngeal teeth	Number	Maximal length [mm]	Number of rings of ringpapillae
72034	39	41	–	5	0	2	12	3
124155	6.4	35	–	2.6	2	1?	2.3	2
125356-1	16	37	+	4.4	0	1?	7.4	?
125356-2	23	37	+	6.5	0	2	5.6	?
149775	42	48	–	8	2	2	7.4	min. 1
149776	34	43	–	6.3	0	2	16	4
157060	5.4	29	–	withdr.	0	?	–	3
157950-1	4.2	47	+	2.6	3	1	1.5	2–3
157950-2	6.9	49	+	3.2	3	1	1.9	?
162907	16	49	–	3.9	0	absent	–	min. 1
162918-1	19	40	–	4.3	1	2	3	?
162918-2	17	41	–	4.3	1	2	10/3.5	?
162922	17	43	–	2.2	0	2	7.4/5.2	?
162936	20	46	–	5	0	2	10/5	2–3
162937-1	14	45	+	4.6	2	2	2.1/2.0	3
162937-2	7	38	+	1.8	2	2	1.4/0.4	min. 1
162937-3	12.1	45	–	1.6	0	2?	1.3	2
162982	18	41	–	9.3	0	?	2.5	2
ZMH V13672	22	41	–	6	2	2	11/?	3–4
ZMH V13673	15	37	–	8.5	0	2	4.5/?	?

0.4 mm long. In SEM samples, the surface of the vesicles is often strongly shrunken. The vesicles are covered by a net-like surface structure of cuticular ridges (Figure 6A and B). Spinulets are scattered over the entire vesicle (Figure 6A–C).

Priapulus tuberculatospinosus

(Figures 7–9, Table 3)

Catalogue numbers: 21401, 21402, 21406, 162940 (two specimens), ZMH V13674.

Six specimens are assigned to *P. tuberculatospinosus*, but three of the specimens (21401, 21402, 21406) were collected outside of the New Zealand vicinity, in circum-Antarctic waters. The largest two specimens have a trunk length of 24 and 32 mm, respectively (both specimens of 162940; Figure 7A), three showed a trunk length of 7.6–13.5 mm (21401, 21402: Figure 7D, ZMH V13674: Figure 7G) and one is a small specimen of 1.9 mm trunk length (21406). The number of annuli that could be counted does not correspond to the trunk length, as the smallest specimen has at least 40 annuli, while in one medium-sized specimen (21401) only 20–25 annuli are counted. This specimen, however, is strongly contracted and the annuli are difficult to recognise.

Introvert: The anterior part of the pharynx with pharyngeal teeth is everted in four of the six specimens, up to six rings are visible (Figures 7B and C and 8A and B). The teeth

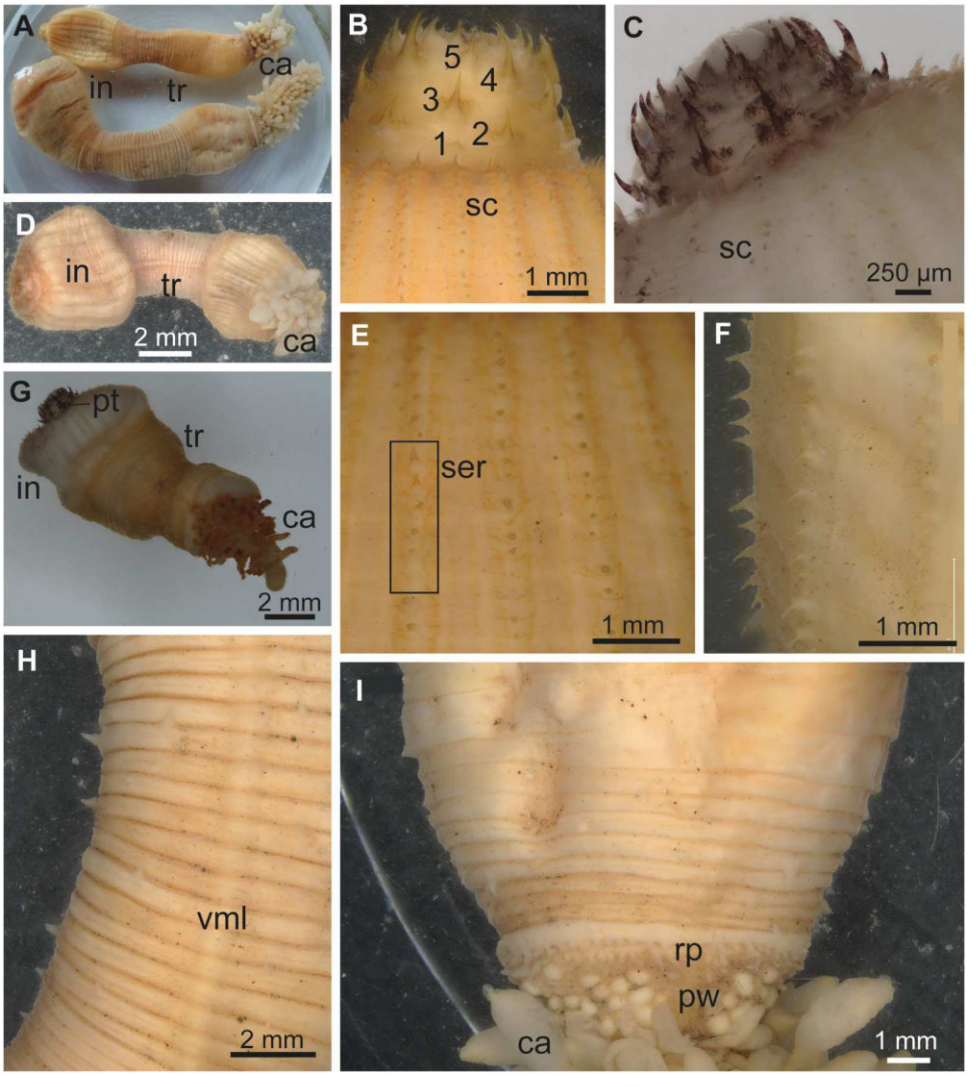

Figure 7. *Priapulus tuberculatospinosus*, light microscopical images. **A,** Two specimens of 162940 with introvert (in), trunk (tr) and one caudal appendage (ca). **B, C,** Everted pharyngeal teeth (rings numbered in B) and scalids (sc). **D,** Specimen 21402. **E, F,** Rows of scalids arranged in series (ser). **G,** Specimen ZMH V13674. **H,** Trunk annuli with trunk papillae and elevated ventral midline (vml). **I,** Posterior end of trunk with ring papillae (rp), posterior warts (pw) and caudal appendage (ca). B, E from 162940-2, C from ZMH V13674, F, H, I from 162940-1.

increase in size from ring 1 to ring 4 and then decrease in size in the posterior rings (Figure 8B). In ring 4, two teeth (presumably the dorsolateral ones) are larger than the remaining teeth in this ring (Figure 8A and B). The teeth of the first ring are the smallest, they either have around 12 cusps (21406; Figure 8D) or have a short central cusp and five lateral cusps (162940-2; Figure 8C). All other teeth have a strong central cusp and five (ring 2) or four (remaining rings) lateral cusps (Figure 8A, B, E and F). Tooth receptors are present on teeth of ring 1 (Figure 8D) and scattered on other teeth (Figure 8G). The

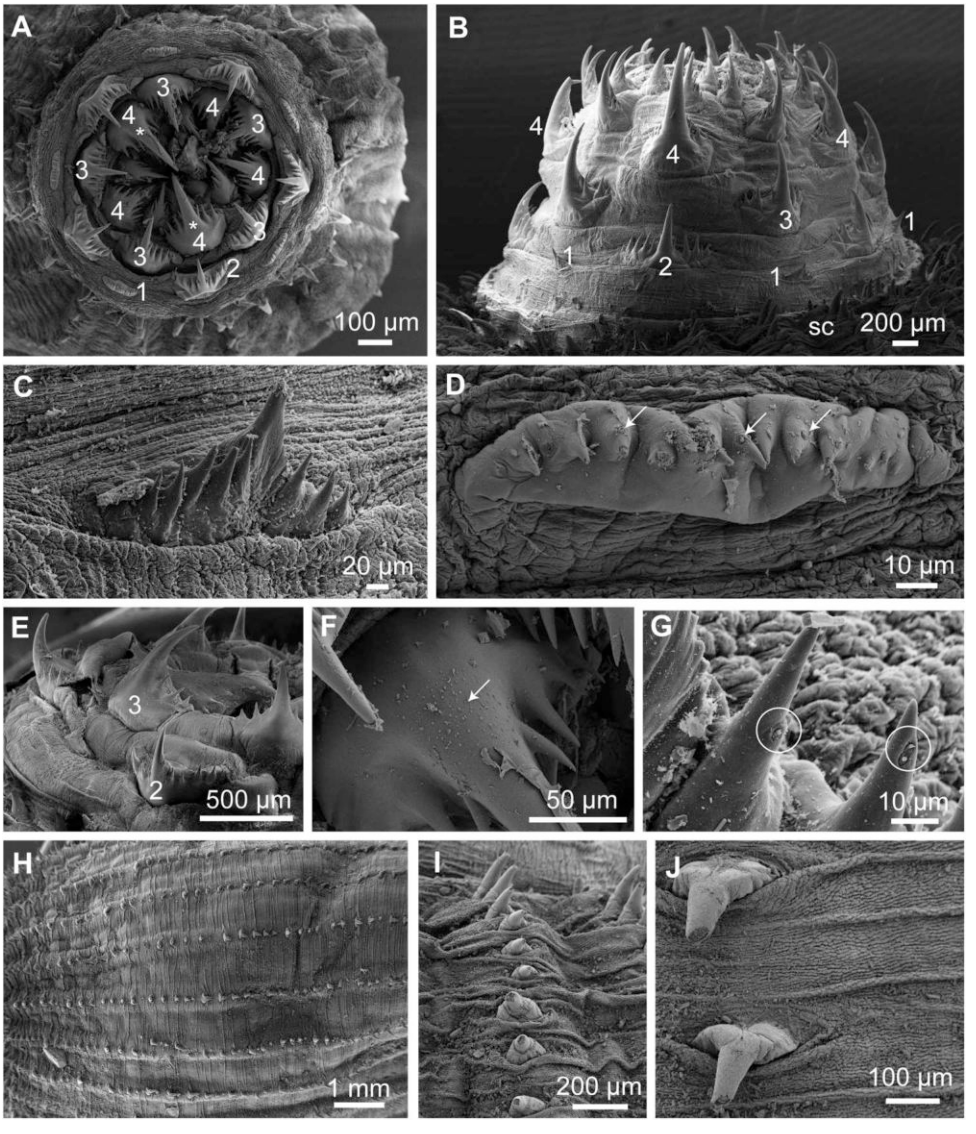

Figure 8. *Priapulus tuberculatospinosus*, pharyngeal teeth and scalids, SEM. **A,** Frontal view on the teeth of rings 1–4. Note that two teeth of ring 4 are larger than the three others (marked with asterisk). **B,** Lateral view on everted pharyngeal teeth. sc = scalids. **C,** First-ring tooth with short central cusp from specimen in B. **D,** First-ring tooth without central cusp from specimen in A. Arrows point at tooth receptors. **E,** Teeth of rings 2 and 3. **F,** Magnification of tooth of ring 4 showing tiny cusps on the upper side (arrow). **G,** Tooth receptors (encircled). **H,** Rows of scalids. **I,** Within a series, scalids decrease in size. **J,** Two scalids and structure of the introvert surface. A, D, F from 21406, B, C, G–J from 162940-2, E from 21402.

outer surface of the teeth of rings 4 and 5 is covered with a few tiny spinose projections (Figure 8F).

Scalids occur regularly spaced in longitudinal rows. Series are present, but only slightly or not separated at all from adjoining series (Figure 7E and F). Series are composed of up

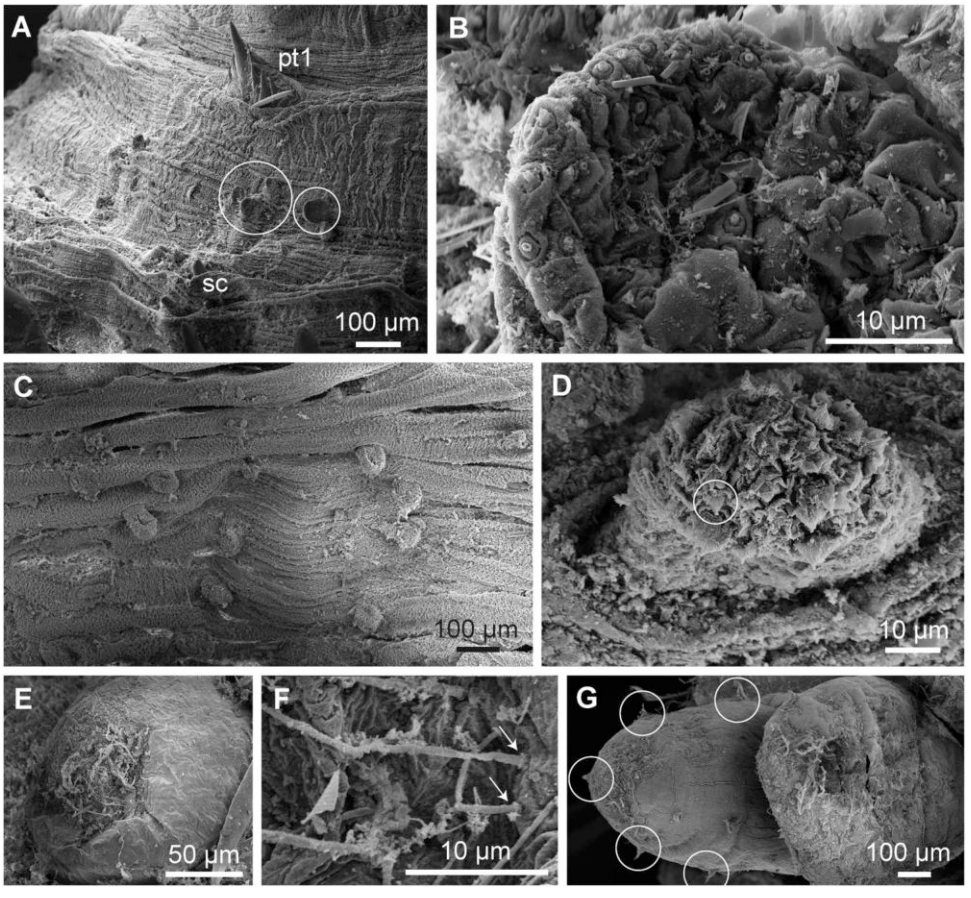

Figure 9. *Priapulus tuberculatospinosus*, SEM. **A,** Structures (encircled) between scalids (sc) and first ring of pharyngeal teeth (pt1). **B,** Higher magnification of encircled structure in A. **C,** Annuli and trunk papillae. **D,** Higher magnification of trunk papilla with apical receptors (one is encircled). **E,** Posterior wart. **F,** Bristles on the apical surface attach at the posterior wart (arrows). **G,** Vesicle of caudal appendage with spinulets (encircled). A, B, E, F from 162940-2, C, D from ZMH V13674, G from 21402.

Table 3. Measurements in *Priapulus tuberculatospinosus*. Number of trunk rings is the counted number of visible rings, additional rings might be present, but are difficult to observe.

Catalogue no.	Trunk length [mm]	Number of trunk rings	Trunk papillae	Introvert length [mm]	Number of visible rings of pharyngeal teeth	caudal appendage	
						number	Maximal length [mm]
21401	10	20–25	+	hardly everted	2	1	3.75
21402	7.6	40	+	5.6	4	1	ca. 1
21406	1.9	min. 40	?	2.1	2	1	0.7
162940-1	32	50	+	17	0	1	14
162940-2	24	43	+	13	6	1	7
ZMH V13674	13.5	33	+	9.5	8	1	11

to six scalids (Figure 8I). The anterior scalids in a series are elongate. Some appear to be composed of one piece (Figure 8J), but in others there is a basal socket, from which the elongate part of the scalid emerges (Figure 8I). The surface of the introvert has a fine striation oblique to the longitudinal axis (Figure 8J). In the region between the anteriormost scalids and the first pharyngeal teeth are irregular structures (Figure 9A) that are densely covered by receptors (Figure 9B).

Trunk: The surface of the trunk annuli is smooth at lower magnifications, with a fine oblique striation at higher magnifications (Figure 9C). Trunk papillae are present (Figures 7H and 9C). In specimen 162940-2 they are pointed and very prominent, in the other specimens they are hemispherical and smaller (Figure 9C). The fine structure resembles the one described for *P. australis*, with several receptors on the apical surface (Figure 9D).

In the posterior part of the trunk there are posterior warts and, at least in some specimens, ring papillae. Ring papillae are observed by light microscopy (Figure 7I) but are not confirmed from the specimens investigated by SEM. Posterior warts are hemispherical structures covering the posterior tip (Figure 7I). With SEM, only some warts could be investigated, these have a smooth surface except for the apical centre, which is covered by numerous bristles (Figure 9E). The bristles attach to the warts with a socket-like structure (Figure 9F) and are therefore likely part of the warts.

Caudal appendage: The caudal appendage is single, the central stem is quite thick and visible in specimen ZMH V13674 (Figure 7G), in the other specimens, the caudal appendage is either very 'bushy' and the central stem is not visible (both specimens of 162940, Figure 7A) or the entire appendage is very short (remaining specimens, e.g. Figure 7D). The surface of the vesicles is smooth, and a few delicate cuticular ridges run predominantly in longitudinal direction (Figure 9G). The spinulets are few and scattered over the entire vesicle (Figure 9G).

Priapulopsis papillatus nov. spec.

(Figures 10–14)

Zoobank: lsid:zoobank.org:pub:D465D9E2-6B02-4AA9-80D3-E15C619174E6.

Diagnosis: Trunk surface with numerous trunk papillae, in part arranged regularly on the trunk annuli. Trunk cuticle without tumuli, instead structured into compartments with radiating ridges. Up to five rings of ring papillae, posterior warts absent, but trunk papillae present on the last trunk annuli. Ring papillae in some rings with lateral flaps. Scalids on introvert not arranged in series. The 10 first ring pharyngeal teeth with blunt cusps. Tooth receptors present only on first ring teeth.

Material examined: holotype and paratype.

Deposition of material: NIWA Invertebrate Collection, Auckland, New Zealand, under the catalogue numbers 63448 (holotype) and 63408 (paratype). Several parts of the holotype were prepared and are stored as three SEM samples (anterior, midbody and posterior parts of the body), from the paratype only a piece of integument of the trunk was prepared for SEM. The remaining parts are kept in ethanol. Type locality: Hikurangi Margin (subduction zone east of the North Island of New Zealand; −41.5195, 175.80683), collected by beam trawl at 723–746 m depth. Paratype also from Hikurangi Margin (−41.55433, 175.82683) at 917–945 m depth.

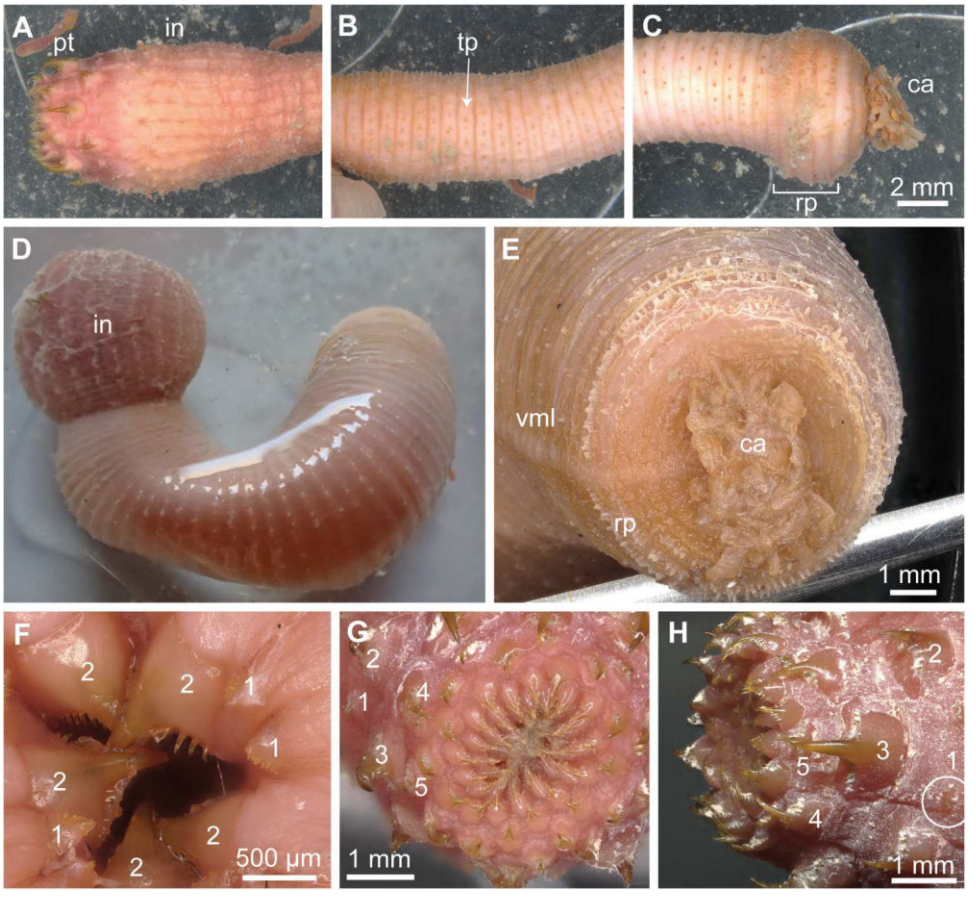

Figure 10. *Priapulopsis papillatus* nov. spec. Light microscopical images. **A–C,** Anterior, middle and posterior part of the holotype (63448). Pharyngeal teeth (pt) are far extended, trunk papillae (tp) are visible on trunk annuli. Ring papillae (rp) are present on the posterior annuli, anterior of the caudal appendage (ca). **D,** Paratype (63408) with bulbously everted introvert (in). **E,** Terminal view on the posterior end with small caudal appendage, ring papillae and elevated ventral midline (vml). **F,** Pharyngeal teeth of rings 1 and 2 are visible in the paratype. **G, H,** Frontal (G) and lateral (H) view on the pharyngeal teeth of the holotype. Scalid rings are numbered, tooth of ring 1 is encircled in H. A–C, G, H, from holotype (63448), D–F from paratype (63408). There is no scale bar in D, but the trunk length is 32 mm.

Etymology: 'papillatus' refers to the conspicuous and abundant papillae on the trunk.

Description: The holotype specimen has a long and slender trunk of 42 mm length and about 59 annuli (Figure 10A–C). The introvert is strongly everted (10 mm; Figure 10A), exposing about 10 rings of pharyngeal teeth (Figures 10G and H). There is a paired, but very short caudal appendage (Figure 10E). The paratype specimen is shorter (32 mm, 46 annuli) and less slender (Figure 10D), the introvert is also strongly everted and bulbous (Figure 10D), but only two rings of pharyngeal teeth are exposed (Figure 10F).

Introvert: The first ring of pharyngeal teeth consists of 10 small teeth (Figures 10F–H and 11A). These are semicircular and have blunt elevations along the apical ridge (Figure 11B). These elevations have up to nine apical depressions, in each of which

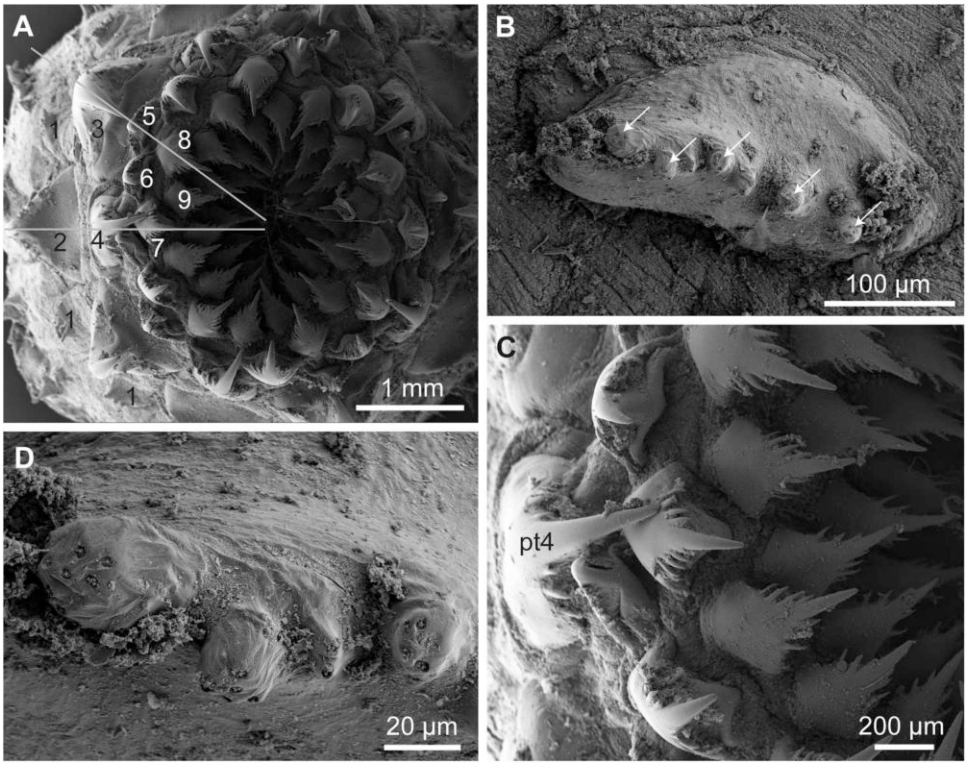

Figure 11. *Priapulopsis papillatus* nov. spec. Pharyngeal teeth, SEM. **A,** Frontal view on the everted pharyngeal teeth with tentative numbering up to ring 9. Radial axes of pentagons are indicated (see text for explanation). **B,** One of ring 1 teeth, arrows point at cusps with receptors. **C,** Fine structure of teeth in ring 4 and following rings. **D,** Magnification from B showing some cusps and their receptors. All images from holotype (63448).

one or two tooth receptors are present (roundish base and apical tubulus) (Figure 11D). The teeth of the following rings are cuspidate teeth with a strong central cusp and four to five lateral cusps (Figure 11A and C). The exact number was hard to observe, because some dirt remained on the teeth. The teeth in ring 3 are the largest (Figures 10H and 11A). They measure from base to tip about 1.5 mm, whereas the teeth of rings 2 and 4 measure about 1 mm (for difficulties in measurements see above). From ring 5 on, the pharyngeal teeth become smaller and the central cusp gets much shorter (Figure 11A). Up to ring 5, pharyngeal teeth are arranged in pentagons, with the rings following each other being shifted against each other, so that the teeth of rings 1, 3 and 5 are on a line radiating out from the mouth opening as well as teeth 2 and 4 (Figure 11A). From ring 6 on this arrangement becomes difficult to follow and some teeth are positioned out of register of the first teeth, probably because their number per ring is higher than five. Figure 11A gives an interpretation of tooth counting, but this is a bit speculative.

No structures are present between the pharyngeal teeth and the scalids (Figure 12A). Scalids were investigated by SEM only in the holotype, but as they are covered by some dirt, the observations are less clear than other structures in this species. The anteriormost

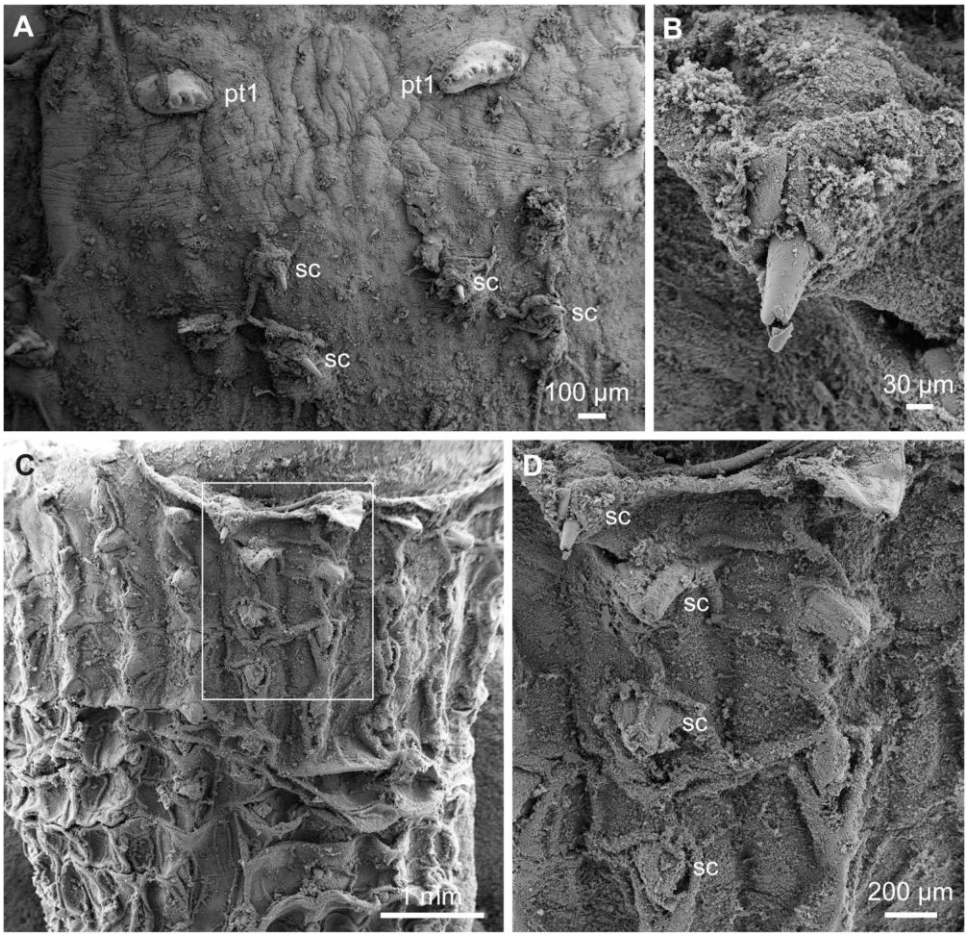

Figure 12. *Priapulopsis papillatus* nov. spec. Scalids, SEM. **A,** Region between first-ring pharyngeal teeth (pt1) and anterior scalids (sc). Scalids are partly covered by dirt. **B,** Magnification of an anterior scalid. **C, D,** Anterior region of the introvert (C overview and D magnification as indicated in C). Scalids (sc) are regularly spaced, but single and not arranged in series. All images from holotype (63448).

scalids are largest and are composed of a conical base and a tubular apical part (Figure 12B). As far as was observed by light microscopy and SEM, scalids are not arranged in series, but are single and equally spaced (Figure 12C and D). The surface structure of the region between scalids could not be observed.

Trunk: Very conspicuous is that the specimens have a large number of trunk papillae, arranged mostly in regular rings on each annulus of the trunk (Figures 10B–D and 13A and D). The trunk papillae observed by SEM are hemispherical structures, which are on the apex covered with different receptive structures. Most abundant are long conical structures, each with an apical tubulus (Figure 13E and G). Single flosculi are present (Figure 13G and G′) and some papillae have a single broad apical structure that has an apical depression, probably with receptors inside (Figure 13F). In the holotype, the trunk papillae are well visible, because they are darker than the trunk surface (Figure 10B and C), but in the paratype surface and papillae have the same colour

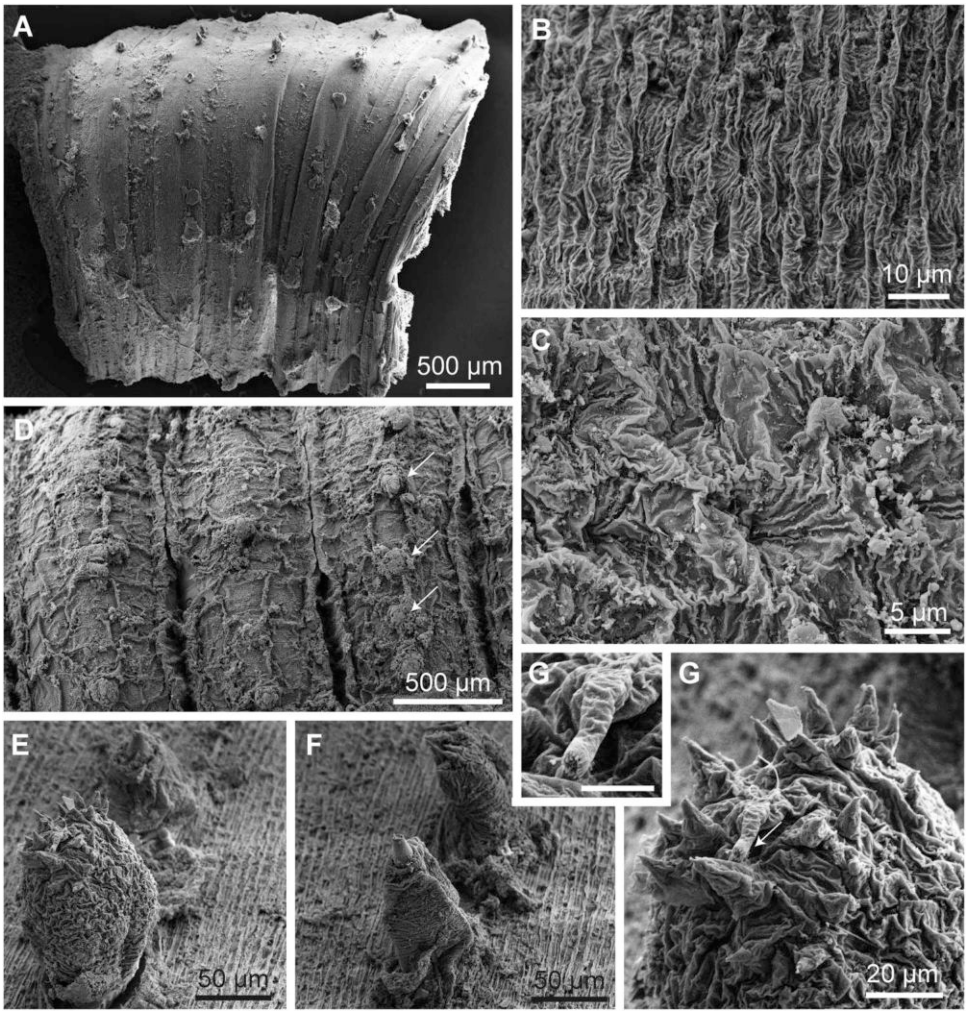

Figure 13. *Priapulopsis papillatus* nov. spec. Trunk, SEM. **A,** Piece of the trunk of the paratype showing numerous trunk papillae. **B, C,** Surface structure of the trunk in paratype (B) and holotype (C). **D,** Trunk annuli with trunk papillae (arrows) in the holotype. **E–G,** Trunk papillae with different apical structures. G´ shows a flosculus as magnification of G. Scale bar in G´ is 10 µm. A, B, E–G from paratype (63408), C, D from holotype (63448).

(Figure 10D). The cuticle of the trunk is structured into almost rectangular (paratype; Figure 13B) or more irregular (holotype; Figure 13C) compartments, in which the cuticle forms ridges radiating from a central depression towards the margin of the compartment. The compartments are 8–10 µm broad and 10–12 µm long.

In the posterior region of the trunk there are four (paratype) or five (holotype) rings of ring papillae (Figures 10E and 14A). These are elongate, about 200 µm long. They originate at the posterior margin of a trunk annulus and are directed anteriorly (Figure 14A–C). In the three posterior rings the ring papillae have a flat extension on one side (Figure 14B–D). Posterior of the ring papillae is a ring of semispherical papillae, these are called here trunk papillae (Figure 14A and C; see discussion).

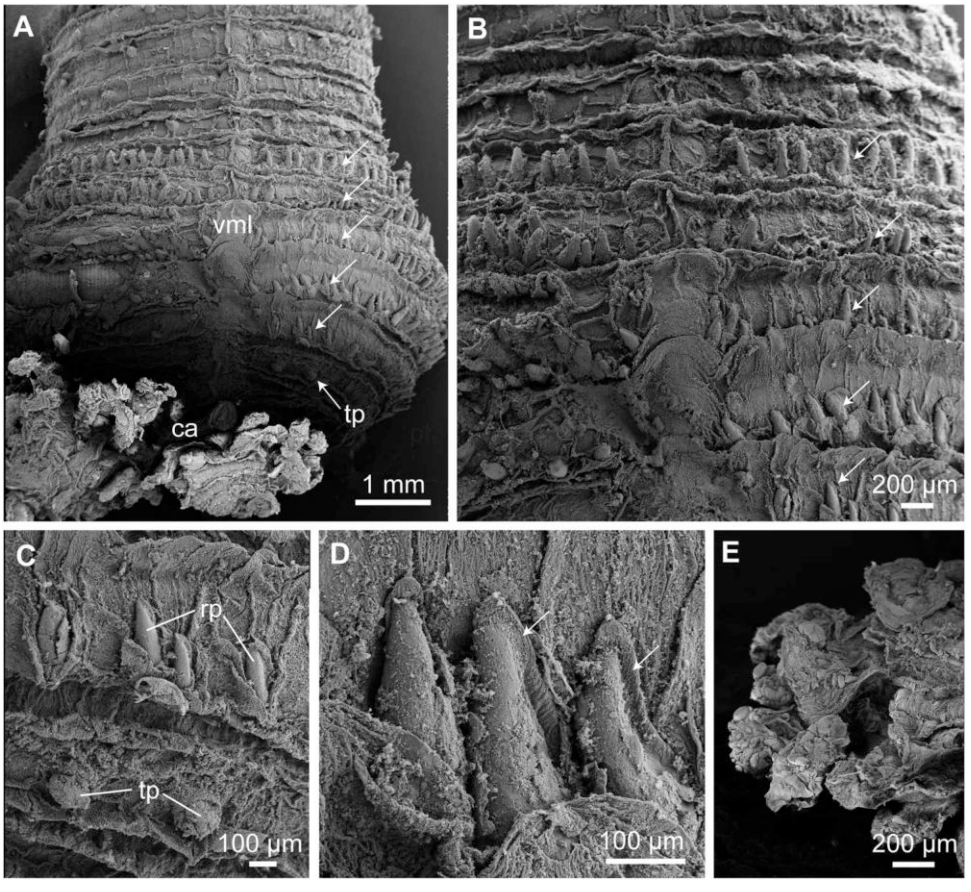

Figure 14. *Priapulopsis papillatus* nov. spec. Caudal trunk and caudal appendage, SEM. **A,** Ventral view on the posterior end with elevated ventral midline (vml), five rings of ringpapillae (arrows), some trunk papillae (tp) and caudal appendage (ca). **B,** Higher magnification from A, showing the anteriorly directed ringpapillae (arrows). **C,** Last ring of ringpapillae (rp) and posterior trunk papillae (tp). **D,** Ringpapillae of the last three rings have lateral flaps (arrows). **E,** Structure of the caudal appendage, see text for description. All images from holotype (63448).

Caudal appendage: The caudal appendage is extremely short (Figure 10E). Although difficult to detect, it is paired. Ultrastructurally, the vesicles appear as covered by plaque-like structures (Figure 14E). Spinulets were not observed.

Larvae

(Figures 15–16, Table 4)
Catalogue numbers: 162925, 162926, 162978, 162981, 162989.

Five catalogue numbers house a total of 15 larvae, all of which were first documented by light microscopy and then investigated by SEM. The larvae have a lorica length of 750–1,020 µm (Table 4). The introvert is everted in almost all larvae, but to a different extent (Table 4). In no larva the introvert is everted far enough to observe the structure of the pharyngeal teeth.

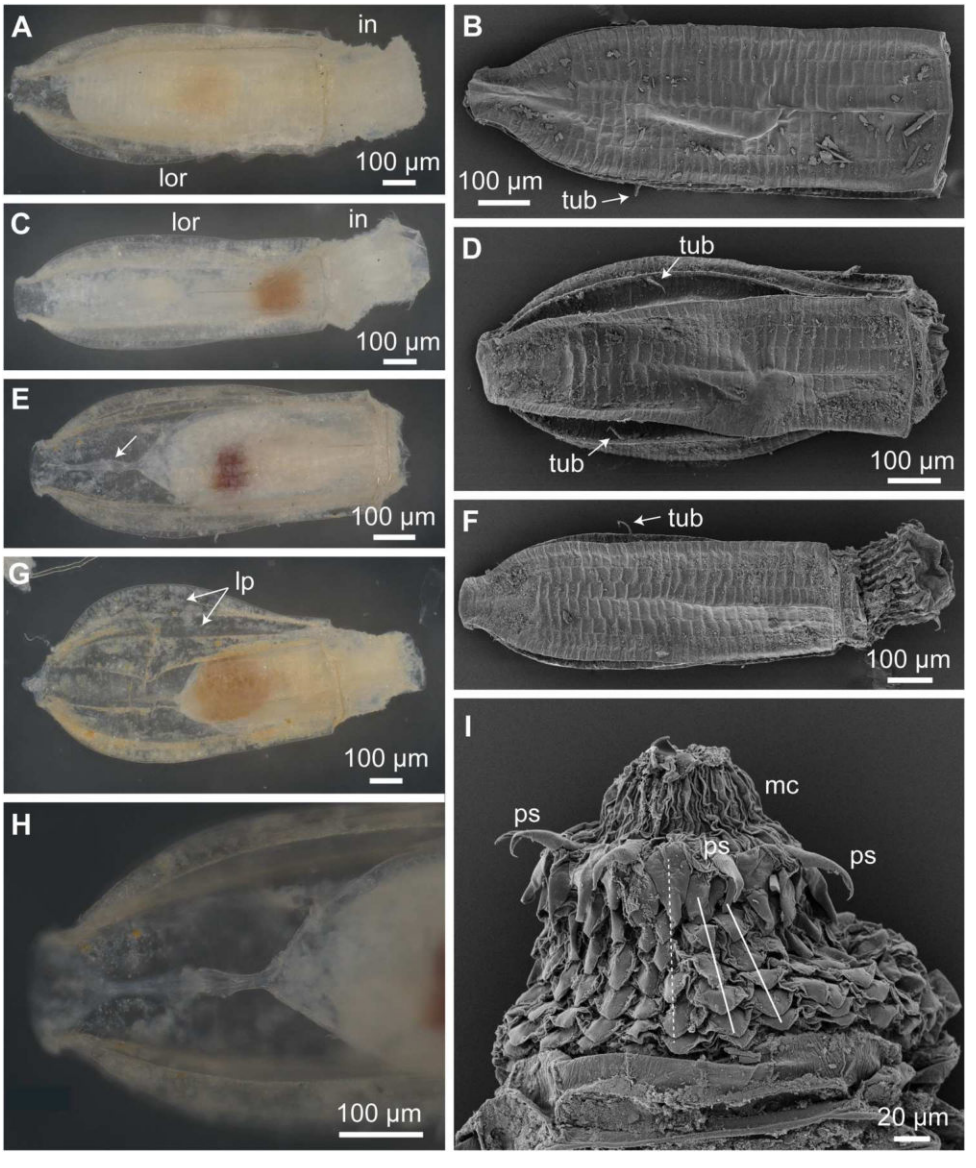

Figure 15. Larvae. **A, C, E, G,** Different larvae as seen with light microscopy. The body of some larvae fills their lorica (lor), in others the body is only in the anterior region of the lorica. In this case, a tissue strand (arrow in E) connects the larval body with the posterior end. In larvae that appear to be broad, the lateral plates (lp in G) are folded out. In some larvae the introvert (in) is everted. **B, D, F,** Larvae as seen with SEM. Note the position of tubuli (tub) in D and F. **H,** Higher magnification of the tissue strand from E. **I,** SEM of the introvert showing the mouth cone (mc) and the arrangement of scalids in two rows (white lines) following a primary scalid (ps) and in one row (dotted line) between primary scalids. A, G two larvae from 162925, B, I two larvae from 162978, C, F same larva from 162989, D, E, H same larva from 162981.

The lorica is composed of a larger dorsal and a larger ventral plate and six lateral plates on each side (Figure 15B, D and F). Dorsal and ventral plates could not be distinguished from each other in the specimens observed, they are therefore termed

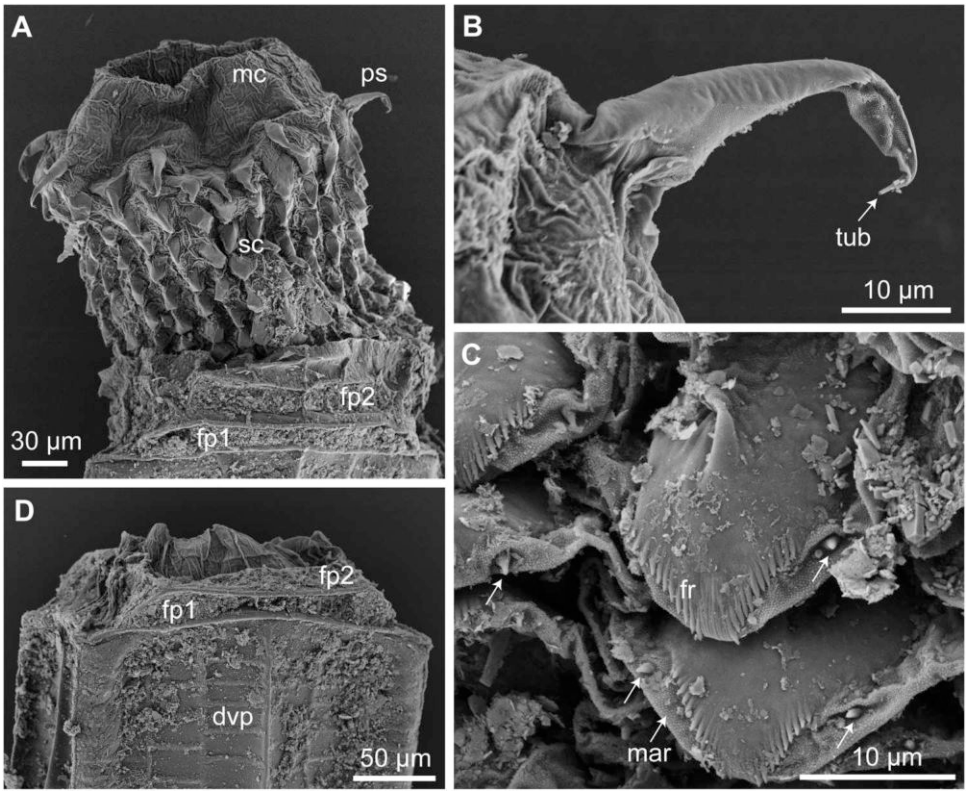

Figure 16. Larvae. **A,** Structure of the introvert with mouth cone (mc), primary scalids (ps) and regular scalids (sc). Visible are also two frontal plates (fp1 and fp2) from the closing apparatus. **B,** Fine structure of a primary scalid with apical tubulus (tub). **C,** Fine structure of regular scalids with lateral receptors (arrows), fringe (fr) and margin (mar). **D,** Dorsoventral plate (dvp) and closed frontal plates. A, B from 162989, C from 162978, D from 162981.

Table 4. Measurements of larvae from light microscopical images.

Catalog no.	lorica length [µm]	Introvert length [µm]
162925 spec. 1	980	120
162925 spec. 2	1020	240
162925 spec. 3	1000	160
162925 spec. 4	1000	220
162926	840	160
162978 spec. 1	850	250
162978 spec. 2	750	250
162978 spec. 3	895	250
162981 spec. 1	962	231
162981 spec. 2	962	–
162981 spec. 3	923	385
162989	962	308

'dorsoventral plate' in the following. The anterior margin of a dorsoventral plate is gently curved and the lateral margins are almost parallel for most of the lorica length. In the posterior region they narrow distinctly and lead to a terminal narrower end region (Figure 15A–C and F). The dorsoventral plates are sculptured by an

orthogonal pattern of longitudinal and transverse ridges (Figure 15B, D and F). There is one stronger median longitudinal ridge and on each side two distinct, but not so prominent ridges. In most specimens, the longitudinal ridge is straight in the anterior part, but runs in a slight zig-zag pattern after about half of the lorica length (Figure 15B). In some specimens, the lateral plates are folded out artificially, creating the impression of quite broad larvae (Figure 15D and G). Anterior to the dorsoventral plates are two broad but short frontal plates (Figure 16A) that close the lorica when the introvert is withdrawn (Figure 16D). A pair of tubuli is attached at between 54% and 65% of the lorica length (measured from the anterior margin) (Figure 15D and F). There is a very slight tendency of a more posterior position in larger larvae (Table 5), but sample size is too low for exact statements. In the specimen figured in Figure 15D the tubuli appear to attach at different levels, which might be due to the artificial outfolding of the lateral plates.

In some larvae, the larval body fills the lorica entirely (Figure 15A and C), in others it is present only in the anterior part of the lorica (Figure 15E and F). In this case, a strand of tissue connects the posterior part of the larval body with the terminal region of the lorica (Figure 15E and H). The inner organs of the larvae are not clearly visible with the exception of parts of the intestine, which can be recognised by their brown colour (Figure 15C, E and G).

The scalids are flat and almost triangular (Figures 15I and 16A and C). The upper surface is smooth and ends in a fringe, which covers a finely granulated margin on which a pair of receptors is present (Figure 16C). The scalids are positioned very close to each other and overlap each other (Figures 15I and 16C). Anteriorly, there are long and slender primary scalids (Figures 15I and 16A). Five primary scalids were observed from one side, which makes it likely that their total number is eight. The upper side of the primary scalids is smooth, the lower side is finely granulated (Figure 16B). Apically, the primary scalids end with a tubulus (Figure 16B). Between the primary scalids are very large scalids (Figure 15I). The arrangement pattern of scalids corresponds to the 'usual' pattern described for scalid arrangement in priapulids, i.e. one longitudinal row of scalids follows the large scalids and two rows follow the primary scalids (Figure 15I). Anterior of the scalids is a slightly conical mouth cone, which ends in the broad mouth opening, but pharyngeal teeth were not observed (Figures 15I and 16A).

Table 5. Position of the lateral tubuli, measured in percent of the entire lorica length from the anterior margin. Measurements are taken from SEM images, which produce smaller measurements than measurements of light microscopical specimens (Table 4). Not all specimens could be assigned to the light microscopical images with certainty, therefore only the general catalogue numbers are given.

Catalogue no.	lorica length [µm]	Position of tubuli in % of lorica length
162989	765	53.8
162978	794	59.3
162981	800	59.4
162981	824	53.6
162925	824	64.3
162978	925	64.9

Discussion

Pripulopsis australis

Morphological data on *Priapulopsis australis* were contributed by De Guerne (1886, 1891), Hurley (1962), Van der Land (1970, 2010), Storch et al. (1995) and Adrianov and Malakhov (1996). The paired nature of the first ring of pharyngeal teeth was not mentioned in the early publications (De Guerne 1891), but first by Van der Land (1970). They are much smaller than teeth in *P. bicaudatus* (see Schmidt-Rhaesa and Raeker 2023), with around 30 µm versus 150 µm width, respectively. Ultrastructurally, the first-ring teeth of both species are quite comparable, bearing a ridge of cusps and tooth receptors (Schmidt-Rhaesa and Raeker 2023). There are, however, some differences compared to images of *P. australis* by Storch et al. (1995). In their images the first-ring teeth are not semicircular structures with an apical ridge of cusps, but papilliform structures with only one cusp that is covered by tooth receptors. This may be the reason why Storch et al. (1995) called this a 'conical sensillum' and a 'modified tooth of the first ring'.

The cushion-like structure in front of the second-ring teeth is also present in figures 3 and 4 of Storch et al. (1995), but was not yet mentioned in any publication. The number of lateral cusps in the teeth of rings 2–4 ranges between three and five (De Guerne 1891; Storch et al. 1995, this report). Tooth receptors were discovered to be quite regular structures on teeth in *P. bicaudatus* (see Schmidt-Rhaesa and Raeker 2023) and were also present on different teeth in *P. australis*, although not as abundant as in the former species. Except for the first-ring teeth (Storch et al. 1995), this is the first report of tooth receptors in *P. australis*. The spiny covering on the outside of the third-ring teeth has not been reported before and is not evident on the images in Storch et al. (1995).

Descriptions of the teeth posterior of ring 5 differ a bit. According to Van der Land (1970), there is a conspicuous gap with no teeth behind the fifth ring. We could not observe such a gap, but teeth are quite closely together. The structure of teeth posterior of ring 6 corresponds with the images in Storch et al. (1995). Their term 'pectinate' for these teeth is nevertheless misleading, as pectinate describes the absence of a central cusp and a comb-like set of about equally long cusps (Schmidt-Rhaesa 2013). The posterior teeth clearly have a central cusp, even if this is very short. The papilliform teeth in the posterior region of the pharynx are described for the first time, but their overall structure is comparable to the teeth anterior of them.

Concerning the scalids, two characters seem to be peculiar for *P. australis*: scalids within a series are closely together and probably even fused basally and there are gaps between series (Van der Land 1970). The gaps between series can be confirmed, but the common base is a bit problematic. Under light microscopical investigation, it indeed appears sometimes as if scalids are basally fused, but this could not be confirmed by SEM. The reason for this difference is unknown. Scalids within a series are indeed close together, but not significantly closer as in, e.g. *P. bicaudatus* (see Schmidt-Rhaesa and Raeker 2023). At least some of the anterior scalids are composed of two parts, which gives them the appearance to be telescopically mobile. This character is assumed to be characteristic for the genus *Priapulopsis* (Van der Land 1970).

In some priapulids there are structures in the region between pharyngeal teeth and scalids. In *P. bicaudatus* these are scalid-like in structure and were therefore termed 'ring 0 scalids' (Schmidt-Rhaesa and Raeker 2023). In most other publications, these

structures are called buccal papillae. Buccal papillae are mentioned to be present by Storch et al. (1995), but are not labelled and not evident from the figure that should illustrate them. As we did not find any such structures, the presence of buccal papillae must remain unclear in *P. australis*. However, the interpretation of structures in this region is difficult and depends on having the right landmarks. It is no problem to identify pharyngeal teeth, but with scalids this is more difficult and needs to be investigated in further detail. There seems to be a common pattern among most priapulids, in which eight primary scalids are the anteriormost scalids, followed by 25 rows of 'regular' scalids. Recognition of these primary scalids, however, is challenging, especially when introverts are not fully everted, because scalids may be hidden in folds and overall patterns not be recognised. In our investigation we could not identify primary scalids with certainty.

The coverage of the trunk by tumuli is regarded a character of the genus *Priapulopsis* (Van der Land 1970), their presence in *P. australis* is confirmed here. Trunk papillae were mentioned to be present by De Guerne (1886) and illustrated by Storch et al. (1995). They are smaller and less abundant than in the other two species investigated here (*P. papillatus* and *P. tuberculatospinosus*). The absence of posterior warts and the presence of ring papillae are characteristic of the genus *Priapulopsis*, but may not be restricted to this genus (see, e.g. Van der Land 1972 for deep sea priapulids). The paired nature of the caudal appendage was already noted by De Guerne (1886), but Hurley (1962) as well as Van der Land (2010) pointed out that the paired nature can be easily overlooked, because the two appendages may be very closely together. This is confirmed by our investigation and in some specimens, which are clearly *P. australis* based on other characters, we were not able to separate two branches of the caudal appendage. We report that the two branches are, in some specimens, distinctly unequal in size. This may be due to damage, e.g. by predation, but it could also be that in some specimens the unequal size is natural. As it was observed in *P. bicaudatus* that the two branches may grow at a different rate (Schmidt-Rhaesa and Raeker 2023), it may be possible that when one branch develops dominantly, the other remains small. The net-like fine structure of the vesicles corresponds to an image in Adrianov and Malakhov (1996), while Van der Land (1970) reported the surface to be smooth, with very few small spinulets being present. Probably the net-like surface structure is not visible by light microscopy and the scattered appearance of spinulets is confirmed.

Priapulus tuberculatospinosus

Morphological data on *Priapulus tuberculatospinosus* were contributed by Baird (1868), Michaelsen (1889), De Guerne (1891), Théel (1911), Van der Land (1970, 1972), Storch et al. (1994) and Adrianov and Malakhov (1996). There was a long debate about whether the southern *Priapulus* specimens represent an own species or are a subspecies of the northern species *P. caudatus*, but since Théel (1911) the debate settled and *P. tuberculatospinosus* (originally described as *P. tuberculato-spinosus*) was considered a distinct species. This was finally supported by Lang's (1951) observation that the attachment of the tubuli on the larval lorica is at different levels in both species.

A significant difference between *P. caudatus* and *P. tuberculatospinosus* is that in the latter species the first ring teeth are smaller than those of the second ring, while they are

of about equal size in *P. caudatus* (Théel 1911; Van der Land 1970). Teeth of the fourth ring are the largest in both species (Théel 1911; Van der Land 1970). Van der Land (1972) noted that the laterodorsal teeth in the fourth ring are larger than the three others in this ring, which has been confirmed by Storch et al. (1994) and by our investigation. For the number of lateral cusps on the anterior teeth different numbers are reported, from 3–4 (Théel 1911) to 4–6 (De Guerne 1891). Our observation of 4–5 lateral cusps supports De Guerne´s counting. Tooth receptors are present: they were documented by Storch et al. (1994) on the first-ring teeth and named as 'cuticular tubules'. The presence of tooth receptors on other teeth is reported here for the first time. The tiny spines on the outside of the teeth from rings 4 and 5 were not observed before, but in the images in Storch et al. (1994) the teeth are only partly everted and only the central and some lateral cusps are visible.

Concerning the scalids, the authors reported the presence of a series and an almost equal distance of scalids in the rows (Baird 1868; Théel 1911). The numbers of scalids per row differ between 50 (Storch et al. 1994) and 60 (De Guerne 1891) and the number of scalids per series varies between two and seven (Storch et al. 1994). Very likely, scalids are added constantly. The presence of scalid-like structures between pharyngeal teeth and scalids has already been mentioned by Théel (1911) and is confirmed here. These may be called buccal papillae, but see the discussion under *Priapulopsis australis*.

Baird (1868) described the trunk annuli to have a smooth surface with 'sharp spines' (= trunk papillae) being present. De Guerne (1891) added the observation of posterior warts and assumed that they contain glandular openings. Although the presence of posterior warts is recognised as an important difference between the genera *Priapulus* (present) and *Priapulopsis* (absent) (Van der Land 1970), they were never described in detail. Van der Land (1972) notes that posterior warts can be very few, small and sometimes hard to observe, which is probably the reason that they were not figured (neither for *P. caudatus* nor for *P. tuberculatorspinosus*) by Storch et al. (1994). The structure observed by us differs from trunk papillae, but it should be checked by further investigations whether the bristles on the surface represent the undamaged surface or not. Ring papillae, meaning rings of elongate papillae on posterior trunk annuli, were not reported for *P. tuberculatospinosus* before, but few specimens investigated here clearly have an accumulation of papillae on the last rings before the posterior warts, which could therefore be ring papillae. However, the absence of such ring papillae in other specimens and especially on specimens investigated by SEM makes it worth placing special attention on this character in future investigations.

The fine structure of the caudal appendage has not been investigated before, but spinulets on the vesicles can be seen to some extent also by light microscopy. Van der Land (1970) sees one difference between the genera *Priapulus* and *Priapulopsis* in the distribution of spinulets, which are reported to be scattered over the entire vesicle (*Priapulus*) or concentrated apically (*Priapulopsis*). As was shown in *P. australis*, this is not correct for *Priapulopsis* and a scattered presence of spinulets must be assumed for both genera.

Priapulopsis papillatus nov. spec. as a new species

Identifying priapulids is sometimes not easy, because characters change during postlarval development, may appear different due to variable states of contraction and may even

vary intraspecifically. Postlarval development is fragmentary known for some species and almost unknown for others. Fine structural (SEM) investigations add new characters to the ones known from light microscopical investigations. Taking all this into account, the description of new species should be made with some caution. Gene comparisons (DNA barcoding) would be a helpful addition but was not tried here because the material had been stored in formalin.

Nevertheless, we find that the two specimens 63408 and 63448 differ in a number of characters from other priapulids and regard the sum of these characters as convincing enough to describe them as a new species, despite their low number (two specimens) and the fact that not all parts of the body could be described with the same quality.

The possession of 10 small pharyngeal teeth in the first ring and of two caudal appendages indicates that *P. papillatus* nov. spec. belongs to the genus *Priapulopsis*.

The holotype is a long and slender worm, quite different from the usual body shapes of other preserved priapulids. However, the paratype is more compact and resembles other priapulids. The bulbous introvert of the paratype is regarded here as an artifact, probably due to high internal pressure from the body cavity fluid.

The introvert is everted much stronger in the holotype than in any other of the priapulids investigated here. Usually only a few anterior rings of pharyngeal teeth are visible and observations on live animals of macroscopic priapulids (*Priapulus caudatus*) by the authors confirm this. An artificially everted pharynx is sometimes observed in meiobenthic priapulids (e.g. Schmidt-Rhaesa et al. 2013, 2017) and is thought to be an artifact of preservation (Schmidt-Rhaesa et al. 2017). Whether or not *P. papillatus* nov. spec. is able to extend its pharynx so strongly in vivo must remain an open question. There are differences in the fine structure of the first-ring teeth of *P. papillatus* nov. spec. and the two other *Priapulopsis* species, *P. australis* and *P. bicaudatus* as the first species has blunt cusps and the others mainly pointed cusps (this investigation, Schmidt-Rhaesa and Raeker 2023). Tooth receptors are present on the first ring teeth but were not found on other teeth. This is another difference to *P. australis* and *P. bicaudatus*, where tooth receptors are also present on other teeth (this investigation, Schmidt-Rhaesa and Raeker 2023). Teeth of ring 3 are the largest in all three species. In *P. australis*, there is a distinct morphological difference between teeth of rings 2–4 and the posterior teeth, as the first ones are cuspidate teeth with a dominant central cusp, while the posterior teeth are still cuspidate, but with a very small central cusp (this investigation). *Priapulopsis bicaudatus* has six rings of large cuspidate teeth, before teeth get smaller in the posterior rings (Schmidt-Rhaesa and Raeker 2023). In *P. papillatus* nov. spec., the central cusp in ring 5 and posterior is also smaller than in ring 4, but not as small as in *P. australis* and the size of the central cusp decreases very gradually in *P. papillatus* nov. spec. Nevertheless, such differences may also be dependent of the developmental stage of the specimen.

Although not observable in the best quality, there seems to be a strong difference in the arrangement of scalids, as series were not observed in *P. papillatus* nov. spec. This is a very surprising observation, as series are present in all *Priapulopsis* species. The scalids themselves appear to be of a structure comparable to *P. australis* and *P. bicaudatus* (this investigation, Schmidt-Rhaesa and Raeker 2023), with anteriormost telescopic scalids and posterior cone-like scalids.

The surface of the trunk annuli in *P. papillatus* nov. spec. is completely different from the two other *Priapulopsis* species due to the absence of tumuli. Instead, the cuticular pattern is very peculiar. As *P. papillatus* nov. spec. clearly belongs to the genus *Priapulopsis*, the presence of tumuli cannot currently be regarded as characteristic for the entire genus anymore. Trunk papillae are present and structurally comparable in all three investigated species, but their abundance, size and arrangement in rings is peculiar and even the first eye-catching character in *P. papillatus* nov. spec. This is the reason why we have chosen the species name '*papillatus*'. Trunk papillae seem to have quite some morphological range concerning their apical structure, but the present observations are still snapshots and more investigations from further specimens would be desirable.

The number of rings of ring papillae is higher than in *P. australis* and *P. bicaudatus* (this investigation, Schmidt-Rhaesa and Raeker 2023) and also the flaps in the posterior ring papillae are peculiar to *P. papillatus* nov. spec. In addition, trunk papillae on annuli posterior of the ring papillae appear to be absent in *P. australis* and *P. bicaudatus* (this investigation, Schmidt-Rhaesa and Raeker 2023), but present in *P. papillatus* nov. spec. Their regular, ring-like distribution makes them different from posterior warts, therefore these structures are assumed to be trunk papillae rather than posterior warts. Further differences may be present in the structure of the vesicles of the caudal appendage, but this appears to be too uncertain to be further discussed here.

Taken together, there are a number of characters that are different between *P. australis, P. bicaudatus* and *P. papillatus* nov. spec. Most of the fine-structural characters were only observed in the holotype, but checked as much as possible by light microscopy in the paratype. Even if some characters turn out to be specimen-specific, we regard the number of differences as convincing enough to describe *P. papillatus* nov. spec. as a new species. In summary, the differences or characteristic features of *P. papillatus* nov. spec. are:

- First ring teeth with blunt cusps
- Longer central cusp in teeth of ring 5 and posterior
- Absence of tooth receptors except for ring 1 teeth
- Scalids not arranged in series
- Trunk surface structure compartments with radial ridges and not tumuli
- Regularly arranged large and abundant trunk papillae
- Larger number (up to 5) of rings of ring papillae
- Flaps on posterior ring papillae
- Trunk papillae present posterior of ring papillae

Diagnosis of the genus *Priapulopsis*

Because the description of *P. papillatus* nov. spec. has implications on the diagnosis of the genus *Priapulopsis*, we provide here an emended diagnosis of this genus:

Genus *Priapulopsis* Koren & Danielssen, 1875: Macroscopic priapulids. First ring of pharyngeal teeth consisting of 10 small teeth, at least rings 2–5 consisting of five cuspidate teeth. Tooth receptors present at least on the first ring teeth. Some scalids composed of two parts (telescopiform). Trunk cuticle either covered with small projections (tumuli)

or with small compartments containing radiating ridges. Trunk papillae and ring papillae are present, posterior warts are absent. Caudal appendage paired.

Additional remark on morphology

All-in-all our SEM observations show that priapulids are strongly receptive animals. As has been mentioned in the general description at the beginning of the results section, the term 'receptor' is here applied very broadly to structures composed of a basis and an apical tube. Such structures are present along the entire body: as tooth receptors, as scalids, on trunk papillae, ring papillae and as spinulets on the caudal appendage. The exact fine structure differs, but the main structure remains. Sometimes the apical margin of the tube shows flower petal-like extensions, which is characteristic for flosculi. Flosculi were found in larvae and adults of all meiobenthic priapulids (Lemburg 1995), but are only reported in larvae and (young) adults of *Halicryptus spinulosus* and *Priapulus caudatus* for macroscopic species (Adrianov and Malakhov 1996). While in larvae of macroscopic species the flosculi can occur as own structures on the neck region and lorica (Storch and Higgins 1991; Higgins et al. 1993; Lemburg 1995; Adrianov and Malakhov 1996), the flosculi in the respective adults only occur in connection with other structures, e.g. on the tip of scalids as one of the types of receptors in *P. caudatus* (Schmidt-Rhaesa 2013) or next to papillae in the posterior trunk in *H. spinulosus* (Adrianov and Malakhov 1996). Recent external investigations of *Priapulopsis bicaudatus* did not report any flosculus-like structures (Schmidt-Rhaesa and Raeker 2023). Here, we also did not observe any flosculus-like structures for *Priapulopsis australis*. For *Priapulopsis papillatus* nov. spec., we only found flosculi associated with tubuli on trunk papillae and not as individual structures. Storch et al. (1994, 1995) have shown that the ultrastructure of the structures called receptive here indeed is the characteristic structure of a receptor with a receptive cilium.

Larvae

The larvae strongly resemble those described for *Priapulopsis bicaudatus* (see Schmidt-Rhaesa and Raeker 2023). The shape and arrangement of scalids corresponds almost exactly, and the only very slight differences may be that the fringe is a bit more extensive in the New Zealand larvae compared to the *P. bicaudatus* larvae. In *P. bicaudatus* larvae, the bipartition of the first ring of pharyngeal teeth is already indicated by a groove (Schmidt-Rhaesa and Raeker 2023). It would have been interesting to observe whether this is also the case in the New Zealand larvae. The closing apparatus of the lorica also corresponds to that of *P. bicaudatus* larvae (Sanders and Hessler 1962, Schmidt-Rhaesa and Raeker 2023) in having two frontal plates. Laterofrontal plates were not observed in the New Zealand larvae, but this may be due to suboptimal preservation rather than absence of these plates. Differences between the New Zealand larvae and the *P. bicaudatus* larvae exist in the shape and the sculpture of the dorsoventral plates. Both larvae have an orthogonal pattern of longitudinal and transversal ridges, but in the *P. bicaudatus* larvae only the median longitudinal ridge runs the entire lorica length, while the other longitudinal ridges fade out. The posterior margin of the

P. bicaudatus lorica narrows more gradually and does not create a distinct narrow posterior endpiece as in the New Zealand larvae.

Larvae of *P. australis* were described and illustrated by drawings by Adrianov and Malakhov (1996) for New Zealand and by Schmidt-Rhaesa and Freese (2019) for Antarctic larvae. The larvae from Adrianov and Malakhov (1996) are the only larvae reported from New Zealand. Their assignment to *P. australis* is only made by their co-occurrence. Characteristic for the *P. australis* larva is a zig-zag-pattern of the median ridge on the lorica. This is also present in the larvae reported here, but not as distinct as in the other records.

In summary, it seems very likely that the larvae belong to the genus *Priapulopsis*, but a clear assignment to *P. australis* is made difficult due to the description of *P. papillatus* nov. spec. Only the relative abundance of *P. australis* makes it likely that the larvae belong to this species.

The New Zealand priapulid fauna

There are different views on which species of Priapulida are present in New Zealand (Schmidt-Rhaesa in press). The first priapulid from New Zealand was reported by Benham (1932). This and the second report by Dell (1955) were stated to be *Priapulus tuberculatospinosus*, which was later doubted (Van der Land 2010). Certainly present in New Zealand is *Priapulopsis australis*, first reported by Hurley (1962) and later from Murina and Starobogatov (1961), Estcourt (1967), Storch et al. (1995), Adrianov and Malakhov (1996) and Van der Land (2010). Two further species are regarded as uncertain (Schmidt-Rhaesa in press): *Priapulus abyssorum* (Menzies, 1959) and *Acanthopriapulus horridus* (Théel, 1911). The first is a postlarval specimen from 3,013 m depth in Hikurangi Trench, mentioned as *P. tuberculatospinosus abyssorum* in Murina and Starobogatov (1961). As this is not an adult specimen, it is very difficult to assign it to a certain species (Van der Land 2010). The second is a rare species (Schmidt-Rhaesa et al. 2022), and the figures in Adrianov and Malakhov (1996) do not correspond to the description of this species (Schmidt-Rhaesa in press). A further, meiobenthic species is mentioned by Van der Land (2010), but on closer investigation it turned out to be a sipunculid (B. Neuhaus, personal communication).

Our results confirm the presence of at least three species of priapulids in New Zealand. While the presence of *P. australis* is no surprise, we can now confirm that *P. tuberculatospinosus* belongs to the New Zealand priapulid fauna. The description of *P. papillatus* nov. spec. shows, that even macroscopic priapulids can still be discovered and the total diversity of priapulids may be larger than currently known (22 species including *P. papillatus*).

Van der Land (2010) states that all priapulids in the NIWA collection are *P. australis*. Compared with the present investigation this statement is surprising. Probably Van der Land has seen not all, but only a fraction of the NIWA material. His name is included in the data spreadsheet for 40 catalogue numbers. Specimens for the present investigation were chosen to largely exclude the specimens Van der Land has seen and only three of 'his' specimens (162905, 162906, 162907) were investigated. The first two of these numbers were found to be unidentified non-priapulid worms, only 162907 is *P. australis*.

Priapulids occur in collections in different shapes, due to different developmental stages, different states of introvert eversion or varying amounts of contraction. This makes them difficult to recognise and easy to confuse with other introvert-bearing organisms, especially sipunculids. This explains why only about one third of the worms labelled as priapulids in the NIWA collection were actually priapulids.

Conclusions

Three species of Priapulida occur in the waters around New Zealand: *Priapulopsis australis*, *Priapulus tuberculatospinosus* and *Priapulopsis papillatus* nov. spec. These are characterised externally, providing a basis for comparison for further records. One of the species, *P. papillatus*, is endemic to New Zealand. Additionally, larvae of presumably *P. australis* are reported and described.

Acknowledgements

The authors express their deep thanks to Michelle Kelly and Sadie Mills for making part of the NIWA collection available for investigation, and to Richard Taylor for supplying new specimens.

Disclosure statement

No potential conflict of interest was reported by the authors.

Funding

No third-party funding was used for this investigation.

ORCID

Jan Raeker http://orcid.org/0000-0002-5387-5471

References

Adrianov AV, Malakhov VV. 1996. Priapulida: structure, development, phylogeny, and classification. Moscow: KMK Scientific Press. [In Russian with English summary].

Adrianov AV, Malakhov VV. 2001a. Symmetry of priapulids (Priapulida). 1. Symmetry of adults. J Morphol. 247:99–110. doi:10.1002/1097-4687(200102)247:2<99::AID-JMOR1005>3.0.CO;2-0.

Adrianov AV, Malakhov VV. 2001b. Symmetry of priapulids (Priapulida). 2. Symmetry of larvae. J Morphol. 247:111–121. doi:10.1002/1097-4687(200102)247:2<111::AID-JMOR1006>3.0.CO;2-C.

Baird W. 1868. Monograph of the species of worms belonging to the subcalss Gephyrea; with notice of such species as are contained in the collection of the British Museum. Proc Zool Soc London.1868:76–114.

Benham WB. 1932. *Priapulus caudatus* in New Zealand waters. Nature. 130:890–890. doi:10.1038/130890a0.

De Guerne J. 1886. Sur les Gèphyriens de la famille des Priapulides recueillis par la mission de Cap horn. C R Seances Acad Sci. 103:760–762.

De Guerne J. 1891. Priapulides. In: Ministéres de la Marine et de l´instruction publique. Mission scientifique de Cap Horn 1882-1883. Vol.VI Zoologie, part 13. Gauthier-Villars et fils, Paris; p. 3-20. In: Tome VI Zoologie, 13e partie. p. 3–20.

Dell RK. 1955. The occurrence of *Priapulus* in New Zealand waters. Trans R Soc New Zealand. 82:1129–1133.

Estcourt IN. 1967. Distributions and associations of benthic invertebrates in a sheltered water soft-bottom environment (Marlborough Sounds, New Zealand). New Zealand J Mar Freshw Res. 1:352–370. doi:10.1080/00288330.1967.9515211.

Higgins RP, Storch V, Shirley TC. 1993. Scanning and transmission electron microscopic observations on the larva of *Priapulus caudatus* (Priapulida). Acta Zool. 74:301–319. doi:10.1111/j.1463-6395.1993.tb01245.x.

Hurley DE. 1962. A second species of *Priapulus* from New Zealand waters. New Zealand J Sci. 5:13–16.

Janssen R, Wennberg S, Budd GE. 2009. The hatching larva of the priapulid worm *Halicryptus spinulosus*. Front Zool. 6:8. doi:10.1186/1742-9994-6-8.

Lang K. 1951. *Priapulus caudatus* Lam. and *Priapulus caudatus* forma *tuberculato-spinosus* Baird represent two different species. Ark Zool. 2:565–568.

Lemburg C. 1995. Ultrastructure of sense organs and receptor cells of the neck and lorica of the *Halicryptus spinulosus* larva (Priapulida). Microfauna Marina. 10:7–30.

Menzies RJ. 1959. *Priapulus abyssorum*, new species, the first abyssal priapulid. Nature. 184:1585–1586. doi:10.1038/1841585a0.

Michaelsen W. 1889. Die Gephyreen von Süd-Georgien nach Ausbeute der Deutschen Station von 1882-1883. Jahrbuch Hamburger Wiss Anst. 6:41–51.

Murina VV, Starobogatov JI. 1961. [Classification and zoogeography of Priapuloidea]. Trudy Inst Okeanol. 46:178–200. [In Russian].

Sanders HL, Hessler RR. 1962. *Priapulus atlantisi* and *Priapulus profundus*. Two new species of priapulids from bathyal and abyssal depth of the North Atlantic. Deep-Sea Res. 9: 125–130.

Schmidt-Rhaesa A. 2013. Priapulida. In: Schmidt-Rhaesa A, editor. Handbook of Zoology: Nematomorpha, Priapulida, Kinorhyncha and Loricifera. Vol. 1. Berlin: Walter de Gruyter; p. 147–180.

Schmidt-Rhaesa A, Canete JI, Mutschke E. 2022. New record and first description including SEM and µCT of the rare priapulid *Acanthopriapulus horridus* (Priapulida, Scalidophora). Zool Anz. 298:1–9. doi:10.1016/j.jcz.2022.03.001.

Schmidt-Rhaesa A, Freese M. 2019. Microscopic priapulid larvae from Antarctica. Zool Anz. 282:3–9. doi:10.1016/j.jcz.2019.06.001.

Schmidt-Rhaesa A. in press. Kingdom Animalia, phylum Priapulida (priapulid worms). In: Kelly M, Mills S, Nelson W, Terezow M, editor. The marine fauna of New Zealand - Marine biota 2023: updating the New Zealand inventory of marine biodiversity. NIWA Biodiversity Memoir Series; p. 472–475.

Schmidt-Rhaesa A, Panpeng S, Yamasaki H. 2017. Two new species of *Tubiluchus* (Priapulida) from Japan. Zool Anz. 267:155–167. doi:10.1016/j.jcz.2017.03.004.

Schmidt-Rhaesa A, Raeker J. 2023. Morphology of larval and postlarval stages of Priapulopsis bicaudatus (Danielssen, 1869) (Priapulida) from the North Atlantic Ocean. Zool Anz. 302:1–16. doi:10.1016/j.jcz.2022.11.006.

Schmidt-Rhaesa A, Rothe BH, García Martínez A. 2013. *Tubiluchus lemburgi*, a new species of meiobenthic Priapulida. Zool Anz. 253:158–163. doi:10.1016/j.jcz.2013.08.004.

Storch V, Higgins RP. 1991. Scanning and transmission electron microscopic observations on the larva of *Halicryptus spinulosus* (Priapulida). J. Morphol. 210:175–194. doi:10.1002/jmor.1052100207.

Storch V, Higgins RP, Anderson P, Svavarsson J. 1995. Scanning and transmission electron microscopic analyses of the introvert of *Priapulopsis australis* and *Priapulopsis bicaudatus* (Priapulida). Invertebr Biol. 114:64–72. doi:10.2307/3226954.

Storch V, Higgins RP, Malakhov VV, Adrianov AV. 1994. Microscopic anatomy and ultrasructure of the introvert of *Priapulus caudatus* and *P. tuberculatospinosus* (Priapulida). J Morphol. 220:281–293. doi:10.1002/jmor.1052200307.

Théel H. 1911. Priapulids and Sipunculids dredged by the Swedish Antarctic expedition 1901–1903 and the phenomen of bipolarity. Kungl Svenska Vet Akad Handl. 47:3–36.

Van der Land J. 1970. Systematics, geography, and ecology of the Priapulida. Zool Verhand Leiden. 112:1–118.

Van der Land J. 1972. *Priapulus* from the deep sea. Zool Mededel Leiden. 47:358–368.

Van der Land J. 2010. Phylum Priapulida, penis worms. In: Gordon DP, editor. New Zealand inventory of biodiversity: Volume 2. Kingdom Animalia, Chaetognatha, Ecdysozoa, ichnofossils. Christchurch: Canterbury University Press; p. 476–479.

Wennberg SA, Janssen R, Budd GE. 2009. Hatching and earliest larval stages of the priapulid worm *Priapulus caudatus*. Invertebr Biol. 128:157–171. doi:10.1111/j.1744-7410.2008.00162.x.

Molecular Phylogenetics and Evolution 204 (2025) 108297

Contents lists available at ScienceDirect

Molecular Phylogenetics and Evolution

journal homepage: www.elsevier.com/locate/ympev

The big, the small and the weird: A phylogenomic analysis of extant Priapulida

Jan Raeker [a], Arianna Lord [b], María Herranz [c,d,e], Gonzalo Giribet [b], Katrine Worsaae [e,*], Andreas Schmidt-Rhaesa [a,*]

[a] Museum of Nature Hamburg - Zoology, Leibniz Institute for the Analysis of Biodiversity Change (LIB) and University Hamburg, Martin-Luther-King-Platz 3 20146 Hamburg, Germany
[b] Museum of Comparative Zoology, Department of Organismic and Evolutionary Biology, Harvard University, 26 Oxford Street, Cambridge, MA 02139, USA
[c] Department of Biology and Geology, Physics and Inorganic Chemistry, Rey Juan Carlos University, Tulipán s/n, 28933 Móstoles, Madrid, Spain
[d] Global Change Research Institute (IICG-URJC), Rey Juan Carlos University, Spain
[e] Marine Biological Section, Department of Biology, University of Copenhagen, Universitetsparken 4, 2100 Copenhagen Ø, Denmark

ARTICLE INFO

Keywords:
Priapulida
Phylogeny
Transcriptome
Genome skimming
Bioinformatics
Morphology

ABSTRACT

Priapulida is a small phylum of 22 described species that are divided into two size classes (microscopic and macroscopic), distinguished by adult and larval morphology. Most priapulidans are rare or live in inaccessible habitats, and freshly collected material for molecular studies is difficult to obtain. With this study, we for the first time aim to resolve the phylogeny of extant Priapulida using transcriptomic, genomic, and morphological data. We analyze six newly assembled transcriptomes alongside existing data, covering seven species and four genera. Additionally, we include genomic data from museum-preserved species, adding another genus via low-coverage genome sequencing. Conserved regions from these data produce a combined phylogenomic tree, augmented by morphological data to suggest positions for the rare taxa *Acanthopriapulus* and *Maccabeus*. Our findings show that the microscopic *Meiopriapulus* consistently groups as a sister taxon to other priapulidans and not with *Tubiluchus*, as suggested in previous studies. *Maccabeus*, which exhibits both size-class characteristics, is the sister taxon to all the macroscopic species, while *Acanthopriapulus* is a sister taxon to *Priapulus*, but molecular data are needed to support their suggested positions. Ancestral state reconstruction suggests that small body size, lack of caudal appendages, and internal fertilization are ancestral traits for Priapulida. This supports the derived evolution of macroscopic size and other traits in the group, aligning with its microscopic sister groups Kinorhyncha and Loricifera. Due to the diversity of priapulidans and the unique morphologies of some species, further fossil studies and potential discoveries of priapulidan microfossils are essential to fully understand the evolutionary history of this phylum.

1. Introduction

Priapulida is the smallest phylum of Ecdysozoa with only 22 valid, described species nested in seven genera (Schmidt-Rhaesa and Raeker, 2024) including both microscopic and macroscopic species. Morphologically they group with the meiofaunal phyla Kinorhyncha and Loricifera, together constituting Scalidophora, characterized by the possession of an introvert with scalids (Nielsen, 2012). Scalidophora is often supported in molecular analyses, yet with unclear sister group relationships (e.g., Giribet and Edgecombe, 2017; Laumer et al., 2019; Howard et al., 2022), and studies not supporting Scalidophora also exist (e.g., Park et al., 2006; Yamasaki et al., 2015). Molecular analyses have proposed different relationships of Priapulida within Ecdysozoa, however, always placed outside Panarthropoda (Giribet and Edgecombe, 2017), and sometimes as a sister group to all remaining ecdysozoans (Laumer et al., 2019). Hence, understanding the evolution of Priapulida and the origin of different body sizes and morphologies within the group will impact broader hypotheses on Ecdysozoan evolution.

Despite the small number of priapulidan (see 4.2. on classification) species, no molecular and only few morphologically-based attempts have been made to resolve the phylogeny of Priapulida. von Salvini-Plawen (1974) and Adrianov and Malakhov (1996) (Fig. 1A), both

* Corresponding authors.
E-mail addresses: j.raeker@leibniz-lib.de (J. Raeker), ariannalord@g.harvard.edu (A. Lord), maria.herranz@urjc.es (M. Herranz), ggiribet@g.harvard.edu (G. Giribet), kworsaae@bio.ku.dk (K. Worsaae), a.schmidt-rhaesa@leibniz-lib.de (A. Schmidt-Rhaesa).

https://doi.org/10.1016/j.ympev.2025.108297
Received 21 November 2024; Received in revised form 25 January 2025; Accepted 27 January 2025
Available online 28 January 2025

proposed the genus *Maccabeus* Por, 1972 (two species, as Chaetostephanidae von Salvini-Plawen, 1974) as sister group to the remaining Priapulida. However, the meiofaunal genus *Tubiluchus* Van der Land, 1968 (10 species, as Tubiluchidae Van der Land, 1970) is placed either as sister group to the clade of macroscopic genera (*Priapulus* Lamarck, 1816 [3 species], *Priapulopsis* Koren and Danielssen, 1875 [3 species], *Acanthopriapulus* Van der Land, 1970 [one species] and *Halicryptus* Von Siebold, 1849 [2 species]) (von Salvini-Plawen, 1974), or as sister group to Priapulidae Gosse, 1855 (*Priapulopsis*, *Priapulus*, *Acanthopriapulus*) (Adrianov and Malakhov, 1996). However, von Salvini-Plawen's (1974) studies lack *Meiopriapulus* as it was not described at that time, and some analyzed morphological data were outdated (e.g., number of scalid rows in *Tubiluchus* [20 instead of 25 rows; e.g., Calloway, 1975]; absence of lorica tubuli in *Halicryptus* larvae [minute lorica tubuli are present; see Storch and Higgins, 1991; Janssen et al., 2009]). In other studies that include fossil species (e.g., Wills, 1998; Lemburg, 1999; Dong et al., 2004; 2005; 2010; Harvey et al., 2010; Wills et al., 2012), the two meiofaunal genera *Tubiluchus* and *Meiopriapulus* constitute a monophyletic group, being sister clade to the remaining macroscopic genera and to the microscopic *Maccabeus* (Fig. 1B). Due to the inconsistent placement of certain groups and the limited morphological characters available for cladistic analysis, further approaches including molecular data are needed to solve the phylogeny within Priapulida.

Molecular analyses that include priapulidans, whether based on a few genes or transcriptomes, are scarce and rarely involve more than one species. Only few species have been included in large phylogenetic analyses not focussing directly on Priapulida (e.g., Giribet et al., 2000; Sørensen et al., 2008; Laumer et al., 2015; 2019). Recently, single gene analyses of different *Priapulus caudatus* Lamarck, 1816 (see Kolbasova et al., 2023) and *Halicryptus spinulosus* Von Siebold, 1849 (see Raeker et al., 2024a) populations have been conducted. Publicly available data on GenBank include single genes (e.g., Sørensen et al., 2012; Schmidt-Rhaesa et al., 2017), transcriptomes (e.g., Martín-Durán et al., 2012; Borner et al., 2014; Cannon et al., 2016), as well as the genomes of *P. caudatus* and, more recently, of the microscopic *Tubiluchus corallicola* Van der Land, 1968 (see Lord et al., 2023). Therefore, new molecular data for additional priapulidan species are needed to generate a molecular based phylogeny of Priapulida.

Two genera, *Acanthopriapulus* and *Maccabeus*, and 12 species across the remaining genera, lack molecular data entirely. The access to many of these species is limited, as some are extremely rare or are only known by few specimens from remote locations (e.g., Por and Bromley, 1974; von Salvini-Plawen, 1974) Malakhov, 1978; Van der Land, 1985; Adrianov et al., 1989; Adrianov and Malakhov, 1991; Schmidt-Rhaesa et al., 2022). In addition, museum specimens are often old and/or preserved in formalin, which leads to DNA fragmentation and cross-linking with proteins, resulting in short sequence fragments (Campos and Gilbert, 2012). Employing methods to generate genomic data from priapulidan specimens from museum collections or not ideally preserved specimens could help to expand the molecular sequence library of Priapulida.

The shallow short-read sequencing method 'genome skimming' allows deep sequencing of the high-copy fraction of the genome (Straub et al., 2012; Dodsworth, 2015). In this method, fragmented DNA is aligned to a reference genome, allowing the usage for phylogenomic analyses (Dodsworth, 2015). Genome skimming has been used in studies on fresh and museum stored samples of vertebrates (e.g., Literman et al., 2023), invertebrates (e.g., Taite et al., 2023) and plants (e.g., Fu et al., 2022). In addition to genome skimming, low-coverage genome sequencing – such as 2x, 5x, 10x or 20x short read coverage – has emerged as a viable method for phylogenomics (Zhang et al., 2019; Ribeiro et al., 2021; Godeiro et al., 2023). These methodologies could contribute to building a molecular phylogeny of Priapulida with existing museum specimens not amenable for PCR amplification.

Priapulidans differ very much in their adult body size, as they are either macroscopic (up to 40 cm; Fig. 2A and B) or microscopic (up to 3 mm excluding the tail; Fig. 2C and D). Hypotheses on the ancestral body size of Priapulida strongly depend on their phylogeny, on outgroup comparison and on the fossil record. The two other taxa within Scalidophora, Loricifera and Kinorhyncha, include exclusively small representatives, but it remains unresolved which of the two taxa, or if both, are the sister group to Priapulida (Giribet and Edgecombe, 2017; 2020; Worsaae et al., 2023). While the fossil record of priapulidans includes only specimens of macroscopic size, it is not always clear which of the priapulidan-like fossils belong to the priapulidan stem lineage and which might represent earlier lineages (e.g., Conway Morris and Robison, 1986; Huang et al., 2004a; Hu et al., 2017). The record of macroscopic fossils may be a preservation or sampling bias. Meiofaunal fossils are found rarely, but exist, as demonstrated by the finding of Cambrian Loricifera (Harvey and Butterfield, 2017) or of the Middle Cambrian *Markuelia* (Dong et al., 2004). For Kinorhyncha, potential questionable stem group fossils were described within meiofaunal size (Zhang et al., 2015; Shao et al., 2020), but undescribed kinorhynch-like fossils of macroscopic size have also been reported (Fu et al., 2019). Due to these uneven reports within Scalidophora, the ancestral body size of Priapulida remains unclear.

Besides body size, further morphological differences occur across and within both size classes of priapulidans, e.g., presence or absence of a posterior appendage (Fig. 2A–D), the type of pharyngeal teeth (Fig. 2E and F), the arrangement of scalids, presence of sensory structures on the body surface, or the presence and appearance of larva (Fig. 2G and H) (Van der Land, 1970; Schmidt-Rhaesa, 2013a; see Supplementary File 2). While most morphological specifications are unique to their respective size class, some species exhibit characters from the other size class or hold completely different characters. For example, microscopic *Maccabeus tentaculatus* Por, 1972 has cuspidate pharyngeal teeth and its larval stages are dorsoventrally flattened (Por and Bromley, 1974), which are characters usually found in macroscopic species (Schmidt-Rhaesa, 2013a). In contrast, the arrangement of scalids or sensory structures on the introvert potentially represent autapomorphies of *Maccabeus* (see Por and Bromley, 1974). Especially, morphological structures on the circumoral field (e.g., the area between the

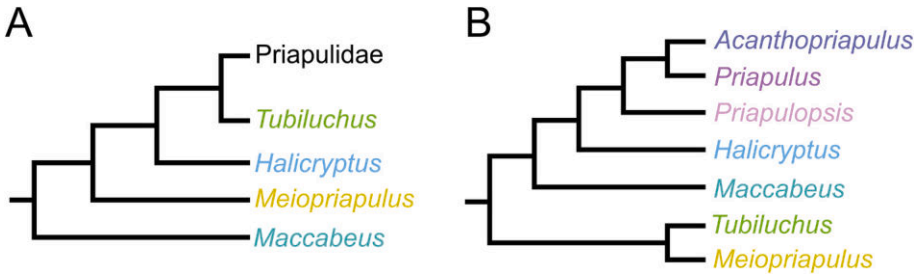

Fig. 1. Simplified phylogenies of extant Priapulida based on morphological data of previous studies. A. Proposed phylogeny by Adrianov and Malakhov (1996). Note that Priapulidae excludes Halicryptus. B. Proposed phylogeny (modified by excluding fossils) by Wills (1998), Lemburg (1999), Dong et al. (2004); Dong et al. (2005); Dong et al. (2010), Harvey et al. (2010) and Wills et al. (2012).

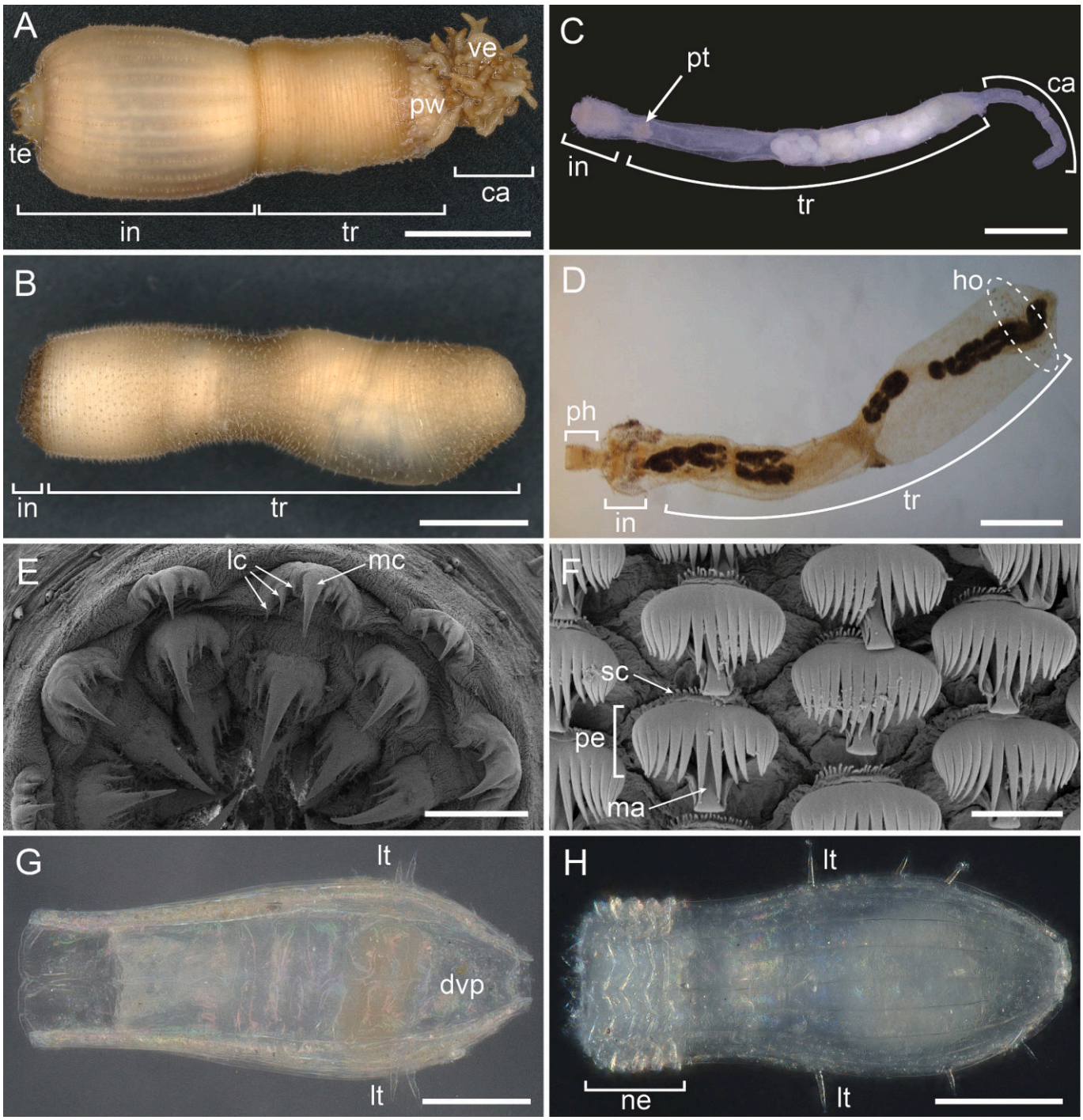

Fig. 2. Morphology of macroscopic (A,B,E,G) and microscopic (C,D,F,H) Priapulida, light microscopical (A-D,G,H) and SEM (E,F) images. A. *Priapulus caudatus* from the White Sea with everted introvert (in) showing pharyngeal teeth (te). B. *Halicryptus spinulosus* from the White Sea with a slightly inverted introvert. C. *Tubiluchus* sp. from Holguin, Cuba. D. *Meiopriapulus fijiensis* from Jeju Island, South Korea with presumably artificially everted pharynx (ph). E. Cuspidate pharyngeal teeth of *P. caudatus* from Gullmarsfjord, Sweden. F. Pectinate pharyngeal teeth of *T. lemburgi* from Tenerife. G. Larval stage of *P. caudatus* from Gullmarsfjord, Sweden. H. Larval stage of *T. lemburgi* from Tenerife with everted neck region (ne). Image D kindly provided by Martin V. Sørensen (Natural History Museum of Denmark). Abbreviations: ca, caudal appendage; dvp, dorso-ventral plate; ho, ring of hook structures; lc, lateral cusp; lt, lorica tubuli; ma, manubrium; mc, median cusp; pe, pecten; sc, secondary comb; tr, trunk; pt, polythyridium; pw, posterior warts; ve, vesicles. Scale bars: A, B = 5 mm; C-E = 500 μm; H = 100 μm; F = 5 μm.

pharyngeal teeth and scalids), and sensory structures on the trunk, are generally not easy to homologize between species. In addition, reinvestigation of specimens has produced a number of new, sometimes previously unknown details (e.g., Sørensen et al., 2012; Schmidt-Rhaesa and Raeker, 2023; 2024; Raeker et al., 2024a; 2024b). There is still a lack of knowledge about many morphological characters in Priapulida, and thus, their character evolution remains unclear.

In this study, we try to clarify the internal phylogeny of Priapulida by combining two different molecular approaches: transcriptomics and genomics. The transcriptomic approach should help to specify the backbone of the phylogeny, given the large number of genes typically used in phylotranscriptomic approaches, but this approach is limited by the availability of fresh samples. With the genomic approach, we add ethanol-preserved specimens to the transcriptomic backbone by

extracting conserved regions from low coverage whole genome sequencing data. In addition, morphological characters of included species are coded based on literature and traced on the combined phylogenomic tree, aiming to place the two genera lacking molecular data and shed light on discussions about body size and character evolution within Priapulida.

2. Material and methods

2.1. Taxon sampling

Specimens from nine species of four genera were obtained from different collection trips and museum collections, and their sequenced data analyzed together with publicly available sequence data from five ingroup and five outgroup taxa (transcriptomes and genomes) (Table 1).

For *de novo* transcriptome sequencing, six priapulidan species of three genera (*Halicryptus spinulosus*, *Priapulus caudatus*, *Tubiluchus corallicola*, *Tubiluchus lemburgi* Schmidt-Rhaesa, Rothe and Martínez, 2013, *Tubiluchus* sp. A [Cuba] and *Tubiluchus* sp. B [Turkey]) were sampled on different collection trips (Table 1). Specimens were preserved in RNA*later* and stored at − 80 °C until RNA extraction. Four publicly available transcriptomes of *P. caudatus*, *H. spinulosus* (by Cannon et al., 2016), *Meiopriapulus fijiensis* Morse, 1981 (by Laumer et al., 2019) and *T. corallicola* were added to the data set (Table 1).

For low coverage genome sequencing and conserved region recovery, ten priapulidan specimens from five genera were analyzed (Table 2). Sequences of four specimens (*T. lemburgi*, *Tubiluchus* sp. [Cuba], *Tubiluchus* sp. [Turkey], *M. fijiensis*) were extracted from transcriptomic data. Conserved loci were also extracted from fresh DNA from the same specimen of each of two species (*H. spinulosus* and *P. caudatus*, both from the White Sea; Table 1), from which new transcriptomes were generated. DNA extractions were also obtained from specimens of three other species (*Halicryptus higginsi* Shirley and Storch, 1999, *Priapulopsis australis* De Guerne, 1886 and *Priapulus tuberculatospinosus* Baird, 1868). These originated from museum collections (Table 1), and were stored in different concentrations of ethanol (70 % and 95 %). The publicly available genome of *T. corallicola* (by Lord et al., 2023) was also included in the conserved region analysis.

Some specimens did not yield sufficient data for locus recovery and were therefore not included in the downstream analyses. These include additional ethanol preserved specimens of *Priapulopsis bicaudatus* (Danielssen, 1869) (Faroe Island Ridge; Zoological Museum Hamburg catalog number: ZMH V13492), *P. caudatus* (Sweden; Museum of Comparative Zoology, Invertebrate Zoology catalog number: MCZ: IZ:135231), *P. tuberculatospinosus* (Chile; Schmidt-Rhaesa collection), *P. australis* (New Zealand; National Institute of Water and Atmospheric Research Invertebrate Collection catalog number: NIC 157950) and *H. spinulosus* (Beaufort Sea; Schmidt-Rhaesa collection).

As outgroups for both analyses, publicly available transcriptomes from two Kinorhyncha (Herranz et al., 2022), one Loricifera (Laumer et al., 2015) and one Nematomorpha (Laumer et al., 2019) were used. One additional nematomorph transcriptome (Cunha et al., 2023) was included in the genomic analysis.

Additional specimens from available collections or body parts from specimens used for DNA extractions were morphologically investigated with a Keyence VHX-7000 digital light microscope. Selected specimens were further prepared for scanning electron microscopy with a LEO SEM 1524 by dehydrating them in an increasing ethanol series, critical point drying with a Leica EM CPD300 and sputter coating with platinum in a Polaron SC7640 Sputter Coater.

2.2. Transcriptome analysis

2.2.1. Transcriptome sequencing and assembly

Scraped-off body wall tissue of the macroscopic species, trunks of adults and whole larvae of meiobenthic priapulidans were rinsed in ddH_2O of RNA*later* residues, transferred to a lysis buffer and incubated 3 min at 72 °C. cDNA synthesis and PCR amplification (16 cycles) were performed using the SMART®-Seq HT Kit (Takara Bio USA, Inc.) following the manufacturer's protocol. Amplified cDNA was purified

Table 1
Species used for phylogenomic analysis with data type, sampling location, data source and Sequence Read Archive (SRA) accession number. Bold highlighted rows show newly generated molecular data deposited under BioProject accession number PRJNA1185466. Data types: g, genome; gs, genome skimming data; t, transcriptome. Catalog numbers: MCZ:IZ, Museum of Comparative Zoology Harvard, Invertebrate Zoology; USNM, United States National Museum; ZMH, Zoological Museum Hamburg.

Phylum	Family	Species	Data type	Sampling location	Source/Catalog number	SRA accession number
Priapulida	Priapulidae	***Halicryptus higginsi***	**gs**	**Beaufort Sea, Point Barrow, USA**	**USNM 186062**	**SRR31406941**
		Halicryptus spinulosus	t	Askö, Sweden	Cannon et al. (2016)	SRR2682062
		Halicryptus spinulosus	**t/gs**	**Kislaya Bay, White Sea, Russia**	**this study**	**t: SRR31406948 gs: SRR31406939**
		Priapulopsis australis	**gs**	**Cape Rodney, New Zealand**	**ZMH V13673**	**SRR31406938**
		Priapulus caudatus	t	Skagerrak, Sweden	N/A (2015)	SRR1800229
		Priapulus caudatus	**t/gs**	**Kislaya Bay, White Sea, Russia**	**this study**	**t: SRR31406947 gs: SRR31406940**
		Priapulus tuberculatospinosus	**gs**	**Peter I Island, Antarctica**	**MCZ:IZ:141165**	**SRR31406946**
	Tubiluchidae	*Tubiluchus corallicola*	g	Castle Harbor, Bermuda	Lord et al. (2023)	JAQGDQ01
		***Tubiluchus corallicola* (A)**	**t**	**Curaçao**	**this study**	**SRR31406945**
		Tubiluchus corallicola (B)	t	Bocas del Toro, Panama	unpublished	SRR2131688
		Tubiluchus lemburgi	**t**	**Los Cerebros (marine cave), Tenerife, Spain**	**this study**	**SRR31406944**
		***Tubiluchus* sp. A**	**t**	**Playa Caletones, Cuba**	**this study**	**SRR31406943**
		***Tubiluchus* sp. B**	**t**	**Kas, Turkey**	**this study**	**SRR31406942**
	Meiopriapulidae	*Meiopriapulus fijiensis*	t	Jeju Island, South Korea	Laumer et al. (2019)	SRR9670664
Kinorhyncha	Campyloderidae	*Campyloderes vanhoeffeni*	t	Gulf of Naples, Italy	Herranz et al. (2022)	SRR14509480
	Dracoderidae	*Dracoderes abei*	t	Gamak Bay, South Korea	Herranz et al. (2022)	SRR14509486
Loricifera	Nanaloricidae	*Armorloricus elegans*	t	Roscoff, France	Laumer et al. (2015)	SRR2131253
Nematomorpha	Gordiidae	*Acutogordius australiensis*	t	New South Wales, Australia	Cunha et al. (2023)	SRR25036554
	Nectonematidae	*Nectonema munidae*	t	Bergen, Norway	Laumer et al. (2019)	SRR8618616

Table 2
Species used in the combined phylogeny with their BUSCO value (complete + partial), number of recovered loci per assembly and % Gap/Ambiguity. Data types: g, genome; gs, genome skimming data; t, transcriptome.

Species	Data type	BUSCO (complete + partial)	Total number of UCE loci matched (raw)	% Gap/Ambiguity in 70p alignment	% Gap/Ambiguity in 80p alignment	% Gap/Ambiguity in 90p alignment
Halicryptus higginsi	gs	126 (13.21 %)	606	73.17	65.54	20.86
Halicryptus spinulosus	gs	609 (63.84 %)	1459	20.52	17.99	18.6
Priapulopsis australis	gs	876 (91.82 %)	1369	6.71	6.13	3.14
Priapulus caudatus	gs	478 (50.10 %)	1312	29.81	27.44	21.65
Priapulus tuberculatospinosus	gs	869 (91.09 %)	1470	8.28	5.98	5.15
Tubiluchus corallicola	g	862 (90.36 %)	1483	8.9	6.16	5.70
Tubiluchus lemburgi	t	908 (95.18 %)	1115	6.44	1.66	1.37
Tubiluchus sp. A (Cuba)	t	707 (74.11 %)	1050	30.76	17.42	12.14
Tubiluchus sp. B (Turkey)	t	608 (63.73 %)	701	41.06	21.25	11.51
Meiopriapulus fijiensis	t	430 (45.07 %)	553	54.05	37.65	22.99
Campyloderes vanhoeffeni	t	885 (92.77 %)	1155	9.71	5.22	3.52
Dracoderes abei	t	928 (97.27 %)	1138	6.81	4.31	3.61
Armorloricus elegans	t	431 (45.18 %)	701	50.16	34.66	20.86
Acutogordius australiensis	t	720 (75.47 %)	1045	14.8	5.65	2.85
Nectonema munidae	t	725 (76.00 %)	1080	17.43	11.79	8.99

using the Agencourt AMPure XP Kit (Beckmann Coulter) followed by a concentration and quality-check using an Agilent 2100 Bioanalyzer (Agilent Biosciences). Dual index libraries were prepared using a Nextera XT DNA Kit (Illumina) with an input of 1 ng of cDNA followed by a clean-up (Agencourt AMPure XP Kit). Concentration and fragment size of the libraries were checked and subsequently sequenced in one lane of an Illumina NovaSeq 6000 system (150 bp paired-end) conducted by Azenta (Genewiz) Leipzig, Germany.

Samples had an average of 45 million raw reads, ranging from 23.1 to 89.1 million (Suppl. Table S1). The new sequence data were deposited in the NCBI sequence read archive (SRA) under the Bioproject number PRJNA1185466 (Table 1). Previously published transcriptomes had an average of 62.5 million raw reads, ranging from 13.1 to 243.2 million (Suppl. Table S1). New and previously published sequence data were processed with the same methods, as follows.

The quality of raw sequences was checked with FASTQC v.0.11.9 and trimmed using Trim Galore! v.0.6.5 (both on https://www.bioinformatics.babraham.ac.uk). Transcriptomes were *de novo* assembled using Trinity v.2.9.1 (Grabherr et al., 2011). Completeness of the assembled transcriptomes was checked against the BUSCO v.5.1.2 (Manni et al., 2021) metazoan library on the software gVolante v.2.0 (Nishimura et al., 2017) with default settings. Transcripts were translated to amino acids and candidates for coding regions (open reading frames with at least 100 amino acids length) were identified with TransDecoder v.5.5.0 (https://github.com/TransDecoder/TransDecoder). Assemblies were conducted on the server of the Biocomputing Core Facility, Department of Biology, University of Copenhagen and the Danish National Supercomputer for Life Sciences, Computerome 2.0.

2.2.2. Phylogenetic analysis of transcriptomes

Phylogenetic analysis of transcriptomes mainly followed Herranz et al. (2022). All analyses were conducted on the High-Performance Computing Cluster (LIB Cluster) of the Leibniz Institute for the Analysis of Biodiversity Change, Germany.

Orthologues were identified using OrthoFinder v.2.5.4 (Emms and Kelly, 2019). Multiple sequence alignment (MSA) gene trees were constructed within OrthoFinder ('-M msa' option) without trimming the alignments ('-z' option). MSAs were compiled with MAFFT v.7.453 (Katoh and Standley, 2013) and corresponding gene trees generated with FastTree v.2.1.11 (Price et al., 2010). These multi-copy gene trees can include duplicates of sequences per species. To obtain only one sequence per gene region of a species, the MSAs and the corresponding multi-copy gene trees were analyzed in PhyloTreePruner v.1.0 (Kocot et al., 2013). The single-copy sequences were realigned with MAFFT and concatenated to supermatrices corresponding to the number of minimum species per gene region (occupancy matrices) with FASconCAT-G v.1.05.1 (Kück and Longo, 2014). Maximum-likelihood (ML) trees of the different occupancy matrices were generated with IQ-Tree2 (Minh et al., 2020) using the unpartitioned automated model selection with ModelFinder (Kalyaanamoorthy et al., 2017). To evaluate the robustness of the inferred tree topologies, 1000 ultrafast bootstrap (UFBoot) replicates with UFBoot2 (Hoang et al., 2018).

A coalescent-based tree framework approach was tested with ASTRAL-III v.5.7.8 (Zhang et al., 2018). The single-copy gene trees of the corresponding occupancy matrices were summarized using a quartet method to estimate the species tree with their corresponding local posterior probabilities (PP) (Sayyari and Mirarab, 2016).

A second coalescent-based tree framework approach with AstralPro2 v.1.15.1.3 (Zhang and Mirarab, 2022) was tested on the 50,723 multi-copy gene trees from the OrthoFinder output. The species tree was estimated with the same method as above. To assess the potential impact of different transcriptomes on the species tree, the topology of the multi-copy gene trees was re-analyzed after (1) excluding transcriptomes with low BUSCO values (*P. caudatus* from the White Sea, *T. corallicola* A and B), (2) excluding *N. munidae* and *A. elegans* outgroups due to their long branches and (3) after removing all outgroups, keeping only Priapulida.

2.3. Conserved region analysis

2.3.1. Probe set design

As part of ongoing work, we used a probe set derived from 58 published genomes across 25 phyla, including two priapulidan genomes (*Priapulus caudatus* [NCBI: GCF_000485595.1] and *Tubiluchus corallicola* [NCBI: GCA_030141605.1]), to identify phylogenetically informative loci from our samples following standard ultraconserved element recovery methods (Faircloth, 2017; https://phyluce.readthedocs.io). This probe set targets 2,146 loci that can be harvested bioinformatically (Derkarabetian, Lord, Giribet, et al., work in progress).

2.3.2. DNA extraction and library preparation

Body tissue from museum samples was used for DNA extraction using the Qiagen DNeasy Blood and Tissue kit (Qiagen). Extractions were quantified using the Qubit fluorometer (Thermo Fisher Scientific). Following DNA quantification we used the Kapa HyperPlus Kit for library preparation. Samples were enzymatically fragmented for 3 min at 37 °C. End repair and A-tailing was conducted at 65 °C for 30 min. This

was followed by ligation of barcodes. After a 0.8x bead cleanup, libraries were eluted in 32 μl of Tris-HCl and quantified using Qubit fluorometer (Thermo Fisher Scientific). From the ligated library, 15 μl were amplified using i5/i7 primer combos (Glenn et al., 2019) at 10–16 cycles (optimized for input DNA). Amplified libraries were cleaned using a 0.7–1x bead cleanup (optimized for each input library) and eluted in 22 μl molecular grade water. Serapure Speedbeads (Rohland and Reich, 2012) were used for all clean-up steps and bead ratios were optimized via assessment of each library's fragment size distribution using Agilent TapeStation. Final library quality was assessed via Agilent TapeStation and pooled in equal concentrations. Sequencing was done on an Illumina Novaseq 6000 S4 with 150 bp paired end reads at the Bauer Core Facility at Harvard University. For each sample we requested 12 million paired end reads, this is estimated to be between 5x and 10x genome coverage. These estimates are based on the assembly sizes of the two currently published priapulidan genomes (345.4 Mb and 511.7 Mb).

2.3.3. Phylogenetic analysis of conserved regions

Raw reads were processed, assembled, and aligned into final matrices using PHYLUCE v.1.7.2 (Faircloth, 2016). Adaptor removal and quality control were conducted using illumiprocessor (Faircloth, 2013), a wrapper for Trimmomatic (Bolger et al., 2014) in the PHYLUCE package. We also subsampled the clean illumina reads used to generate the published *Tubiluchus corallicola* (NCBI: SRX18921368) genome to 5x genome coverage. All processed reads were assembled using SPAdes v.3.15.4 (Bankevich et al., 2012). Contigs in these assemblies and the additional transcriptomes (four priapulidans, five outgroup taxa) were matched to probes using a modified version of the PHYLUCE script 'phyluce_assembly_match_contigs_to_probes' to allow for duplicates, using minimum coverage and minimum identity values of 65. Through wrappers in the PHYLUCE package contigs matching probes were aligned using MAFFT (Katoh and Standley, 2013) and Gblocks (Castresana, 2000; Talavera and Castresana, 2007) was run with conservative settings (–b1 0.5 –b2 0.85 –b3 4 –b4 8) to trim and remove highly divergent sequences for each locus. Following this, loci alignments were imported into Geneious (Kearse et al., 2012) for visual inspection and additional curation of short and divergent sequences. Following these quality control and filtering steps, three occupancy matrices (70 %, 80 % and 90 %) were generated, and each used for phylogenetic reconstruction. Each occupancy matrix was analyzed using Bayesian (unpartitioned dataset) and ML methods (both partitioned and unpartitioned datasets). The unpartitioned Bayesian analyses were run in ExaBayes v.1.5.1 (Aberer et al., 2014) using the default GTR + GAMMA model. The Markov Chain Monte Carlo was configured with two runs, each with one cold and three heated chains and ran for 10 million generations sampling every 500 until the average standard deviation of split frequencies (ASDSF) was < 0.02. Maximum likelihood analyses including model testing, tree reconstruction, and branch support assessment with 1500 ultrafast bootstraps (Hoang et al., 2018), were conducted in IQ-Tree2 v.2.2.2 (Minh et al., 2020) on matrices using both unpartitioned and partitioned approaches. Partitions were identified with ModelFinder (Kalyaanamoorthy et al., 2017) using the relaxed hierarchical clustering algorithm (Lanfear et al., 2014). The best model was selected according to Bayesian Information Criterion via ModelFinder's automated model selection (Kalyaanamoorthy et al., 2017).

2.4. Ancestral state reconstruction of morphological characters of extant priapulidans

Sixteen informative morphological characters were assembled from literature and a matrix prepared in Mesquite v.3.80 (Maddison and Maddison, 2023) (see Suppl. Table S3). Characters were coded from literature research of all extant priapulidan species and outgroup taxa (see Supplementary File 2), as well as own examinations on several species (*P. caudatus*, *P. tuberculatospinosus*, *P. bicaudatus*, *P. australis*, *H. spinulosus* and *H. higginsi*). Codings of character states were depicted either as "0″ (absence) or "1" (presence), or as specific characters (e.g., "0" as microscopic body size and "1" as macroscopic body size) (see Supplementary File 2). Inapplicable characters were coded as "-" and unknown character states as "?". Linked characters were coded using "C-coding" *sensu* Pleijel (1995), where absence/presence depict one character state and linked expressions another character. As the morphological data were mostly congruent between species of the same genus, they were summarized to genus level.

For ancestral character state reconstruction, a simplified version (i.e. species branches collapsed to genus level) of the phylogenetic tree generated from the combined 80 % occupancy matrix was imported into Mesquite. Ancestral states were reconstructed on the tree with the 'Trace Character History' option (setting: Parsimony Ancestral States). The likelihood of character states was determined in Mesquite using the maximum likelihood (Mk1 model; default settings) ancestral state reconstruction.

Due to missing molecular data of *Acanthopriapulus* and *Maccabeus*, we tried to identify their phylogenetic positions by entering their morphological data in the morphological matrix. The morphological matrix was analyzed both including and excluding outgroups (instead rooting with *Meiopriapulus*), using the 'Heuristic Add & rearrange' function in Mesquite (settings: Tree length; SPR Rearranger; 100 trees). Consensus trees were constructed from the stored trees with default 'Majority-Rule Consensus' options in Mesquite. When excluding outgroups the generated consensus tree based on morphological data only fully concurred with the topology of the simplified tree generated from the combined 80 % occupancy matrix (see above). However, when including outgroups the topologies were not fully congruent, as polytomies occurred containing in- and outgroup taxa. Therefore, we restricted the positions of taxa included in the simplified tree to its topology, and reanalyzed and identified the positions of *Acanthopriapulus* and *Maccabeus* on the tree including outgroups. Ancestral character states were reconstructed on this tree as above.

3. Results

3.1. Sequence quality

Overall percentage of BUSCO values (complete + partial) present in transcriptomes and assembled contigs ranged from 13.1 % to 95.18 % (Table 2), while the number of loci initially matched per sample used in the combined phylogeny ranged from 553 to 1470 (Table 2; Fig. 3A). The 5x coverage genomic assembly of *T. corallicola* contained 90.36 % complete and partial BUSCOs and had initial matches to 1483 loci, while the newly sequenced *P. tuberculatospinosus* and *P. australis* genomes both also contained over 90 % complete and partial BUSCOs and had initial matches to 1470 and 1369 loci respectively. This suggests that assemblies generated from a low coverage genome sequencing approach are generally able to generate sufficient data to recover many loci for this group, even if they do not generate otherwise contiguous assemblies. While not all samples generated optimal assemblies, there is a positive trend between BUSCOs recovered and number of loci matched (Fig. 3B). As one would expect there is also a negative correlation between the completeness of the assembly and the percentage of missing data in the final matrices, with the samples that generate the most incomplete assemblies also having the greatest percent of gaps/ambiguity in the final alignments (Table 2).

3.2. Transcriptomic analyses

Information of analyzed occupancy matrices is shown in Supplementary Table S2. In all but one ML analysis, Priapulida forms a fully supported clade with Kinorhyncha as sister group, when using Nematomorpha to root the tree (Fig. 4; Suppl. Figs. S1; S3–S8). Only in the analysis of the 100 % occupancy matrix (only 11 loci), Loricifera is sister

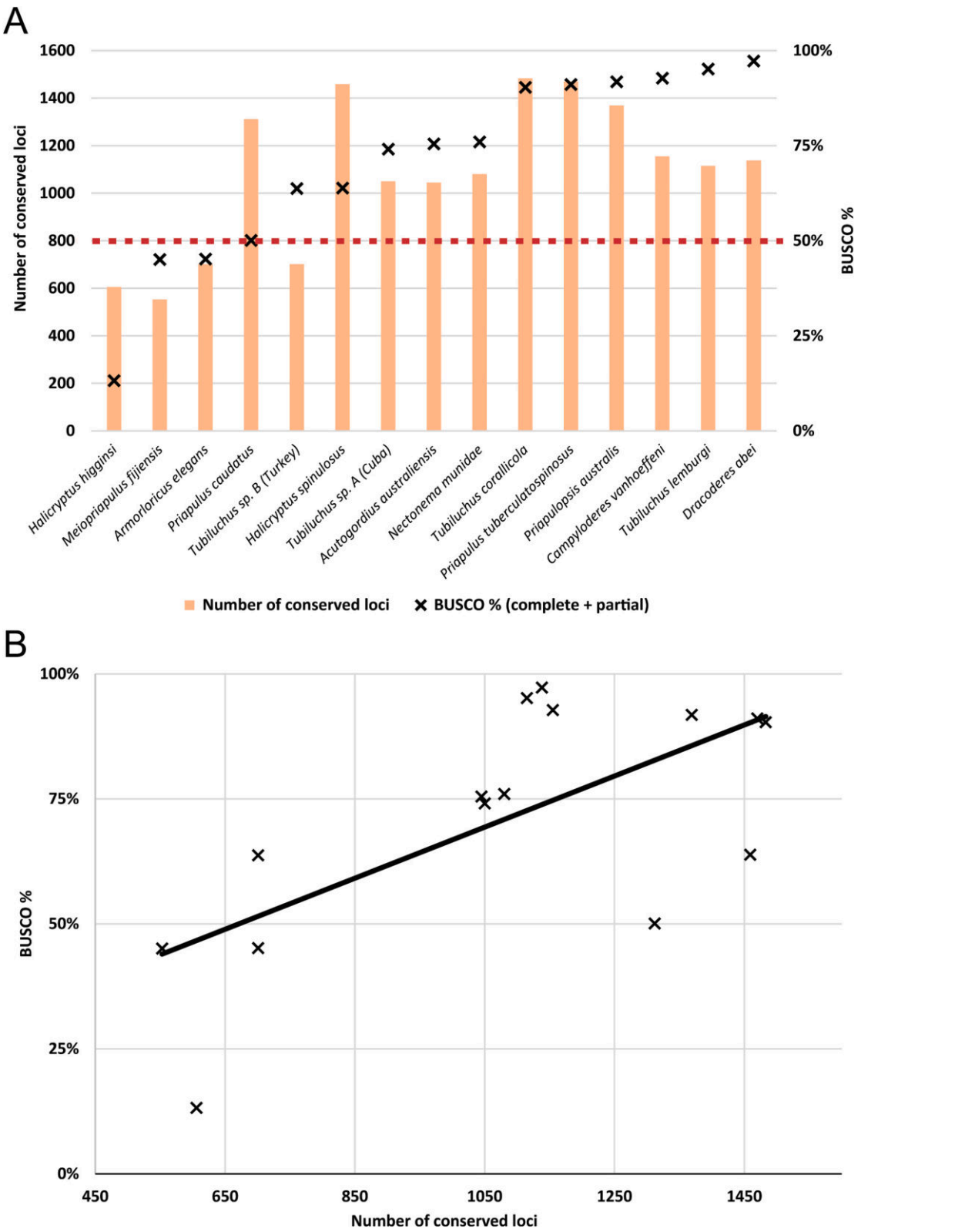

Fig. 3. Overview of conserved loci recovery and BUSCO values. A. Specimens used in the combined phylogenetic analysis and their respective number of recovered loci (bars) and BUSCO values (complete + partial) (crosses). Taxa are sorted by increasing BUSCO values. B. Comparison of number of recovered loci and their respective BUSCO values. Trend line shows a positive trend.

group to Priapulida, albeit with low support (UFBoot = 54 %) (Suppl. Fig. S2). In the coalescent-based species tree estimation (single-copy and multi-copy gene trees), Kinorhyncha is sister group to Priapulida with full support in all analyses, except in the analysis of the 100 % occupancy matrix (11 single-copy gene trees), where this relationship receives low support (PP = 0.72) (Suppl. Figs. S9–S14).

In all analyses, the meiofaunal *Meiopriapulus* is the sister group to all remaining Priapulida (Fig. 4; Suppl. Figs. S1–S14). This arrangement is

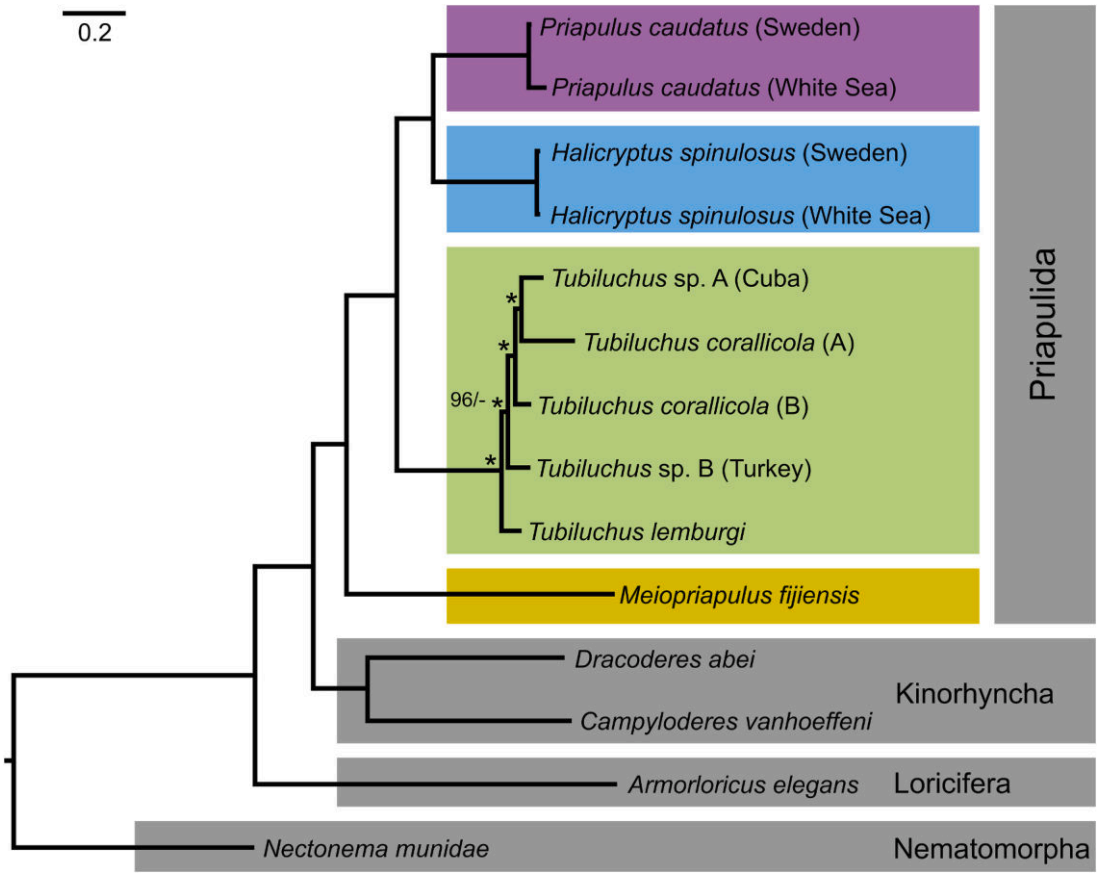

Fig. 4. Maximum likelihood tree showing relationships of Priapulida based on transcriptomic data. Branch lengths, topology and support values (bootstrap/Astral posterior probabilities) based on the 55 % occupancy matrix (≥8 species; 1376 gene regions; 805,039 amino acids) generated with IQ-Tree2. Nodes without support values show maximum support (100/1). Nodes with asterisk (*) in the *Tubiluchus* clade show deviations compared to the coalescent-based species tree of the 55 % occupancy matrix generated with ASTRAL-III (Suppl. Fig. S15).

always fully supported (UFBoot = 100 %, PP = 1.00), except in the 100 % occupancy matrix of the ML analysis (UFBoot = 87 %; Suppl. Fig. S2) and in the 100 % occupancy matrix of the coalescent-based single-copy analysis (PP = 0.97; Suppl. Fig. S9). The meiofaunal *Tubiluchus* always form a fully supported clade and are in all analyses the sister group to the macroscopic Priapulidae (here *Halicryptus* and *Priapulus*) (Fig. 4; Suppl. Figs. S1–S14). Within Priapulidae, *Halicryptus* and *Priapulus* form fully supported clades throughout all analyses (Fig. 4; Suppl. Figs. S1–S14).

Minor changes occur within the genus *Tubiluchus* throughout all analyses. In the ML analyses, either both *T. corallicola* specimens form a clade (Suppl. Figs. S1–S5) or *T. corallicola* A forms a highly supported monophyletic group with *Tubiluchus* sp. from Cuba (Suppl. Figs. S6–S8). Either *Tubiluchus lemburgi* and *Tubiluchus* sp. from Turkey form a monophyletic group with varying support values (Suppl. Figs. S1–S5) or they are paraphyletic with maximum support (Suppl. Figs. S6–S8). Similar changes within the Caribbean specimens occur in the coalescent-based single-copy analyses, and *T. lemburgi* and *Tubiluchus* sp. from Turkey always form a highly supported monophyletic group (Suppl. Figs. S9–S16).

In the coalescent-based single-copy analyses, *T. corallicola* A is sister taxon to *T. corallicola* B in some of the matrices (PP = 0.67 – 0.58) (Suppl. Figs. S9–S10). In other occupancy matrices, *T. corallicola* A and *Tubiluchus* sp. from Cuba are sister groups (Suppl. Figs. S11–S16), albeit not well supported (PP = 0.75 – 0.44). *Tubiluchus lemburgi* and *Tubiluchus* sp. from Turkey always form a monophyletic group with high support (PP = 1.00 – 0.83; Suppl. Figs. S9–S16).

In the coalescent-based multi-copy analysis with all transcriptomes, the topology is the same as starting with the 85 % single-copy occupancy matrix (Suppl. Fig. S17). Also, testing the topology without certain transcriptomes (see above), reveal *Tubiluchus* sp. from Cuba being the sister taxon to *T. corallicola* (from Curaçao and the Caribbean coast of Panama), although with low support (Suppl. Figs. S18–20). The remaining topology stays the same.

3.3. Combined phylogenetic analysis

Due to concern with the unstable placement of low quality samples in preliminary analyses, only the best representative (in terms of recovered loci) per species was included for analysis in cases where both transcriptomic and genomic data were available. In our final dataset the number of initial loci matched to assemblies ranged from 553 to 1483 (Table 2). We generated matrices at 70 %, 80 % and 90 % occupancy, which contained 724, 378, and 208 loci respectively. In the unpartitioned IQ-Tree analysis, models were selected with ModelFinder based on BIC score, with K3PU + F + I + G4 as the best model for the 70 % and 80 % matrices, while TIM + F + I + G4 was used for the 90 % matrix.

The topology of the ML tree of the combined unpartitioned 80 % occupancy matrix (Fig. 5) corresponds almost completely to the topology of the transcriptome analyses (Fig. 4).

In the combined analysis newly added species *P. tuberculatospinosus* and *H. higginsi* form clades with their respective congener in all phylogenetic analyses (Fig. 5). *Priapulopsis australis* is positioned as the sister branch to the *Priapulus* spp. clade with moderate support in the 80 % occupancy matrix (Fig. 5). This sister group relationship occurs in the 90 % occupancy matrix as well, however in the 70 % occupancy matrix *Priapulopsis* is sister group to *Priapulus* + *Halicryptus* (Suppl. Figs. S27–S29).

Similar to the transcriptomic analyses, there are minor topological

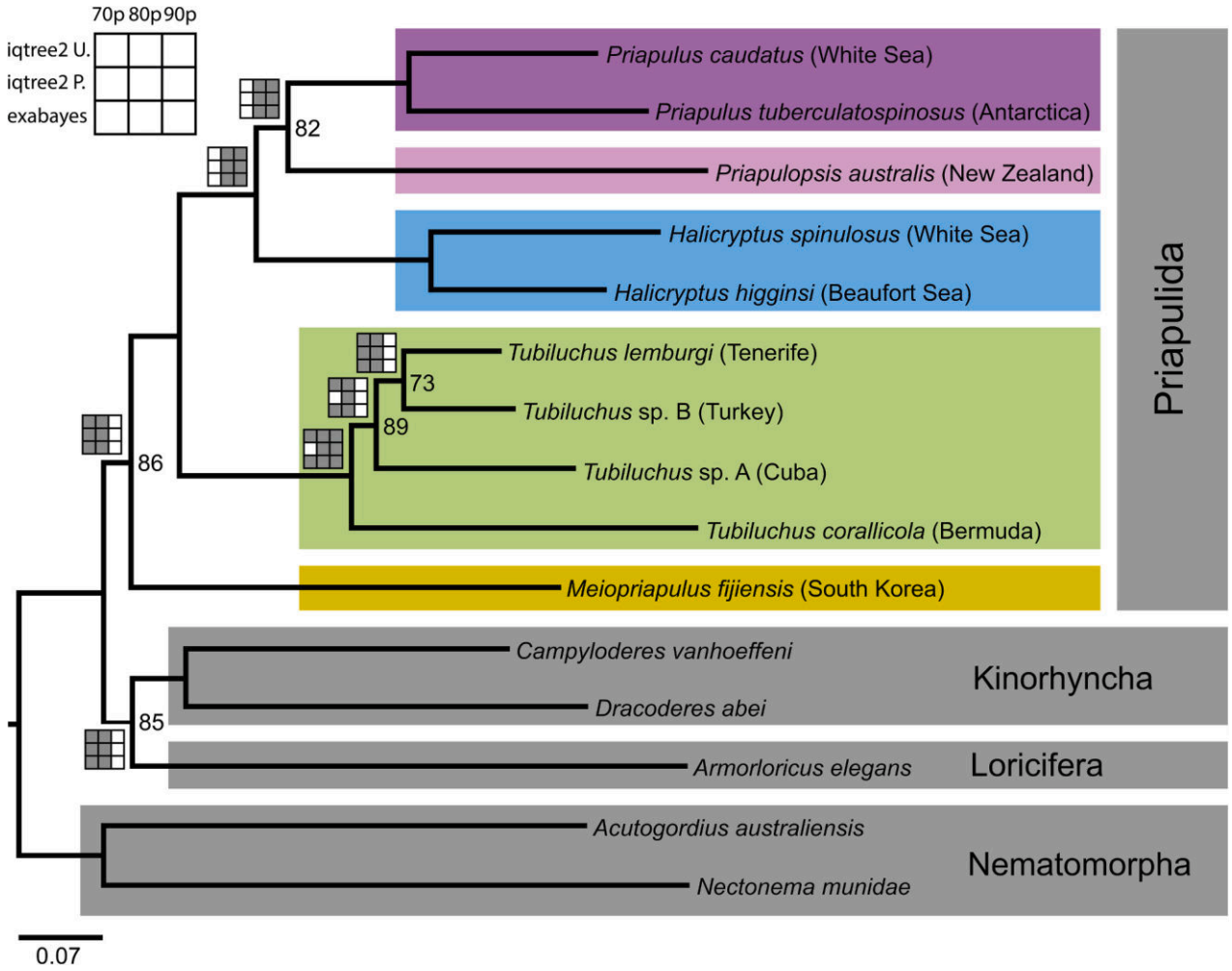

Fig. 5. Maximum likelihood tree showing relationships of Priapulida based on combined (transcriptomic and genomic) data. Branch lengths, topology and bootstrap support values are based on the 80% occupancy matrix (378 loci) of the unpartitioned ML analysis generated with IQ-Tree2. Nodes without bootstrap value show maximum support (100). Squares on nodes show used analysis methods and respective occupancy matrices. Grey squares show identical nodes, white squares show deviations (see Suppl. Figs. S21–S29).

differences within *Tubiluchus* across the combined analyses (Fig. 5; Suppl. Figs. S21–S29). While *T. lemburgi* and *Tubiluchus* sp. from Turkey group together in the 70 % and 80 % occupancy matrices (Fig. 5; Suppl. Figs. S24–S29), *T. lemburgi* swaps positions with *Tubiluchus* sp. (Cuba) in the 90 % occupancy matrix, so that it becomes the sister group to *Tubiluchus* sp. (Turkey) + *Tubiluchus* sp. (Cuba) (Suppl. Figs. S21–S23).

Another noticeable difference to the transcriptome analyses is the relationships of outgroup taxa. While these analyses show Priapulida and Kinorhyncha as sister groups, the 70 % and 80 % occupancy matrices in the combined analyses yield Loricifera and Kinorhyncha as sister groups, next to Priapulida (Fig. 5; Suppl. Figs. S24–S29). In the 90 % occupancy matrix, Loricifera groups together with the priapulidan *M. fijiensis*, though with moderate support (Suppl. Figs. S21–S23).

3.4. Ancestral states of morphological characters

A total of 16 morphological characters were traced on a simplified phylogenetic tree based on the topology of the combined 80 % occupancy matrix analysis (Fig. 6A) as well as on a tree including *Acanthopriapulus* and *Maccabeus* (Fig. 6B). Based on a phylogenetic analysis of the morphological matrix, constraining the topology of the remaining taxa, *Acanthopriapulus* is here positioned as sister taxon to *Priapulus*, and *Maccabeus* as sister taxon to the macroscopic Priapulidae (Fig. 6B). The ability of the morphological matrix to resolve their positions was tested by analyzing the matrix without outgroups and rooting the generated tree at *Meiopriapulus*, resulting in the same topologies as in Fig. 6A and B. The coding of characters 1–16 is justified in Supplementary File 2. The likelihoods of the character states per character are shown in Supplementary Figs. S30–S61. Names and classification of clades given in Fig. 6B is discussed below.

Adult body size (1). The ancestral state of the adult body size is reconstructed as microscopic, supported by moderate and high likelihoods (likelihood l = 0.88/0.96; Fig. 6). The macroscopic adult body size occurs within Priapulidae (Fig. 6).

Presence of loricate larval stage (2). Without analyzing outgroup character states, the ancestral state would be ambiguous, as *M. fijiensis* is the only priapulidan with direct development and it is positioned as sister group to the remaining Priapulida with loricate larval stages. As only Loricifera among the outgroup taxa have loricate larval stages, and Kinorhyncha (without a loricate larva) is the sister group to Priapulida, they are traced to ancestrally lack loricate larval stages, albeit with low support (l = 0.64/0.67; Suppl. Figs. S31 and S47; Fig. 6).

Shape of lorica of larval stages (3). As Eupriapulida (Priapulidae + *Maccabeus*) have dorsoventrally flattened larval shapes and their sister group *Tubiluchus* a round shape, the most ancestral larval shape remains ambiguously reconstructed (Fig. 6).

Presence of caudal appendage in postlarval stages and adults (4). Ancestrally, Priapulida are reconstructed to lack a caudal

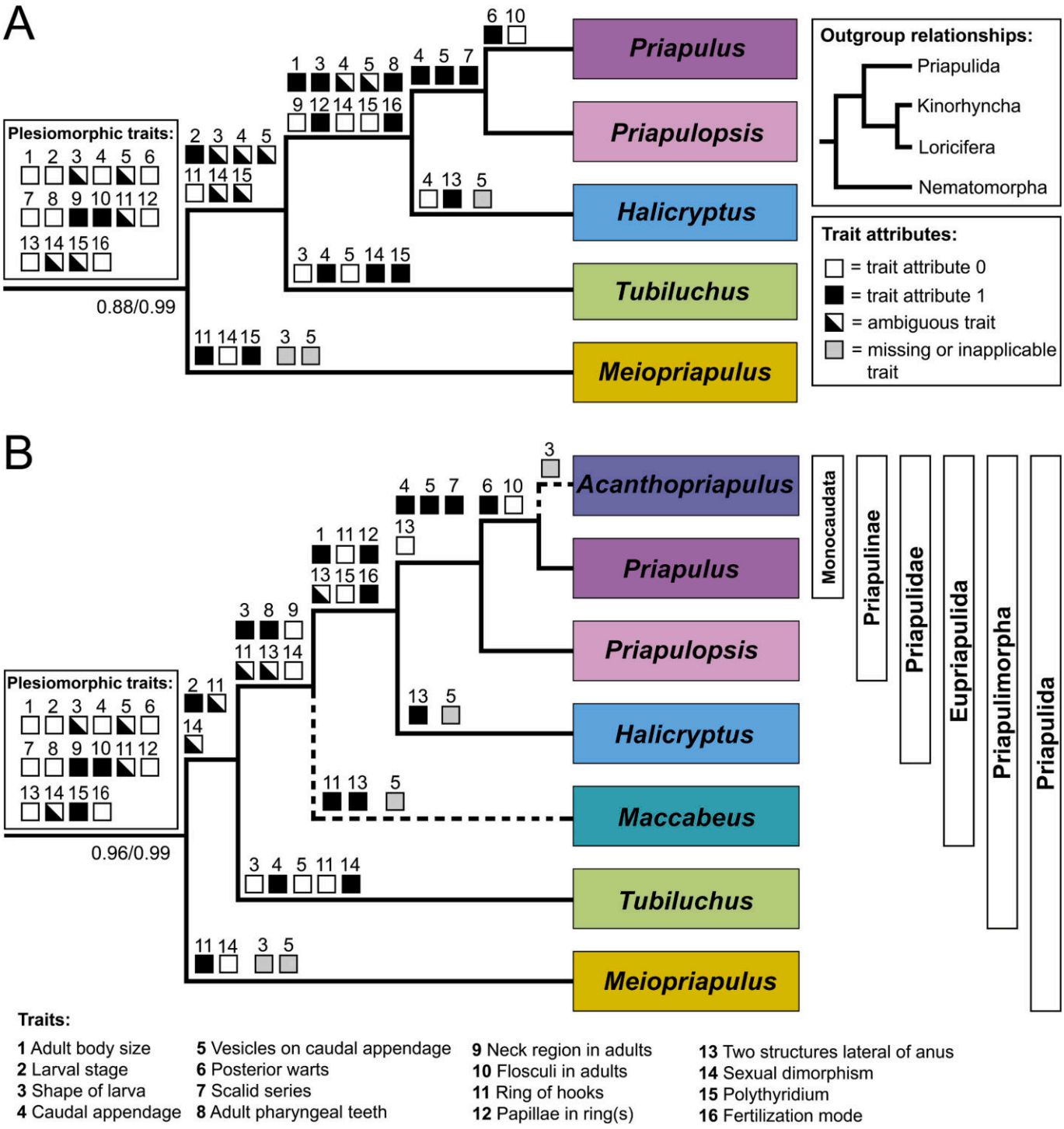

Fig. 6. Parsimonious ancestral state reconstruction of selected morphological traits of Priapulida. Support values on the first node show the likelihoods for an ancestral small body size and internal fertilization mode. For the remaining likelihoods for character states see Supplementary Figs. S30–S61. Outgroups and character attributes of outgroup taxa not shown. A. Traced traits on a simplified (= species collapsed to genus level) phylogeny of the combined 80 % occupancy matrix of the unpartitioned ML analysis. B. Inferred positions of *Acanthopriapulus* and *Maccabeus* on the phylogenetic tree based on analyzed morphological traits. Boxes on branches show attributes (different grey scales) of traced traits (numbers above boxes).

appendage with moderate support (l = 0.86/0.93; Suppl. Figs. S33 and S49; Fig. 6). A caudal appendage appeared two times, and potentially independently, throughout priapulidan evolution, first within *Tubiluchus* and second within Priapulinae (*Acanthopriapulus* + *Priapulus* + *Priapulopsis*) (Fig. 6).

Presence of vesicles on caudal appendage (5). Whether the presence or absence of vesicles on the caudal appendage is the ancestral state, is equivocal (Fig. 6). The long, thin tail of *Tubiluchus* is always free of vesicles, whereas vesicles are present at least partially throughout postlarval development on the appendages of Priapulinae.

Presence of posterior warts (6). Posterior warts on the posterior trunk are reconstructed as ancestrally absent in Priapulida (l = 0.99; Suppl. Figs. S35 and S51; Fig. 6). Only macroscopic Monocaudata (*Acanthopriapulus* + *Priapulus*) have posterior warts (Fig. 6).

Presence of scalid series in decreasing size (7). Ancestrally, the scalid rows of Priapulida are reconstructed to lack scalid series (l = 0.99; Suppl. Figs. S36 and S52; Fig. 6). Scalid series with several scalids in decreasing sizes occur within Priapulinae (Fig. 6).

Appearance of pharyngeal teeth (8). Priapulida are ancestrally reconstructed to have pectinate teeth with moderate support (l = 0.66/0.79; Suppl. Figs. S37 and S53; Fig. 6). Cuspidate pharyngeal teeth evolve in Eupriapulida (Fig. 6).

Presence of neck region in adults (9). A neck region which is separated from the introvert and trunk is reconstructed as ancestrally present in adult Priapulida (l = 0.89/0.91; Suppl. Figs. S38 and S54; Fig. 6). The neck region was lost within Eupriapulida (Fig. 6).

Presence of flosculi in adults (10). The presence of flosculi is traced as an ancestral state in Priapulida (l = 0.96/0.98; Suppl. Figs. S38 and S55; Fig. 6). Only in Monocaudata, this type of sensory structure is absent (Fig. 6).

Ring of hooks on posterior trunk (11). A ring of cuticular hooks occurs in *Meiopriapulus* and *Maccabeus* (Fig. 6). As *Tubiluchus* and Priapulidae lack these structures, the ancestral states traced as ambiguous here (Suppl. Figs. S39 and S56).

Ring(s) of papillae on posterior trunk (12). Papillae organized in ring(s) are present in all adults of macroscopic priapulidans (Fig. 6). In microscopic species such organized papillae are absent, reconstructing a lack of ring papillae as ancestral trait in priapulidans (l = 0.99; Suppl. Figs. S40 and S57).

Presence of two tube-like structures lateral of anus (13). The lack of two tube-like structures on the terminal posterior end of the trunk is traced as an ancestral state in Priapulida (l = 0.99; Suppl. Figs. S41 and S58; Fig. 6). This trait either evolved twice in *Maccabeus* and in *Halicryptus*, or evolved once in Eupriapulida and is secondary lost in Priapulinae (Fig. 6).

Presence of sexual dimorphism (14). The ancestral state of sexual dimorphism in Priapulida is reconstructed as ambiguous (Fig. 6). All outgroup taxa have sexual dimorphism, but only *Tubiluchus* in Priapulida displays such state.

Presence of muscular polythyridium (15). The presence of a muscular polythyridium is reconstructed as an ancestral state in Priapulida, albeit with low support (l = 0.6/0.79; Suppl. Figs. S44 and S60), as *Meiopriapulus* and *Tubiluchus* both feature one (Fig. 6). A presumably homologous structure occurs in *Maccabeus* (Fig. 6B). The polythyridium got lost in the ancestor of Priapulidae (Fig. 6).

Fertilization mode (16). The ancestral fertilization mode in Priapulida is reconstructed as internal (l = 0.99; Fig. 6). External fertilization is derived in the macroscopic Priapulidae.

4. Discussion

This study shows the first phylogenetic analysis of Priapulida with molecular data from species of five out of seven priapulidan genera. The position of both missing rare priapulidans *Acanthopriapulus* and *Maccabeus* on the tree is hypothesized by analyzing selected morphological traits.

Our analyses largely confirm previously recovered topologies within extant Priapulida based on morphological data (see Fig. 1B; Wills, 1998; Lemburg, 1999; Dong et al., 2004; 2005; 2010; Harvey et al., 2010; Wills et al., 2012). Discrepancies lie in the position of *Meiopriapulus*, which in these studies formed a clade together with *Tubiluchus*, as sister group to all remaining priapulidans. Our phylogeny, however, shows *Meiopriapulus* as sister taxon to the remaining priapulidans, and *Tubiluchus* branching off next, which has a strong impact on the interpretation of character evolution.

Other phylogenetic analyses based on morphological data by von Salvini-Plawen (1974), though not including a range of present day data, and Adrianov and Malakhov (1996) both propose *Maccabeus* as sister taxon to all remaining priapulidans. Another difference to our proposed phylogeny is their stated sister group relationship of *Tubiluchus* and Priapulidae (excluding *Halicryptus*) (see Fig. 1A).

4.1. Advantages of conserved region analysis for exploiting museum material

Across many taxonomic groups, target enrichment sequencing of ultra conserved elements has proven a valuable approach for generating phylogenomic datasets, including ecdysozoans (Faircloth et al., 2015; Derkarabetian et al., 2023; Geburzi et al., 2024; Sato et al., 2024). An advantage of this approach over transcriptomes is that it is an accessible approach for specimens preserved in ethanol. This allows for the inclusion of museum materials that otherwise may be excluded from phylogenomic studies. This is particularly valuable for species that are rare or difficult to collect but are available as historical museum specimens preserved in 70 – 80 % ethanol stored at room temperature (Derkarabetian et al., 2019). Furthermore, due to the drop in cost of sequencing technology it is becoming increasingly possible to sequence low to mid coverage genomes and bioinformatically extract conserved regions from subsequent assemblies (as we have done in this study), also including museum specimens (Liu et al., 2021; Quattrini et al., 2024). This approach proves to be a promising alternative to target enrichment that is both more efficient and economical. However, there may be limitations to this approach based on probe set and bait design, and variability in genome size and content across the target group.

4.2. Classification of Priapulida

Members of the phylum Priapulida have been mainly referred to as ‘priapulids’ by many authors. This was comprehensible until the discovery of microscopic species, as all described species to that time belong to the exclusively macroscopic Priapulidae. However, microscopic species are also referred to as ‘priapulids’ (*Tubiluchus*: e.g., Van der Land, 1982; Todaro and Shirley, 2003; *Maccabeus*: Por and Bromley, 1974; *Meiopriapulus*: Morse, 1982). Other authors refer to the phylum as ‘Priapula’ (e.g. Nielsen, 2012) and use the term ‘priapulans’ instead, to distinguish between members of Priapulida and Priapulidae (e.g., Giribet and Edgecombe, 2020). In this study, we use the anglicized term ‘priapulidans’ for all members of the phylum Priapulida to keep the connection to the original name of the phylum.

Published classifications of Priapulida include several redundant names to “fill in” levels of Linnean hierarchies (Van der Land, 1970; von Salvini-Plawen, 1974; Adrianov and Malakhov, 1995; Lemburg, 1999). Meiopriapulomorpha Adrianov and Malakhov, 1995 and Meiopriapulidae are redundant with *Meiopriapulus fijiensis*, Tubiluchidae is redundant with *Tubiluchus*, and Seticoronaria von Salvini-Plawen, 1974 and Chaetostephanidae are redundant with *Maccabeus*. We reject these redundant names and have not included them in the present study (Table 3).

Eupriapulida Lemburg, 1999 is the sister group to *Tubiluchus* and includes microscopic *Maccabeus* and all macroscopic Priapulidae. Within Priapulidae, Halicryptinae von Salvini-Plawen, 1974 or Halicryptidae is redundant with *Halicryptus*. There also is a miscitation of these names (Halicryptinae and Halicryptidae) between von Salvini-Plawen (1974) and Adrianov and Malakhov (1995), as Salvini-Plawen introduced Halicryptinae and Adrianov and Malakhov cited it as Halicryptidae.

Priapulinae von Salvini-Plawen, 1974 (synonymous with Megintroverta Lemburg, 1999) is the sister group of *Halicryptus* and includes *Priapulopsis*, *Priapulus* and *Acanthopriapulus*. *Priapulus* and *Acanthopriapulus* are together named Monocaudata Lemburg, 1999.

von Salvini-Plawen (1974) grouped Priapulidae and *Tubiluchus* together in the taxon Priapulimorpha von Salvini-Plawen, 1974 (not ‘Priapulomorpha’ as cited by Adrianov and Malakhov, 1995). In our phylogeny this taxon is polyphyletic, thus, we propose to include *Maccabeus*, resulting in Priapulimorpha consisting of Eupriapulida + *Tubiluchus* (Table 3).

Table 3
Classification of Priapulida without redundant names.

Priapulida Théel, 1906
Priapulimorpha von Salvini-Plawen, 1974
Eupriapulida Lemburg, 1999
Priapulidae Gosse, 1855
Halicryptinae von Salvini-Plawen, 1974
Priapulinae von Salvini-Plawen, 1974 (synonymous with **Megintroverta** Lemburg, 1999)
Monocaudata Lemburg, 1999

Meiopriapulus Morse, 1981	***Tubiluchus*** Van der Land, 1968	***Maccabeus*** Por, 1972	***Halicryptus*** Von Siebold, 1849	***Priapulopsis*** Koren and Danielssen, 1875	***Priapulus*** Lamarck, 1816	***Acanthopriapulus*** Van der Land, 1970

4.3. Morphological characters

Heuristic ancestral state reconstructions of 16 selected morphological characters predicted 12 of them as having an ancestral origin in extant priapulidans.

Meiopriapulus holds the identified ancestral priapulidan character states and is separated from the remaining priapulidans by having a direct development without loricate larval stages (Higgins and Storch, 1991). An ancestral direct development would correspond to direct development in Cambrian *Markuelia* (Dong et al., 2005). In several characters of the introvert, *Meiopriapulus* differs strongly from the remaining extant priapulidans: 'sensory scalids' in three rings with [8 + 9 + 8] scalids, approximately 150 rows of 'locomotory scalids' and the anterior trunk region with 'trunk scalids' (Morse, 1981; Sørensen et al., 2012). Additionally, a true coelom is present in the introvert (Storch et al., 1989). A typical character for Priapulidae and *Tubiluchus* is having eight primary scalids in the first ring, followed by 25 longitudinal rows of scalids on the introvert (Adrianov and Malakhov, 1996; Lemburg, 1999). Additional types of scalids or papillae occur in many macroscopic species on the circumoral field (see Raeker et al., 2024b). For *Meiopriapulus*, this scalid pattern does not exist, but two interpretations of its anterior scalids are possible. There is a first ring of eight scalids, followed by a second and third ring with nine and eight scalids. Either, the first ring is interpreted as primary scalids, but then the number of scalids of the second and third ring (together 17) does not fit into the pattern of 25 scalid rows. Or, all three rings sum up to 25 scalids, but then the eight primary scalids would be lacking. Additionally, the about 150 rows of locomotory scalids may not represent "true" scalids, as they differ morphologically and number-wise from other priapulidans. Due to significant differences to other priapulidans, Park et al. (2006) even speculated on a polyphyly of Priapulida.

Introvert structures of *Maccabeus* likewise differ compared to the "general" bauplan of introvert structures of Priapulida (see Por and Bromley, 1974; von Salvini-Plawen, 1974; Malakhov, 1978). The first two rings of structures form a distinct tentacle crown consisting of eight circumoral trigger spines and 25 double tentacles. Such a tentacle crown is unique for Priapulida. It is followed by three structures: one ring of 16 or 20 sensory spines, two rings of 25 trifid spines and three to four rings of 25 glandular spines. The tentacle crown of *Maccabeus* may represent highly modified scalids of the first two scalid rings (primary scalids and first ring of scalids), due to comparable numbers and their positions. Only the number of sensory spines is not comparable to structures of other priapulidans. As these structures are lacking in postlarval stages and seemingly only develop in adults (Por and Bromley, 1974), they may represent an autapomorphy of *Maccabeus*. Trifid spines and glandular spines are present in postlarval stages of *Maccabeus* and may be modified scalids as well. However, functions of these modified scalid types remain obscure, but they may be linked to the tubicolous life of *Maccabeus*, similar to the ring of anal spines on the posterior trunk (Por and Bromley, 1974). *Meiopriapulus* holds a ring of preanal hooks as well, but they differ in their morphology and hold a sensory structure (Sørensen et al., 2012). However, the ring of hooks of both taxa are considered as homologous structures (Morse, 1981; Wills, 1998; Wills et al., 2012). As *Tubiluchus* lacks such a ring of hooks, it arose two times in Priapulida, but the ancestral state remains unclear. In contrast, ring papillae (Priapulinae) and flosculus-tubulus-complexes (*Halicryptus*) found in macroscopic priapulidans may be homologous structures that are ancestrally absent (see Raeker et al., 2024b).

Scalids are organized in longitudinal rows on the introvert of priapulidans and appear in slightly different shapes among species (conical or basally flattened). In Priapulinae, scalid rows are composed of several scalid series, each consisting of a small number of conical scalids decreasing in size (Van der Land, 1970). In the remaining priapulidans (macroscopic *Halicryptus* and all microscopic species), scalid series are absent. Although the "true scalids" of *Maccabeus* and *Meiopriapulus* are still obscure, no scalid-like structure on the introvert has series with the same structures decreasing in size, thus, making absent scalid series an ancestral trait in Priapulida. Related taxa Kinorhyncha and Loricifera exhibit scalids that decrease in length but do not form distinct scalid series (Bang-Berthelsen et al., 2013; Neuhaus, 2013).

Pharyngeal teeth occur in two types in Priapulida: pectinate and cuspidate. Two microscopic extant taxa, *Tubiluchus* and *Meiopriapulus*, have pectinate pharyngeal teeth in adults (Schmidt-Rhaesa, 2013a). From our analysis, pectinate teeth is the ancestral state in extant priapulidans, and cuspidate teeth arose later in microscopic *Maccabeus* and macroscopic species. However, fossil priapulidan teeth resemble more intermediate types with characters of both other types (e.g., Smith et al., 2015; Slater et al., 2017; Wernström et al., 2023), making it possible that the pectinate and cuspidate teeth of extant priapulidans may have deviated from these intermediate types, eventually due to varying feeding preference. Interestingly, teeth of larval stages of Priapulidae differ morphologically to those of adults, resulting in a shift towards the morphospace of pectinate teeth of *Meiopriapulus* and *Tubiluchus*, assuming a detritivorous feeding contrary to the predatory adults (Wernström et al., 2023). In larval stages of *P. caudatus* and *P. australis*, the anterior tooth rings all differ from each other and distinct pectinate teeth occur in approximately rings three to four (e.g., Figs. 13.46, 13.47 and 13.48 in Adrianov and Malakhov, 1996), confirming a detritivorous feeding. On the contrary, teeth of larval stages of *Tubiluchus* also differ from those of adults, but correspond more to cuspidate teeth, and pectinate teeth as in adults are absent (e.g., Figs. 43–53 in Kirsteuer, 1976 for *T. corallicola*; Figs. 8D-G in Todaro and Shirley, 2003 for *T. troglodytes*). As larval stages and their respective adult stages differ in the type of pharyngeal teeth, the ancestral pectinate tooth type only represents the adults.

Between the teeth-covered pharynx and the midgut of microscopic *Tubiluchus* and *Meiopriapulus* there is a prominent, roundish organ positioned, the polythyridium. The polythyridium consists of cuticular plates and strong circular muscles (see Schmidt-Rhaesa, 2013b). It presumably functions as a filtering organ to only let small food particles pass by (Van der Land, 1970) or as collection structure for scratched off food particles from detritus (Morse, 1981). In *Maccabeus*, instead of a polythyridium, gastric spines are present (Por and Bromley, 1974). These spines are assumed to function as closure structures for small swallowed prey and are presumably homologous to a polythyridium (Por and Bromley, 1974). The presence of a polythyridium seems to be related to the food source of priapulidans, as this ancestral character got lost in macroscopic Priapulidae, mainly feeding on animal organisms.

The majority of extant priapulidans of both size classes have a caudal appendage. Only microscopic *Meiopriapulus* and *Maccabeus*, and macroscopic *Halicryptus* lack a caudal appendage, which is from our data reconstructed as an ancestral priapulidan trait. However, some Cambrian fossils of Priapulida show supposably evidence of a caudal appendage (e.g., *Xiaoheiqingella peculiaris*; *Paratubiluchus bicaudatus* [both see Han et al., 2004]; *Corynetis brevis* [see Huang et al., 2004b]). Additionally, the only Carboniferous species, *Priapulites konecniorum*, has a caudal appendage (presumably two, but fossils are poorly preserved; Schram, 1973) and are considered as extinct sister taxon to Priapulinae (e.g., Adrianov and Malakhov, 1996; Wills, 1998; Dong et al., 2010). As *Tubiluchus* also has a caudal appendage, but its composition differs from the ones of Priapulinae, both appendages are assumed to have different functions: anchor-like function due to its contractility and length in *Tubiluchus*, and an assumed (but debated) respiratory function in Priapulinae (see Van der Land, 1970). Caudal appendages may have arisen two times in extant priapulidans, which is expressed in the fact that the caudal appendage in *Tubiluchus* (and only there) is generally called "tail". Related taxa Kinorhyncha, Loricifera and Nematomorpha all lack posterior appendages (Neuhaus, 2013; Bang-Berthelsen et al., 2013; Schmidt-Rhaesa, 2013b).

Two of the genera lacking a caudal appendage, *Maccabeus* and *Halicryptus*, have a pair of spine-like anal tubuli lateral to the anus. In *Halicryptus*, anal tubuli presumably have a sensory or secretory function and are associated by several smaller papillae (Raeker et al., 2024a). For *Maccabeus*, these structures are not well documented, but sometimes few smaller papillae are found along the two prominent anal tubuli (see von Salvini-Plawen, 1974). The detailed function of the pair of anal tubuli is not yet clarified, but due to morphological similarities, these structures may represent homologous structures. From our data, anal tubuli arose two times in both taxa in Priapulida. Both related outgroup taxa Kinorhyncha and Loricifera lack caudal appendages and anal tubuli (Bang-Berthelsen et al., 2013; Neuhaus, 2013).

Two types of larval stages exist in Priapulida mainly differing in their lorica shape (Schmidt-Rhaesa, 2013a). Larval stages of all macroscopic species have a dorso-ventrally flattened lorica, e.g. two large dorsal and ventral lorica plates connected by lateral plates in a zig-zag pattern on each side. In between the lateral plates, in the posterior half of the lorica, are two lorica tubuli attached on each side, whose number is not reported to change throughout larval development (Fig. 2G). *Acanthopriapulus horridus* and *Priapulopsis papillatus* are the only macroscopic species without reports of larval stages. Microscopic *Tubiluchus* on the other side have larval stages with a roundish shaped lorica, consisting of 20 similar large cuticular plates (Fig. 2H). Lorica tubuli are arranged in circlets of four to five tubuli and the number of circlets increases from one to five throughout larval stages (Kirsteuer, 1976; Todaro and Shirley, 2003). Interestingly, microscopic *Maccabeus* develops from dorso-ventrally flattened larvae like macroscopic priapulidans, but differs from them in having two additional pairs of lorica tubuli in the anterior part (see Por and Bromley, 1974). Introvert structures of larval stages of both body size classes do not differ distinctly from each other. From our data, loricate larval stages are ancestrally absent in Priapulida. This may be due to the absence of loricate larval stages in outgroup taxa Nematomorpha and Kinorhyncha. However, Nematomorpha have larval stages that distinctly differ from their adults, but they lack a lorica (Schmidt-Rhaesa, 2013b). Only Loricifera have larval stages with a lorica, similar to most priapulidans (Bang-Berthelsen et al., 2013). Kinorhyncha have a direct postembryonic development (Neuhaus, 2013). *Meiopriapulus fijiensis* is the only priapulidan with a direct development (Higgins and Storch, 1991).

Loricate larval stages of priapulidans have a distinct neck region, characterized by cuticular folds with flosculi (Van der Land, 1970; Schmidt-Rhaesa, 2013a). In adults, a neck region is only reported for *Tubiluchus* (Van der Land, 1970). The neck region of *Tubiluchus* does not have tumuli, which are cuticular elevations arranged in rows on the trunk (Van der Land, 1970). In *M. fijiensis*, a neck region is not directly reported, but may be present in the anterior trunk region, which has trunk scalids. The trunk of *M. fijiensis* is covered in tubercles (small spherical cuticular protrusions), which do not seem to appear in the anterior trunk, similar to the tumuli of *Tubiluchus* (cf. Figs. 15 and 16 in Morse, 1982). A neck region is not reported for adult Eupriapulida. Both related taxa, Kinorhyncha and Loricifera, have neck regions in adults (Bang-Berthelsen et al., 2013; Neuhaus, 2013). Thus, the presence of a neck region in adult priapulidans is reconstructed as an ancestral trait that got lost in Eupriapulida.

Many morphological structures of priapulidans have sensory structures associated with them. These receptors are often similarly composed with a basis and an apical tube (see Schmidt-Rhaesa and Raeker, 2024). Another type of receptors are flower-like structures, the flosculi, which are remarkable due to their petal-like apical extensions (Van der Land, 1970). Flosculi have been reported recently in adults of all microscopic genera, but also in (post-)larval stages of *H. spinulosus* and *P. caudatus* (see Schmidt-Rhaesa, 2013a). Flosculi have been reported recently in adult *H. spinulosus* (Raeker et al., 2024a) and *P. papillatus* (Schmidt-Rhaesa and Raeker, 2024), but not yet in adult *Priapulus* and *Acanthopriapulus*. Thus, the presence of flosculi is ancestral in adults of Priapulida and got lost in evolution in Monocaudata. Similar flosculus-like structures are also present in Loricifera (N-flosculi; Bang-Berthelsen et al., 2013) and Kinorhyncha (type-3 and 5 sensory spots; Neuhaus, 2013).

4.4. Are Priapulida ancestrally small?

Our phylogenomic results based on combined molecular data and tracing of selected morphological characters conclude extant Priapulida as having ancestrally small body sizes. An ancestrally microscopic body size of Priapulida was already argued by Lemburg (1999) due to the most parsimonious evolution, if including microscopic related outgroups (Kinorhyncha, Loricifera, Gastrotricha, Nematoda) in the analyses. Other studies that include fossil data in their analyses lean towards a macroscopic ancestral body size (e.g., Adrianov and Malakhov, 1996). All described priapulidan-like fossils exceed the microscopic size and are therefore treated as macroscopic species, thus, a macroscopic body size seems plausible. However, detailed phylogenetic analyses including all extant and fossil priapulidans and incorporating thorough reexaminations and revisions of the coding of morphological traits is needed. Moreover, extinct microscopic priapulidans may very well have existed and just not been found due to the major sampling and preservation bias against microscopic fossils (Worsaae et al., 2023). Small carbonaceous fossils (SCFs) that presumably resemble priapulidan teeth or scalids have been found frequently (e.g., Butterfield and Harvey, 2012; Smith et al., 2015; Slater et al., 2017). Priapulidan teeth-like SCFs often reach tooth base widths of more than 50 μm, whereas tooth bases of extant microscopic species range between 5 and 15 μm (*Meiopriapulus*, see Sørensen et al., 2012; *Tubiluchus*, see Schmidt-Rhaesa et al., 2013; *Maccabeus*, see von Salvini-Plawen, 1974). Therefore, it seems likely that the specimens belonging to the SCFs were larger than microscopic priapulidans. The exact phylogenetic position is difficult, but it should be noted that a few SCFs share morphological similarities with pectinate teeth of extant *Tubiluchus* (see Figs. 3, 9A and 10B,D,F in Smith et al., 2015; Fig. 4B in Slater et al., 2017). Both have a basal crescent-like shape with an anterior part holding spines (e.g., prong holding denticles in fossils; manubrium holding pecten in *Tubiluchus*, see Fig. 2F) and a posterior part bending towards the anterior (e.g., spur in fossils; posterior part of the manubrium in *Tubiluchus*). These observations support the need for further analyses of the phylogeny of priapulidans including extinct species.

The fertilization mode differs between both size classes of Priapulida. Macroscopic species have external fertilization, releasing gonad products into the water (Van der Land, 1970). The spermatozoa of macroscopic species are of a round-headed type with a cilium (Afzelius and Ferraguti, 1978; Schmidt-Rhaesa, 2013a). In contrast, microscopic

species are all assumed to have internal fertilization, due to sexual dimorphism (species-specific male genital region in *Tubiluchus*), modified spermatozoa (*Tubiluchus*; Alberti and Storch, 1983; Ferraguti and Garbelli, 2006), internal brooding of embryos (*Meiopriapulus*; Storch and Higgins, 1991) and low number of oocytes (*Tubiluchus*, *Meiopriapulus* and *Maccabeus*; Storch and Higgins, 1991). Although *Meiopriapulus* is assumed to have internal fertilization, similar round-headed spermatozoa (i.e. spermatozoa with a spherical front part including nucleus, mitochondria and acrosome, and a posteriorly attaching cilium) as in macroscopic species have been reported (Storch et al., 1989). *Tubiluchus* on the other hand has modified spermatozoa with an elongate corkscrewed head (Alberti and Storch, 1983; Ferraguti and Garbelli, 2006). A correlation between sperm structure and fertilization mode (round-headed spermatozoa in external fertilizers and diversely modified spermatozoa in internal fertilizers) as well as body size and fertilization mode (large-sized external fertilizers and small-sized internal fertilizers) of marine invertebrates is commonly assumed (e.g., Franzén, 1977; Jarvis and Marshall, 2023). *Meiopriapulus* is an exception from such assumptions, combining round-headed spermatozoa and internal fertilization. Our phylogeny suggests internal fertilization as ancestral for Priapulida, which is surprising, as external fertilization and round-headed spermatozoa are usually regarded as ancestral. However, as *Meiopriapulus* has preserved round-headed spermatozoa, the ancestor of Eupriapulida may have returned to external fertilization and spermatozoa were modified only in the ancestor of *Tubiluchus*. Related microscopic taxa, Kinoryncha and Loricifera, are assumed to have exclusively internal fertilization modes (see Bang-Berthelsen et al., 2013; Neuhaus, 2013) which might reinforce the hypothesis of internal fertilization being the ancestral mode of reproduction in Priapulida.

5. Conclusions

We provide a phylogenetic tree of Priapulida with molecular data from ten species representing five of the seven genera. In addition, positions of the rare priapulidan genera *Acanthopriapulus* and *Maccabeus* were inferred by analyzing morphological data, as molecular data are still lacking. *Maccabeus* holds morphological characters of both priapulidan size classes, which makes it important for understanding priapulidan evolution and their ecological transitions. Our suggested position of *Maccabeus* as sister taxon to the remaining macroscopic priapulidans is congruent with the majority of morphological phylogenies of previous studies, but molecular data from fresh material should be added to future studies. Additionally, a much-needed morphological reinvestigation of *Maccabeus* could help refine our understanding of the evolution of morphological characters in Priapulida.

Similarly, we recommend generating novel molecular (transcriptomic or genomic) data for *M. fijiensis* and the loriciferan *A. elegans* (or other Loricifera), which are here represented by low quality transcriptomes. Especially, *M. fijiensis* could benefit from high quality molecular data, as this species deviates in multiple morphological characteristics from other priapulidans (introvert characters; direct development; presence of coelom) and additional molecular data could further test its position as sister taxon to the remaining extant priapulidans.

Our character optimization suggests that extant Priapulida have an ancestrally small body size from which large-sized species derived. Potential findings of priapulidan microfossils are needed to support this reconstructed ancestral small body size. However, our optimization also suggests that internal fertilization would be ancestral in Priapulida while external fertilization is derived. This contrasts with the “common” hypothesis for marine invertebrates where broadcast spawning appears as the primitive mode of fertilization with subsequent mechanisms for internal fertilization evolving in the more derived groups. Nonetheless, our study sheds light on the phylogeny of one of the most primitive-looking ecdysozoan phyla.

CRediT authorship contribution statement

Jan Raeker: Writing – review & editing, Writing – original draft, Visualization, Software, Project administration, Methodology, Investigation, Formal analysis, Data curation, Conceptualization. **Arianna Lord:** Writing – review & editing, Writing – original draft, Software, Project administration, Methodology, Investigation, Formal analysis, Data curation, Conceptualization. **María Herranz:** Writing – review & editing, Writing – original draft, Supervision, Resources, Project administration, Methodology, Formal analysis, Conceptualization. **Gonzalo Giribet:** Writing – review & editing, Writing – original draft, Supervision, Project administration, Funding acquisition, Conceptualization. **Katrine Worsaae:** Writing – review & editing, Writing – original draft, Supervision, Resources, Project administration, Methodology, Funding acquisition, Conceptualization. **Andreas Schmidt-Rhaesa:** Writing – review & editing, Supervision, Resources, Project administration, Funding acquisition, Conceptualization.

6. Data availability

Raw sequences are deposited in the NCBI sequence read archive (SRA) under the BioProject accession number PRJNA1185466. Input and output files, concatenated matrices and tree files generated during the analyses are deposited on the Harvard Dataverse under https://doi.org/10.7910/DVN/VYCIGX.

Declaration of competing interest

The authors declare that they have no known competing financial interests or personal relationships that could have appeared to influence the work reported in this paper.

Acknowledgements

We are deeply thankful for helping us to collect, or allocating us specimens to use in this study: Alejandro Martínez García (Water Research Institute, National Research Council, Verbania, Italy); Anna J. Phillips (Smithsonian Institution, Natural Museum of Natural History, Washington, DC, USA); Ekin Tilic (Senckenberg Natural History Museum Frankfurt, Germany); Glafira Kolbasova (White Sea Biological Station, Lomonosov Moscow State University, Russia); Katrin Iken (College of Fisheries and Ocean Sciences, University of Alaska Fairbanks, USA); Saskia Brix (Deutsches Zentrum für Marine Biodiversitätsforschung, Hamburg, Germany).

We would also like to thank Shahan Derkarabetian (San Diego Natural History Museum), who designed and generously shared with us the probe set which we used to bioinformatically harvest loci for our combined phylogenetic analysis.

This study was funded by the Deutsche Forschungsgemeinschaft (DFG, German Research Foundation) with the grant number SCHM 1278/20-1 to Andreas Schmidt-Rhaesa and Katrine Worsaae. With additional internal funding from the Museum of Comparative Zoology, Harvard University.

Appendix A. Supplementary data

Supplementary data to this article can be found online at https://doi.org/10.1016/j.ympev.2025.108297.

Data availability

Data will be made available on request.

References

Aberer, A.J., Kobert, K., Stamatakis, A., 2014. ExaBayes: massively parallel Bayesian tree inference for the whole-genome era. Mol. Biol. Evol. 31 (10), 2553–2556. https://doi.org/10.1093/molbev/msu236.

Adrianov, A.V., Malakhov, V.V., Chesunov, A.V., Tsetlin, A.B., 1989. *Tubiluchus arcticus* sp. n. from the White Sea (Priapulomorpha Tubiluchidae). Zool. Zh. 68, 126–131.

Adrianov, A.V., Malakhov, V.V., 1991. First findings of dwarf priapulids of the genus *Tubiluchus* (Priapulida Tubiluchidae) in Oceania (New-Hebrides). Zool. Zh. 70, 23–32.

Adrianov, A.V., Malakhov, V.V., 1995. The phylogeny and classification of the phylum Cephalorhyncha. Zoosyst. Ross. 3, 181–201.

Adrianov, A.V., Malakhov, V.V., 1996. Priapulida: Structure, development, phylogeny, and classification. KMK Scientific Press, Moscow [In Russian with English summary].

Afzelius, B.A., Ferraguti, M., 1978. The spermatozoon of *Priapulus caudatus* Lamarck. J. Submicrosc. Cytol. 10, 71–80.

Alberti, G., Storch, V., 1983. Fine structure of developing and mature spermatozoa in *Tubiluchus* (Priapulida, Tubiluchidae). Zoomorphology 103, 219–227. https://doi.org/10.1007/BF00310479.

Bang-Berthelsen, I., Schmidt-Rhaesa, A., Kristensen, R.M., 2013. Loricifera. In: Schmidt-Rhaesa, A., editor, Handbook of Zoology: Nematomorpha, Priapulida, Kinorhyncha and Loricifera. Volume 1. Berlin: De Gruyter, 349-378. https://doi.org/10.1515/9783110272536.349.

Baird, W., 1868. Monograph of the species of worms belonging to the subclass Gephyrea; with a notice of such species as are contained in the collection of the British Museum. Proc. Zool. Soc. Lond. 76–114.

Bankevich, A., Nurk, S., Antipov, D., Gurevich, A.A., Dvorkin, M., Kulikov, A.S., Lesin, V. M., Nikolenko, S.I., Pham, S., Prjibelski, A.D., Pyshkin, A.V., Sirotkin, A.V., Vyahhi, N., Tesler, G., Alekseyev, M.A., Pevzner, P.A., 2012. SPAdes: a new genome assembly algorithm and its applications to single-cell sequencing. J. Comput. Biol. 19, 455–477. https://doi.org/10.1089/cmb.2012.0021.

Bolger, A.M., Lohse, M., Usadel, B., 2014. Trimmomatic: A Flexible Trimmer for Illumina Sequence Data. Bioinformatics 30, 2114–2120. https://doi.org/10.1093/bioinformatics/btu170.

Borner, J., Rehm, P., Schill, R.O., Ebersberger, I., Burmester, T., 2014. A transcriptome approach to ecdysozoan phylogeny. Mol. Phylogenetics Evol. 80, 79–87. https://doi.org/10.1016/j.ympev.2014.08.001.

Butterfield, N.J., Harvey, T.H.P., 2012. Small carbonaceous fossils (SCFs): a new measure of early Paleozoic paleobiology. Geology 40 (1), 71–74. https://doi.org/10.1130/G32580.1.

Calloway, C.B., 1975. Morphology of the introvert and associated structures of the priapulid *Tubiluchus corallicola* from Bermuda. Mar. Biol. 31, 161–174. https://doi.org/10.1007/BF00391628.

Campos, P., Gilbert, T.P., 2012. DNA Extraction from Formalin-Fixed Material. In: Shapiro, B., Hofreiter, M. (Eds.), Methods in Molecular Biology, Vol. 840. Humana Press, pp. 81–85. https://doi.org/10.1007/978-1-61779-516-9_11.

Cannon, J.T., Vellutini, B.C., Smith, J., Ronquist, F., Jondelius, U., Hejnol, A., 2016. Xenacoelomorpha is the sister group to Nephrozoa. Nature 530, 89–93. https://doi.org/10.1038/nature16520.

Castresana, J., 2000. Selection of conserved blocks from multiple alignments for their use in phylogenetic analysis. Mol. Biol. Evol. 17, 540–552. https://doi.org/10.1093/oxfordjournals.molbev.a026334.

Conway Morris, S., Robison, R.A., 1986. Middle Cambrian priapulids and other soft-bodied fossils from Utah and Spain. Univ. Kans. Paleontol. Contrib. 117, 1–22.

Cunha, T.J., de Medeiros, B.A.S., Lord, A., Sørensen, M.V., Giribet, G., 2023. Rampant loss of universal metazoan genes revealed by a chromosome-level genome assembly of the parasitic Nematomorpha. Curr. Biol. 33 (16), 3514–3521. https://doi.org/10.1016/j.cub.2023.07.003.

Danielssen, D.C., 1869. To maerkelige Sodyr. Forhandlinger Skand. naturforsk. Mode Christiania 1868, 541–542.

De Guerne, J., 1886. Sur les Gèphyriens de la famille des Priapulides recueillis par la mission de Cap Horn. C. R. Acad. Sci. Paris 103, 760–762.

Derkarabetian, S., Benavides, L.R., Giribet, G., 2019. Sequence capture phylogenomics of historical ethanol-preserved museum specimens: Unlocking the rest of the vault. Mol. Ecol. Resour. 19 (6), 1531–1544. https://doi.org/10.1111/1755-0998.13072.

Derkarabetian, S., Lord, A., Angier, K., Frigyik, E., Giribet, G., 2023. An Opiliones-specific ultraconserved element probe set with a near-complete family-level phylogeny. Mo. Phylogenetics Evol. 187, 107887. https://doi.org/10.1016/j.ympev.2023.107887.

Dodsworth, S., 2015. Genome skimming for next-generation biodiversity analysis. Trends Plant Sci. 20, 525–527. https://doi.org/10.1016/j.tplants.2015.06.012.

Dong, X.-P., Donoghue, P.C.J., Cheng, H., Liu, J.-B., 2004. Fossil embryos from the middle and late Cambrian period of Hunan, south China. Nature 427, 237–240. https://doi.org/10.1038/nature02215.

Dong, X.-P., Bengtson, S., Gostling, N.J., Cunningham, J.A., Harvey, T.H.P., Kouchinsky, A., Val'kov, A.K., Repetski, J.E., Repetski, J.E., Stampanoni, M., Marone, F., Donoghue, P.C.J., 2010. The anatomy, taphonomy, taxonomy and systematic affinity of *Markuelia*: Early Cambrian to Early Ordovician scalidophorans. Palaeontology 53, 1291–1314. https://doi.org/10.1111/j.1475-4983.2010.01006.x.

Dong, X.-P., Donoghue, P.C., Cunningham, J.A., Liu, J.B., Cheng, H., 2005. The anatomy, affinity, and phylogenetic significance of *Markuelia*. Evol. Dev. 7 (5), 468–482. https://doi.org/10.1111/j.1525-142X.2005.05050.x.

Emms, D.M., Kelly, S., 2019. OrthoFinder: phylogenetic orthology inference for comparative genomics. Genome Biol. 20, 238. https://doi.org/10.1186/s13059-019-1832-y.

Faircloth, B.C., 2013. Illumiprocessor: a trimmomatic wrapper for parallel adapter and quality trimming. https://doi.org/10.6079/J9ILL.

Faircloth, B.C., Branstetter, M.G., White, N.D., Brady, S.G., 2015. Target enrichment of ultraconserved elements from arthropods provides a genomic perspective on relationships among Hymenoptera. Mol. Ecol. Resour. 15 (3), 489–501. https://doi.org/10.1111/1755-0998.12328.

Faircloth, B.C., 2016. PHYLUCE is a software package for the analysis of conserved genomic loci. Bioinformatics 32, 786–788. https://doi.org/10.1093/bioinformatics/btv646.

Ferraguti, M., Garbelli, C., 2006. The spermatozoon of a "living fossil": *Tubiluchus troglodytes* (Priapulida). Tiss. Cell 38, 1–6. https://doi.org/10.1016/j.tice.2005.05.001.

Franzén, A., 1977. Sperm structure with regard to fertilization biology and phylogenetics. Verh. Dtsch. Zool. Ges. 1977, 123–138.

Fu, D., Tong, G., Dai, T., Liu, W., Yang, Y., Zhang, Y., Cui, L., Li, L., Yun, H., Wu, Y., Sun, A., Liu, C., Pei, W., Gaines, R.R., Zhang, Z., 2019. The Qingjiang biota—A Burgess Shale–type fossil Lagerstätte from the early Cambrian of South China. Science 363, 1338–1342. https://doi.org/10.1126/science.aau8800.

Fu, C.N., Mo, Z.Q., Yang, J.B., Cai, J., Ye, L.J., Zou, J.Y., Qin, H.T., Zheng, W., Hollingsworth, P.M., Li, D.Z., Gao, L.M., 2022. Testing genome skimming for species discrimination in the large and taxonomically difficult genus *Rhododendron*. Mol. Ecol. Resour. 22, 404–414. https://doi.org/10.1111/1755-0998.13479.

Geburzi, J.C., Rodríguez-Flores, P.C., Derkarabetian, S., Giribet, G., 2024. From the shallows to the depths: A new probe set to target ultraconserved elements for Decapoda and other Malacostraca. Front. Mar. Sci. 11, 1429314. https://doi.org/10.3389/fmars.2024.1429314.

Giribet, G., Distel, D., Polz, M., Sterrer, W., Wheeler, W., 2000. Triploblastic relationships with emphasis on the acoelomates and the position of Gnathostomulida, Cycliophora, Plathelminthes, and Chaetognatha: a combined approach of 18S rDNA sequences and morphology. Syst. Biol. 49 (3), 539–562. https://doi.org/10.1080/10635159950127385.

Giribet, G., Edgecombe, G.D., 2017. Current understanding of Ecdysozoa and its internal phylogenetic relationships. Integr. Comp. Biol. 57, 455–466. https://doi.org/10.1093/icb/icx072.

Giribet, G., Edgecombe, G.D., 2020. The Invertebrate Tree of Life. Princeton University Press.

Godeiro, N.N., Ding, Y., Cipola, N.G., Jantarit, S., Bellini, B.C., Zhang, F., 2023. Phylogenomics and systematics of Entomobryoidea (Collembola): marker design, phylogeny and classification. Cladistics 39 (2), 101–115. https://doi.org/10.1111/cla.12521.

Gosse, P.H., 1855. A manual of marine zoology for the British Isles (Vol. 1). J. Van Voorst. https://doi.org/10.5962/bhl.title.32503.

Grabherr, M.G., Haas, B.J., Yassour, M., Levin, J.Z., Thompson, D.A., Amit, I., Adiconis, X., Fan, L., Raychowdhury, R., Zeng, Q., Chen, Z., Mauceli, E., Hacohen, N., Gnirke, A., Rhind, N., di Palma, F., Birren, B.W., Nusbaum, C., Lindblad-Toh, K., Friedman, N., Regev, A., 2011. Full-length transcriptome assembly from RNA-Seq data without a reference genome. Nat. Biotechnol. 29 (7), 644–652. https://doi.org/10.1038/nbt.1883.

Han, J., Shu, D., Zhang, Z., Liu, J., 2004. The earliest-known ancestors of recent Priapulomorpha from the early Cambrian Chengjiang Lagerstätte. Chi. Sci. Bull. 49, 1860–1868. https://doi.org/10.1007/BF03183414.

Harvey, T.H.P., Dong, X.-P., Donoghue, P.C.J., 2010. Are palaeoscolecids ancestral ecdysozoans? Evo. Dev. 12, 177–200. https://doi.org/10.1111/j.1525-142X.2010.00403.x.

Harvey, T.H.P., Butterfield, N.J., 2017. Exceptionally preserved Cambrian loriciferans and the early animal invasion of the meiobenthos. Nat. Ecol. Evol. 1, 0022. https://doi.org/10.1038/s41559-016-0022.

Herranz, M., Stiller, J., Worsaae, K., Sørensen, M.V., 2022. Phylogenomic analyses of mud dragons (Kinorhyncha). Mol. Phylogenetics Evol. 168, 107375. https://doi.org/10.1016/j.ympev.2021.107375.

Higgins, R.P., Storch, V., 1991. Evidence for the direct development in *Meiopriapulus fijiensis*. Trans. Am. Microsc. Soc. 110, 37–46. https://doi.org/10.2307/3226738.

Hoang, D.T., Chernomor, O., von Haeseler, A., Minh, B.Q., Vinh, L.S., 2018. UFBoot2: improving the ultrafast bootstrap approximation. Mol. Biol. Evol. 35 (2), 518–522. https://doi.org/10.1093/molbev/msx281.

Howard, R.J., Giacomelli, M., Lozano-Fernandez, J., Edgecombe, G.D., Fleming, J.F., Kristensen, R.M., Ma, X., Olesen, J., Sørensen, M.V., Thomsen, P.F., Wills, M.A., Donoghue, P.C.J., Pisani, D., 2022. The Ediacaran origin of Ecdysozoa: Integrating fossil and phylogenomic data. J. Geol. Soc. 179 (4), jgs2021-107. https://doi.org/10.1144/jgs2021-107.

Hu, S.X., Zhu, M.Y., Zhao, F.C., Steiner, M., 2017. A crown group priapulid from the early Cambrian Guanshan Lagerstätte. Geol. Mag. 154, 1329–1333. https://doi.org/10.1017/s001675681700019x.

Huang, D.Y., Vannier, J., Chen, J.Y., 2004a. Recent Priapulidae and their Early Cambrian ancestors: comparison and evolutionary significance. Geobios 37, 217–228. https://doi.org/10.1016/j.geobios.2003.04.004.

Huang, D.Y., Vannier, J., Chen, J.Y., 2004b. Anatomy and lifestyles of Early Cambrian priapulid worms exemplified by *Corynetis* and *Anningvermis* from the Maotianshan Shale (SW China). Lethaia 37 (1), 21–33. https://doi.org/10.1080/0024116041000508.

Janssen, R., Wennberg, S.A., Budd, G.E., 2009. The hatching larva of the priapulid worm *Halicryptus spinulosus*. Front. Zool. 6, 1–7. https://doi.org/10.1186/1742-9994-6-8.

Jarvis, G.C., Marshall, D.J., 2023. Fertilization Mode Covaries with Body Size. Am. Nat. 202 (4), 448–457. https://doi.org/10.1086/725864.

Kalyaanamoorthy, S., Minh, B.Q., Wong, T.K.F., Von Haeseler, A., Jermiin, L.S., 2017. ModelFinder: Fast model selection for accurate phylogenetic estimates. Nat. Methods 14, 587–589. https://doi.org/10.1038/nmeth.4285.

Katoh, K., Standley, D.M., 2013. MAFFT multiple sequence alignment software version 7: improvements in performance and usability. Mol. Biol. Evol. 30, 772–780. https://doi.org/10.1093/molbev/mst010.

Kearse, M., Moir, R., Wilson, A., Stones-Havas, S., Cheung, M., Sturrock, S., Buxton, S., Cooper, A., Markowitz, S., Duran, C., Thierer, T., Ashton, B., Meintjes, P., Drummond, A., 2012. Geneious Basic: An integrated and extendable desktop software platform for the organization and analysis of sequence data. Bioinformatics 28 (12), 1647–1649. https://doi.org/10.1093/bioinformatics/bts199.

Kirsteuer, E., 1976. Notes on adult morphology and larval development of *Tubiluchus corallicola* (Priapulida), based on *in vivo* and scanning electron microscopic examinations of specimens from Bermuda. Zool. Scripta 5, 239–255. https://doi.org/10.1111/j.1463-6409.1976.tb00706.x.

Kocot, K.M., Citarella, M.R., Moroz, L.L., Halanych, K.M., 2013. PhyloTreePruner: a phylogenetic tree-based approach for selection of orthologous sequences for phylogenomics. Evolut. Bioinf. 9, 429–435. https://doi.org/10.4137/EBO.S12813.

Kolbasova, G., Schmidt-Rhaesa, A., Syomin, V., Bredikhin, D., Morozov, T., Neretina, T., 2023. Cryptic species complex or an incomplete speciation? Phylogeographic analysis reveals an intricate Pleistocene history of *Priapulus caudatus* Lamarck, 1816. Zool. Anz. 302, 113–130. https://doi.org/10.1016/j.jcz.2022.11.013.

Koren, J., Danielssen, D.C., 1875. Bidrag til de norske Gephyreers Naturhistorie. Nyt Magazin Naturv. 21, 108–138.

Kück, P., Longo, G.C., 2014. FASconCAT-G: extensive functions for multiple sequence alignment preparations concerning phylogenetic studies. Front. Zool. 11, 81. https://doi.org/10.1186/s12983-014-0081-x.

Lamarck, J.B. de, 1816. Histoire naturelle des animaux sans vertébrés, 3, 1-586.

Lanfear, R., Calcott, B., Kainer, D., Mayer, C., Stamatakis, A., 2014. Selecting optimal partitioning schemes for phylogenomic datasets. BMC Evol. Biol. 14, 1–14. https://doi.org/10.1186/1471-2148-14-82.

Laumer, C.E., Bekkouche, N., Kerbl, A., Goetz, F., Neves, R., Sørensen, M., Kristensen, R., Hejnol, A., Dunn, C., Giribet, G., Worsaae, K., 2015. Spiralian phylogeny informs the evolution of microscopic lineages. Curr. Biol. 25 (15), 2000–2006. https://doi.org/10.1016/j.cub.2015.06.068.

Laumer, C.E., Fernández, R., Lemer, S., Combosch, D.J., Kocot, K.M., Riesgo, A., Andrade, S.C.S., Sterrer, W., Sørensen, M., Giribet, G., 2019. Revisiting metazoan phylogeny with genomic sampling of all phyla. Proc. r. Soc. b. 286, 20190831. https://doi.org/10.1016/j.cub.2015.06.068.

Lemburg, C., 1999. Ultrastrukturelle Untersuchungen an den Larven von *Halicryptus spinulosus* und *Priapulus caudatus*. Hypothesen Zur Phylogenie Der Priapulida Und Deren Bedeutung Für Die Evolution Der Nemathelminthes.

Literman, R., Windsor, A.M., Bart Jr, H.L., Sage Hunter, E., Deeds, J.R., Handy, S.M., 2023. Using low-coverage whole genome sequencing (genome skimming) to delineate three introgressed species of buffalofish (*Ictiobus*). Mol. Phylogenetics Evol. 182, 107715. https://doi.org/10.1016/j.ympev.2023.107715.

Liu, B.B., Ma, Z.Y., Ren, C., Hodel, R.G., Sun, M., Liu, X.Q., Liu, G.N., Hong, D.Y., Zimmer, E.A., Wen, J., 2021. Capturing single-copy nuclear genes, organellar genomes, and nuclear ribosomal DNA from deep genome skimming data for plant phylogenetics: A case study in Vitaceae. J. Syst. Evol. 59 (5), 1124–1138. https://doi.org/10.1111/jse.12806.

Lord, A., Cunha, T.J., de Medeiros, B.A.S., Sato, S., Khost, D.E., Sackton, T.B., Giribet, G., 2023. Expanding on our knowledge of ecdysozoan genomes, a contiguous assembly of the meiofaunal priapulan *Tubiluchus corallicola*. Genome Biol. Evol. 15, evad103. https://doi.org/10.1093/gbe/evad103.

Maddison, W.P., Maddison, D.R., 2023. Mesquite: a modular system for evolutionary analysis. accessed on 14. April 2023 Version 3, 80. http://www.mesquiteproject.org.

Malakhov, V.V., 1978. New representative of sedentary priapulid *Chaetostephanus cirratus* sp.n. Zool. Zhurn. 58, 1410–1412.

Manni, M., Berkeley, M.R., Seppey, M., Simão, F.A., Zdobnov, E.M., 2021. BUSCO update: novel and streamlined workflows along with broader and deeper phylogenetic coverage for scoring of eukaryotic, prokaryotic, and viral genomes. Mol. Biol. Evol. 38, 4647–4654. https://doi.org/10.1093/molbev/msab199.

Martín-Durán, J.M., Janssen, R., Wennberg, S., Budd, G.E., Hejnol, A., 2012. Deuterostomic development in the protostome *Priapulus caudatus*. Curr. Biol. 22, 2161–2166. https://doi.org/10.1016/j.cub.2012.09.037.

Minh, B.Q., Schmidt, H.A., Chernomor, O., Schrempf, D., Woodhams, M.D., von Haeseler, A., Lanfear, R., 2020. IQ-TREE 2: New models and efficient methods for phylogenetic inference in the genomic era. Mol. Biol. Evol. 37, 1530–1534. https://doi.org/10.1093/molbev/msaa015.

Morse, M.P., 1981. *Meiopriapulus fijiensis* n. gen., n. sp.: an interstitial priapulid from coarse sand in Fiji. Trans. Am. Microsc. Soc. 100 (3), 239–252. https://doi.org/10.2307/3225549.

Neuhaus, B., 2013. Kinorhyncha (= Echinodera). In: Schmidt-Rhaesa, A. (Ed.), Handbook of Zoology: Nematomorpha, Priapulida, Kinorhyncha and Loricifera, Volume 1. De Gruyter, Berlin, pp. 181–348. https://doi.org/10.1515/9783110272536.181.

Nielsen, C., 2012. Animal evolution: interrelationships of the living phyla, 3rd ed. Oxford University Press, Oxford.

Nishimura, O., Hara, Y., Kuraku, S., Hancock, J., 2017. gVolante for standardizing completeness assessment of genome and transcriptome assemblies. Bioinformatics 33 (22), 3635–3637. https://doi.org/10.1093/bioinformatics/btx445.

Park, J.K., Rho, H.S., Kristensen, R.M., Kim, W., Giribet, G., 2006. First molecular data on the phylum Loricifera–an investigation into the phylogeny of Ecdysozoa with emphasis on the positions of Loricifera and Priapulida. Zoological Science 23 (11), 943–954. https://doi.org/10.2108/zsj.23.943.

Pleijel, F., 1995. On character coding for phylogeny reconstruction. Cladistics 11 (3), 309–315. https://doi.org/10.1016/0748-3007(95)90018-7.

Por, F.D., 1972. Priapulida from deep bottoms near Cyprus. Israel Journal of Zoology 21 (3–4), 525–528. https://doi.org/10.1080/00212210.1972.10688375.

Por, F.D., Bromley, H.J., 1974. Morphology and anatomy of *Maccabeus tentaculatus* (Priapulida: Seticoronaria). J. Zool. Lond. 173, 173–197. https://doi.org/10.1111/j.1469-7998.1974.tb03125.x.

Price, M.N., Dehal, P.S., Arkin, A.P., Poon, A.F.Y., 2010. FastTree 2 - approximately maximum-likelihood trees for large alignments. PLoS ONE 5 (3), e9490.

Quattrini, A.M., McCartin, L.J., Easton, E.E., Horowitz, J., Wirshing, H.H., Bowers, H., Mitchell, K., González-García, M.P., Sei, M., McFadden, C.S., Herrera, S., 2024. Skimming genomes for systematics and DNA barcodes of corals. Ecol. Evol. 14 (5), e11254. https://doi.org/10.1002/ece3.11254.

Raeker, J., Worsaae, K., Schmidt-Rhaesa, A., 2024a. David versus Goliath: an interspecific comparison between small-sized *Halicryptus spinulosus* and large-sized *Halicryptus higginsi* (Priapulida). Zool. Anz. 313, 1–20. https://doi.org/10.1016/j.jcz.2024.08.003.

Raeker, J., Worsaae, K., Schmidt-Rhaesa, A., 2024b. New morphological structures of *Priapulus caudatus*, Lamarck 1816 (Priapulida) and analysis of homologous characters across macroscopic priapulids. Zool. Anz. 312, 135–152. https://doi.org/10.1016/j.jcz.2024.08.005.

Ribeiro, P.G., Torres Jiménez, M.F., Andermann, T., Antonelli, A., Bacon, C.D., Matos-Maraví, P., 2021. A bioinformatic platform to integrate target capture and whole genome sequences of various read depths for phylogenomics. Mol. Ecol. 30 (23), 6021–6035. https://doi.org/10.1111/mec.16240.

Rohland, N., Reich, D., 2012. Cost-effective, high-throughput DNA sequencing libraries for multiplexed target capture. Genome Res. 22, 939–946. https://doi.org/10.1101/gr.128124.111.

von Salvini-Plawen, L., 1974. Zur Morphologie und Systematik der Priapulida: *Chaetostephanus praeposteriens*, der Vertreter einer neuen Ordnung Seticoronaria. Z. Zool. Syst. Evolut. Forsch. 12, 31–54. https://doi.org/10.1111/j.1439-0469.1974.tb00156.x.

Sato, S., Derkarabetian, S., Lord, A., Giribet, G., 2024. An ultraconserved element probe set for velvet worms (Onychophora). Mol. Phylogenetics Evol., 108115 https://doi.org/10.1016/j.ympev.2024.108115.

Schmidt-Rhaesa, A., 2013a. Priapulida. In: Schmidt-Rhaesa, A. (Ed.), Handbook of Zoology: Nematomorpha, Priapulida, Kinorhyncha and Loricifera, Volume 1. De Gruyter, Berlin, pp. 147–180. https://doi.org/10.1515/9783110272536.147.

Schmidt-Rhaesa, A., 2013b. Nematomorpha. In: Schmidt-Rhaesa, A. (Ed.), Handbook of Zoology: Nematomorpha, Priapulida, Kinorhyncha and Loricifera, Volume 1. De Gruyter, Berlin, pp. 29–146. https://doi.org/10.1515/9783110272536.29.

Schmidt-Rhaesa, A., Cañete, J.I., Mutschke, E., 2022. New record and first description including SEM and μCT of the rare priapulid *Acanthopriapulus horridus* (Priapulida, Scalidophora). Zool. Anz. 298, 1–9. https://doi.org/10.1016/j.jcz.2022.03.001.

Schmidt-Rhaesa, A., Rothe, B.H., Martínez, A.G., 2013. *Tubiluchus lemburgi*, a new species of meiobenthic Priapulida. Zool. Anz. 253 (2), 158–163. https://doi.org/10.1016/j.jcz.2013.08.004.

Schmidt-Rhaesa, A., Panpeng, S., Yamasaki, H., 2017. Two new species of *Tubiluchus* (Priapulida) from Japan. Zool. Anz. 267, 155–167. https://doi.org/10.1016/j.jcz.2017.03.004.

Schmidt-Rhaesa, A., Raeker, J., 2023. Morphology of larval and postlarval stages of *Priapulopsis bicaudatus* (Danielssen, 1869) (Priapulida) from the North Atlantic Ocean. Zool. Anz. 302, 1–16. https://doi.org/10.1016/j.jcz.2022.11.006.

Schmidt-Rhaesa, A., Raeker, J., 2024. Review of the Priapulida of New Zealand with the description of a new species. New Zealand J. Zool. (online First). https://doi.org/10.1080/03014223.2023.2278738.

Schram, F.R., 1973. Pseudocoelomates and a nemertine from the Illinois Pennsylvanian. Journal of Paleontology 47 (5), 985–989. http://www.jstor.org/stable/1303083.

Shao, T.Q., Wang, Q., Liu, Y.H., Qin, J.C., Zhang, Y.N., Liu, M.J., Shao, Y., Zhao, J.Y., Zhang, H.Q., 2020. A new scalidophoran animal from the Cambrian Fortunian Stage of South China and its implications for the origin and early evolution of Kinorhyncha. Precambrian Res. 349, 105616. https://doi.org/10.1016/j.precamres.2020.105616.

Shirley, T.C., Storch, V., 1999. *Halicryptus higginsi* n.sp. (Priapulida) – a giant new species from Barrow, Alaska. Invertebr. Biol. 118, 404–413. https://doi.org/10.2307/3227009.

Slater, B.J., Harvey, T.H.P., Guilbaud, R., Butterfield, N.J., 2017. A cryptic record of Burgess Shale-type diversity from the early Cambrian of Baltica. Palaeontology 60, 117–140. https://doi.org/10.1111/pala.12273.

Smith, M.R., Harvey, T.H.P., Butterfield, N.J., 2015. The macro- and microfossil record of the Cambrian priapulid *Ottoia*. Palaeontology 58, 705–721. https://doi.org/10.1111/pala.12168.

Sørensen, M.V., Hebsgaard, M.B., Heiner, I., Glenner, H., Willerslev, E., Kristensen, R.M., 2008. New Data from an Enigmatic Phylum: Evidence from molecular sequence data supports a sister group relationship between Loricifera and Nematomorpha. J. Zool. Syst. Evol. Res. 46, 231–239. https://doi.org/10.1111/j.1439-0469.2008.00478.x.

Sørensen, M.V., Rho, H.S., Min, W.-G., Kim, D., 2012. A new recording of the rare priapulid *Meiopriapulus fijiensis*, with comparative notes on juvenile and adult morphology. Zool. Anz. 251, 364–371. https://doi.org/10.1016/j.jcz.2011.10.001.

Storch, V., Higgins, R.P., Morse, M.P., 1989. Internal Anatomy of *Meiopriapulus fijiensis* (Priapulida). Trans. Am. Microsc. Soc. 108, 245–261. https://doi.org/10.2307/3226343.

Storch, V., Higgins, R.P., 1991. Scanning and transmission electron microscopic observations on the larva of *Halicryptus spinulosus* (Priapulida). J. Morphol. 210, 175–194. https://doi.org/10.1002/jmor.1052100207.

Straub, S.C.K., Parks, M., Weitemier, K., Fishbein, M., Cronn, R.C., Liston, A., 2012. Navigating the tip of the genomic iceberg: next-generation sequencing for plant systematics. Am. J. Bot. 99, 349–364. https://doi.org/10.3732/ajb.1100335.

Taite, M., Fernández-Álvarez, F.Á., Braid, H.E., Bush, S.L., Bolstad, K., Drewery, J., Mills, S., Strugnell, J.M., Vecchione, M., Villanueva, R., Voight, J.R., Allcock, A.L., 2023. Genome skimming elucidates the evolutionary history of Octopoda. Mol. Phylogenetics Evol. 182, 107729. https://doi.org/10.1016/j.ympev.2023.107729.

Talavera, G., Castresana, J., 2007. Improvement of Phylogenies After Removing Divergent and Ambiguously Aligned Blocks from Protein Sequence Alignments. Syst. Biol. 56, 564–577. https://doi.org/10.1080/10635150701472164.

Théel, H., 1906. Northern and Arctic Invertebrates in the Collection of the Swedish State Museum (Riksmuseum). II. Priapulids, Echiurids etc. Kungl. Svenska Vetenskapsakademiens Handlingar 40 (4), 1–28.

Todaro, M.A., Shirley, T.C., 2003. A new meiobenthic priapulid (Priapulida, Tubiluchidae) from a Mediterranean submarine cave. Ital. J. Zool. 70, 79–87. https://doi.org/10.1080/11250000309356499.

Van der Land, J., 1968. A new aschelminth, probably related to the Priapulida. Zoologische Mededelingen 42 (22), 237–250.

Van der Land, J., 1970. Systematics, geography, and ecology of the Priapulida. Zool. Verhand. Leiden. 112, 1–118.

Van der Land, J., 1982. A new species of *Tubiluchus* (Priapulida) from the Red Sea. Neth. J. Zool. 32, 324–335.

Van der Land, J., 1985. Two new species of *Tubiluchus* (Priapulida) from the Pacific Ocean. Proc. Nederl. Akad. Wet. Sect. C 88, 371–377.

Von Siebold, C.T., 1849. Beiträge zur Fauna Preussens. Neue Preuss. Provincialbl. 7, 184–185.

Wernström, J.V., Slater, B.J., Sørensen, M.V., Crampton, D., Altenburger, A., 2023. Geometric morphometrics of macro-and meiofaunal priapulid pharyngeal teeth provides a proxy for studying Cambrian "tooth taxa". Zoomorphology 142 (4), 411–421. https://doi.org/10.1007/s00435-023-00617-4.

Wills, M.A., 1998. Cambrian and Recent disparity: the picture from priapulids. Paleobiology 24, 177–199. https://doi.org/10.1666/0094-8373(1998)024[0177:CARDTP]2.3.CO;2.

Wills, M.A., Gerber, S., Ruta, M., Hughes, M., 2012. The disparity of priapulid, archaeopriapulid and palaeoscolecid worms in the light of new data. J. Evol. Biol. 25 (10), 2056–2076. https://doi.org/10.1111/j.1420-9101.2012.02586.x.

Worsaae, K., Vinther, J., Sørensen, M.V., 2023. Evolution of Bilateria from a Meiofauna perspective - Miniaturization in the focus. In: Giere, O., Schratzberger, M. (Eds.), New Horizons in Meiobenthos Research. Springer, Cham, pp. 1–31. https://doi.org/10.1007/978-3-031-21622-0_1.

Yamasaki, H., Fujimoto, S., Miyazaki, K., 2015. Phylogenetic position of Loricifera inferred from nearly complete 18S and 28S rRNA gene sequences. Zoological Letters 1, 1–9. https://doi.org/10.1186/s40851-015-0017-0.

Zhang, H., Xiao, S., Liu, Y., Yuan, X., Wan, B., Muscente, A.D., Shao, T., Gong, H., Cao, G., 2015. Armored kinorhynch-like scalidophoran animals from the early Cambrian. Sci. Rep. 5 (1). https://doi.org/10.1038/srep16521.

Zhang, C., Rabiee, M., Sayyari, E., Mirarab, S., 2018. ASTRAL-III: Polynomial Time Species Tree Reconstruction from Partially Resolved Gene Trees. BMC Bioinform. 19 (S6), 153. https://doi.org/10.1186/s12859-018-2129-y.

Zhang, F., Ding, Y., Zhu, C.D., Zhou, X., Orr, M.C., Scheu, S., Luan, Y.X., 2019. Phylogenomics from low-coverage whole-genome sequencing. Methods Ecol. Evol. 10 (4), 507–517. https://doi.org/10.1111/2041-210X.13145.

Zhang, C., Mirarab, S., 2022. ASTRAL-Pro 2: ultrafast species tree reconstruction from multi-copy gene family trees. Bioinformatics 38, 49–50. https://doi.org/10.1093/bioinformatics/btac620.